# Ultrafast Optoelectronics and Electronics

CLEO Short Course, May 1999

Mark Rodwell

Department of Electrical and Computer Engineering

University of California, Santa Barbara, CA 93106

805-893-3244

rodwell@ece.ucsb.edu

# Outline

- Outlook and motivation
- 2-Terminal Devices
  - Photodiodes
  - Photoconductors
  - SRDs
  - Schottky Diodes
  - RTDs
- Transistors
  - FETS (HEMTs)
  - HBTs
- Transmission Lines
  - Types
  - Skin Effect Losses
  - Radiation Losses
  - Parasitic modes
- Antennas
  - Types
  - Substrate Lenses
- Circuit Design
  - Figures-of-Merit
  - Resistive-Loaded Circuits
  - Matched Circuits
  - Distributed Circuits
- Nonlinear Wave Devices
  - Shock-wave NLTLs
  - Sampling Circuits
  - Soliton NLTLs:
  - Traveling-Wave RTDs
- RTD array oscillators
- Instruments
  - Motivation
  - Types
  - Network Analysis
  - Time-Domain
  - Reflectometry
  - Signal Measurements
  - Photoconductive Testing
  - Electrooptic Probing
  - Laser sources
  - Active Probes
  - femtosecond
  - spectroscopy

## Ultrafast Optoelectronics and Electronics: What?

Generation, propagation, and detection of picosecond (and femtosecond) electrical & optical transients

## Why?

- Basic Technology/Science:
  - Generation and detection of pulse & CW signals in the 100 GHz-10 THz region (the spectral "black hole")
- Characterization of mm-wave circuits and devices.
  - Network analysis, waveform measurements, internal probing
- Measurement of semiconductor material and electron transport properties relevant to devices.
  - 50 GHz circuit needs ≈100-200 GHz transistors.
  - 200 GHz transistor needs ≈1 ps carrier transit times.
- Optoelectronic, Electronic Devices for High-Speed Applications
  - fiber and wireless communications at 10 GHz and beyond.

## Future High-Frequency Applications:

- 10 / 40 / 100 / 160... GB/sec fiber-optic data transmission
- Wireless microwave & mm-wave digital radio links
  - capacity for the data explosion
  - bandwidth is cheap at mm-waves
- mm-wave radar & imaging, car collision avoidance
  - runway imaging, fly-by-night, military
  - small antennas, high resolution
- Radio astronomy / Earth remote sensing
  - THz heterodyne radiometers on Satellites
  - ozone depletion
- ... & instrumentation for these applications

## The Electronic Bottleneck?

The issue:

- Can we make electronics at 100 GHz and above?

Today's solid-state devices:

- III/V HBTs: $f_{max} \approx$ 400 GHz
- Si/Ge HBTs: $f_{max} \approx$ 100 GHz planar,180 GHz mesa
- HEMTs: $f_{max} \approx$ 500 GHz
- Schottky Diodes: $f_c \approx$ 20 THz

Assertions (research objectives):

- device $f_{max}$ can be improved
- at $f_{max} / 4$ many circuits can be implemented.

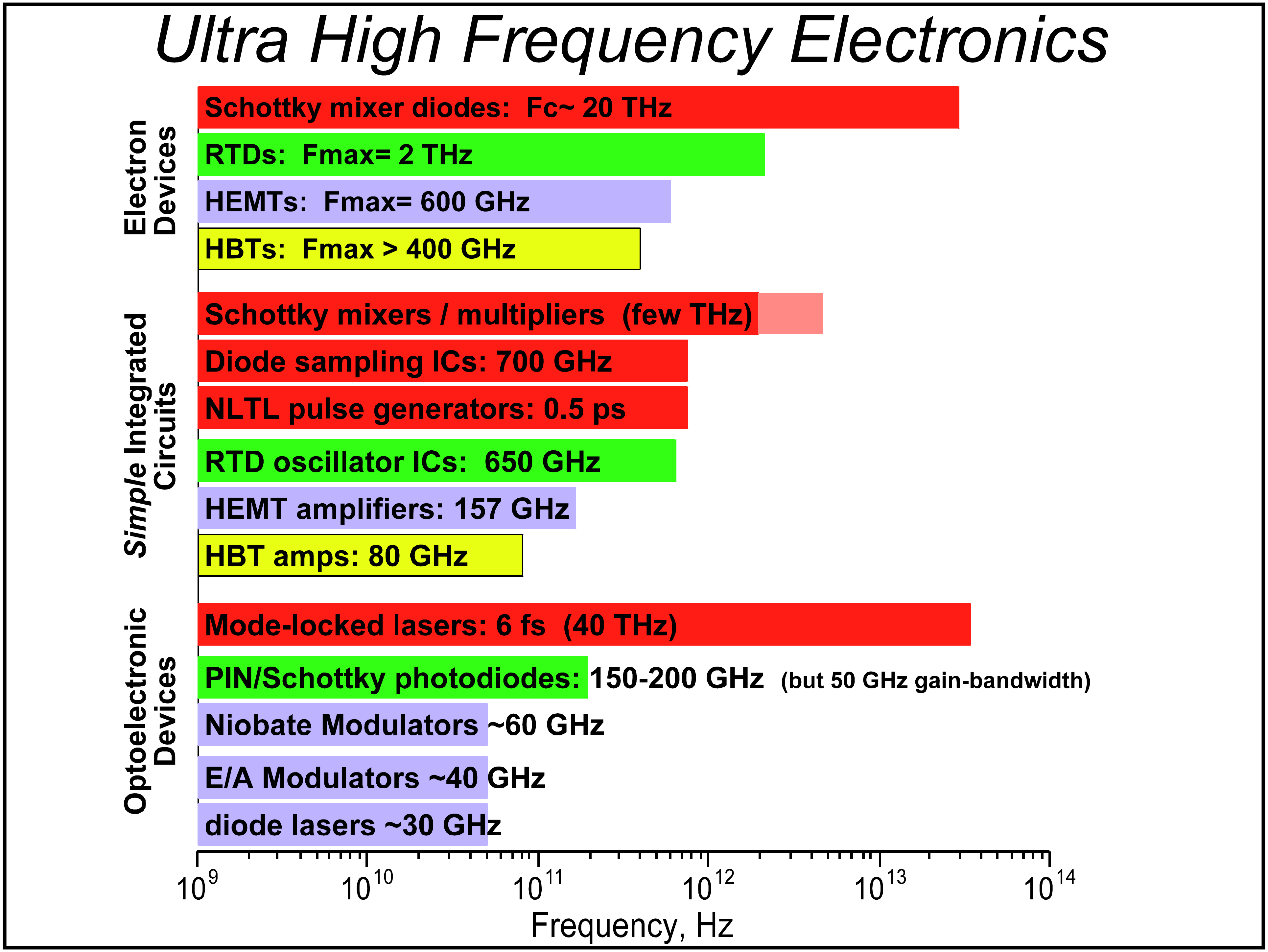
Ultra High Frequency Electronics
Electron Devices
Schottky mixer diodes: Fc~ 20 THz
RTDs: Fmax= 2 THz
HEMTs: Fmax= 600 GHz
HBTs: Fmax > 400 GHz
Simple Integrated Circuits
Schottky mixers / multipliers (few THz)
Diode sampling ICs: 700 GHz
NLTL pulse generators: 0.5 ps
RTD oscillator ICs: 650 GHz
HEMT amplifiers: 157 GHz
HBT amps: 80 GHz
Optoelectronic Devices
Mode-locked lasers: 6 fs (40 THz)
PIN/Schottky photodiodes: 150-200 GHz (but 50 GHz gain-bandwidth)
Niobate Modulators ~60 GHz
E/A Modulators ~40 GHz
diode lasers ~30 GHz
$10^9$
$10^{10}$
$10^{11}$
$10^{12}$
$10^{13}$
$10^{14}$
Frequency, Hz

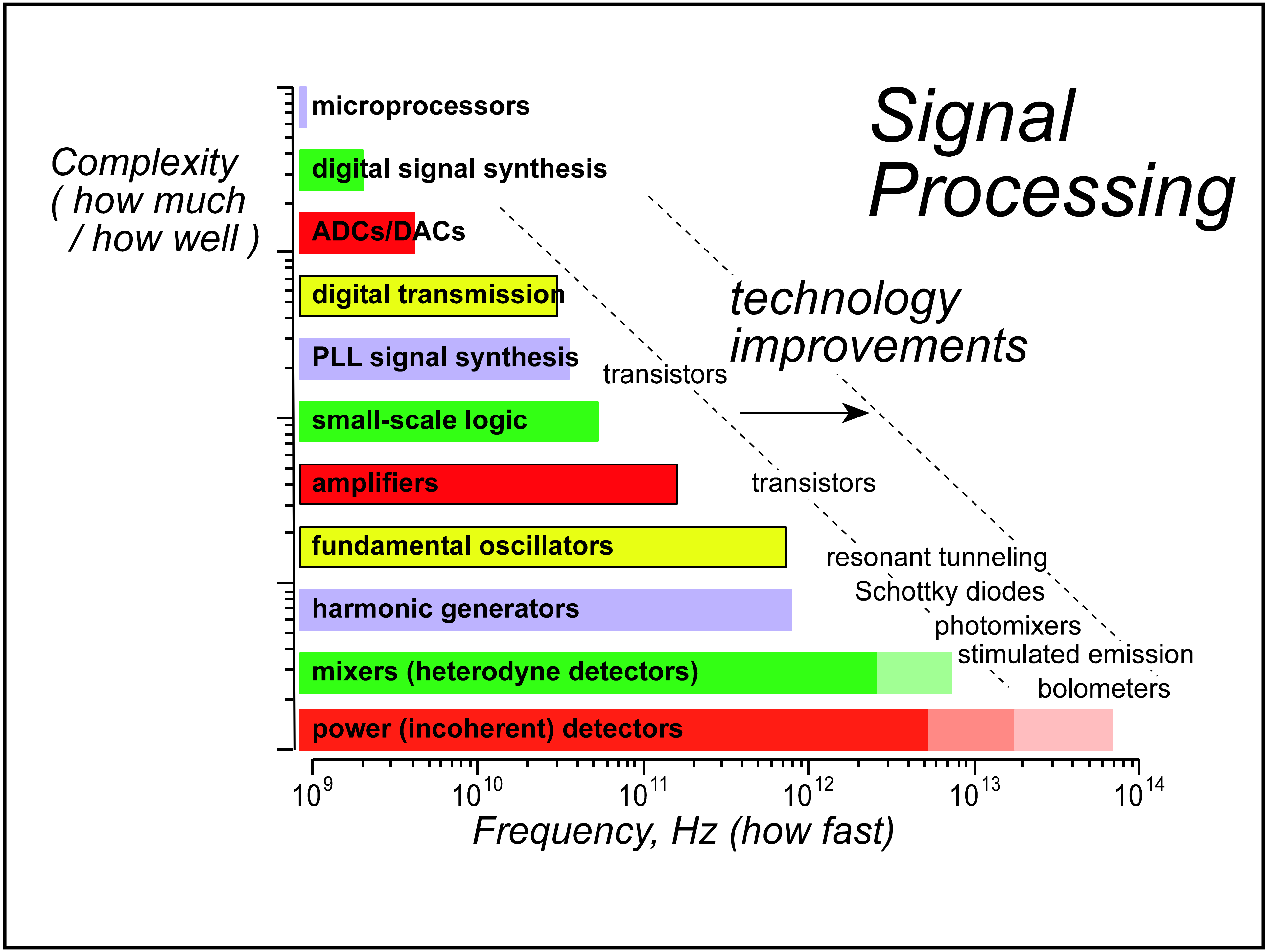

Signal Processing
Complexity ( how much / how well )
microprocessors
digital signal synthesis
ADCs/DACs
digital transmission
PLL signal synthesis
small-scale logic
amplifiers
fundamental oscillators
harmonic generators
mixers (heterodyne detectors)
power (incoherent) detectors
technology improvements
transistors
transistors
resonant tunneling
Schottky diodes
photomixers
stimulated emission
bolometers
$10^9$
$10^{10}$
$10^{11}$
$10^{12}$
$10^{13}$
$10^{14}$
Frequency, Hz (how fast)

## High-Speed Optoelectronics: $$$ Realities

- devices, circuits feasible to ≥ 100 GHz.

- expensive technology: small, high-value market
  military, instruments, satellites, high-capacity fiber

- mm-waves: bandwidth is cheap, ICs are expensive

- goal: cheap mm-wave ICs for high-volume markets
  ... lower-cost III-V devices???
  ... mm-wave silicon ICs???

Feasiblity of 100 + GHz electronics is mainly an economic issue

# Bandwidth of Semiconductor Devices

Interaction of transit time
and RC charging time sets bandwidth

Applies to most semiconductor devices
- Schottky diodes, photodiodes, RTDs
- bipolar transistors, field-effect transistors, …

# How Do Semiconductor Devices Work?

Signal power generated by sweeping carrier through field.

Current independent of output voltage

Current controlled by input voltage

Alternative:
negative-resistance devices

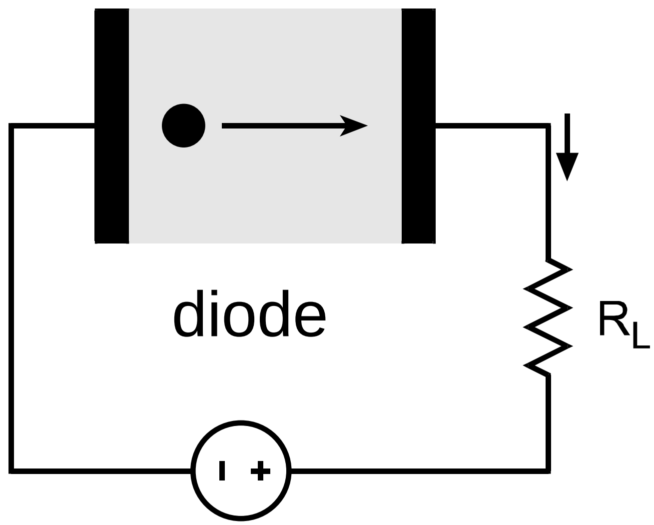


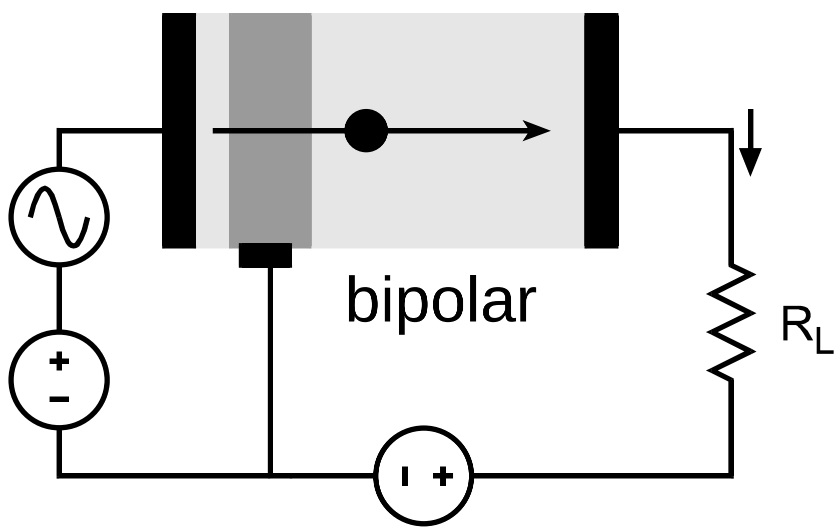


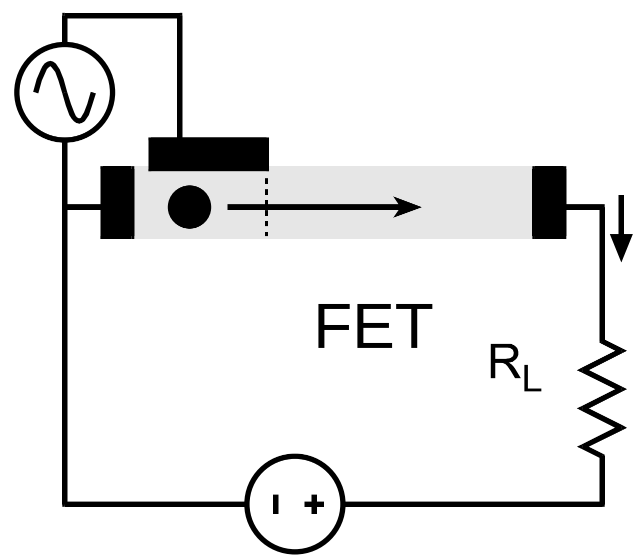

# Total effective time constant and scaling

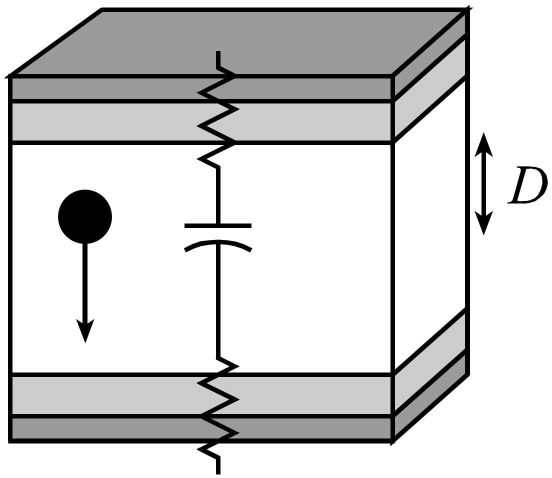


$$R_{contact} C_{depl} = \rho_{contact} \varepsilon / D$$

$$\tau_{transit} \propto D / v_{electron}$$

$$\boxed{T_{effective} \propto \sqrt{\tau_{transit}(RC)} = \sqrt{\frac{\varepsilon \rho_{contact}}{v_{electron}}}}$$

Vertical Ohmic Contacts

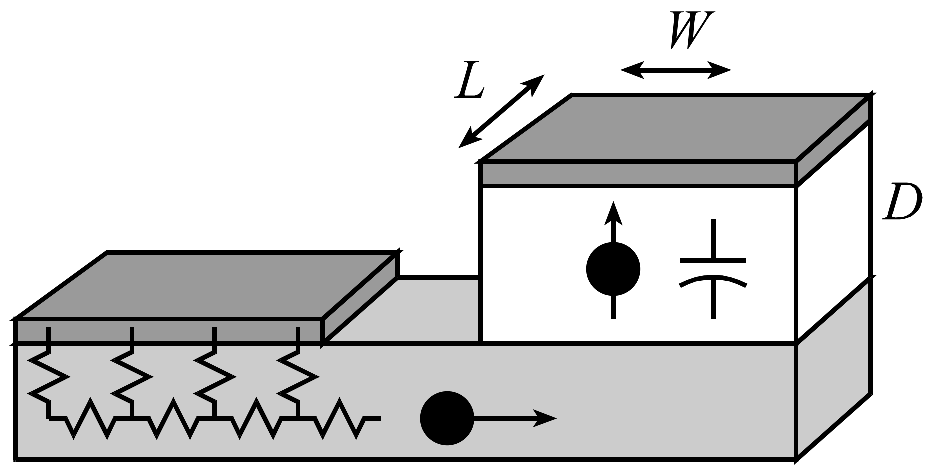


$$R_{cont,horiz} C_{depl} \propto (1/L)(\varepsilon A / D) = \varepsilon W / D$$

$$\tau_{transit} \propto D / v_{electron}$$

$$\boxed{T_{effective} \propto \sqrt{\tau_{transit}(RC)} = \sqrt{\frac{\varepsilon}{v_{electron}}} \sqrt{\frac{1}{W}}}$$

Horizontal Ohmic Contact
Vertical Schottky Contact

- Note the differing scaling laws !

# What Limits Semiconductor Device Bandwidth?

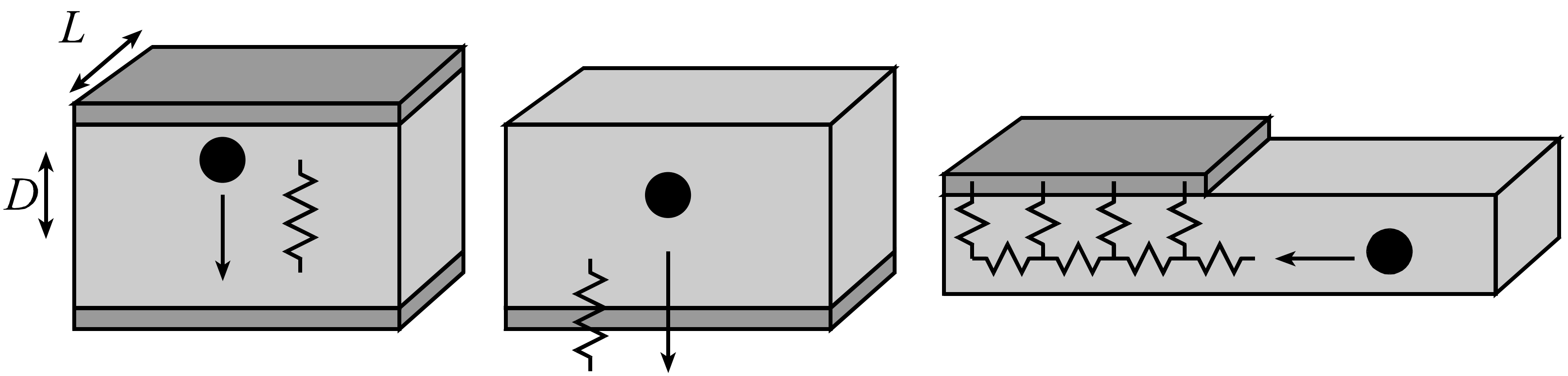


$R_{bulk} = \rho D / A$ $\qquad$ $R_{contact} = \rho_{contact} / A$ $\qquad$ $R_{cont,horiz} \propto 1/L$

- Bulk resistances
- Ohmic contact resistances
- Lateral contact access resistances
- These are for <u>undepleted</u> semiconductor layers

# What Limits Semiconductor Device Bandwidth?

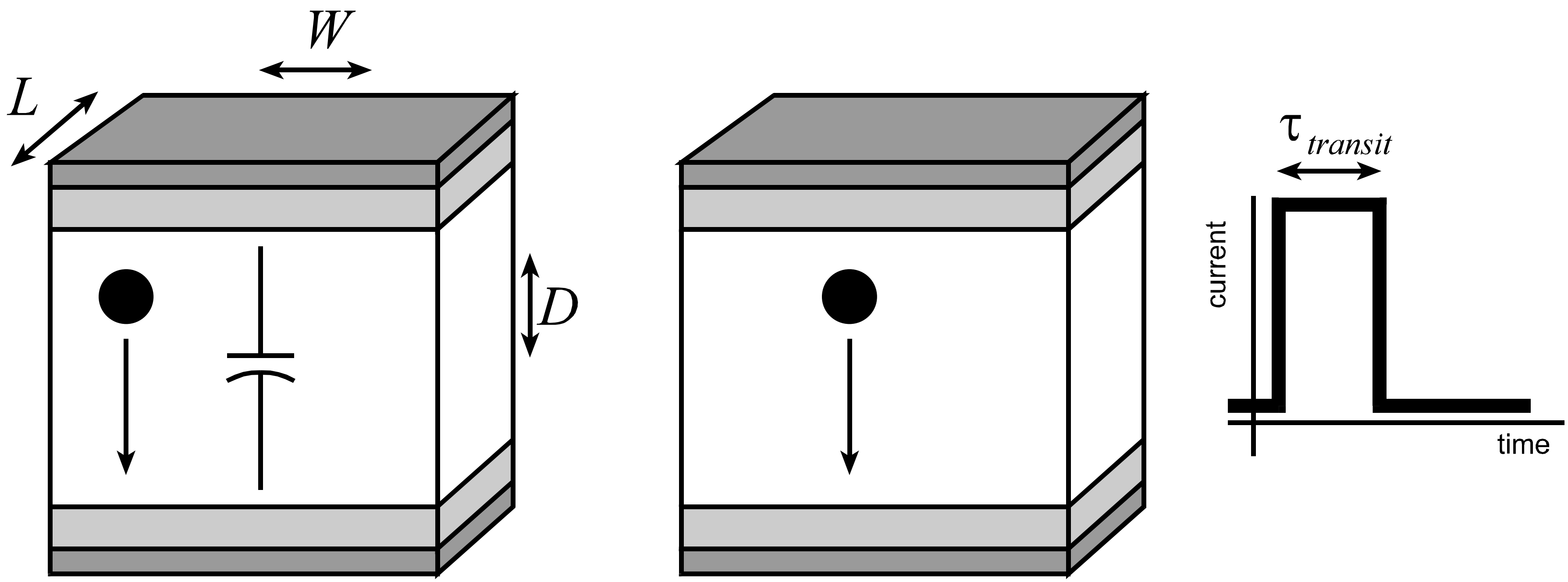


$C_{depl} = \varepsilon A / D$

$\tau_{transit} \propto D / v_{electron}$

- Depletion layer capacitances
- Depletion layer transit times

# RC Charging Times And Scaling

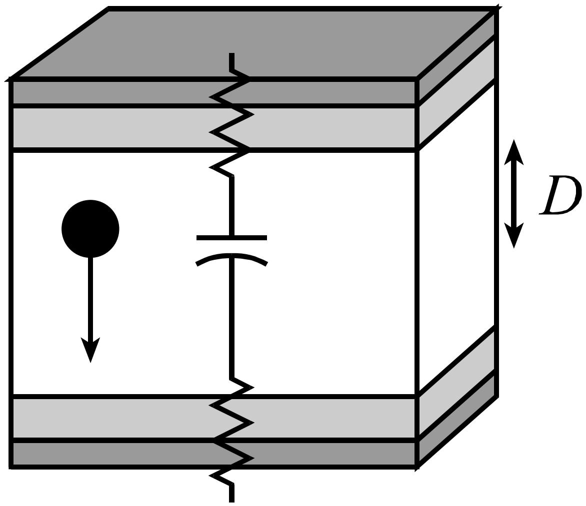


$$C_{depl} = \varepsilon A / D$$

$$R_{contact} \propto \rho_{contact} / A$$

$$\boxed{R_{contact} C_{depl} = \rho_{contact} \varepsilon / D}$$

Vertical Ohmic Contacts

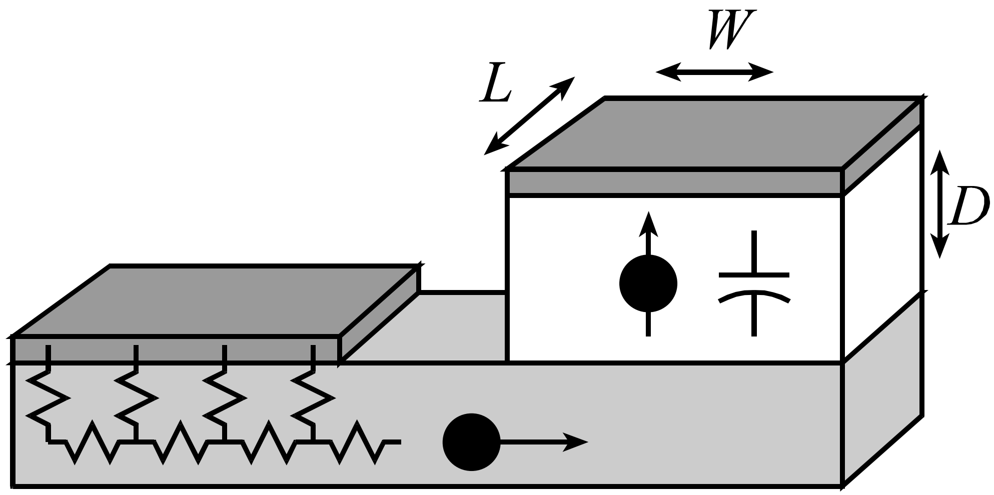


$$R_{cont,horiz} \propto 1 / L$$

$$C_{depl} = \varepsilon A / D$$

$$\boxed{R_{cont,horiz} C_{depl} \propto (1/L)(\varepsilon A / D) = \varepsilon W / D}$$

Horizontal Ohmic Contact
Vertical Schottky Contact

- note the different scaling law

# Super-Scaled, THz-Bandwidth Devices

Principle of Scaling

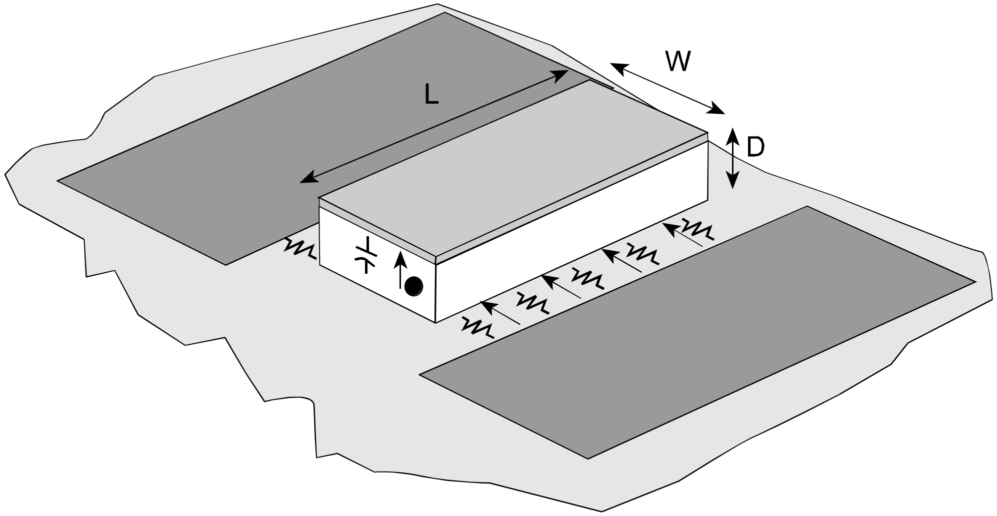


$$C \propto WL / D$$

$$\tau_{transit} \propto D / v_{electron}$$

$$R \propto 1 / L$$

$$\rightarrow RC \propto W / D$$

*deep submicron junction stripe widths,*

*deep submicron epitaxial layer thicknesses*

*--> THz device bandwidths*

Transferred-Substrate HBT

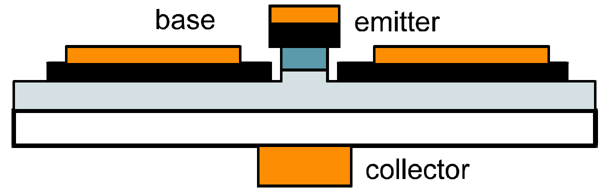


Schottky-collector RTD

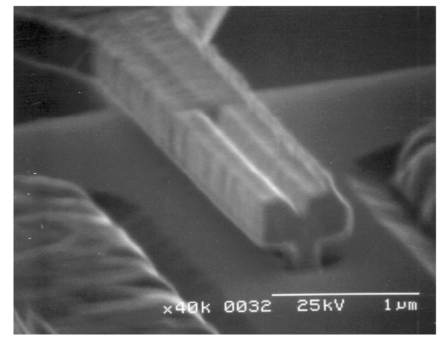


Opposed-Gate HEMT

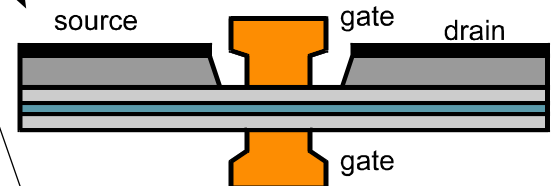


Super-Scaled Schottky

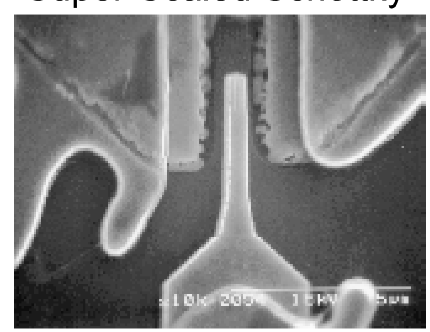

## 2-Terminal Devices

- Photodiodes & Photconductors
- Schottky Diodes
  Resonant Tunnel Diodes

## Photodiodes

Photoconductors: light-controlled resistors

Photodiodes: light-contolled current sources:

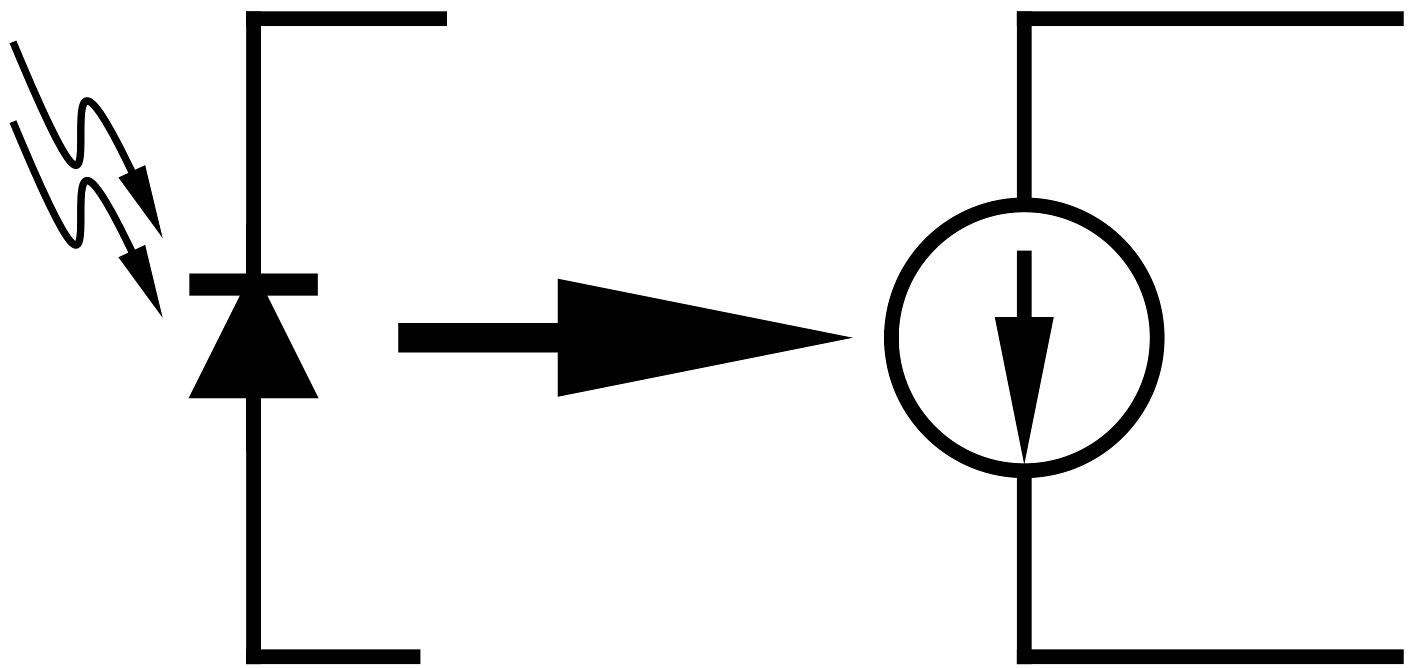

# Photodiode Structures:

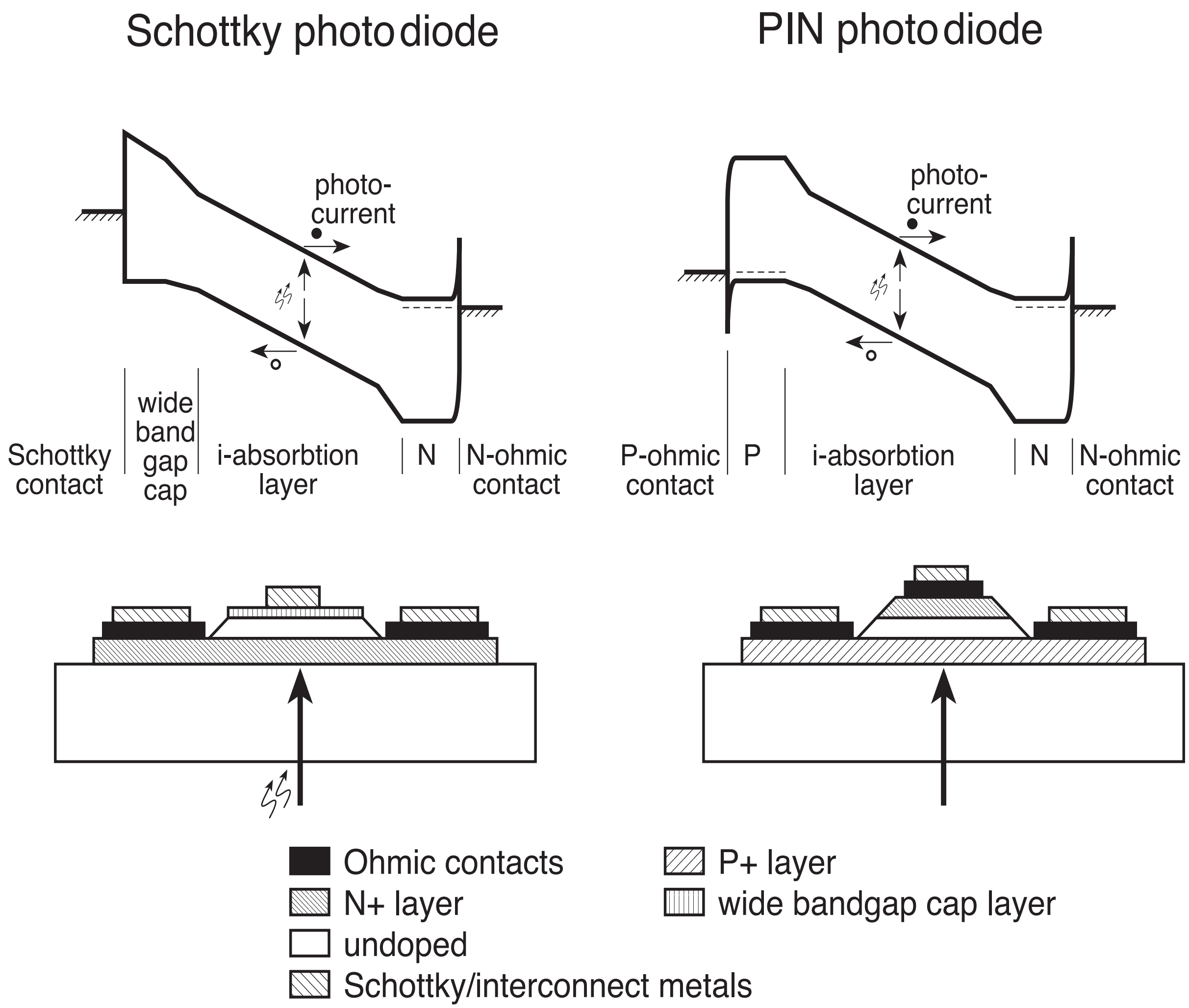


Schottkys are simpler: smaller, faster but are difficult on many materials: need AlInAs cap on InGas Schottky

Narrow band-gap (absorbing) I-region (N+ and P+ regions are wider-bandgap, hence transparent)

# Photodiode Carrier Transit-Time

-Short-circuit current response to a single electron-hole pair

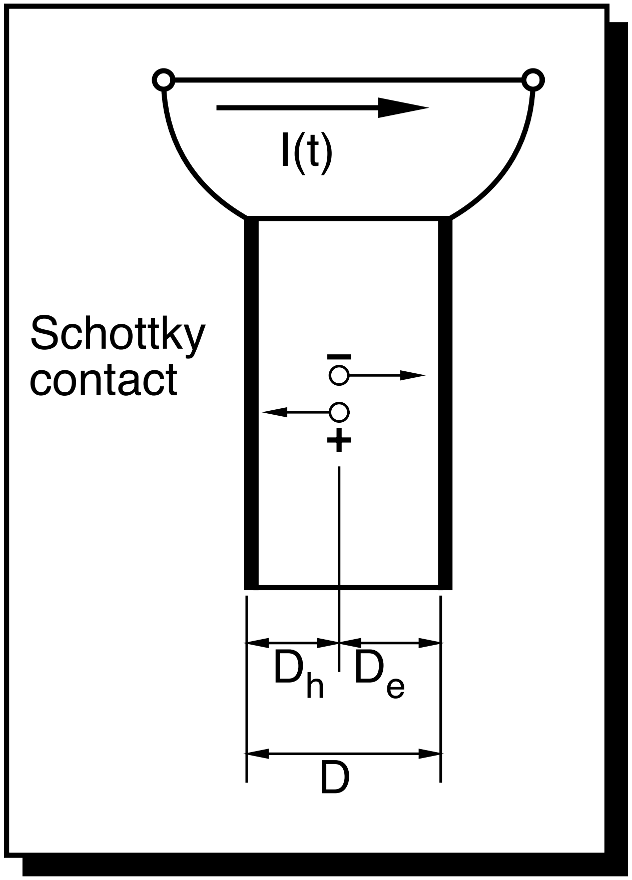


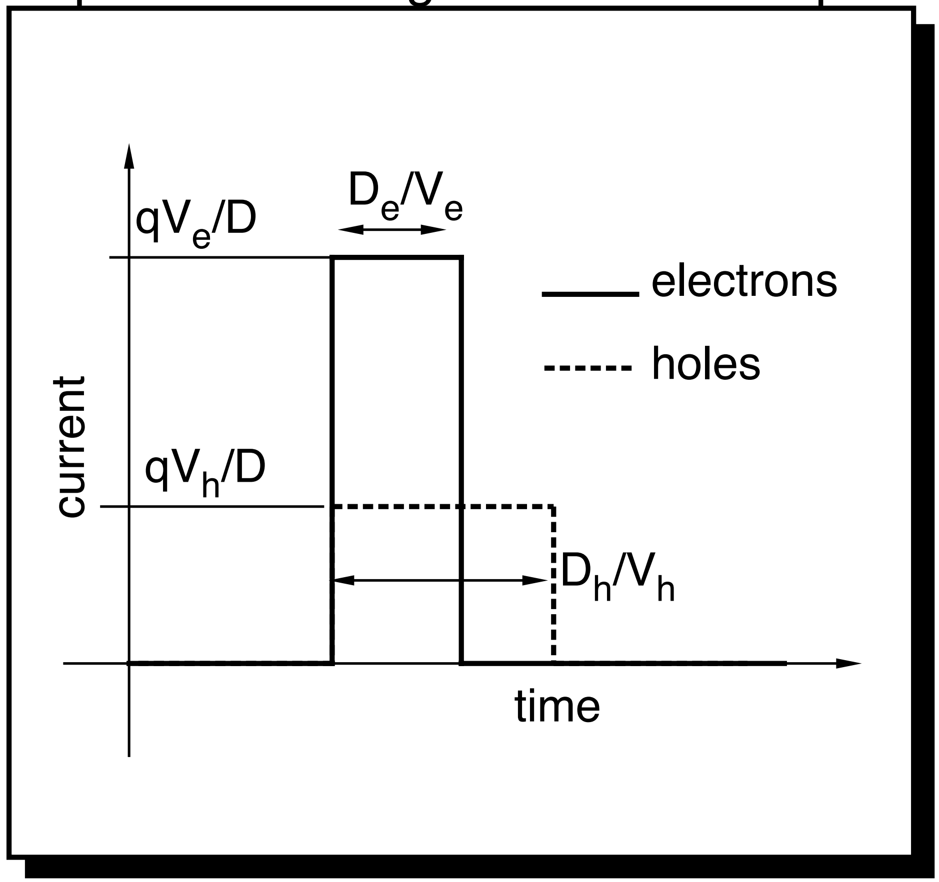


GaAs Electron velocity: $\approx$1-2($10^7$) cm/sec , higher for D<1000 å

GaAs Hole velocity: $\approx$6($10^6$) cm/sec (?), never ballistic

# Photodiode Transit Time II

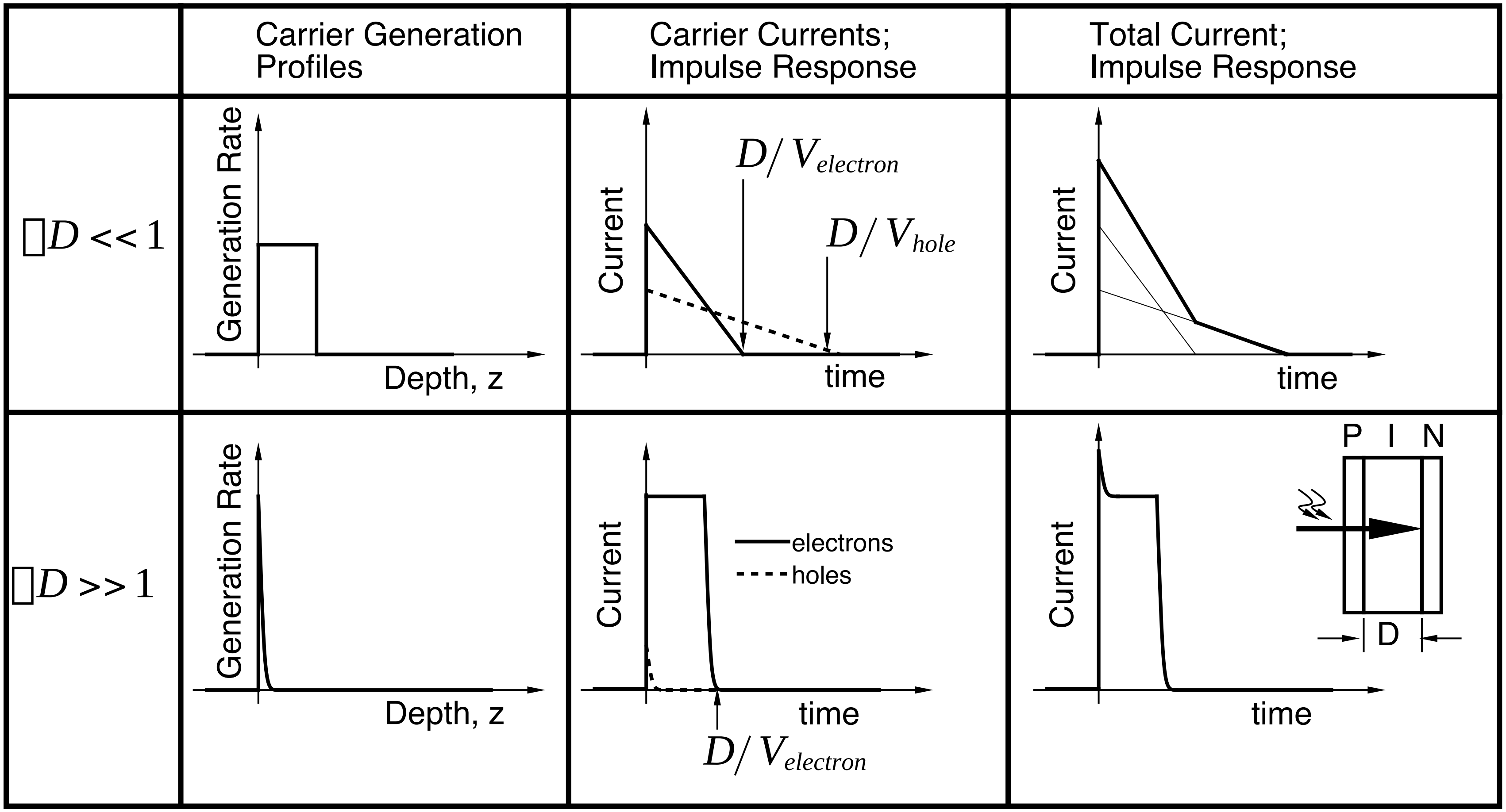


$$G(z,t) = \frac{(1-R)}{h\nu}\frac{E_0\delta(t)}{A}\alpha\left(e^{-\alpha z}\right) \quad \text{for } P_{incident}(t) = E_o\delta(T)$$

# Photodiodes: Optimization of I-layer Thickness

## Photodiodes: Optimization of Absorbtion Layer Thickness

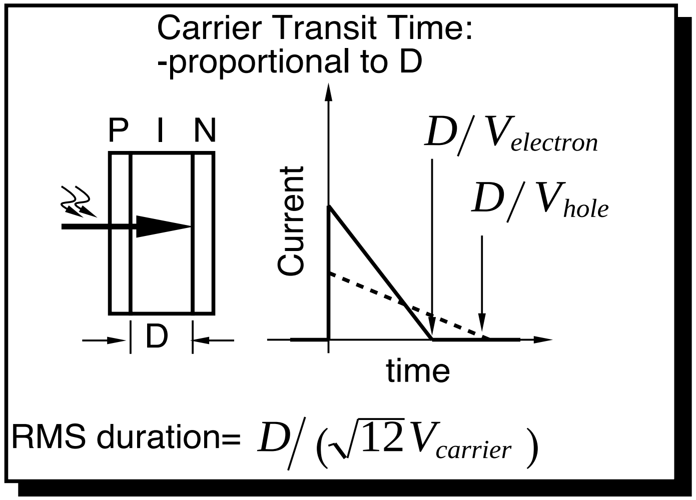


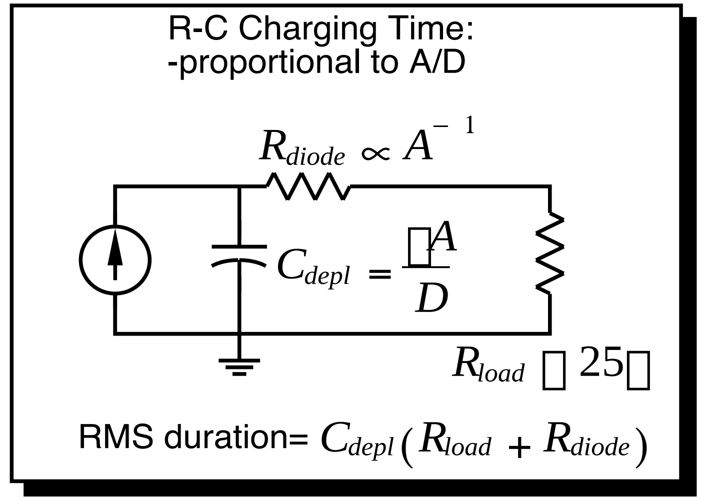


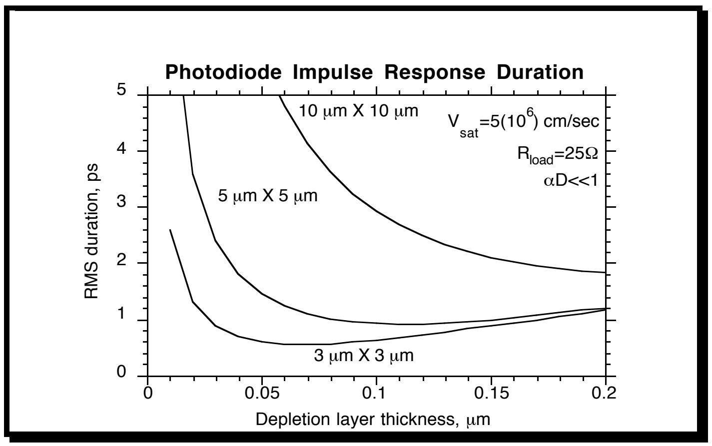


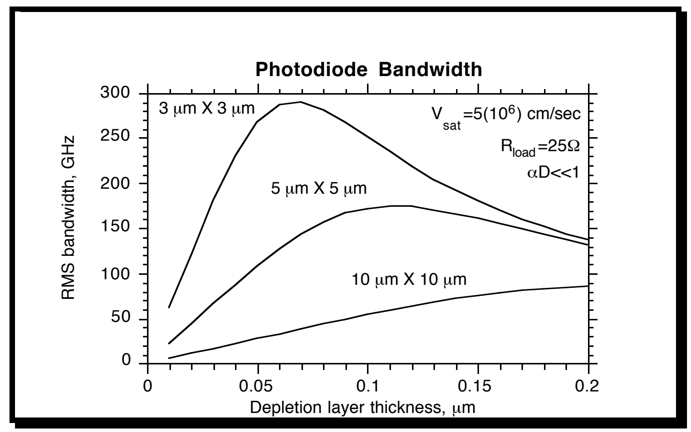


Analysis neglects diode series resistance (process-dependent, significant for smaller diodes). $f_{-3dB} = 0.83 f_{RMS}$ for Guassian response

# High-Speed InGaAs Photodetector

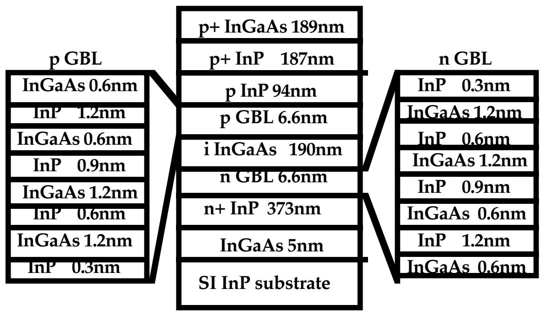


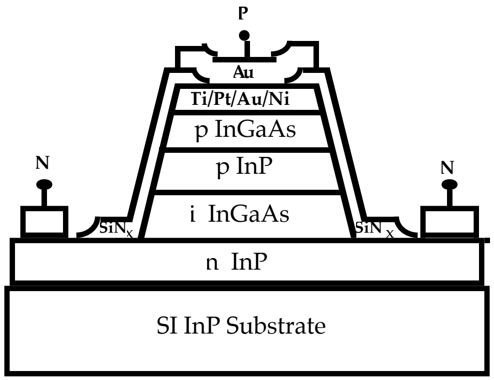


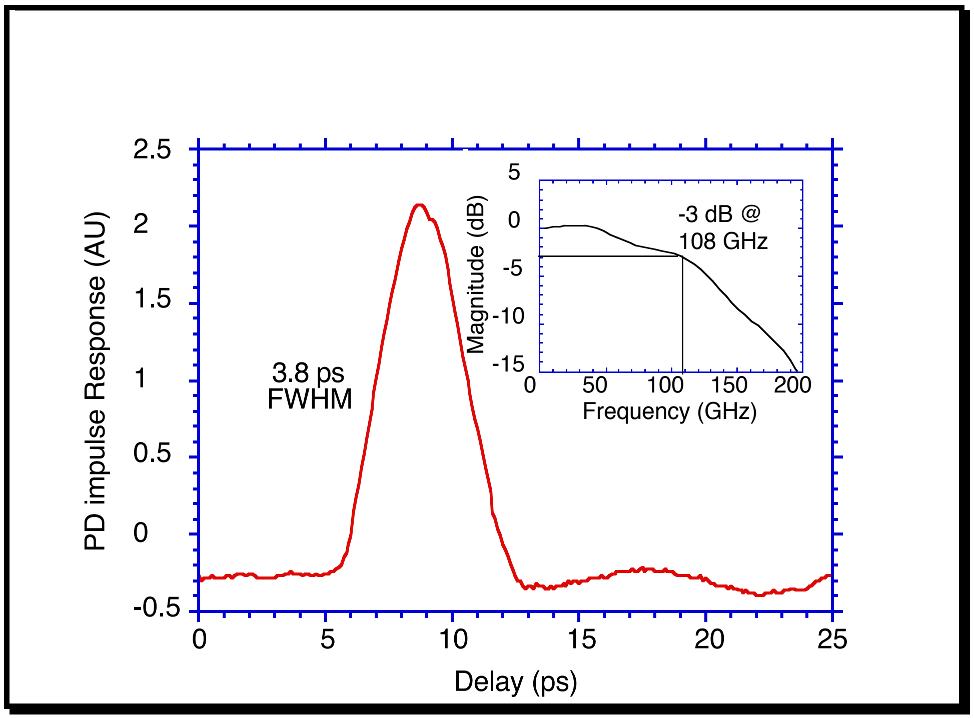

# Photodiode Efficiency-Bandwidth Limit

Quantum Efficiency:

$$\eta = (1 - R)\left(1 - e^{-\alpha D}\right) \cong \alpha D$$

Assuming:

- Antirelection coating: $R = 0$
- Thin absorbtion layer: $\alpha D << 1$

Bandwidth

$$f_{3dB} = 0.445 V_{carrier} / D$$

Assuming:

- Transit time >> RC charging time
- Thin absorbtion layer: $\alpha D << 1$

Efficiency-Bandwidth Product

$$f_{3dB}\eta = 0.445 V_{carrier}\alpha$$

strongly wavelength-dependent

# Beating the Efficiency Bandwidth Limit 1

## PIN RCE photodiodes

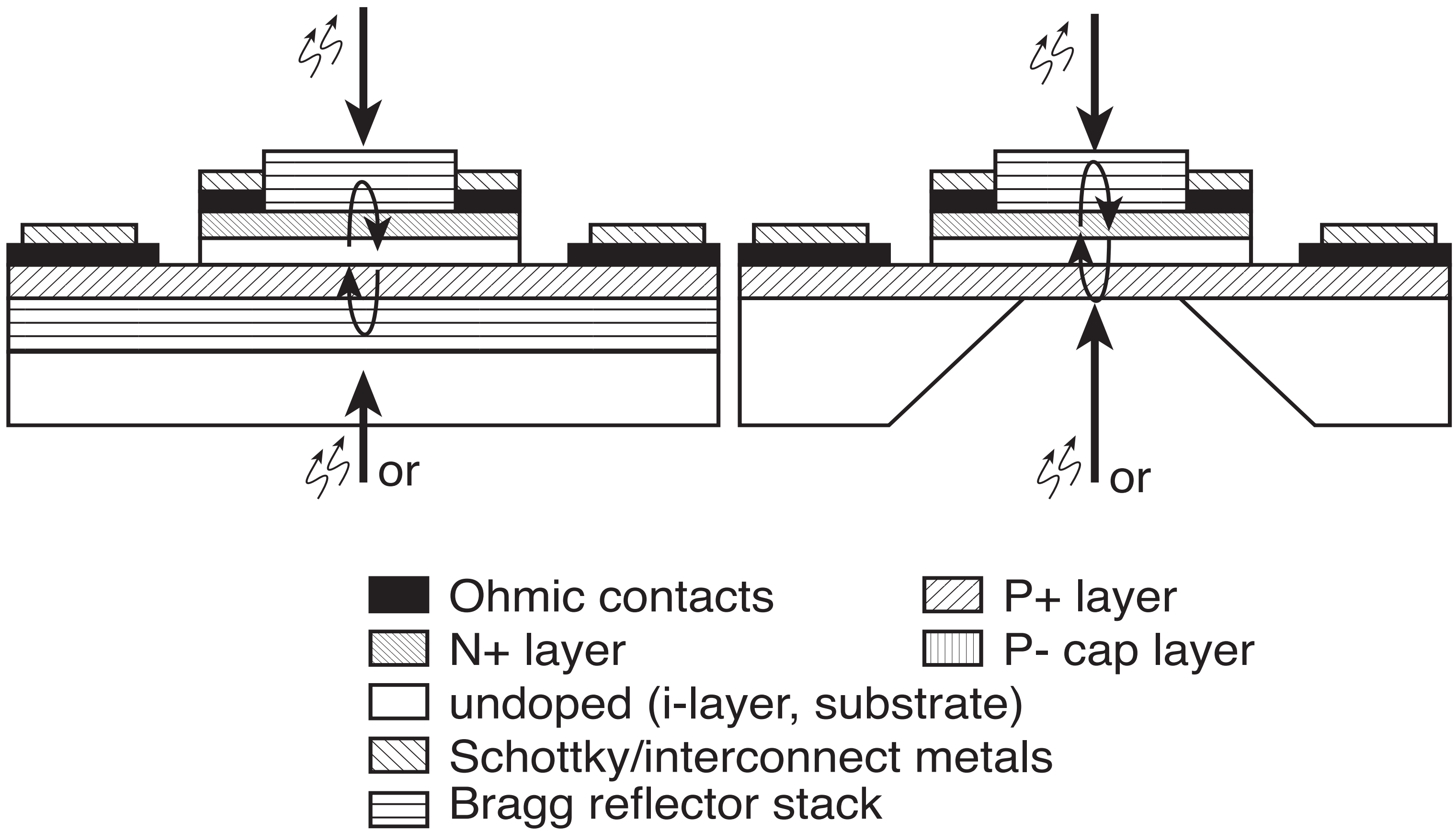


- Mirrors result in mulitiple transits of absorbing region by incident light
- Optical impedance-matching problem (use Smith Chart!)
- Thin absorbing layers (fast device) and high efficiency both possible

# Other RCE detector configurations

PIN RCE photodiode

Schottky RCE photodiodes

via-etched

flip-chip

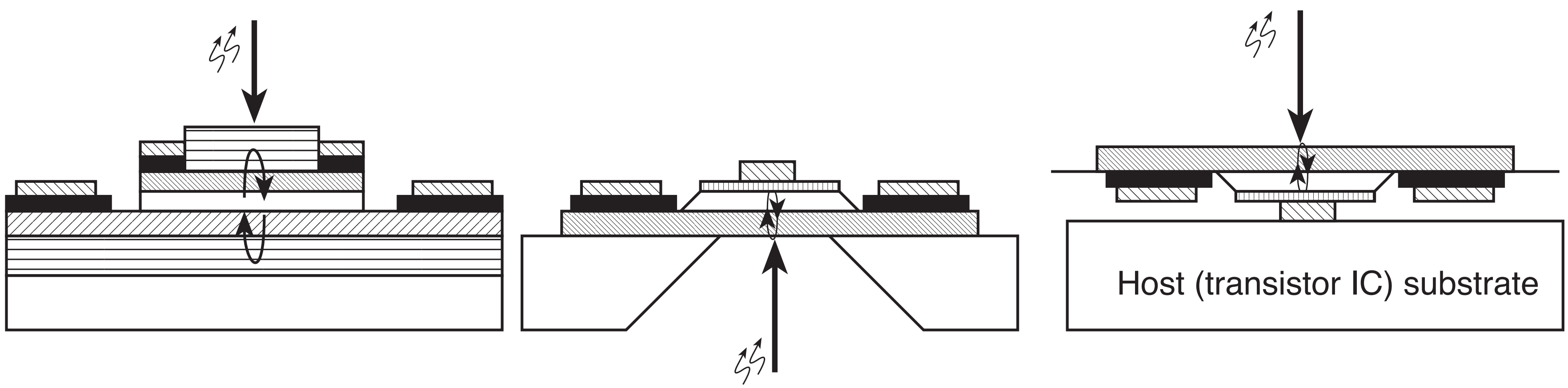


- Ohmic contacts
- N+ layer
- undoped (i-layer, substrate)
- Schottky/interconnect metals
- Bragg reflector stack
- P+ layer
- wide band-gap cap layer

# Beating the Efficiency Bandwidth Limit 2

Waveguide Photodetector
with 172 GHz Bandwidth and
76 GHz Bandwidth-Efficiency Product

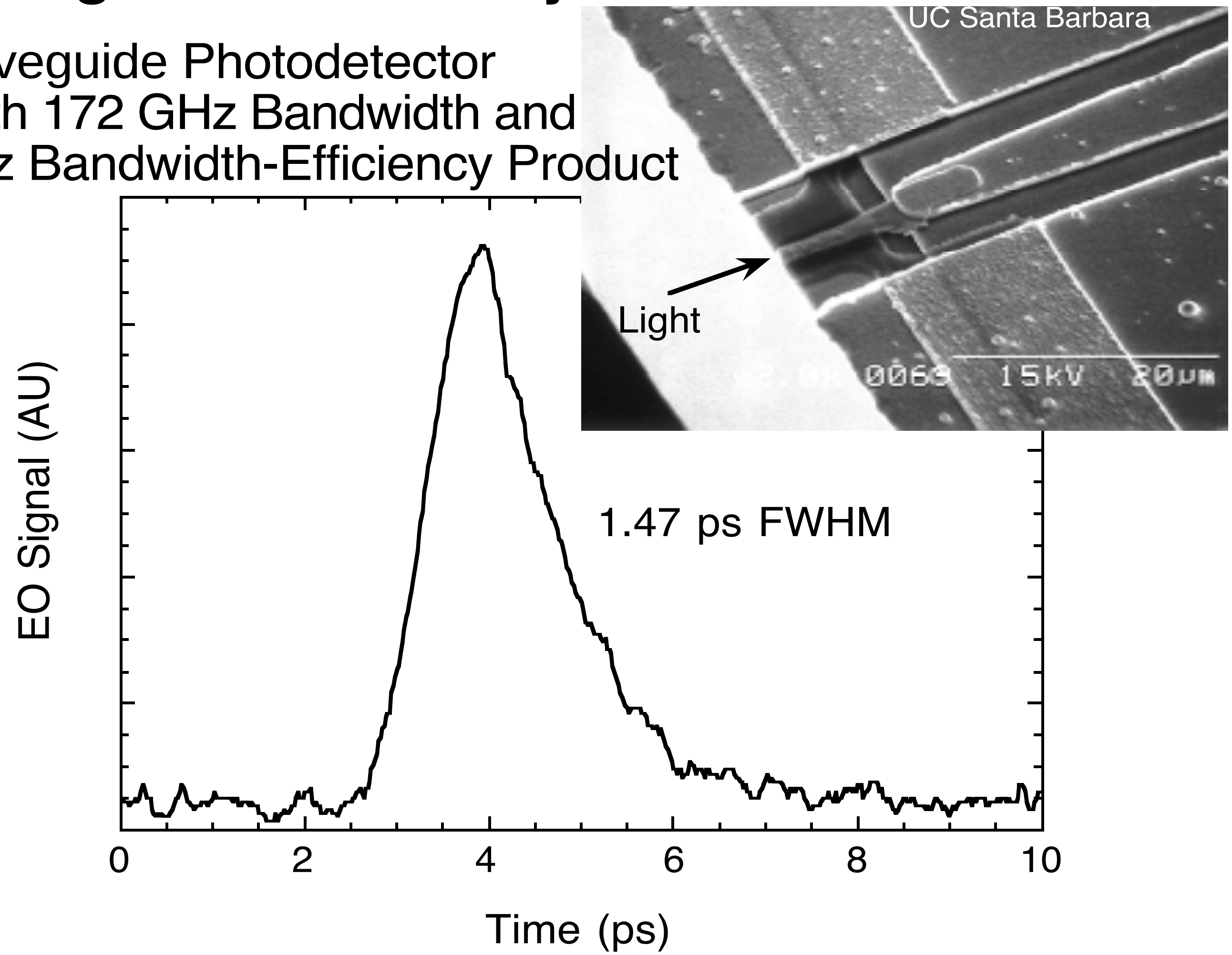


Waveguide (and traveling-wave) photodiodes.

• Optical Illumination perpernicular to electron transport- independent dimensions
• Very small optical aperture....coupling can be hard

# Saturation in Photodiodes: Field-Screening

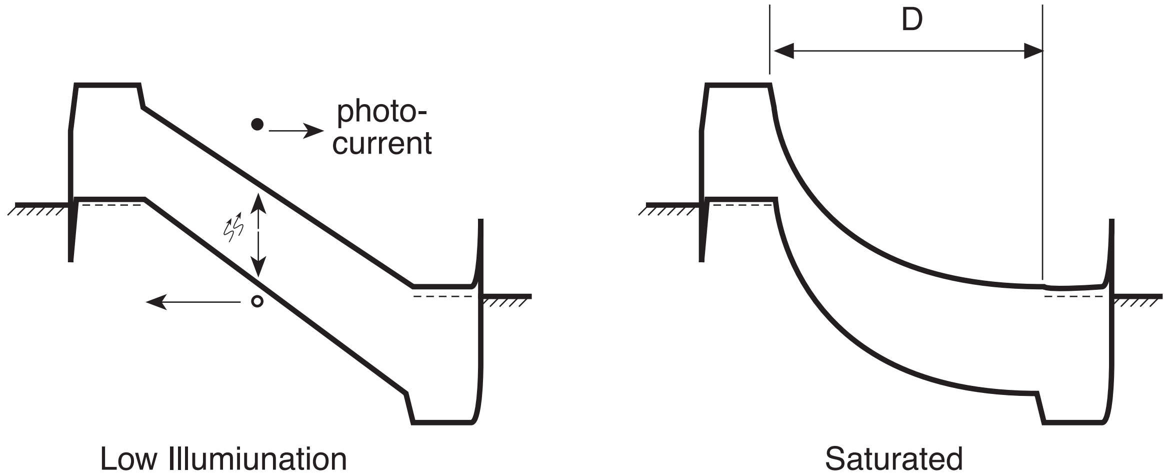


back-of-envelope calculation (skipping integrals)

Electron velocity >> Hole velocity --> hole stored charge dominates

$$Q_{hole} \approx J\tau_{hole} = JD / v_{hole}$$

$$\Delta E \approx Q_{hole}/\varepsilon = JD/v_{hole}\varepsilon$$

$$\Delta V \approx \Delta E \cdot D \approx JD^2/v_{hole}\varepsilon$$

$$V_{bias} + \phi \approx JD^2/v_{hole}\varepsilon$$

$$\longrightarrow \boxed{J_{\max} \approx \left(V_{bias} + \phi\right)\frac{\varepsilon v_{hole}}{D^2}}$$

$\dfrac{D^2}{\varepsilon v_{hole}}$ is called the space-charge resistance

Vbias is limited by breakdown

# Photoconductor: Fast Optical-Electrical Converter

Photoconductors are optically-controlled resistors

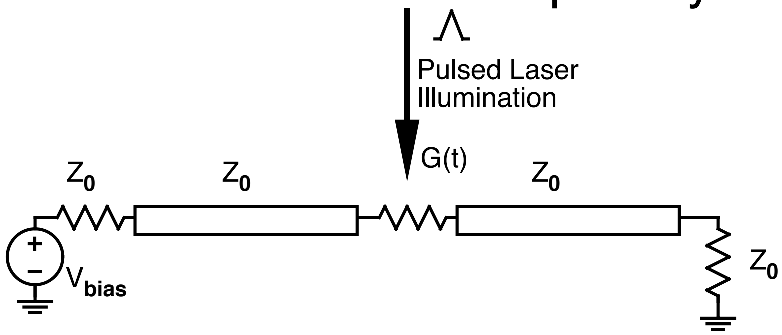


$$\frac{V_{out}}{V_{bias}} = \frac{1}{2}\left(\frac{Z_0}{Z_0 + 1/G}\right)$$

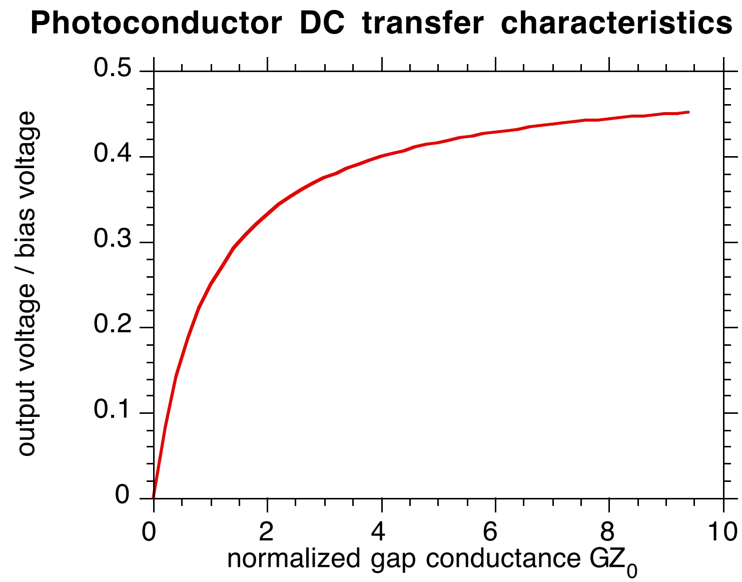


•$GZ_0$<<1: linear photodetector

•For $GZ_0$>>1, laser-gated switch

- Subpicosecond optical-electrical converters
- Subpicosecond electrical sampling gates

# Photoconductive Detectors: DC Characteristics

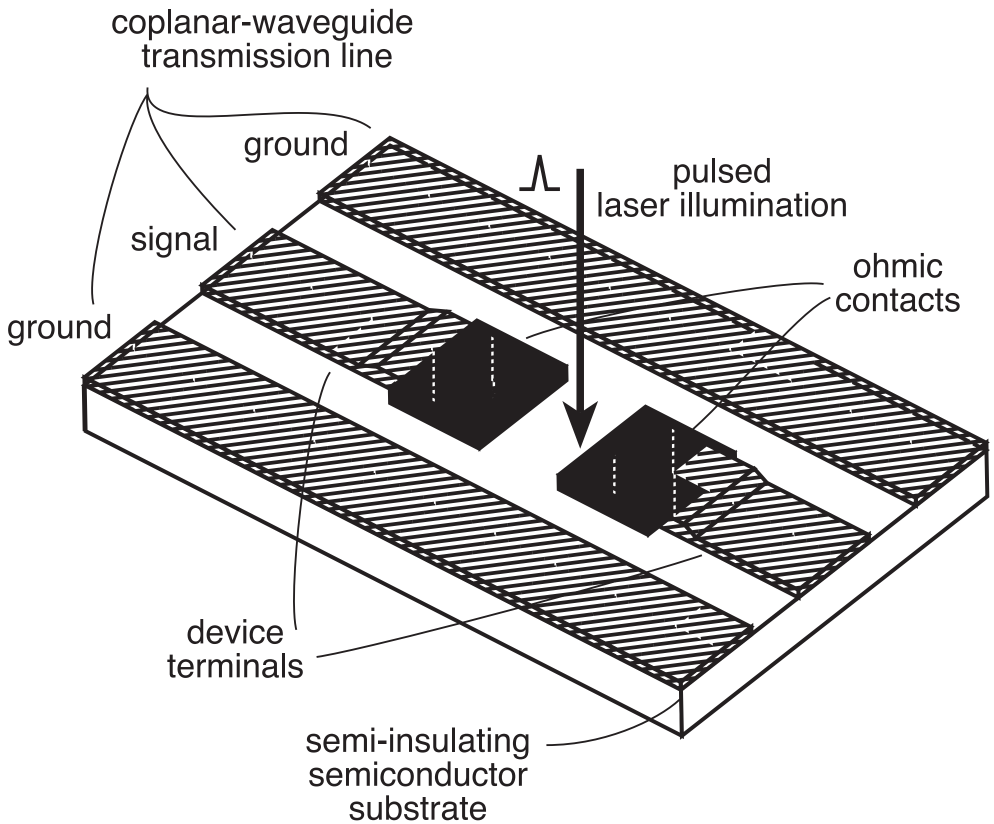


R is the reflectivity,
tau is the carrier
lifetime,
L is the gap length,
W the gap width

Responsivity varies as $1/L^2$

$$G(t) \propto (W/L)(thickness)(\mu_n n + \mu_p p)$$

$$n \bullet (thickness) = p \bullet (thickness) = (1 - R)\frac{q}{h\upsilon}\frac{P_{optical}}{WL}\tau$$

# Photoconductor Impulse Response (bandwidth)

## •Carrier recombination time

$$n(t) = n_o e^{-t/\tau} \ , \ p(t) = p_o e^{-t/\tau}$$

Radiation damaged GaAs

reduces $\tau$ and $\mu$: increases bandwidth, decreases sensitivity.

Low-Temperature-Growth GaAs:

reduces $\tau$ but mainains good mobility, hence good sensitivity.
(Arsenic clusters as recombination centers?)

## •Gap capacitance charging time

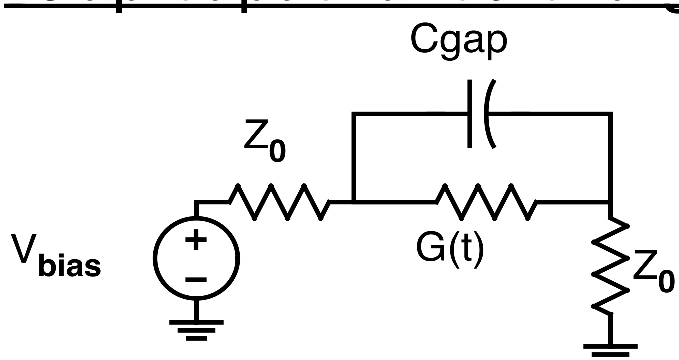


Small-signal ($GZ_0<<1$):

$$\tau = 2Z_0 C_{gap}$$

# Photodiodes vs Photoconductors

Photodiode

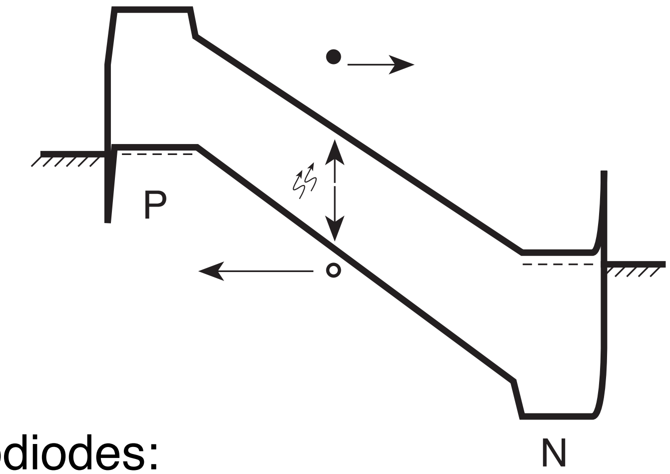


Photo-conductor

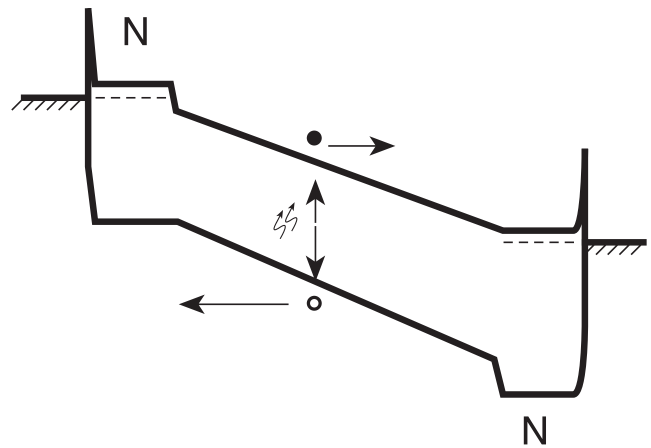


Photodiodes:
contacts block carrier enty into drift region
total charge collected is exactly # photons absorbed
current duration is electron + hole transit times

N-I-N photoconductor (vice-versa for P-I-P photoconductor)
N contacts block hole entry, do not block electron entry
**by charge neutrality, more electrons enter from cathode as holes leave**
current pulse duration is hole recombination or sweep-out time
current gain is (hole lifetime)/(electron lifetime)

# Metal-Semiconductor-Metal Photodetectors

band diagram

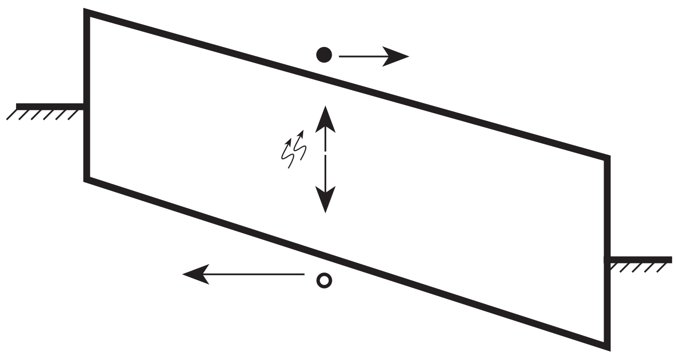

structure

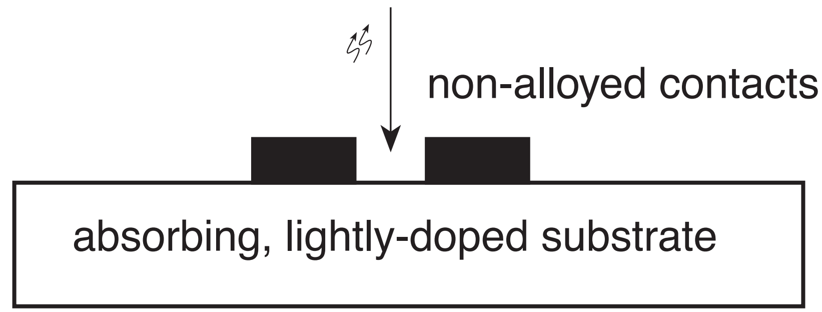


Unless Ohmic contacts are used, MSMs are photodiodes, not photoconductors

Published Ultrafast MSM detectors show no photoconductive gain

Observed change in responsivity with bias  due to increased depletion depth ?

# The Step Recovery Diode

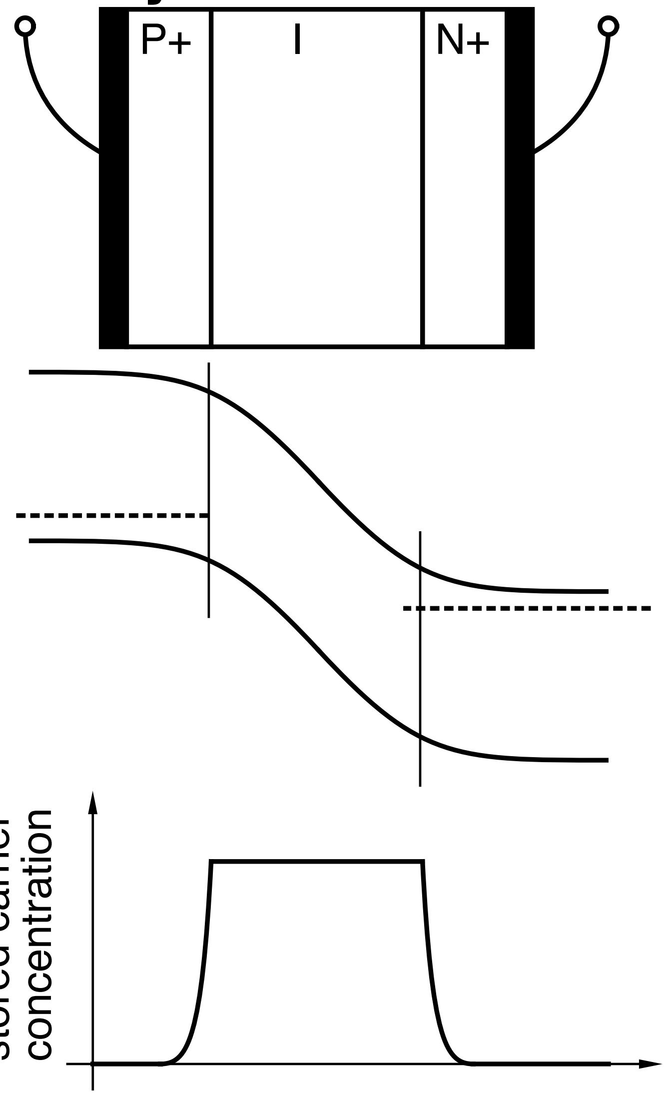


Under bias, carriers are stored in the intrinsic region

Charge control model:

•Stored charge

$$Q_s = Q_0\left(\exp(qV / kT) - 1\right)$$

•Diode current

$$I = \frac{dQ_s}{dt} + \frac{Q_s}{\tau}$$

•Widely used as a pulse generator in microwave instruments

# Electrical Falltime Compression with SRD's

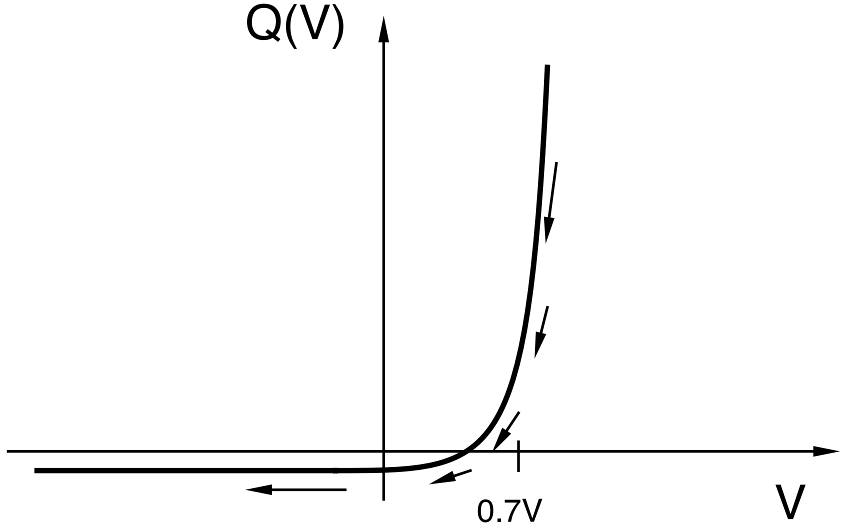


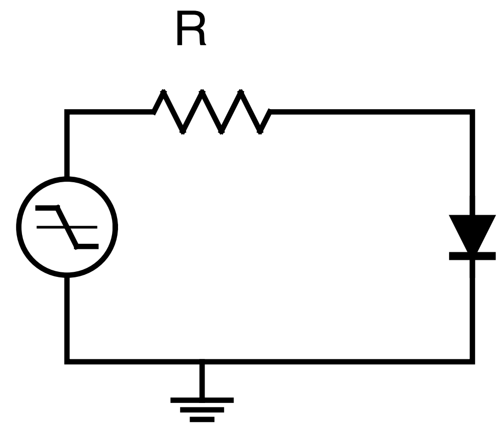


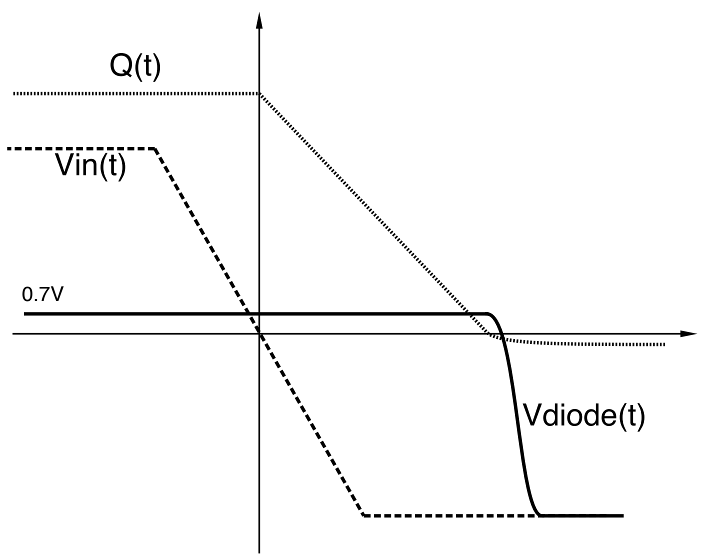


$$I = \left(V_{diode} - V_{in}\right)/R$$
$$dQ/dt \cong -I$$

For a fast-changing input signal, the SRD acts as a nonlinear capacitor.

# Transition time limits of SRD's

Depletion Capacitance:

$\tau = R_{load} C_{SRD}$

Carrier Diffusion Time

Time in which minority carriers are swept from the intrinsic region. No simple closed-form expression. Moll (1969) estimates ≈10 ps/μm of intrinsic layer thickness.

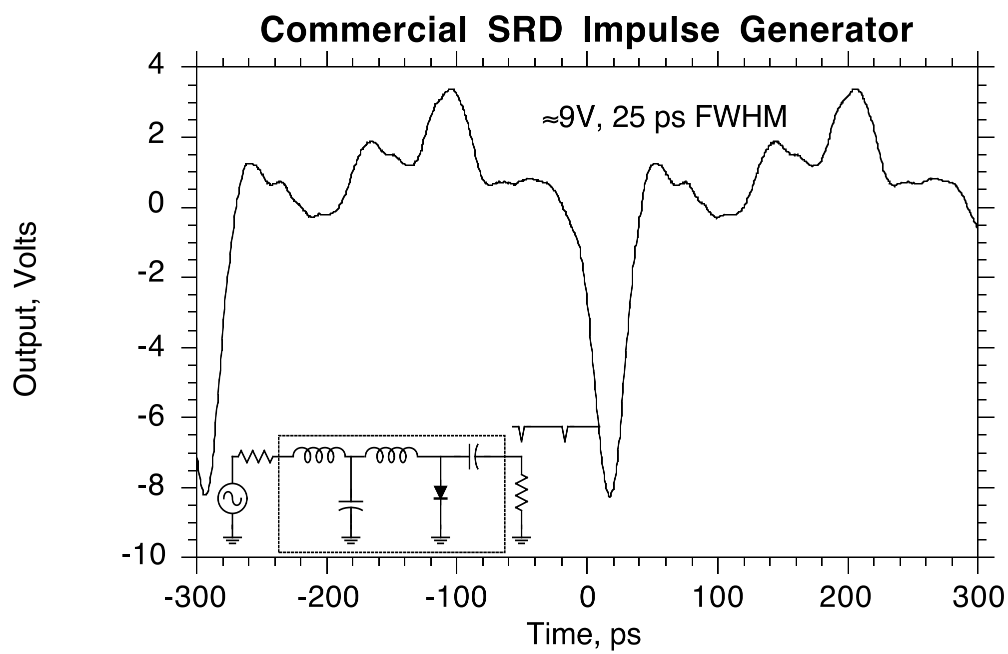

# Schottky Diodes

**Forward bias: nonlinear conductance**

**Reverse Bias: Nonlinear Charge Storage Element**

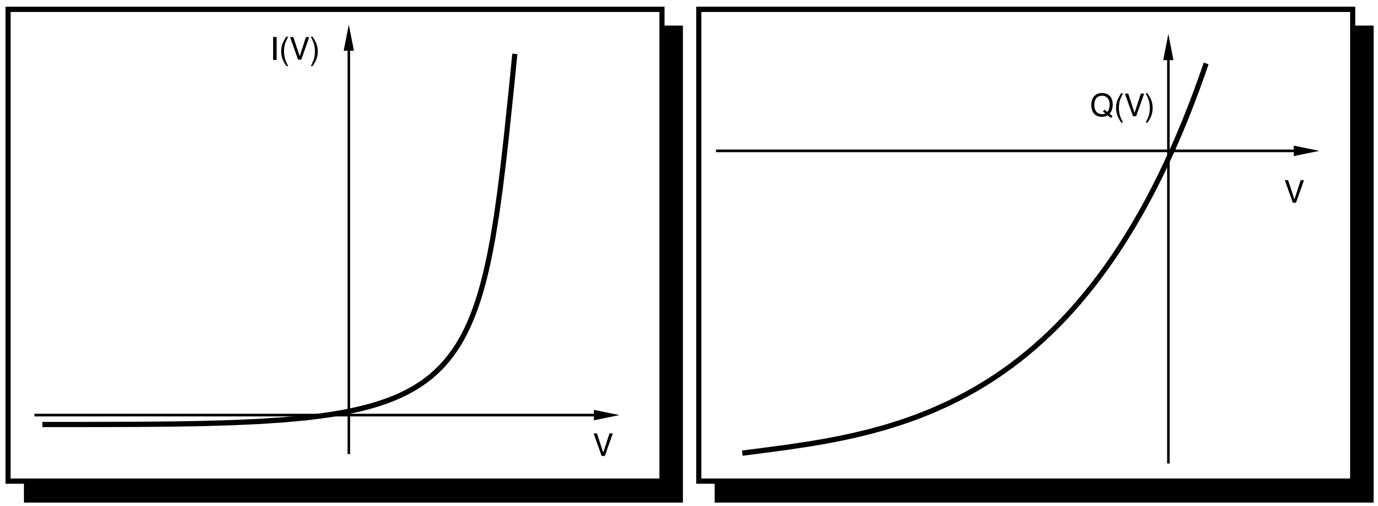


$$I(V) = I_s\left(e^{qV/kT} - 1\right) \qquad Q(V) = C_0 V + C_1 V^2 + \ldots$$

so if $v(t) = v_1 e^{j\omega_1 t} + v_1 e^{j\omega_2 t}$ , then, $I(t) = \sum_{l,m} I_{l,m} e^{j(l\omega_1 + m\omega_2)t}$

•Sum and difference-frequency generation ("mixing"), frequency multiplication.

•Schottky diodes are fastest semiconductor devices, perform as mixers to ≈10-20 THz

# Schottky Diode Millimeter-Wave Circuits

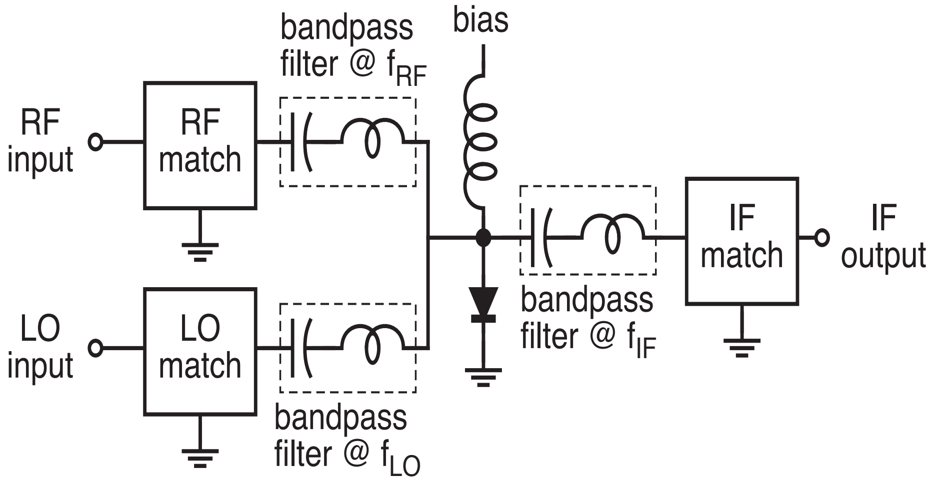


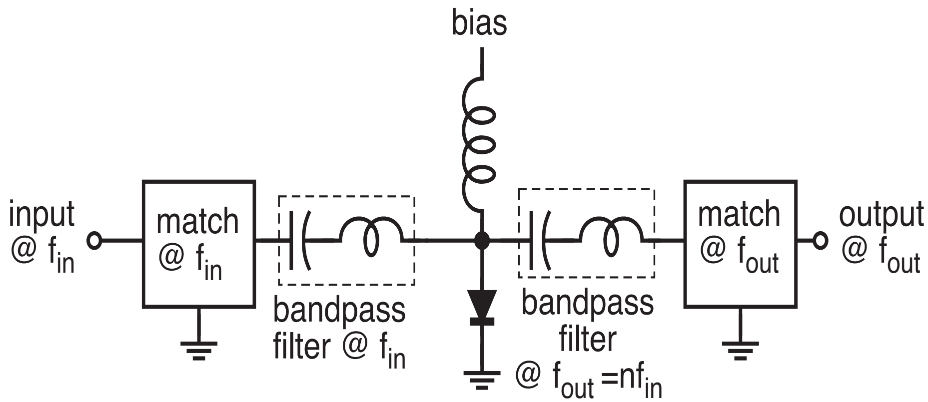


"Canononical" mixer and frequency multiplier are shown.

Millimeter-wave implementations in waveguide or on-wafer, submillimeter-wave versions in quasi-optical form.

Mixing and harmonic generation at low THz frequencies.

Circuits shown are narrowband.

# Schottky Diode Structure and Parasitics

$$f_{diode} = \frac{1}{2\pi C_{diode}\left(R_{N-} + R_{N+} + R_{contact}\right)}$$

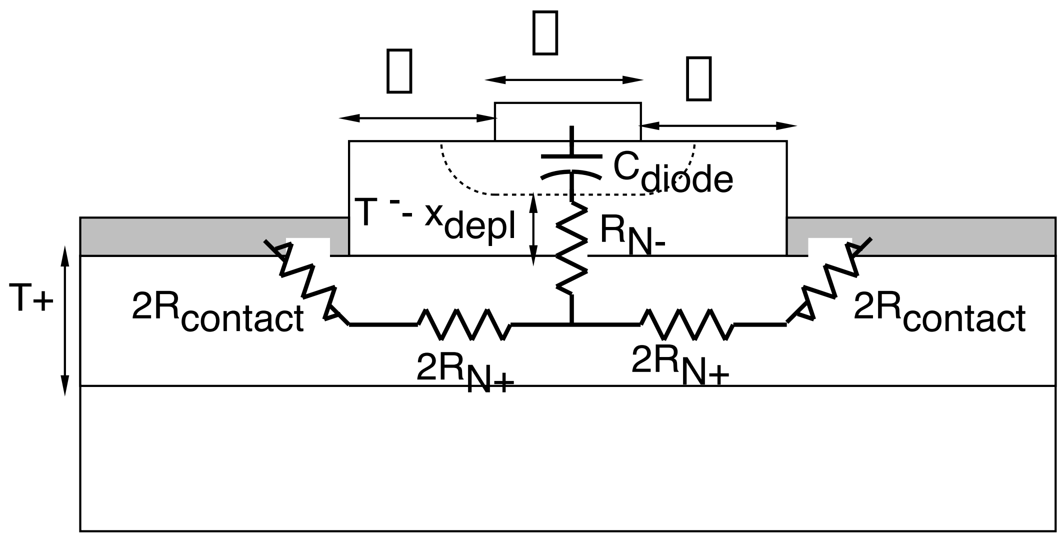

# Exponential Hyperabrupt Varactor Diodes

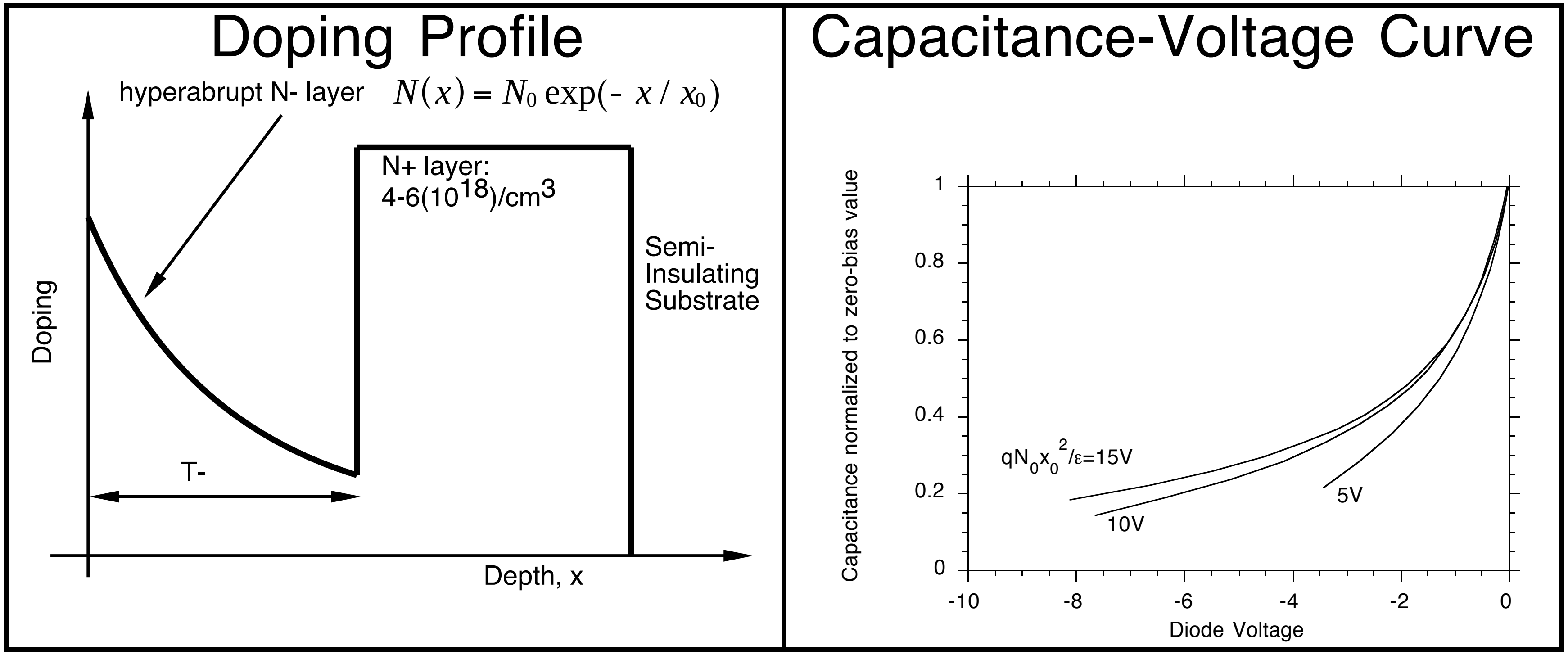


$$V_{reverse} + \phi = \int_0^{x_{depletion}} \left(qN_d(x)/\varepsilon\right) x\,dx \quad , \; C = \varepsilon A / x_{depletion}$$

•Hyperabrupt profiles increase capacitive change but decrease cutoff frequency and reverse breakdown voltage.

# Bandwidth of Uniform Varactors vs Geometry

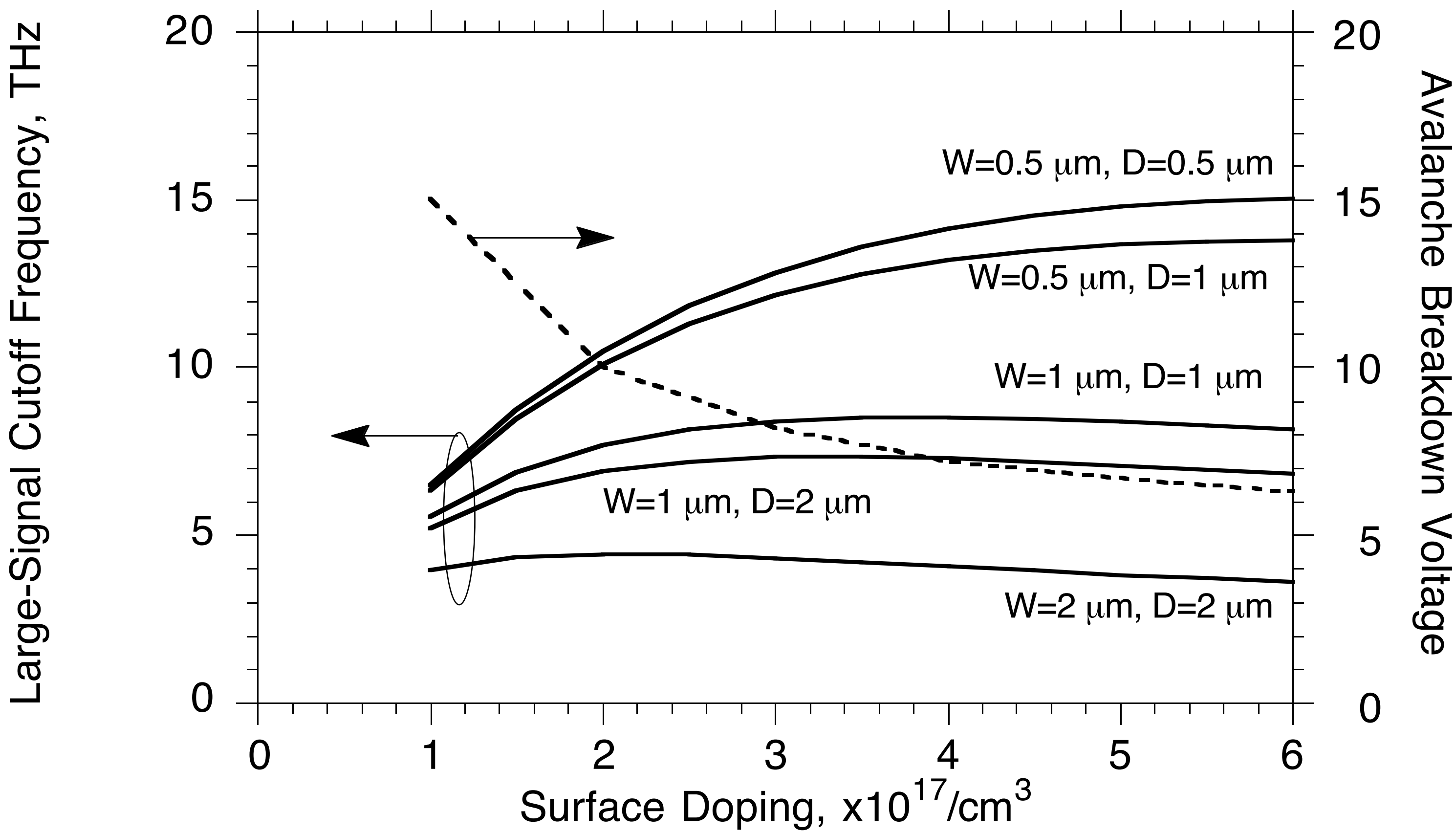

# Bandwidth of Hyperabrupt Varactors vs Geometry

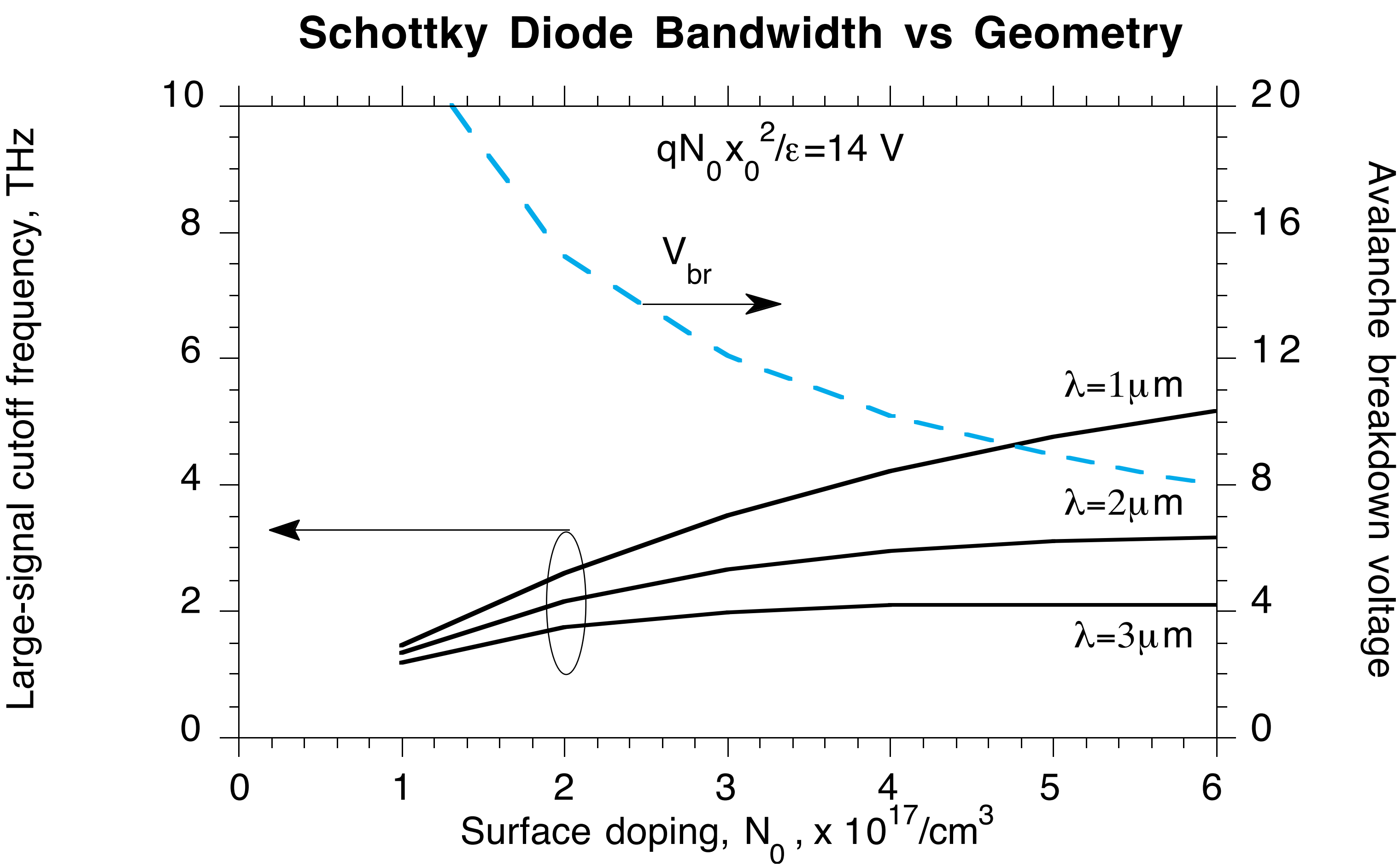

# THz Mixing and Detection with Schottky Diodes

Fetterman et al.: Submillimeter detection and mixing

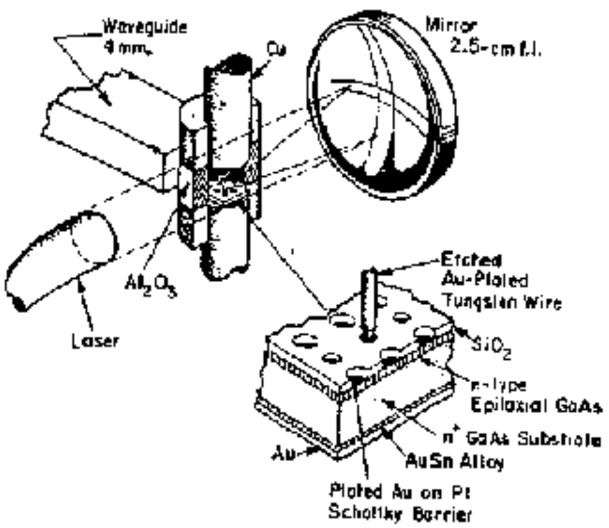


FIG. 1. Quasioptical configuration for harmonic mixing of submillimeter lasers with a V-band klystron. The dashed line indicates the laser beam coupled into the Schottky diode.

Whisker contact as antenna coupling to Schottky diode

VOLUME 17, NUMBER 1 APPLIED PH

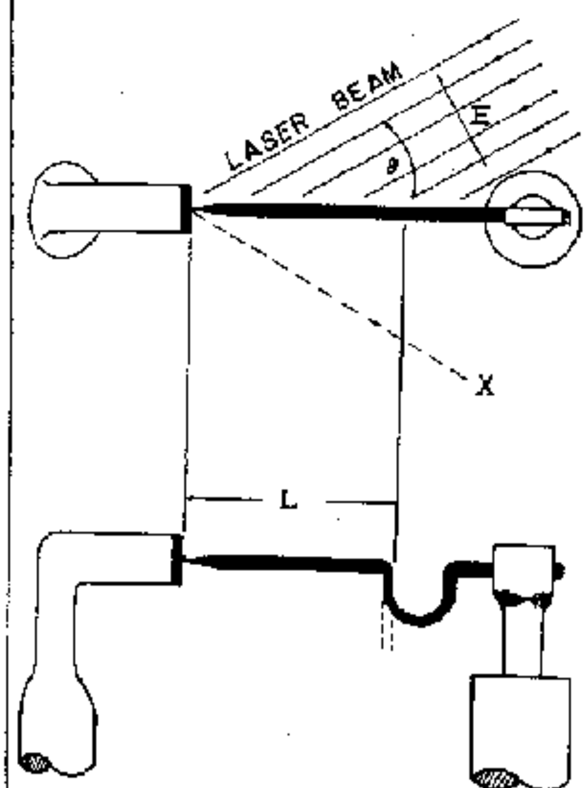


FIG. 1. Whisker diode geometry (not to scale). Top view is in plane of polarization of the laser beam. Dashed lines in lower view are for alternate whisker construction (see text). X marks possible location of reflector.

Mixing of 33rd harmonic of 74 GHz Klystron (2.44 THz) with 119 μm laser radiation

Fetterman et. al., Applied Physics Letters, Vol 24., No 2, 15 January 1974

# Antenna-Coupled Mott Mixer Diodes

**Objectives**

- Low-noise focal-plane array receiver/downconverters for 184/203/2500 GHz radiometers
- Advanced mixer diode technology integrable with diode LO frequency multipliers

**Approach**

- Antenna-coupled diode SMMIC
- Low capacitance: 0.05 $\mu m^2$ contact
- Low transit time: 150å depletion layer
- Low resistance: N++ / I / metal diode
- 12 THz circuit bandwidth
- $\approx$20 THz diode bandwidth

# Resonant Tunneling Diodes

(Sollner, MIT Lincoln Labs)
(Esaki)

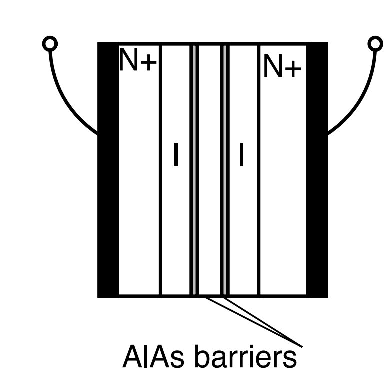


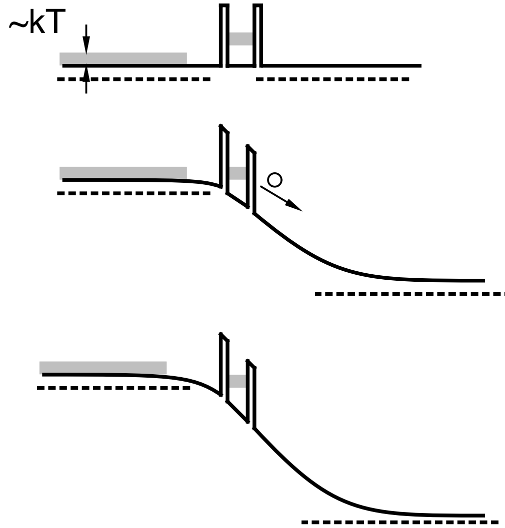


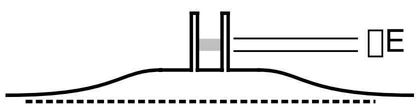


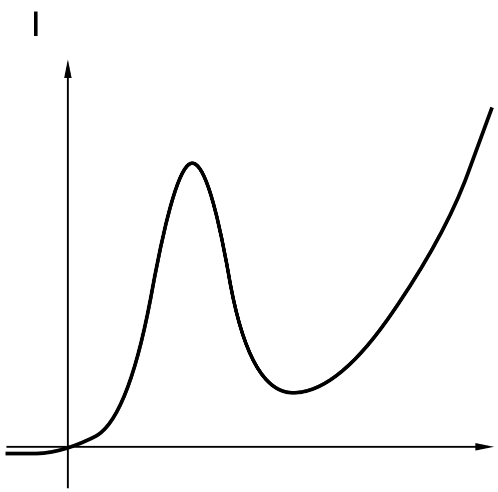


Strong current flow when electron reservoir and confined state are aligned in energy.

Narrower AlAs barriers decrease the electron trapping time, increasing ΔE, and increasing the peak current density. Increasing the emitter doping increases the electron supply and therefore also increases the current density.

# Parameters Determining RTD Fmax

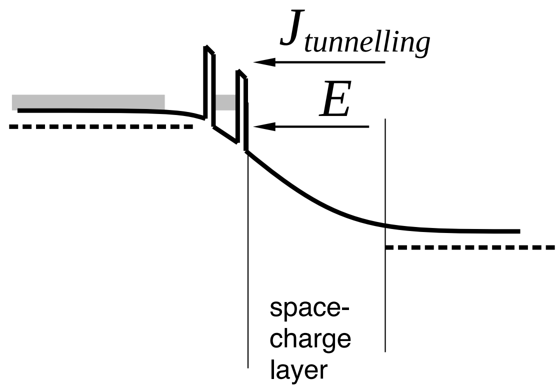


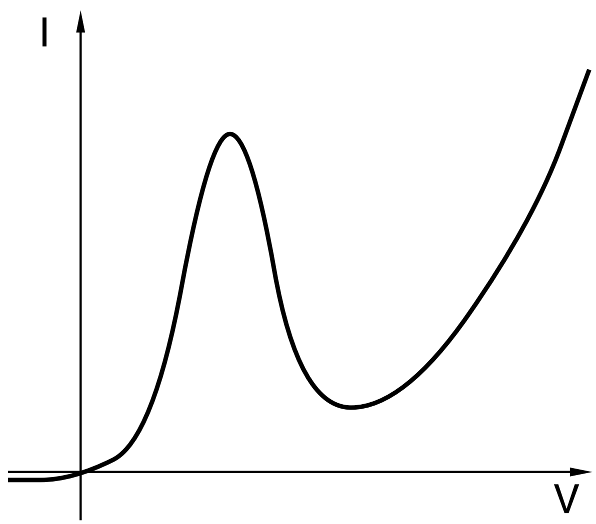


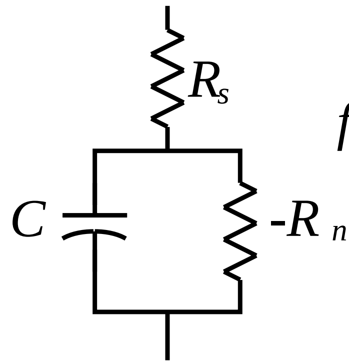


$$f_{\max} = \frac{1}{2\pi R_n C}\sqrt{\frac{R_n - R_s}{R_s}}$$

$$\frac{1}{R_n C} = \frac{1}{\varepsilon}\frac{dJ}{dE}$$

-Maximized by designing for high current density (reliability limits)

-$R_s$ then limits $f_{max}$:
InAs/AlSb RTD's have very low ($10^{-7}$ $\Omega$-cm$^2$) contact resistance, & have attained $f_{max}$=1.3 THz.

# RTDs as negative-resistance oscillators

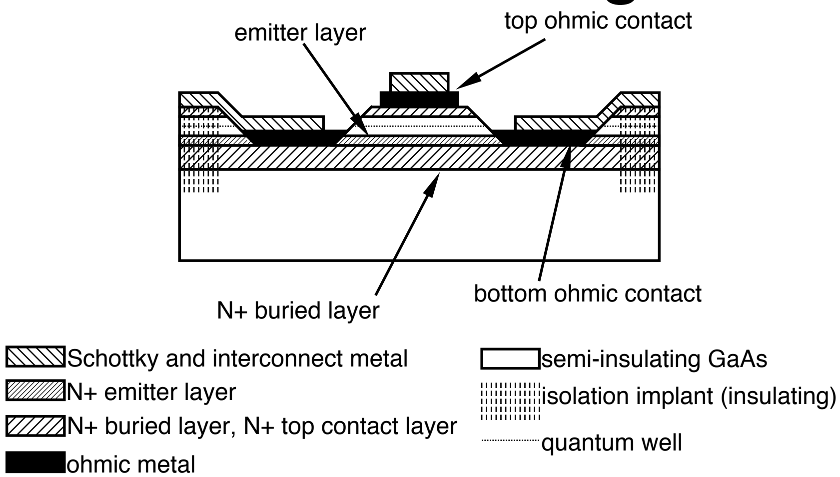


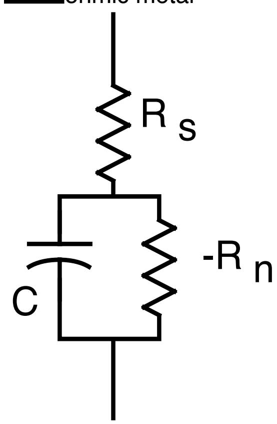


Coupled to the conjugate impedance -jX(ω), the RTD will oscillate if R(ω) <0

$$Z(\omega) = R_s + \frac{-R_n}{1 - j\omega R_n C}$$

$$= R(\omega) + jX(\omega)$$

$$R(\omega) = R_s - \frac{R_n}{1 + \omega^2 R_n^2 C^2}$$

$$R(\omega_{\max}) = 0$$

$$\omega_{\max} = \frac{1}{R_n C}\sqrt{\frac{R_n - R_s}{R_s}}$$

RTD oscillators have been demonstrated to 712 GHz

# Well Transmission Probability vs Energy

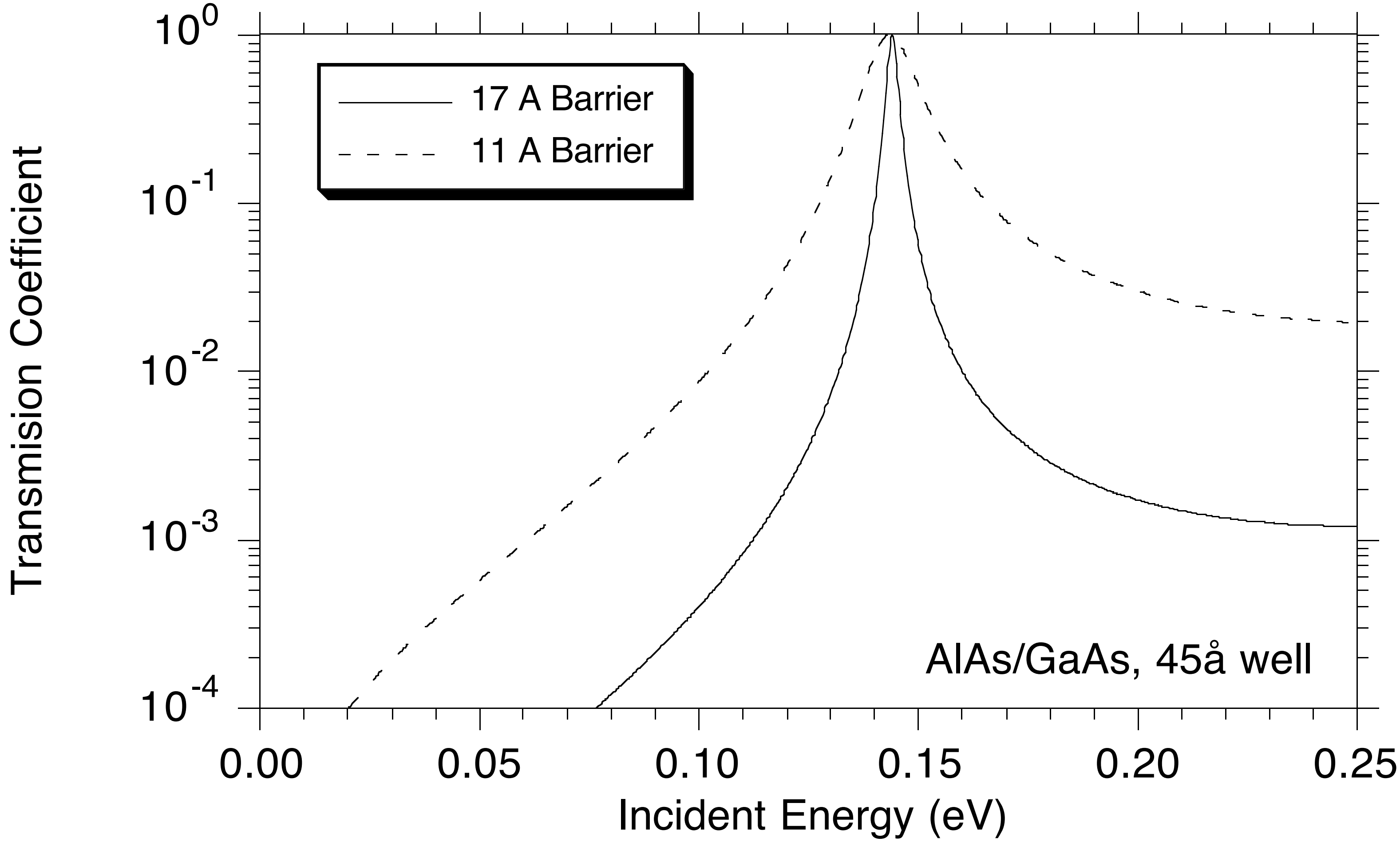

# Quantum Well Inductance

Transit time through well:

$$\tau = \frac{2\hbar}{\Delta E}$$

$\Delta E$ is the F.W.H.M. of the transmission probability

Equivalent inductance:

$$L_W = \frac{\tau}{G_N}$$

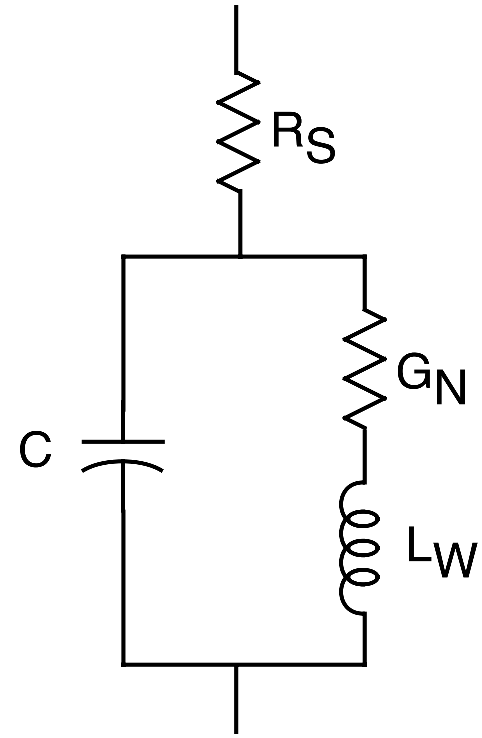


- In the negative resistance region $G_n$ and $L_W$ are negative.
- $f_{max}$ is decreased
- Space charge transit time $\tau_t = d_{\text{space-charge}} / v_{\text{electron}}$ also effects $f_{\max}$, but with $d_{\text{space-charge}} \cong 500$ å, $v_{\text{electron}} >> 10^7$ cm/sec and $\tau_t \approx 100$ fs

# Schottky-Collector Resonant Tunnel-Diodes

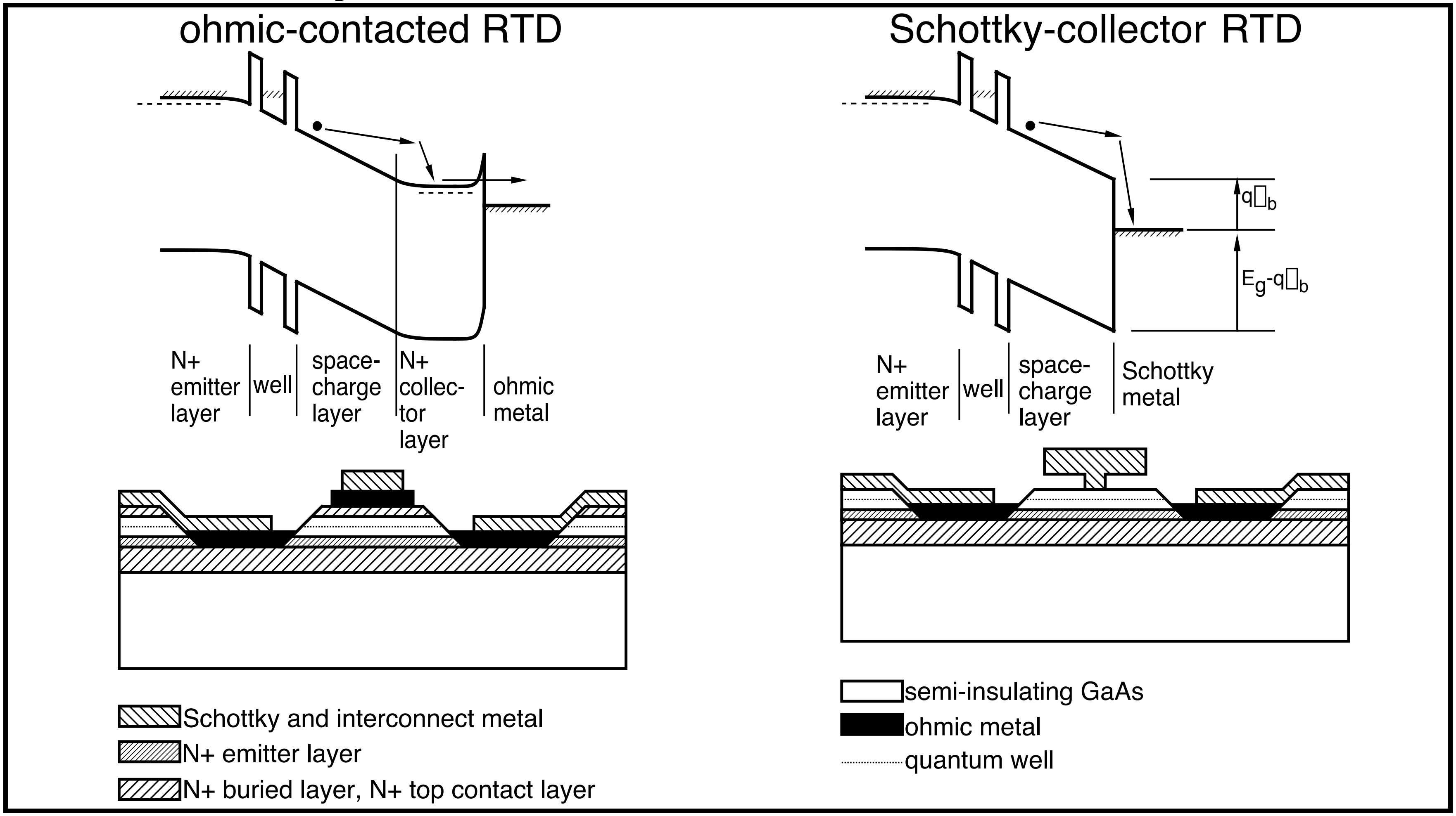


Top ohmic contact is eliminated. Decreased Rs, increased fmax

# Bandwidth of Submicron Schottky-Collector RTDs

## RTDs vs. SRTDs in AlAs/GaAs and $In_{0.53}Ga_{0.47}As$/AlAs

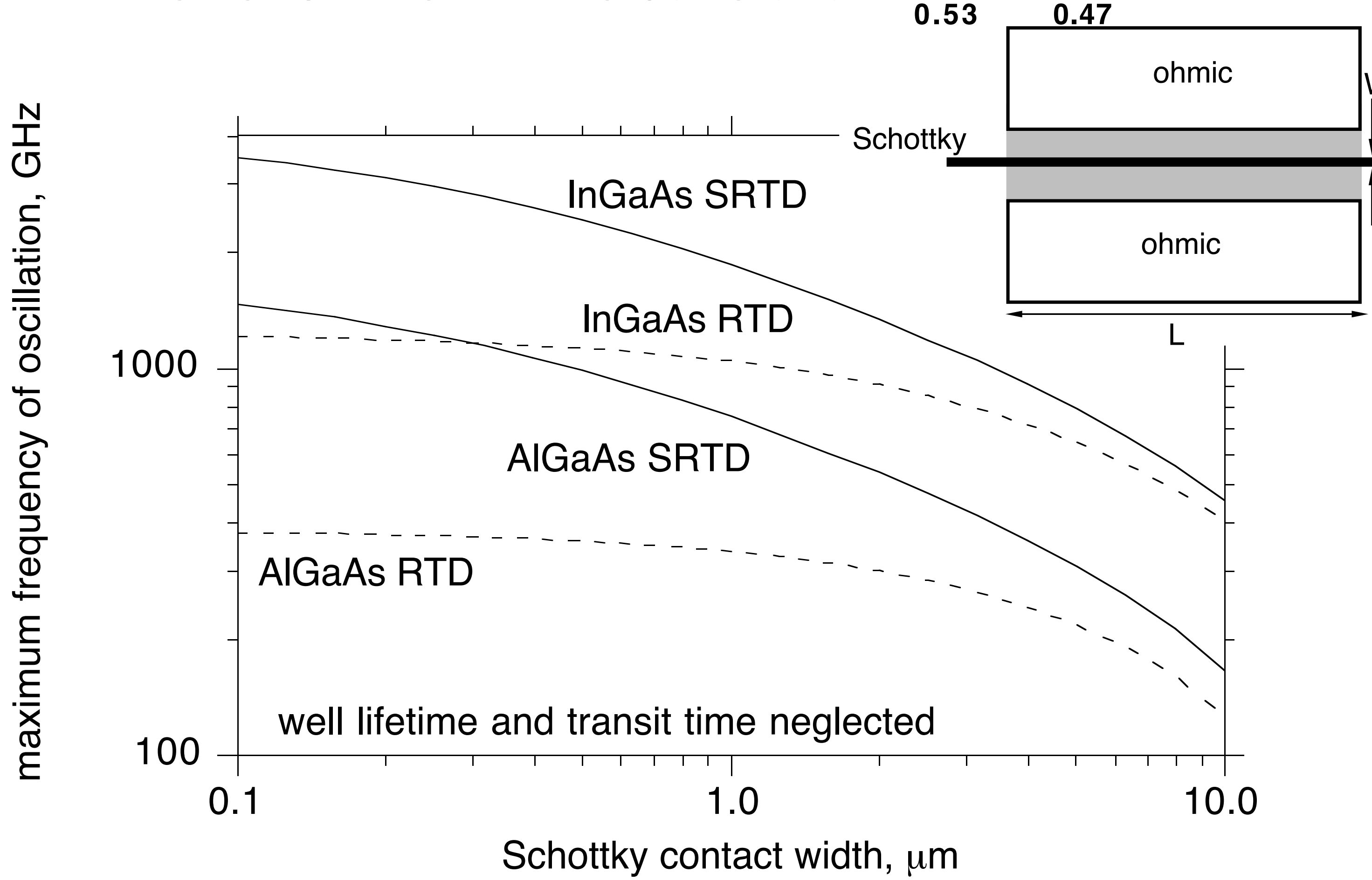


- Scaling to submicron dimensions increases RTD periphery/area ratio
- Periphery-dependent parasitic resistance terms driven towards zero (bottom ohmic contact resistance, buried N+ layer)

## Schottky-Collector RTDs for 0.3-3 THz Oscillators

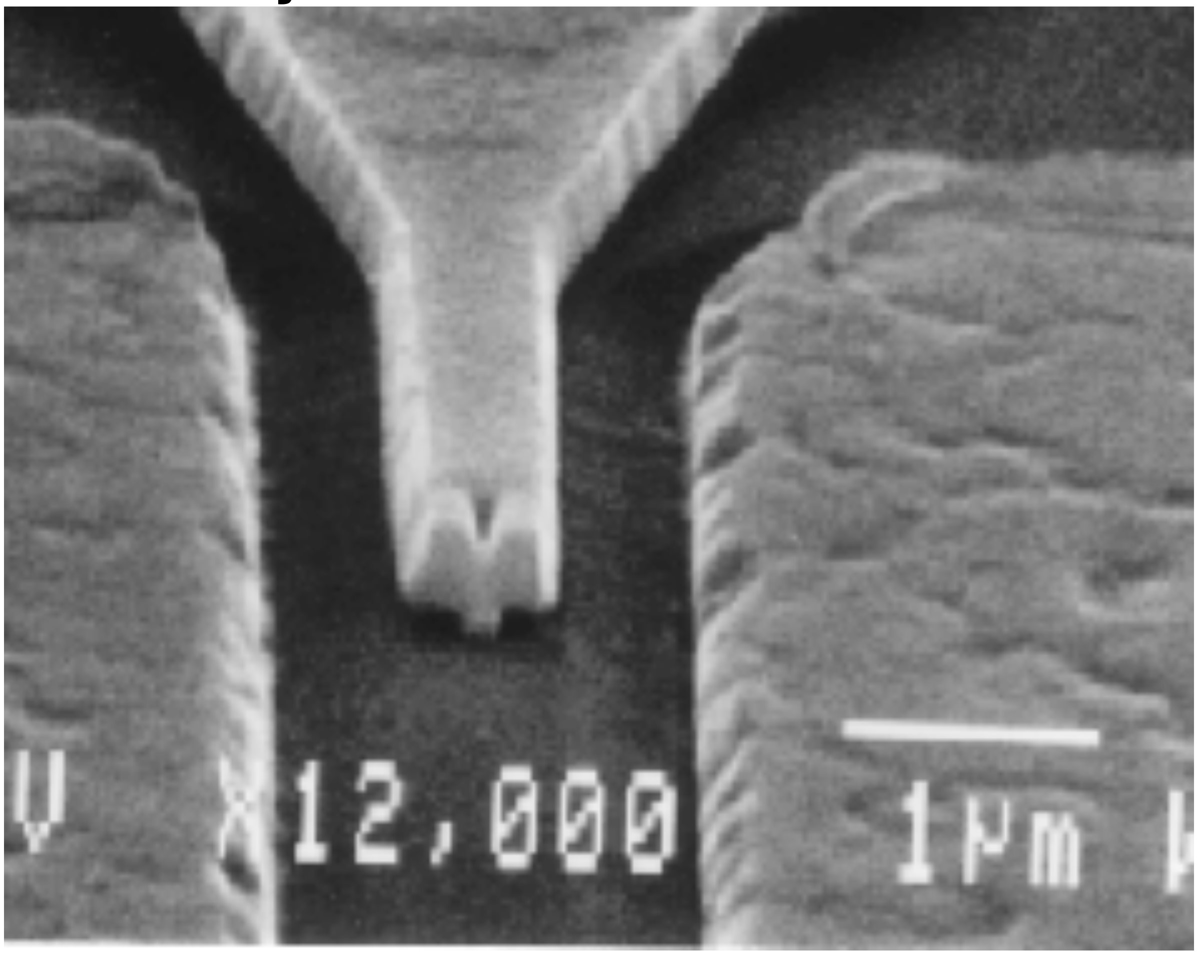


0.12-μm AlAs/InGaAs/InP device

•Schottky (metal) electron collector, 0.1 -μm geometry.

•Greatly reduced series resistance, large increase in $f_{max}$

AlAs/GaAs SRTDs: 900 GHz $f_{max}$ estimated
InGaAs/AlAs SRTDs: 2.2 THz $f_{max}$ estimated
Application: 0.3-1.5 THz quasi-optical power oscillator arrays

# RTD Switching Speed Considerations

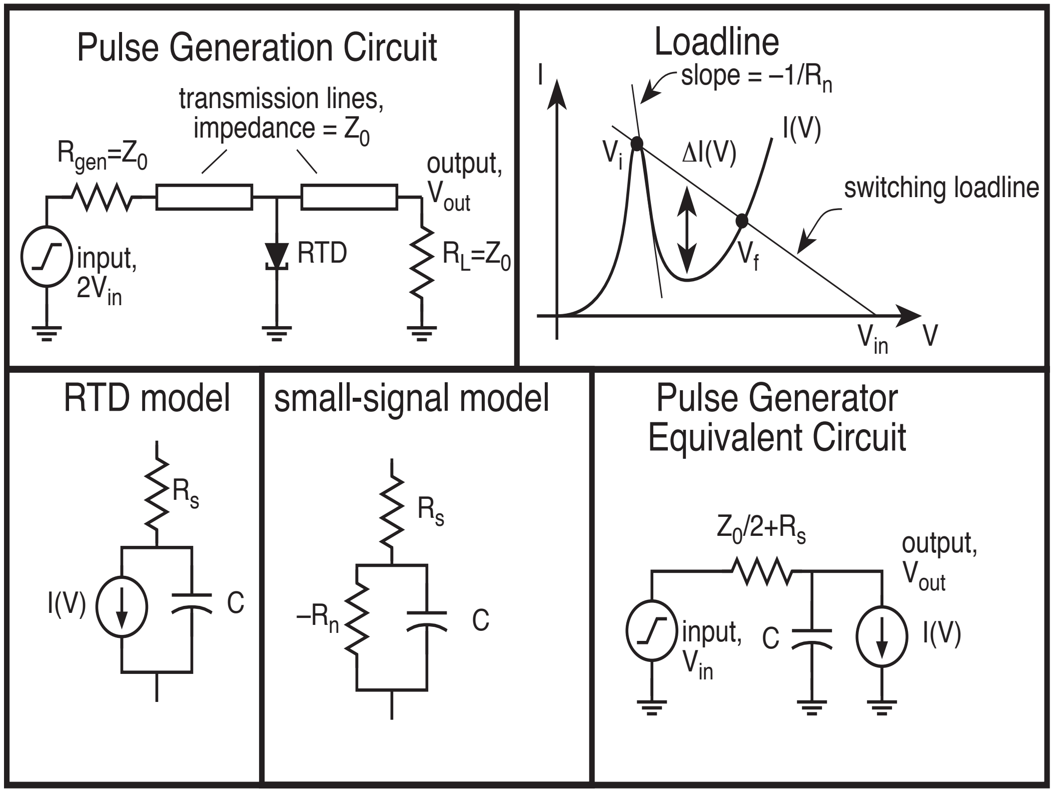


$$T_{10\%-90\%} = \int_{0.9V_{initial}+0.1V_{final}}^{0.1V_{initial}+0.9V_{final}} CdV / \Delta I(V)$$

$$\approx 3-5R_nC$$

Governing law is

$$I = C\frac{dV}{dt}$$

Even if Rs=0 (inifinite fmax), risetime is not zero

For fast risetimes, need high RTD $I_{peak}/C$ ratio. 8 ps risetimes in AlGaAs ($\approx 10^5$ A/cm$^2$current density), 1.8 ps in InAs/AlSb ($3.5 \cdot 10^5$ A/cm$^2$)

# 3-Terminal Devices (Transistors)

# Heterojunction Field-Effect Transistors

Current state of art:

InAlAs/InGaAs / InP HEMTs, 0.1 $\mu$m gate (R&D device)
250-500 GHz $f_{max}$, 2-3 Volt breakdown
1 dB noise figure amplifiers at 65 GHz

AlGaAs/InGaAs/GaAs HEMTs, 0.25 $\mu$m gate (mass production device)
100-150 GHz ft, 100-150 GHz $f_{max}$, 5-8 Volt breakdown
50 GHz ft, 180 GHz fmax, 10-15 Volt breakdown

Circuits:

5-10 dB gain 150 GHz monolithic narrowband (low-noise) amplifiers
5 dB gain, 1-155 GHz broadband amplifiers (Agarwal et. al. 1998 MTT)

Monolithic mm-wave ICs for radar (mixers, phase shifters, preamps, power ampifiers,...)

# Device Circuit Models vs Device Physics: FET as example

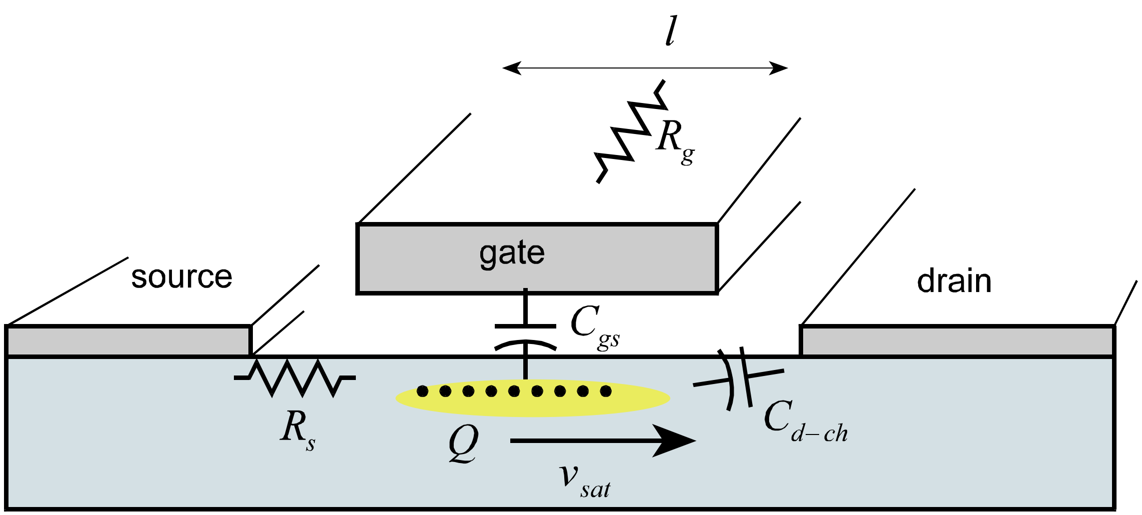


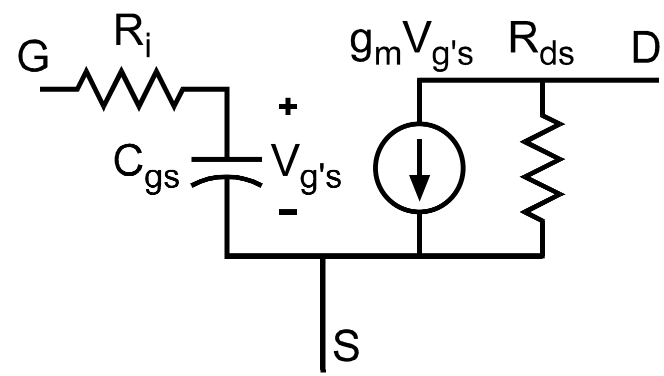


$$I_d = \frac{Q}{l} v_{sat}, \text{ where } \quad \frac{dQ}{dV_{gs}} = C_{gs} \text{ and } \frac{dQ}{dV_{gd}} = C_{d-ch}$$

so :

$$g_m = \frac{dI_d}{dV_{gs}} = C_{gs}\frac{v_{sat}}{l} = C_{gs}\tau_{gate} \text{ and } G_{ds} = \frac{dI_d}{dV_{ds}} \cong C_{d-ch}\frac{v_{sat}}{l} = C_{d-ch}\tau_{gate}$$

# Heterojunction Field-Effect Transistors

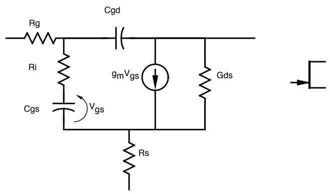


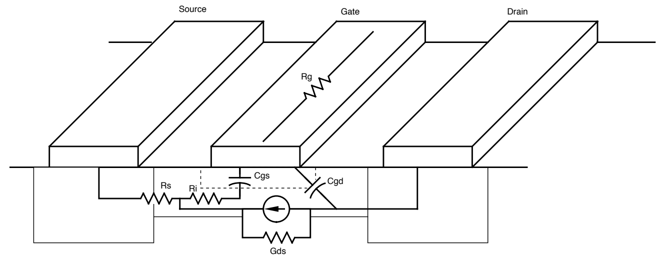


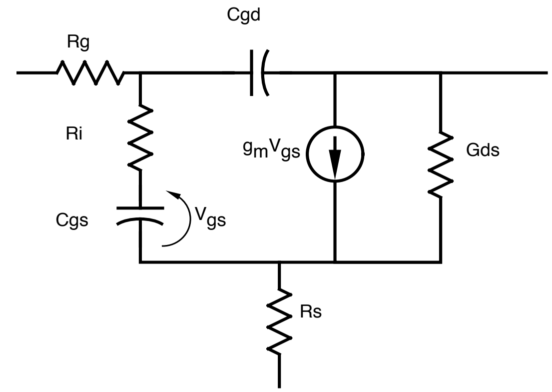


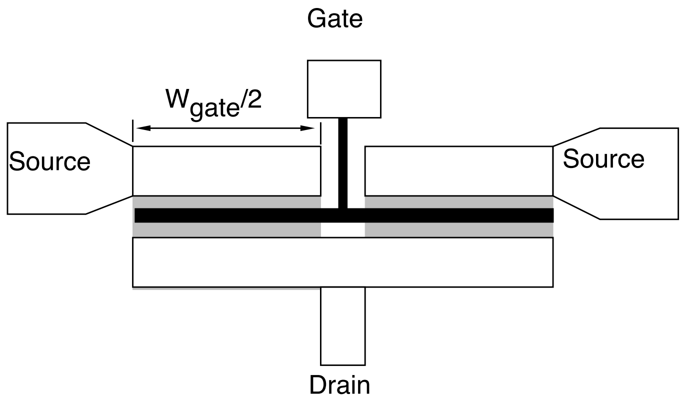


$$\omega_\tau = g_m / C_{gs} = v_{sat} / l_g$$

current gain cutoff frequency

$$\omega_{\max} \cong \frac{\omega_\tau}{2\sqrt{\left(R_g + R_i + R_s\right)/R_{ds}}}$$

POWER gain cutoff frequency

# Scaling of the Schottky-Barrier FET (HEMT)

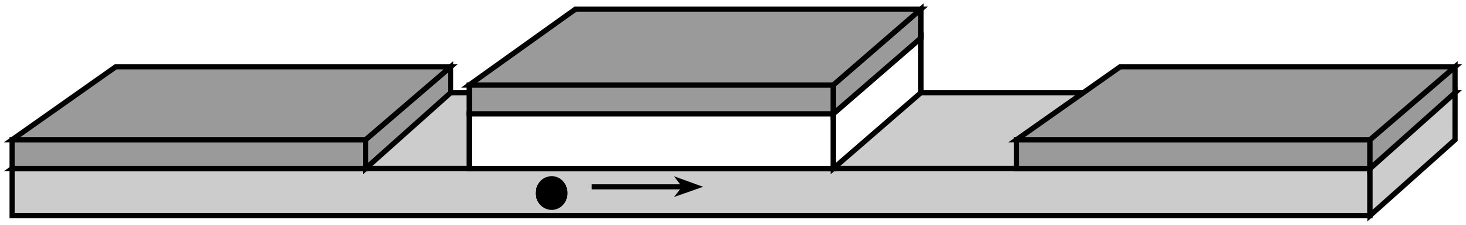

- Reducing gate length by lithographic scaling  decreases the carrier transit time (Cgs/gm ratio) and increases device bandwidth
- Use of Schottky vertical contact essential if RC time constants are to scale (Schottky MESFET vs PN JFET)
- Gate length must be 5-10 times gate-channel separation to screen channel charge from drain potential
- Mimimum gate channel separation (tunneling limit) sets limit on gate length scaling.

# Heterojunction Bipolar Junction Transistors

GaAs/AlGaAs devices: $f_{max} \approx 200$ GHz
AlInAs/GaInAs devices: $f_{max} \approx$ 70-200 GHz (but ...*)
InP/GaInAs devices: $f_{max} \approx 220$ GHz for $ft \approx 220$ GHz
Si/SiGe devices: $f_{max} \approx 70$ GHz (production), 180 GHz (mesa device)

HBTs have generally poorer $f_{max}$ and noise figure than HEMTs, but are more predictably-behaved devices more suitable for higher-complexity analog and mixed analog-digital applications.

Representative circuit result: 37 GHz static frequency dividers (e.g. master-slave flip-flops), DC-40 GHz amplifiers, chip-sets for 40 Gbit/s fiber transmission, A-D converters at a few Gigasamples/sec.

## HBT Device Structure

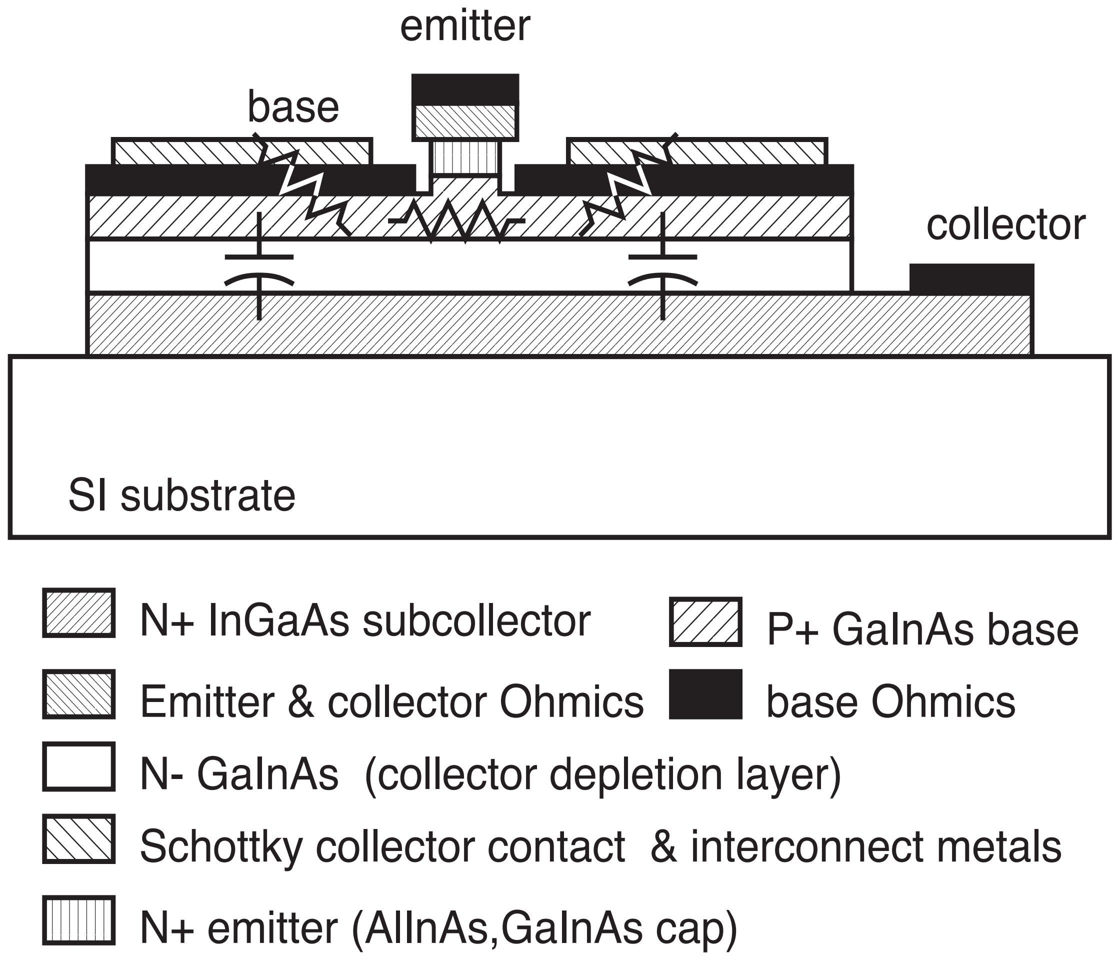


note the indicated base resistance and base-collector capacitance

# HBT DC I-V characteristics

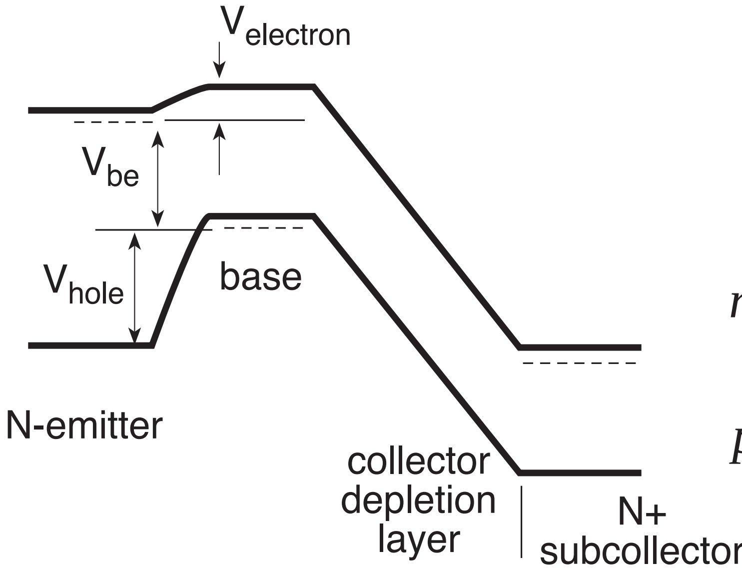


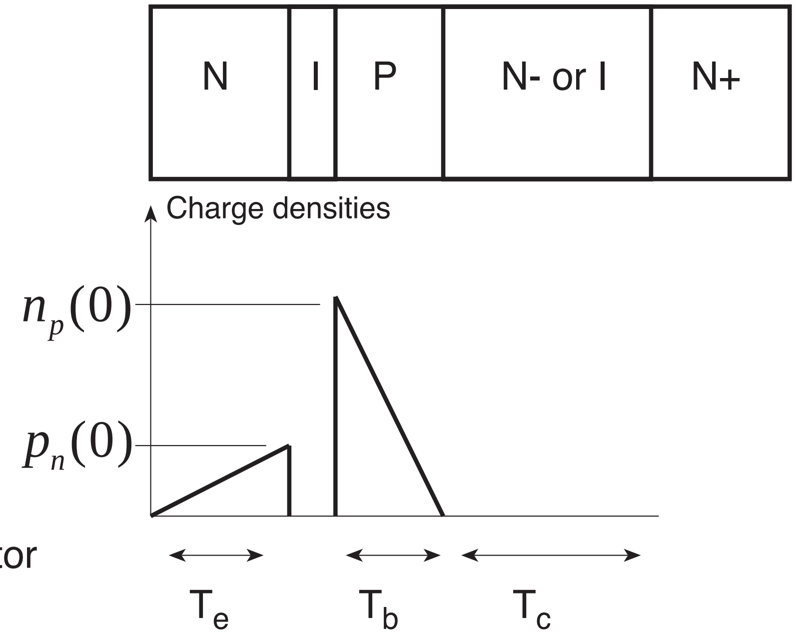


$$n_p(0) = qN_c e^{-qV_{electron}/kT} \propto e^{+qV_{be}/kT}$$

electron concentration at emitter edge of base

$$p_n(0) = qN_v e^{-qV_{hole}/kT} \propto e^{+qV_{be}/kT}$$

hole concentration at base edge of emitter
heterojunction makes this small

$$I_{electron} = \frac{D_n q A_e N_c}{T_b} e^{-qV_{electron}/kT} \propto e^{+qV_{be}/kT}$$

electron current from emitter to collector

$$g_m \equiv \frac{dI_c}{dV_{be}} = \frac{qI_c}{kT}$$

transconductance

# HBT Stored Charge & Diffusion Capacitance

## Base Transit Time

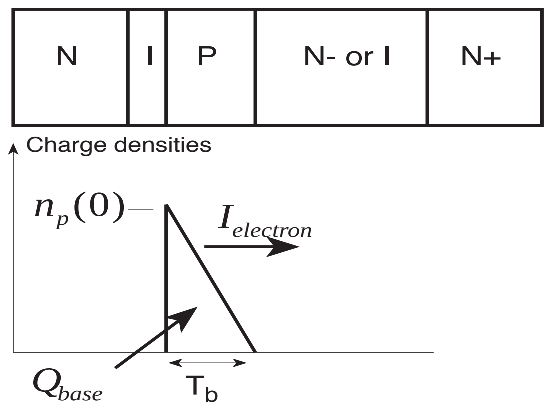


electron concentration at emitter edge of base

$$n_p(0) = qN_c e^{-qV_{electron}/kT} \propto e^{+qV_{be}/kT}$$

electron current from emitter to collector

$$I_{electron} = qn_p(0)D_n / T_b$$

stored base charge

$$Q_{base} = qA_e n_p(0)T_b / 2$$

$$= I_{electron}T_b^2 / 2D_n = \tau_b I_{electron}$$

## Collector Transit Time

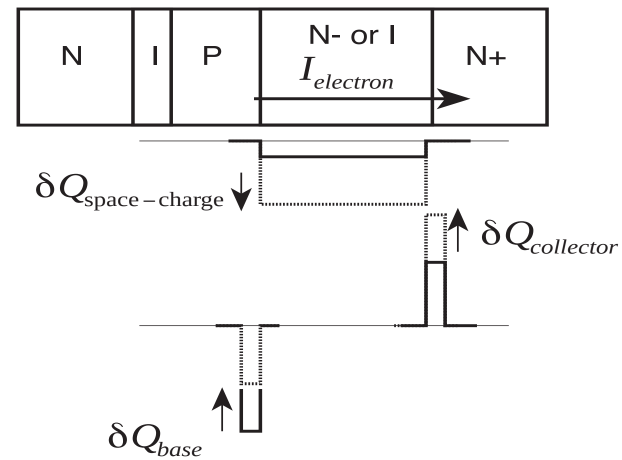


depletion-layer space-charge

$$\delta Q_{\text{space-charge}} = \frac{T_c}{v_{sat}} \delta I_{collector}$$

change in base stored charge

$$\delta Q_{base} = \delta Q_{collector} = \delta Q_{\text{space-charge}} / 2$$

$$= \delta I_{collector}\left(T_c / 2v_{sat}\right) = \tau_c \delta I_{collector}$$

## "Diffusion Capacitance"

$$C_{diffusion} \equiv \frac{dQ_{base}}{dV_{be}} = \frac{dQ_{base}}{dI_c}\frac{dI_c}{dV_{be}} = \left(\tau_b + \tau_c\right)g_m$$

$$C_{\text{be, diffusion}} = g_m\left(\tau_b + \tau_c\right)$$ fictitious capacitance between base & emitter modelling charge storage

# Bandwidth of Bipolar Transistors

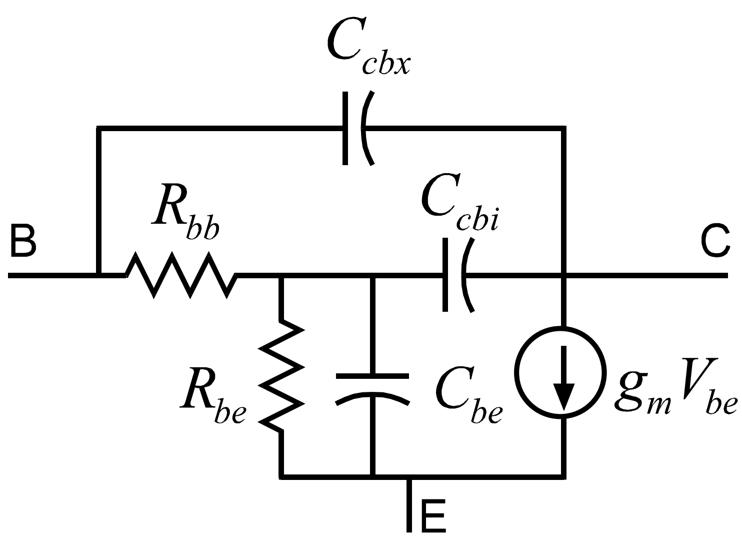


$$f_\tau = \frac{(1/2\pi)}{\tau_{base} + \tau_{collector} + \left(C_{je} kT / qI_e\right)}$$

$$f_{\max} = \sqrt{\frac{f_\tau}{8\pi R_{bb} C_{cbi}}}$$

$f_\tau$ , $f_{\max}$ , and $C_{cbx}$ are all important for high - speed circuits

$R_{bb}C_{cbi}$ and $R_{bb}C_{cbx}$ must be reduced

# HBT Design Tradeoffs

Thin base & collector depletion layers result in small transit times, high ft.

Thin base & collector result in high base resistance, high c-b capacitance ...low fmax!

There are thus optimum thicknesses for these layers.

Very high base doping used to minimize base sheet and ohmic contact resistance.

Etch & implant techniques used to reduce extrinsic CB capacitance.

# Lithographic Scaling & Transistor Bandwidth

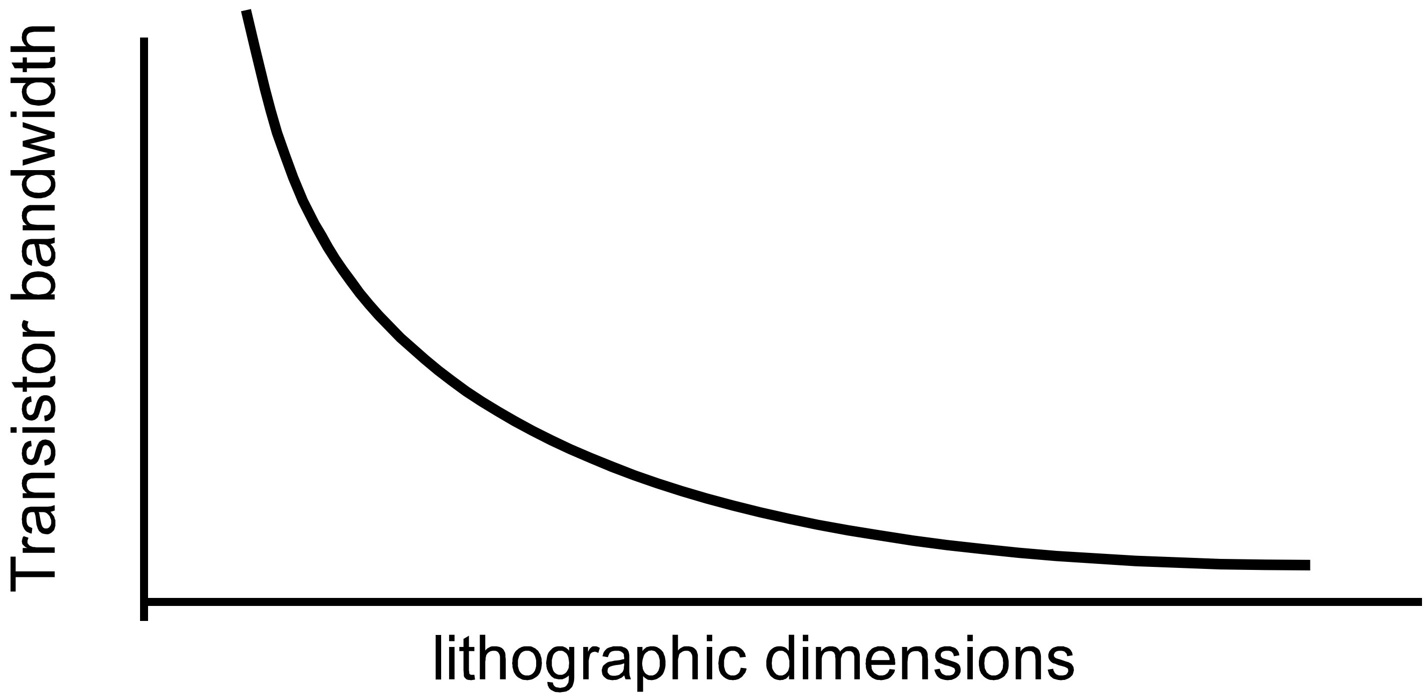


- Transistor bandwidth improves as dimensions are reduced
  - 0.1 µm HEMTs
  - 0.25 µm CMOS (VLSI)
- HBTs typically built at $\approx$1 µm lithography
  - smaller devices not generally faster
- *Goal: a scalable HBT*

# Why are HEMTs smaller & faster than HBTs ?

- **FETs have deep submicron dimensions.**

  0.1 μm HEMTs with 400 GHz bandwidths (satellites).

  5 million 1/4-μm MOSFETs on a 200 MHz, $500 CPU.

  FET lateral scaling decreases transit times.

  FET bandwidths then increase.

- **HBTs, RTDs, Schottky diodes have ≈1 $\mu$m junctions.**

  vertical scaling **decreases** electron transit times.

  vertical scaling **increases** RC charging times.

  lateral scaling **should** decrease RC charging times.

  HBT & RTD bandwidths **should** then increase.

**But, HBTs & RTDs must first be modified . . .**

# Excess Collector-Base Capacitance in Mesa HBT s

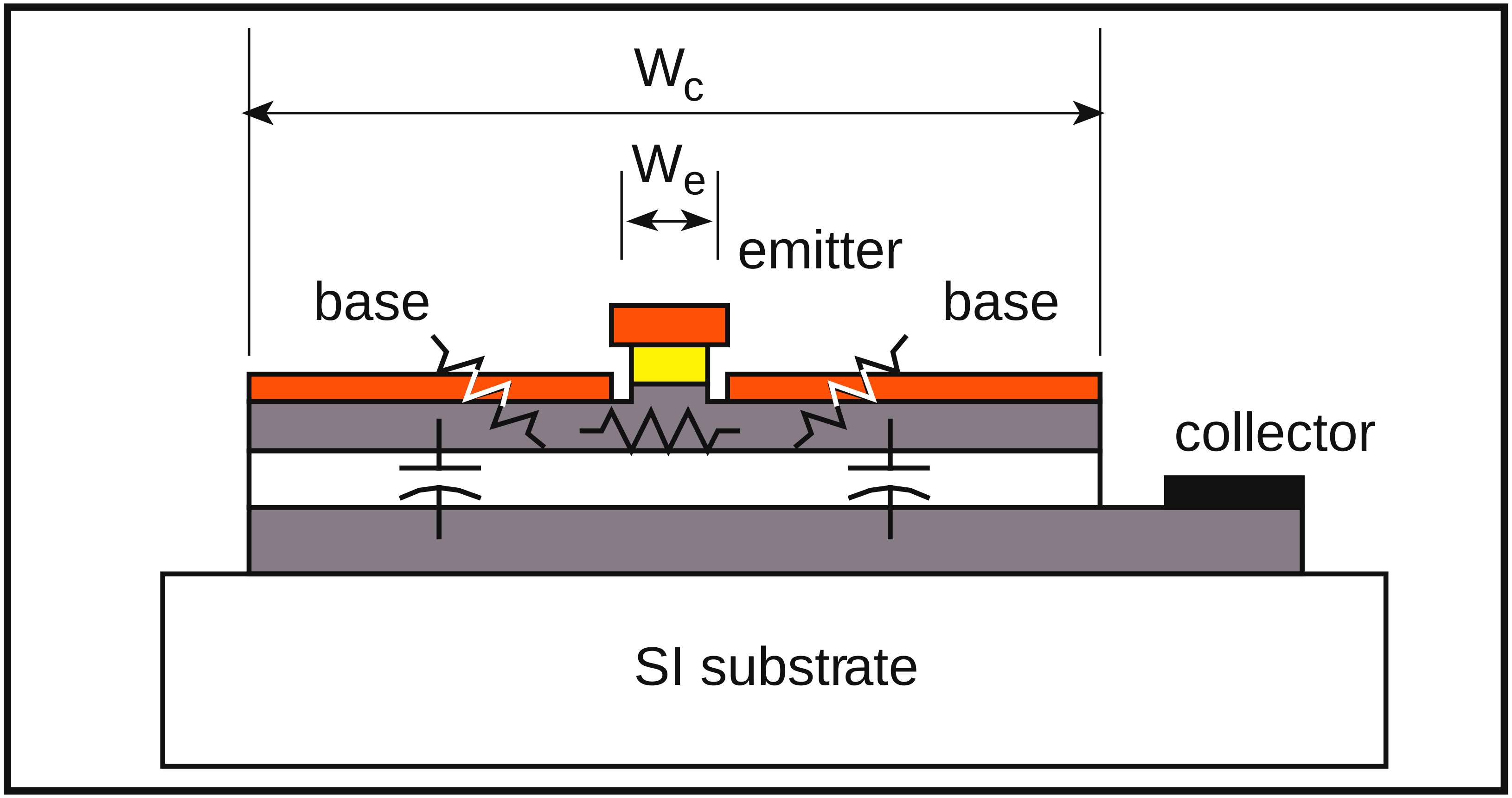


- collector-base capacitance independent of emitter width
- base resistance independent of emitter width for < 1µm
- $f_{max}$ does not improve for emitter stripe widths < 1µm

# Transferred-Substrate HBTs

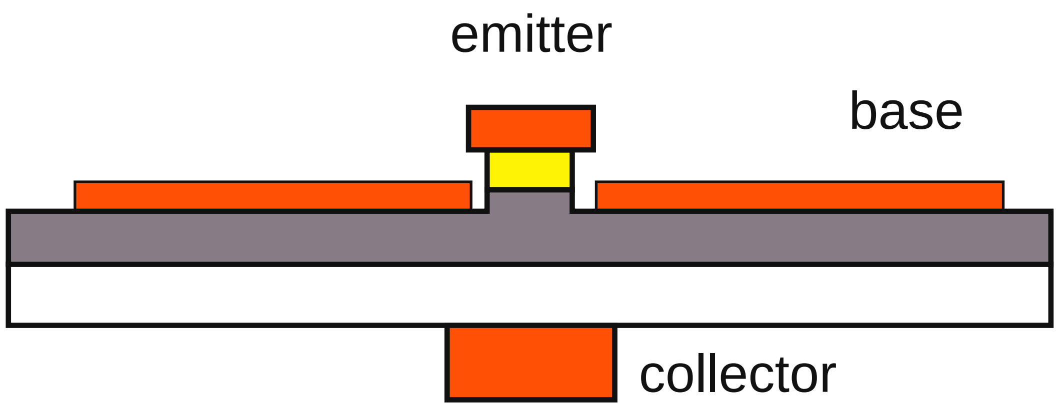


- Flip-chip process : narrow collector
- narrow collectors feasible $\rightarrow$
  large decrease in $R_b C_c$
- consequent large increase in bandwidth
- submicron collector and emitter scaling
  $\rightarrow f_{max} \approx 700$ GHz

## Transferred-Substrate HBTs: a **Scalable** HBT technology

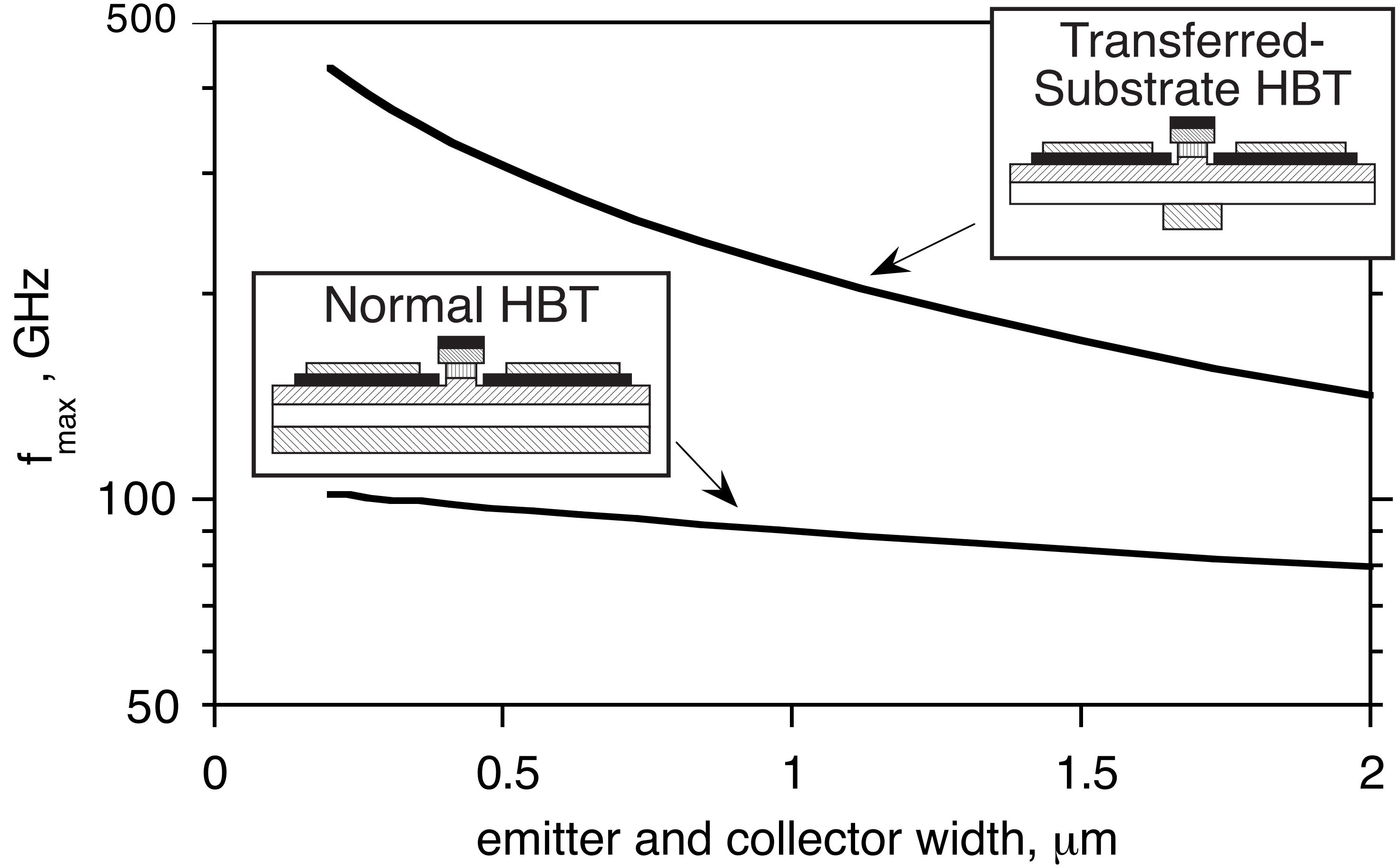


- Collector capacitance reduces with scaling: $C_{cb} \propto W_e$
- Bandwidth increases rapidly with scaling: $f_{\max} = \sqrt{1/W_e}$

# Transferred-Substrate HBT Process

## Objectives:

- 500 GHz transistor bandwidth
- Thermal management for high power density
- Low wiring & packaging parasitics at 100+ GHz

## Approach:

- BCB process: standard IC materials
- Metal substrate, thermal vias
- Microstrip wiring:
  ground vias
  backside ground plane
  $\varepsilon_r$=2: low capacitance

1) Normal emitter, base processes.
Deposit silicon nitride insulator.

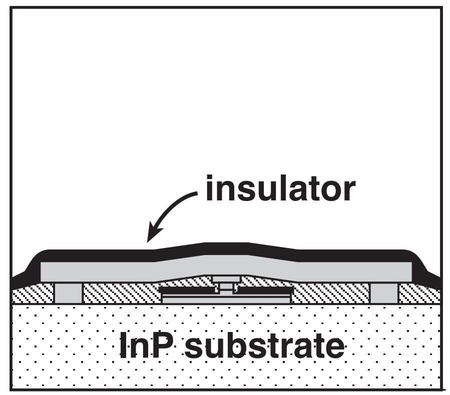


2) Coat with BCB polymer.
Etch vias.

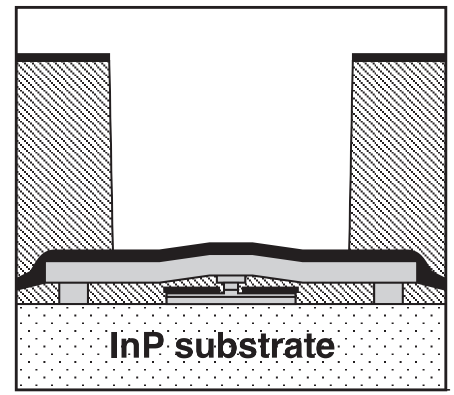


3) Electroplate with gold.
Die attach to copper substrate.

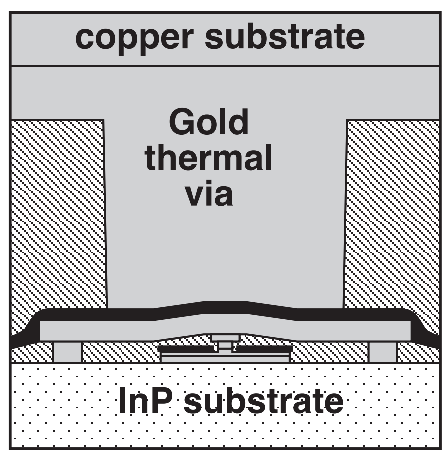


4) Invert wafer.
Remove InP substrate.
Deposit collector.

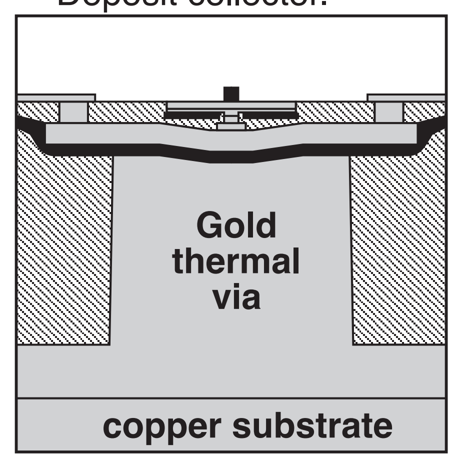

# AlInAs/GaInAs graded base HBT

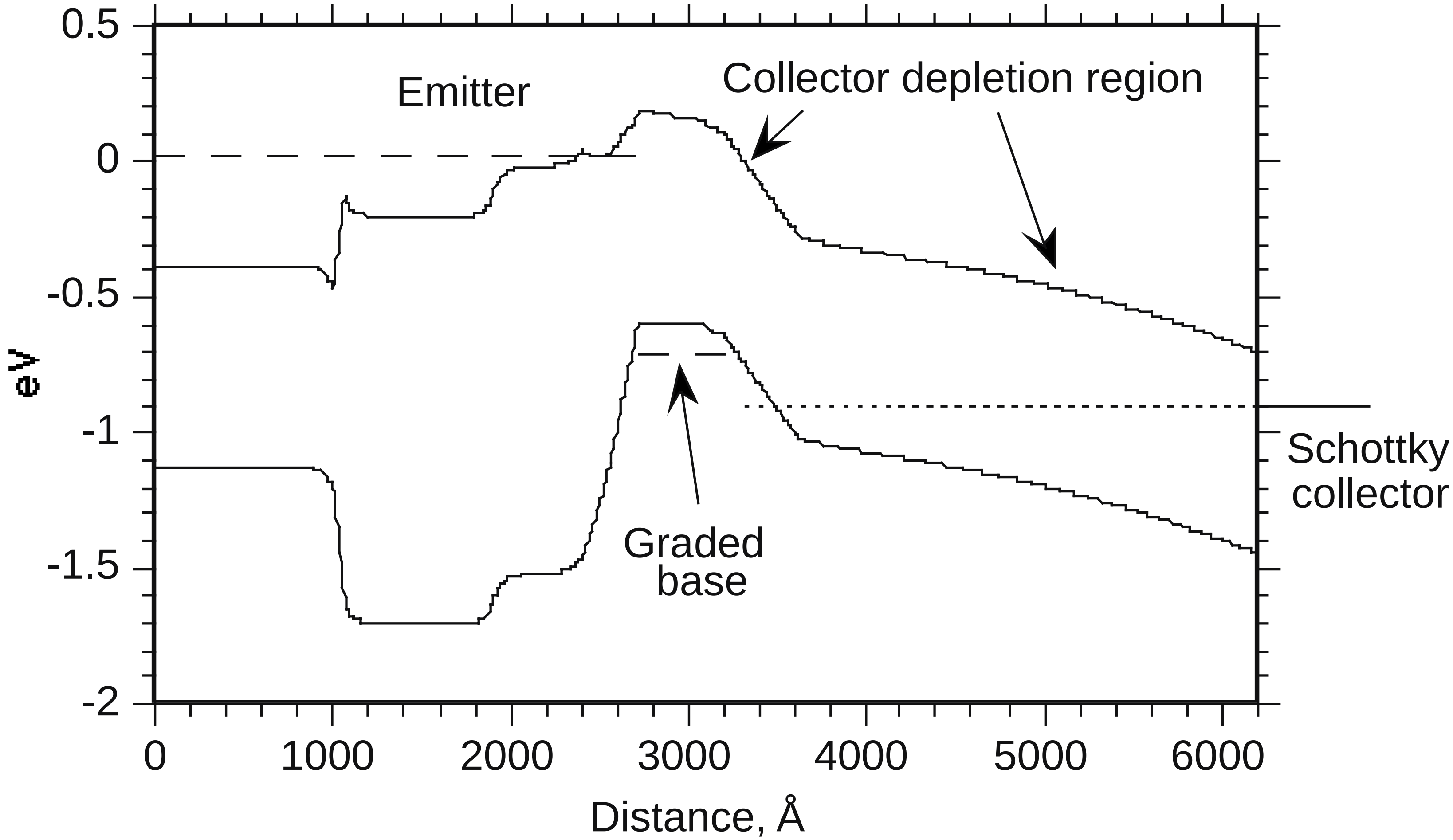


Band diagram under normal operating voltages
$V_{ce}$ = 0.9 V, $V_{be}$= 0.7 V

- 500 Å 5E19 graded base ( $\Delta E_g$ = kT), 3000 Å collector

# Transferred-Substrate Heterojunction Bipolar Transistor

Device with 0.6 $\mu$m emitter & 0.8 $\mu$m collector
extrapolated fmax = 560 GHz (?)

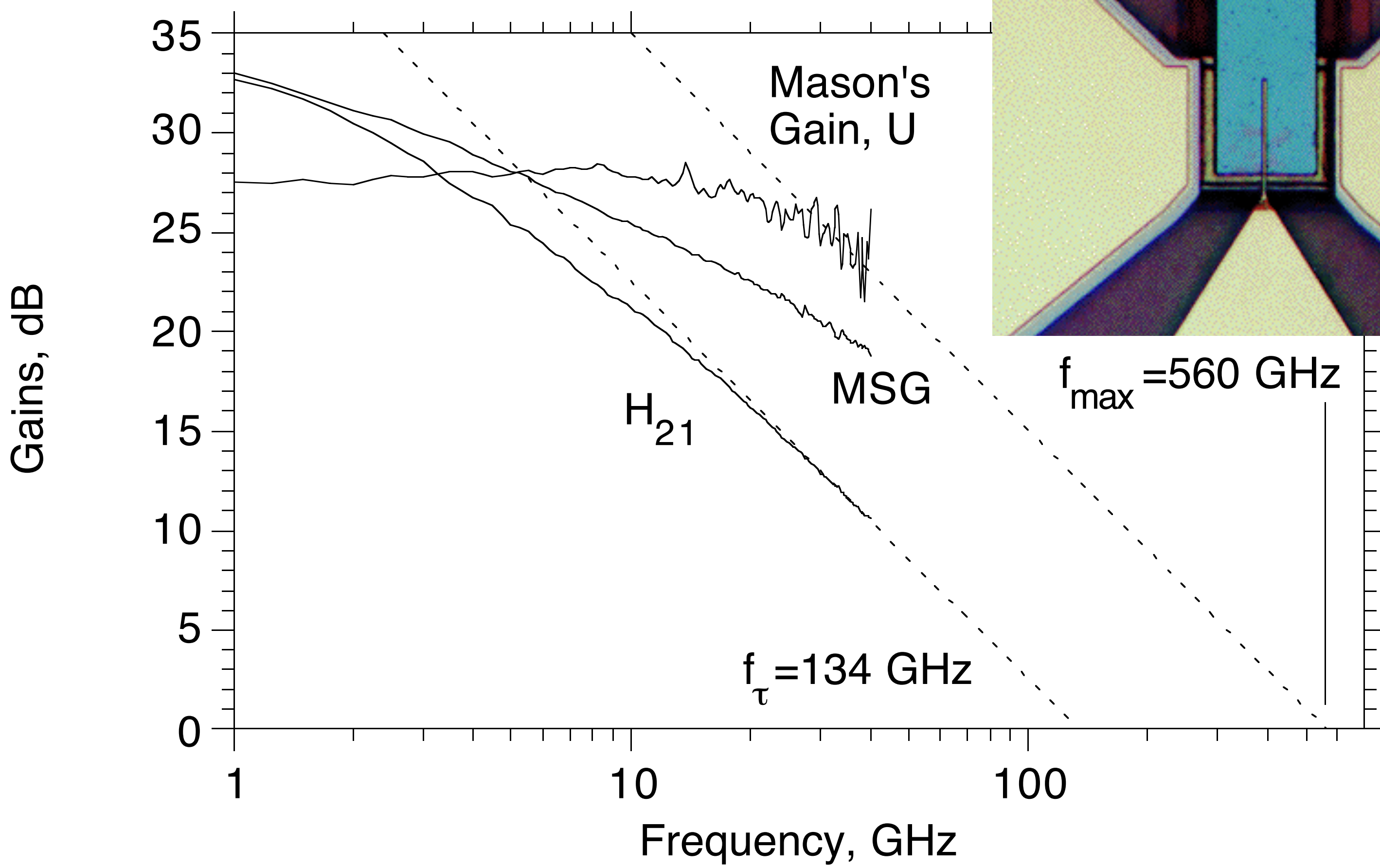


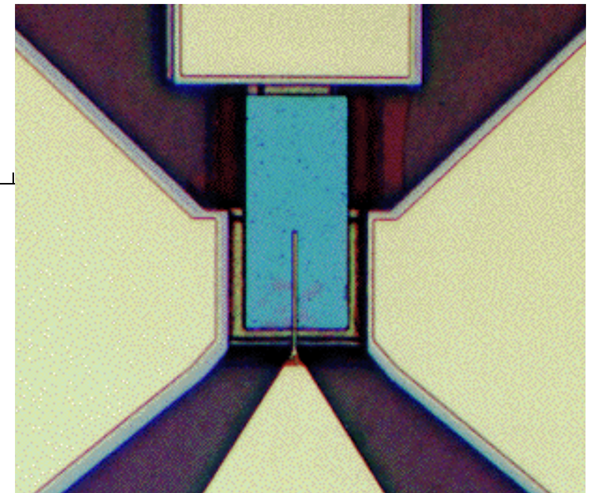

0.25 $\mu$m devices should obtain 600-700 GHz fmax

# Transferred-Substrate Heterojunction Bipolar Transistor

*Device with 0.6  µm emitter & 1.8 µm collector*
*extrapolated fmax at instrument limits*

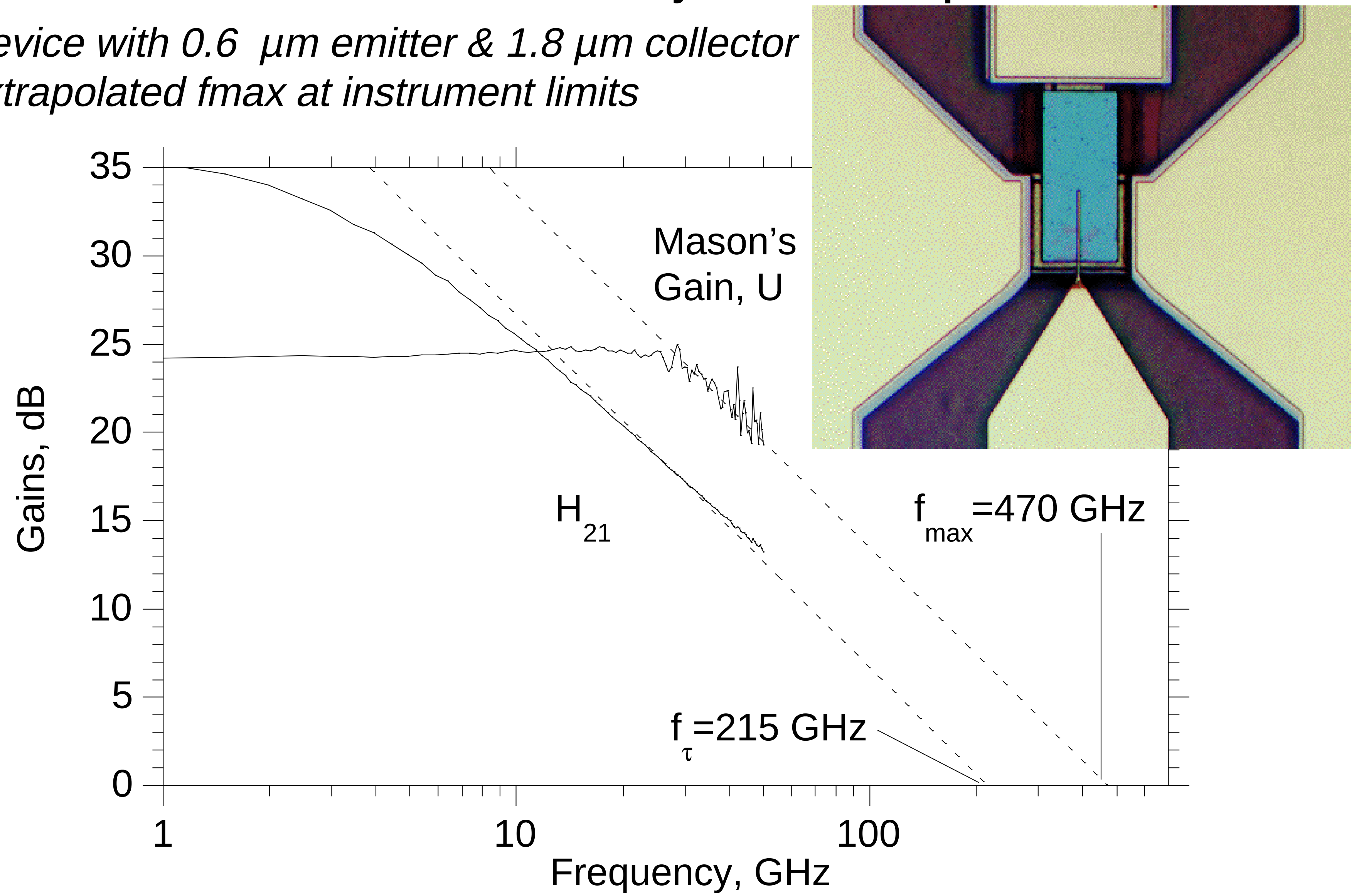


*0.25 µm devices should obtain 600-700 GHz fmax*

# In Fabrication: Deep Submicron HBTs

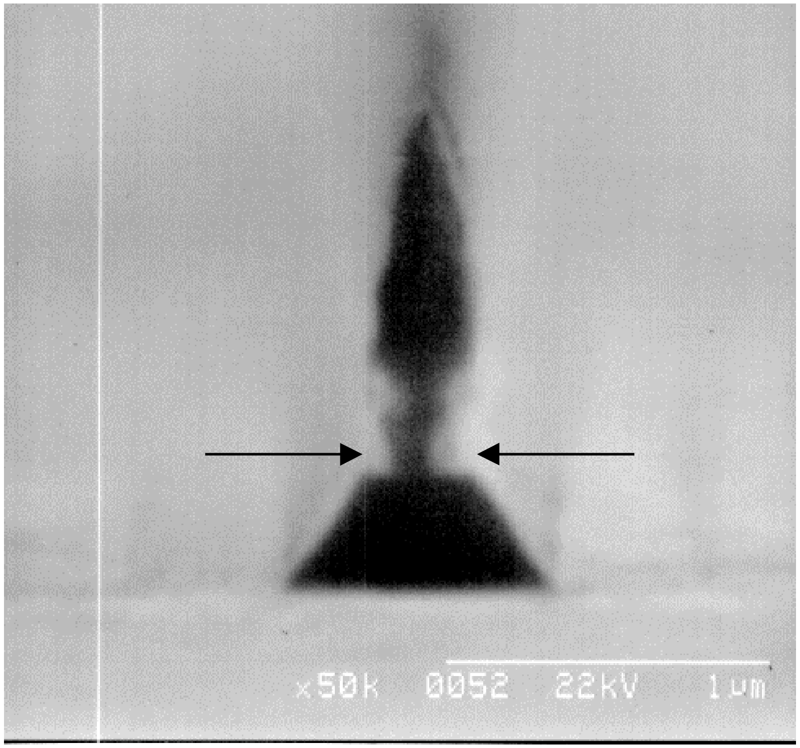


0.15 µm emitter

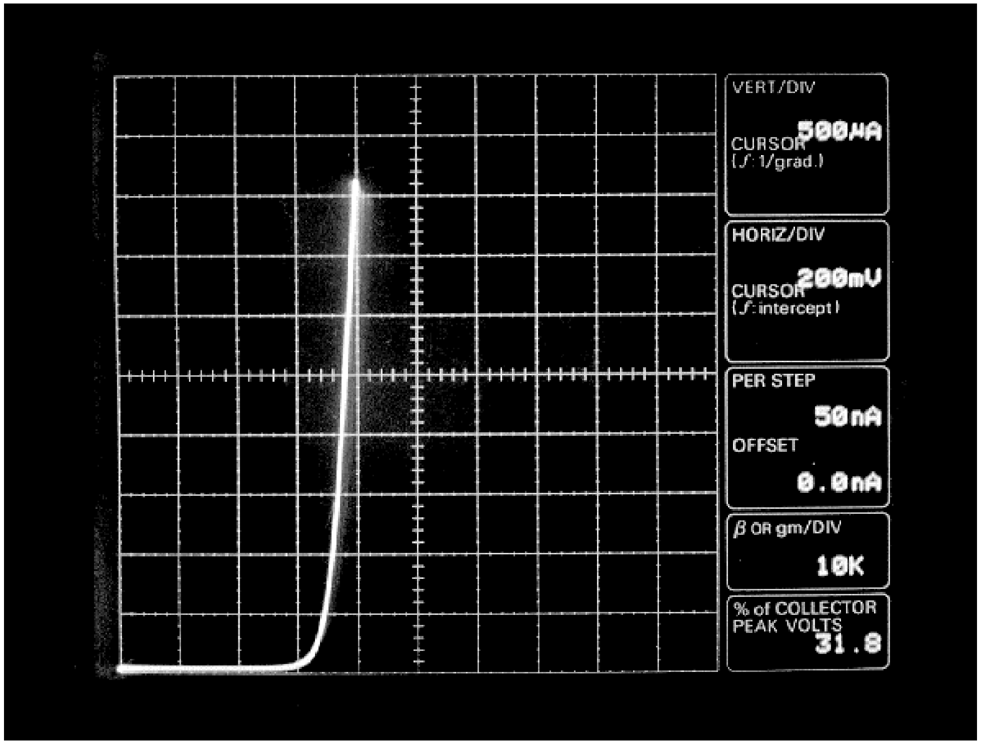


base-emitter diode
IV Charactersitics

*In development:* 0.15 µm emitter/ 0.3 µm collector HBT

*Credit: Michelle Lee, Dino Mensa, UCSB; S. Martin, R.P. Smith, JPL*

# Transferred-Substrate HBT Integrated Circuits

11 dB, 50+ GHz AGC / limiting amplifier

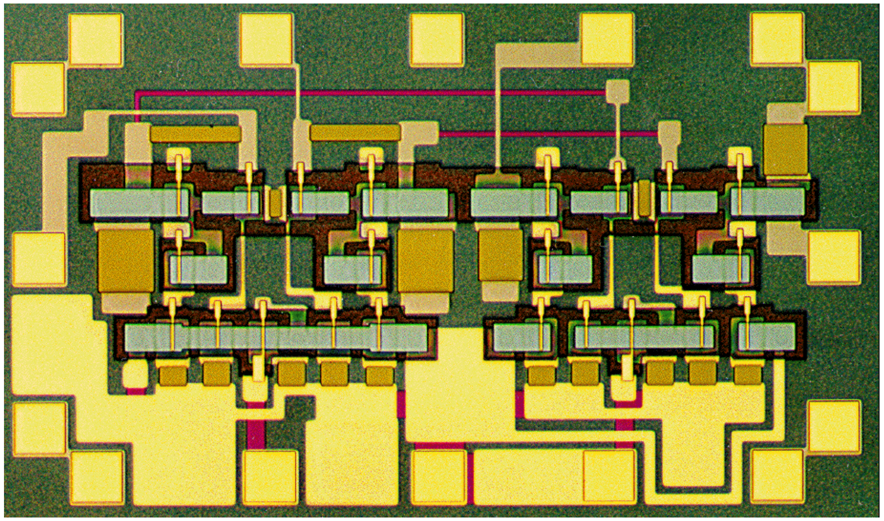

47 GHz master-slave flip-flop

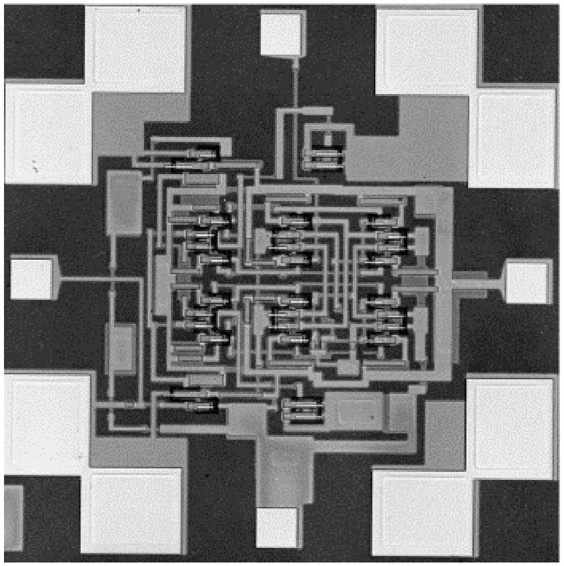

10 dB, 50+ GHz feedback amplifier

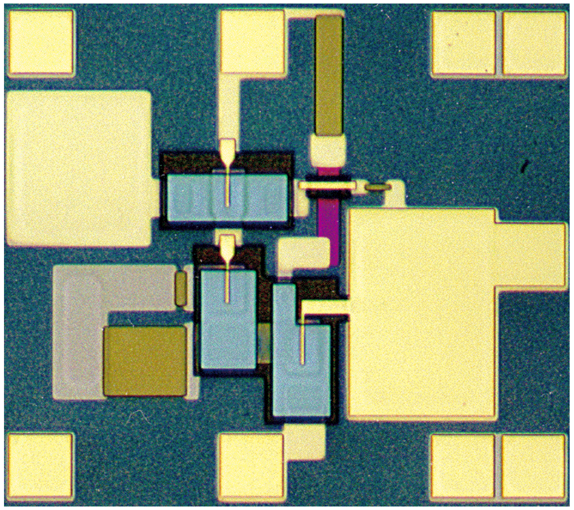

7 dB, 5-80 GHz distributed amplifier

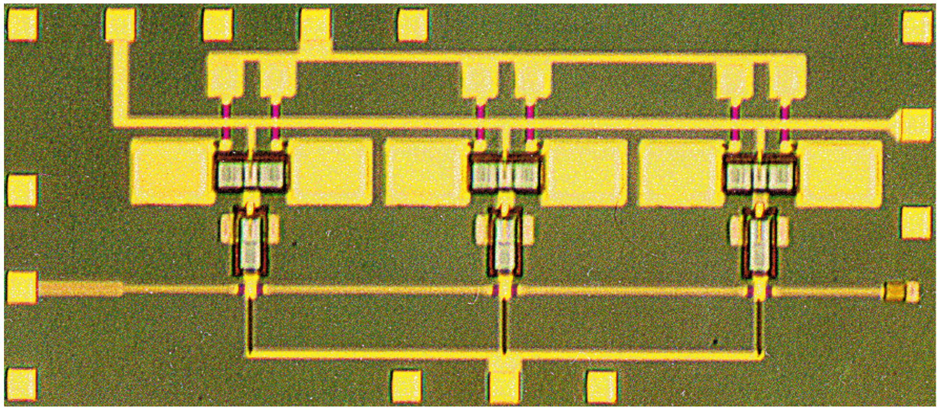

## Transmission Lines

Geometries

Characteristic Impedances

Group Velocity Dispersion

Skin effect losses

(substrate) radiation losses

Excitation of undesired modes & resulting problems

# Types of Planar Transmission Lines

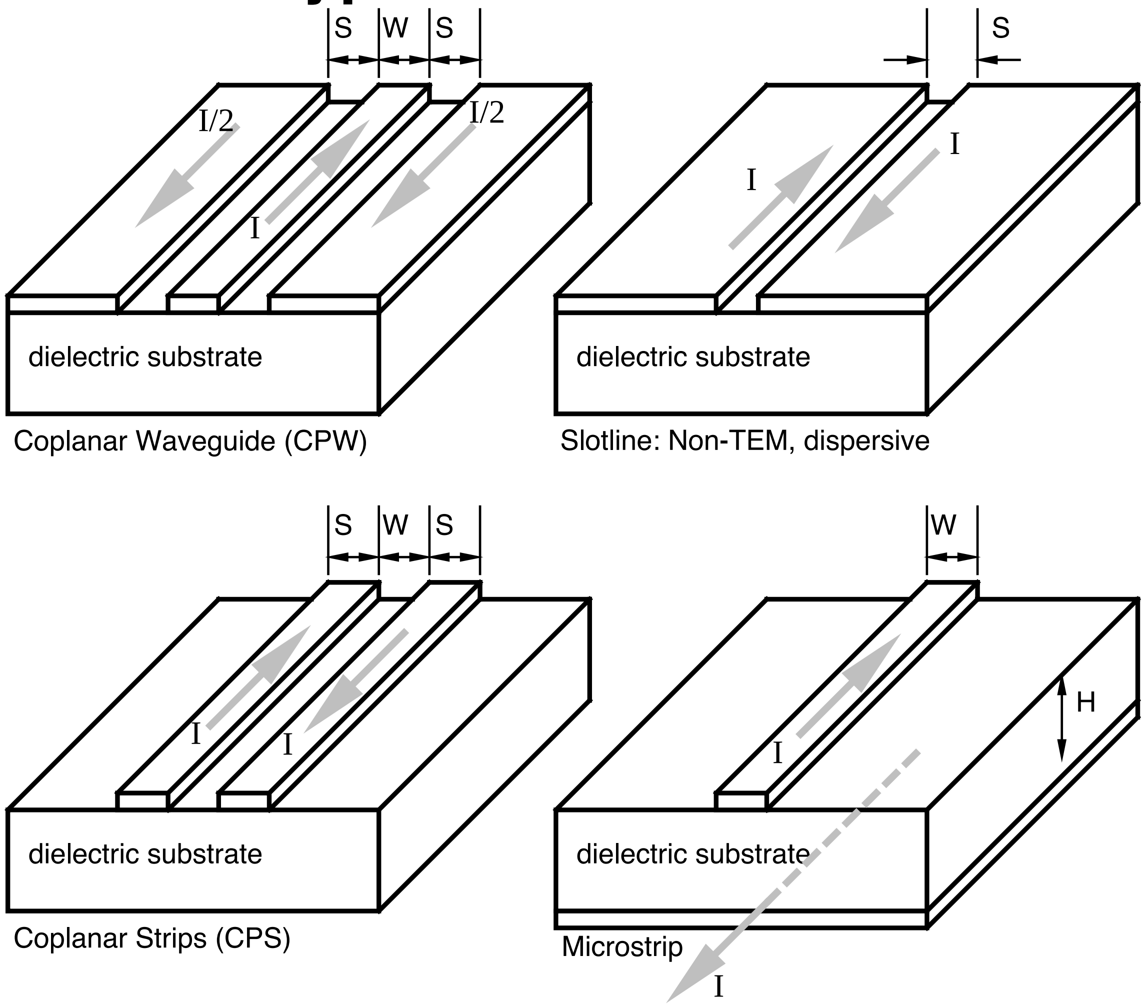


Well designed CPW and CPS have (S+2W)<<h (better than 2:1 ratio)

# Microstrip Line

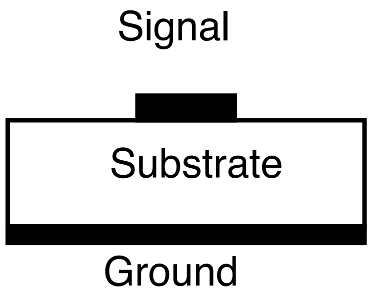


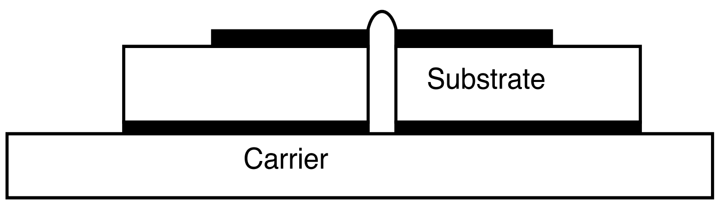


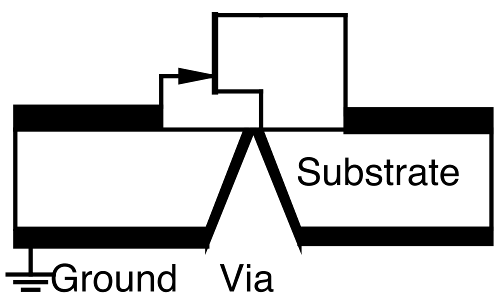


Dominant transmission medium in microwave IC's

Key advantage: IC interconnections have very low ground lead inductance- more important than signal line inductive parasitics in amplifiers

Key problem: through-wafer grounding holes (vias).
Via inductance forces progressively thinner wafers at higher frequencies. Microstrip is used with good performance in 65 GHz monolithic circuits

# Ground Bound Noise in ICs

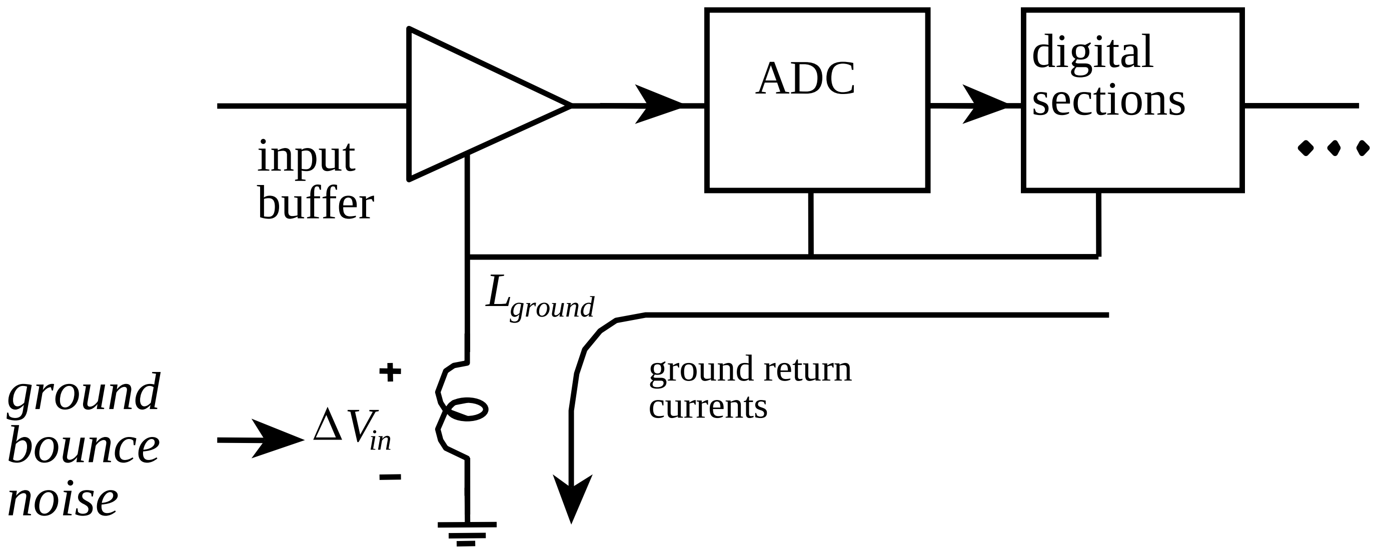


Ground bounce noise must be 98 dB below full-scale input

Differential input will partly suppress ground noise coupling

- ~ 30 to 40 dB common-mode rejection feasible
- CMRR insufficient to obtain 98 dB SNR

*Eliminate ground bounce noise by good IC grounding*

# Microstrip IC wiring to Eliminate Ground Bounce Noise

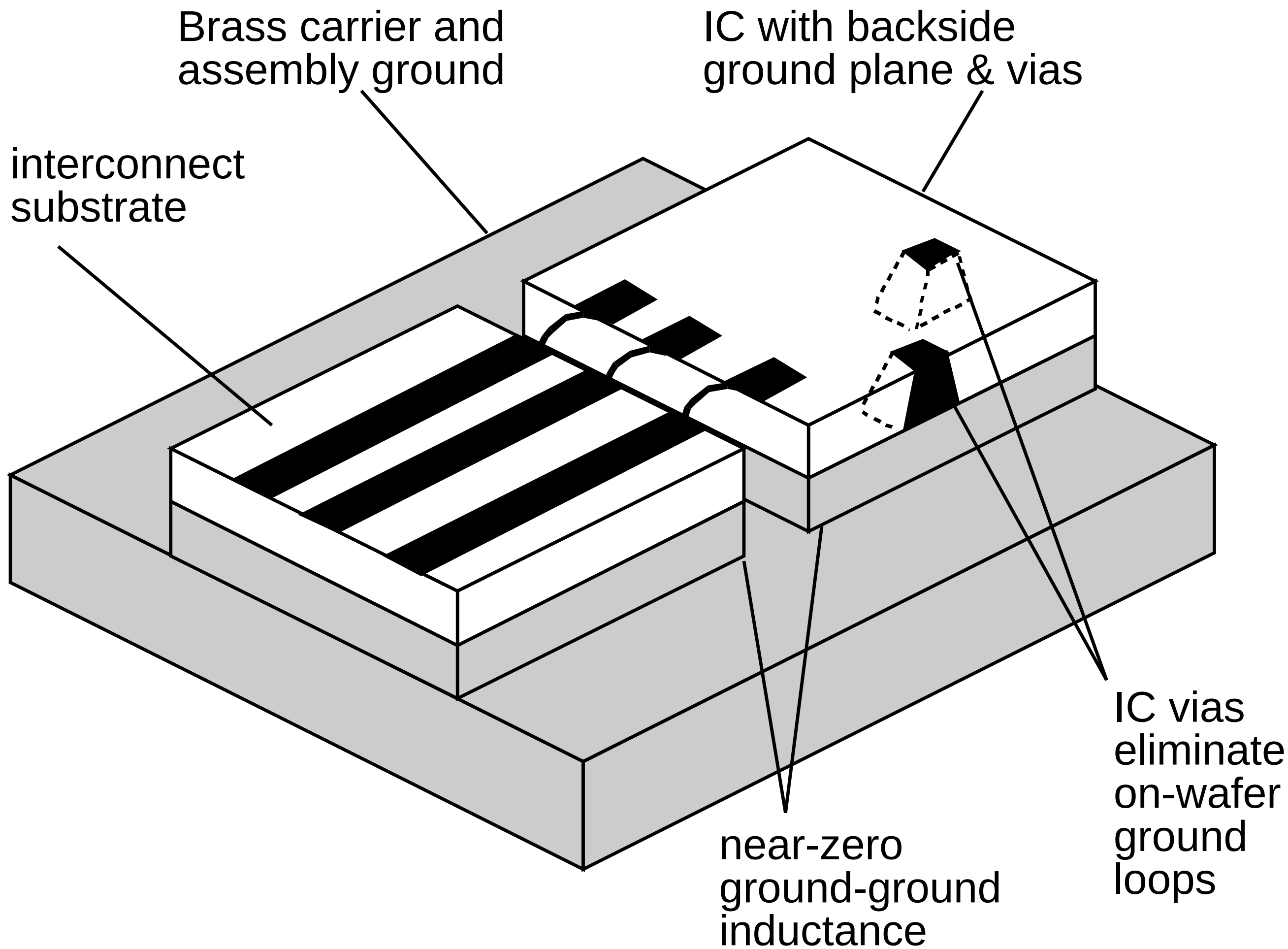

# Skin Effect Losses, I

$$\gamma_{metal} = \sqrt{j\omega\mu\left(j\omega\varepsilon + \sigma\right)}$$
$$\cong \sqrt{j\omega\mu\sigma}$$
$$\alpha_{metal} + j\beta_{metal} = \sqrt{\omega\mu\sigma/2} + j\sqrt{\omega\mu\sigma/2}$$
$$= \left(1/\delta\right)\left(1 + j\right)$$
$$where \;\; \delta = \sqrt{2/\omega\mu\sigma}$$
$$Z_{series} = \gamma_{metal}/\sigma P$$
$$= \left(1/\delta\sigma P\right) + j\left(1/\delta\sigma P\right)$$

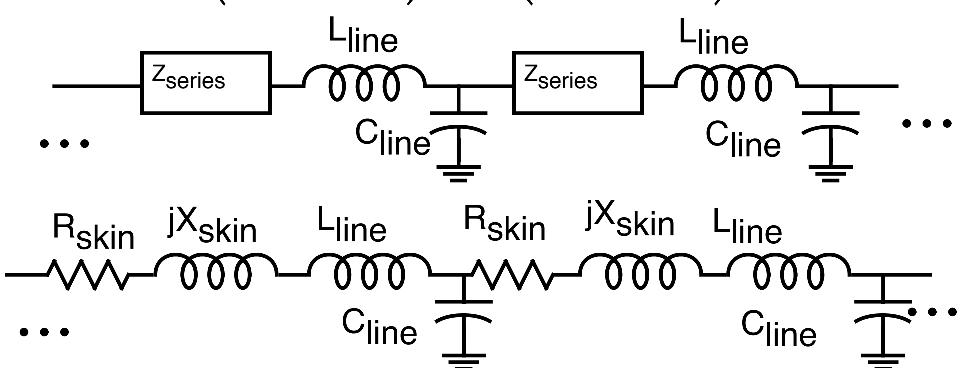


Surface impedance of the metal interconnections of a transmission line introduces loss proportional to the square root of frequency.

Dispersion is also introduced, as the skin impedance has equal real and complex parts

# Skin Effect Losses II

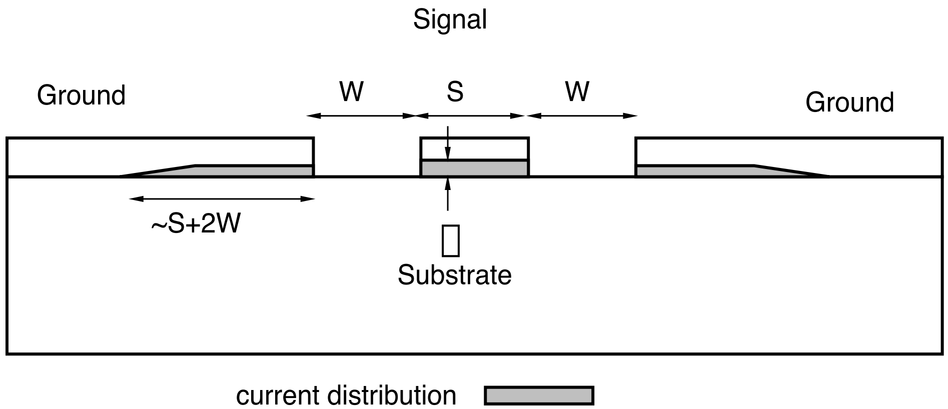


For a coplanar line the effective current carrying periphery P is approximately the width of the center conductor (IF S is relatively small compared to W, a higher-impedance line)

$$\gamma_{line} = \sqrt{j\omega C\left(j\omega L_{line} + Z_{series}\right)}$$

$$= j\omega\sqrt{LC}\sqrt{1+\left(Z_{series}/j\omega L_{line}\right)}$$

$$\cong j\omega\sqrt{LC}\left(1+\left(Z_{series}/2j\omega L_{line}\right)\right)$$

$$= j\omega\sqrt{LC} + \frac{Z_{series}}{2Z_0}$$

$$Z_0 = \sqrt{L/C}$$

Following this, the line propagation constant $\gamma$ can be found, and the transfer function for a line of length $l$ is $\exp(-\gamma l)$

$$Z_{series} = \left(1/\delta\sigma P\right) + j\left(1/\delta\sigma P\right)$$

# Skin Effect Losses III

The impulse response of the transmission line can then be found. (Wiginton and Nahman, Proc. IRE, February 1957)

$$h(t) \cong C * U(t/\tau) \frac{(t/\tau)^{-3/2} \exp(-\tau/t)}{\tau\sqrt{\pi}}$$

$$where \quad \tau = \left[ l\sqrt{\frac{\mu}{\sigma}} \Big/ 4Z_0 P \right]^2$$

Skin effect causes pulse broadening proportional to distance$^2$

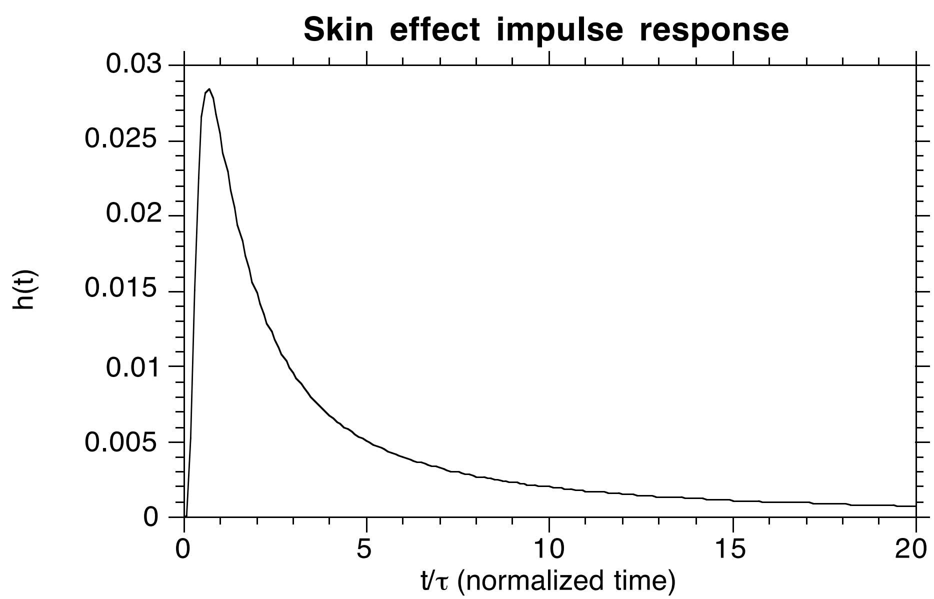

# Skin Effect Losses IV

The step response is the integral of the impulse response.
Note the initial fast rise and the subsequent "dribble-up" characteristic of skin effect losses.

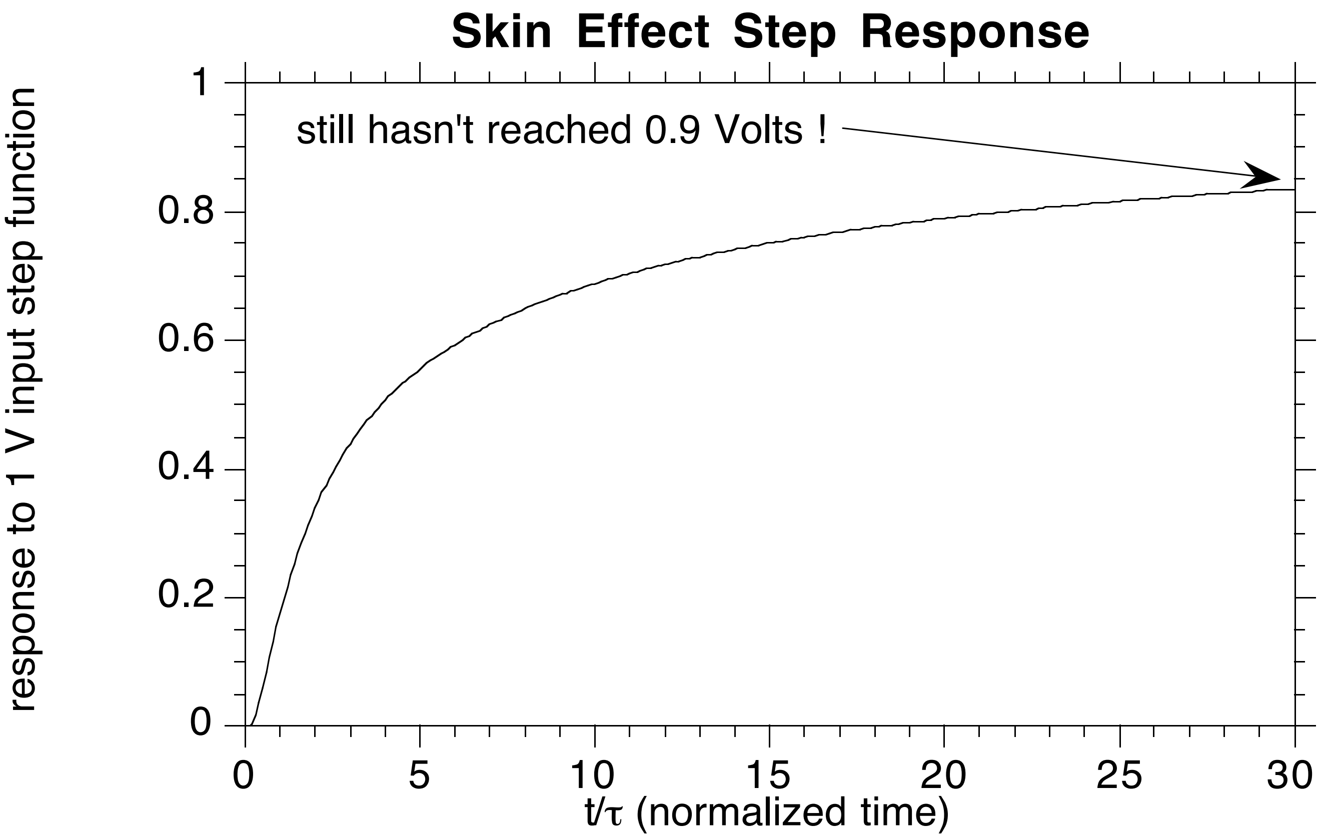

# Transmission-Line Radiation Losses

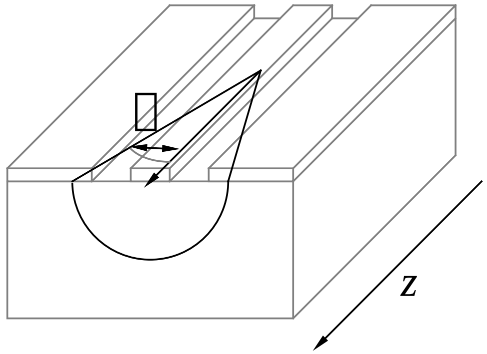


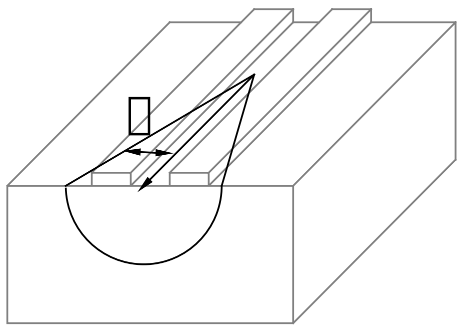

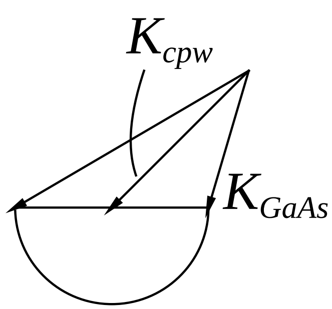


Transmission line velocity is

$v = c/\sqrt{(1+\varepsilon_r)/2}$

Velocity of a plane wave in the substate is $v = c/\sqrt{\varepsilon_r}$ , which is slower.

Power radiates at angle $\psi$ determined by matching $K_z$.

WIth substrate of finite thickness, radiation shows frequency structure due to substrate modes

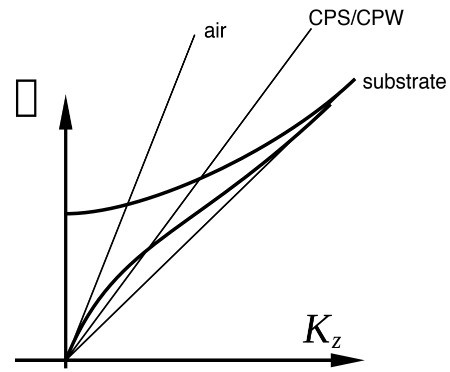

# Radiation Losses II

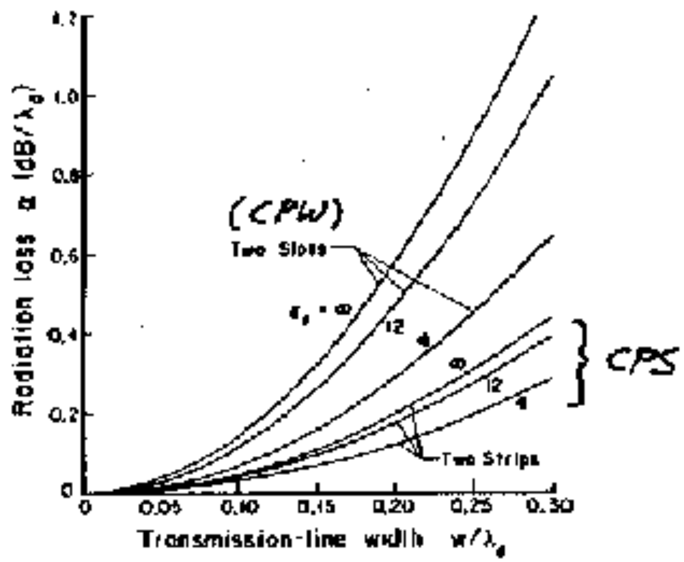


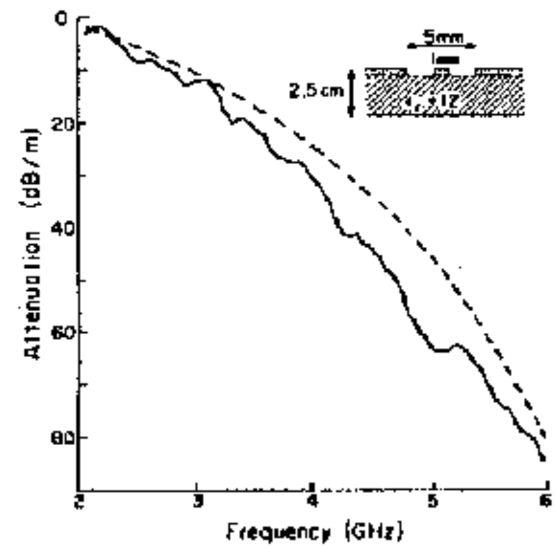


FIG. 22 Measured loss (——) of a two-slot ($k = 1$) transmission line on a thick substrate ($\epsilon_r = 12$) compared to theory (– – –) [Eq. 144)].

Loss (in dB) per wavelength is proportional to frequency$^2$ and to the square of the transverse dimensions of the line

Experimental confirmation -scale model measurements

From Rutledge et al (see reference list)

# Skin and Radiation Losses, 50Ω CPW

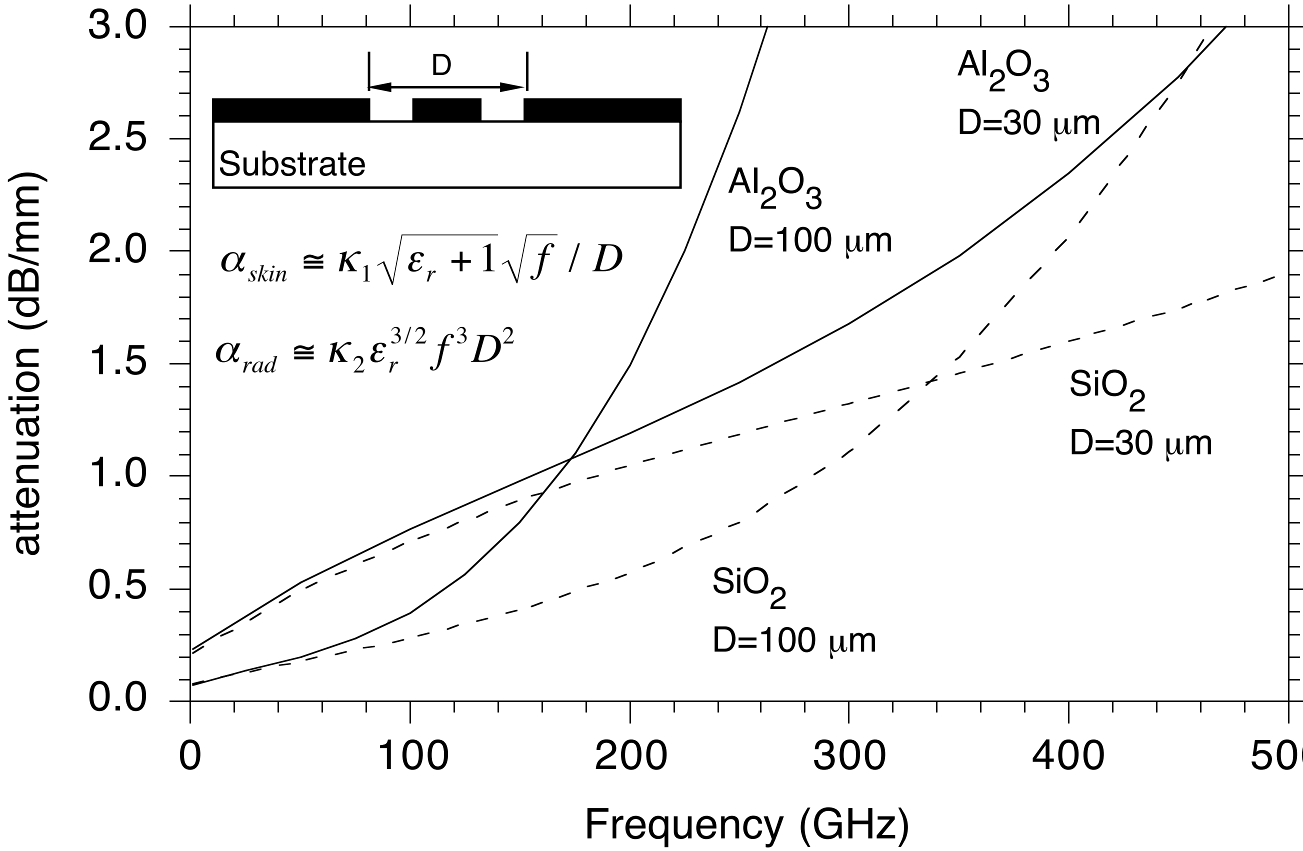

# On-wafer interference from line radiation

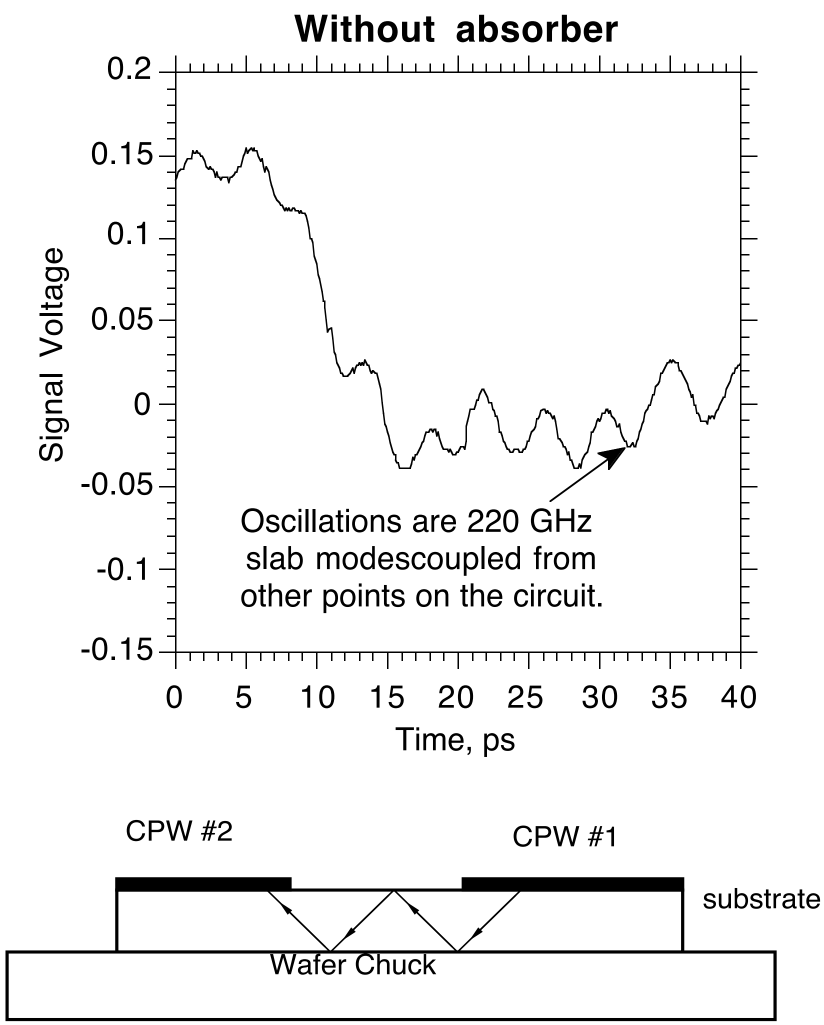


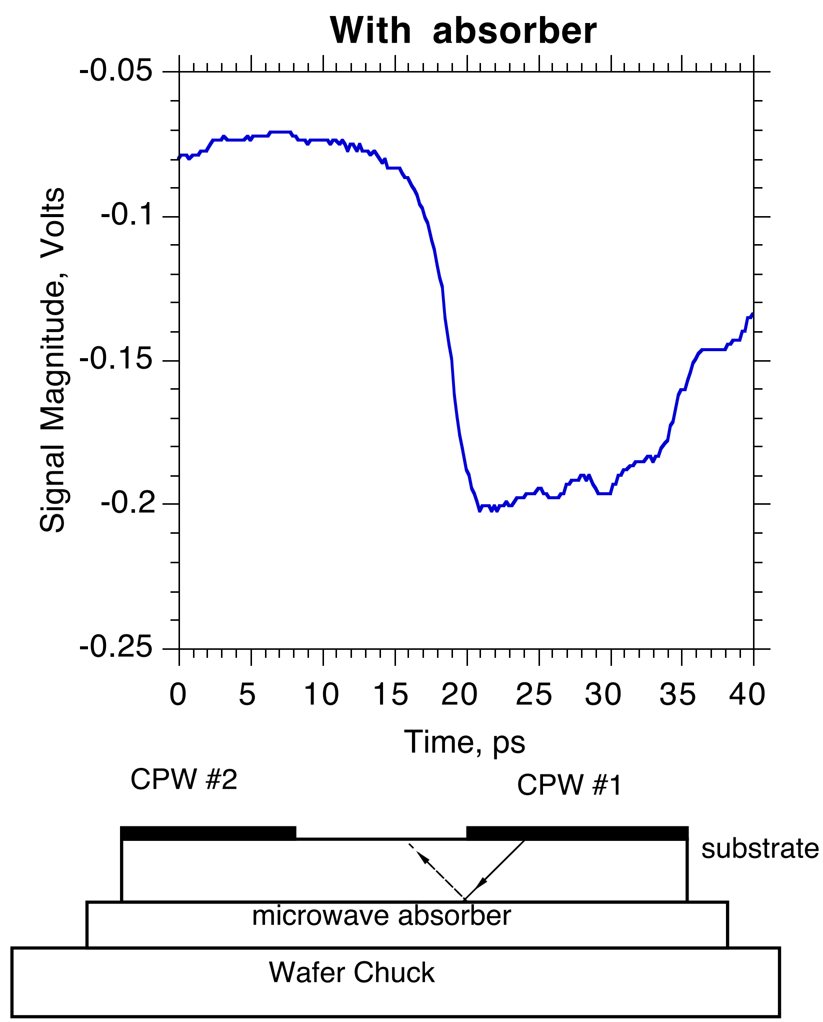

# Tranmission Line Parasitic Modes

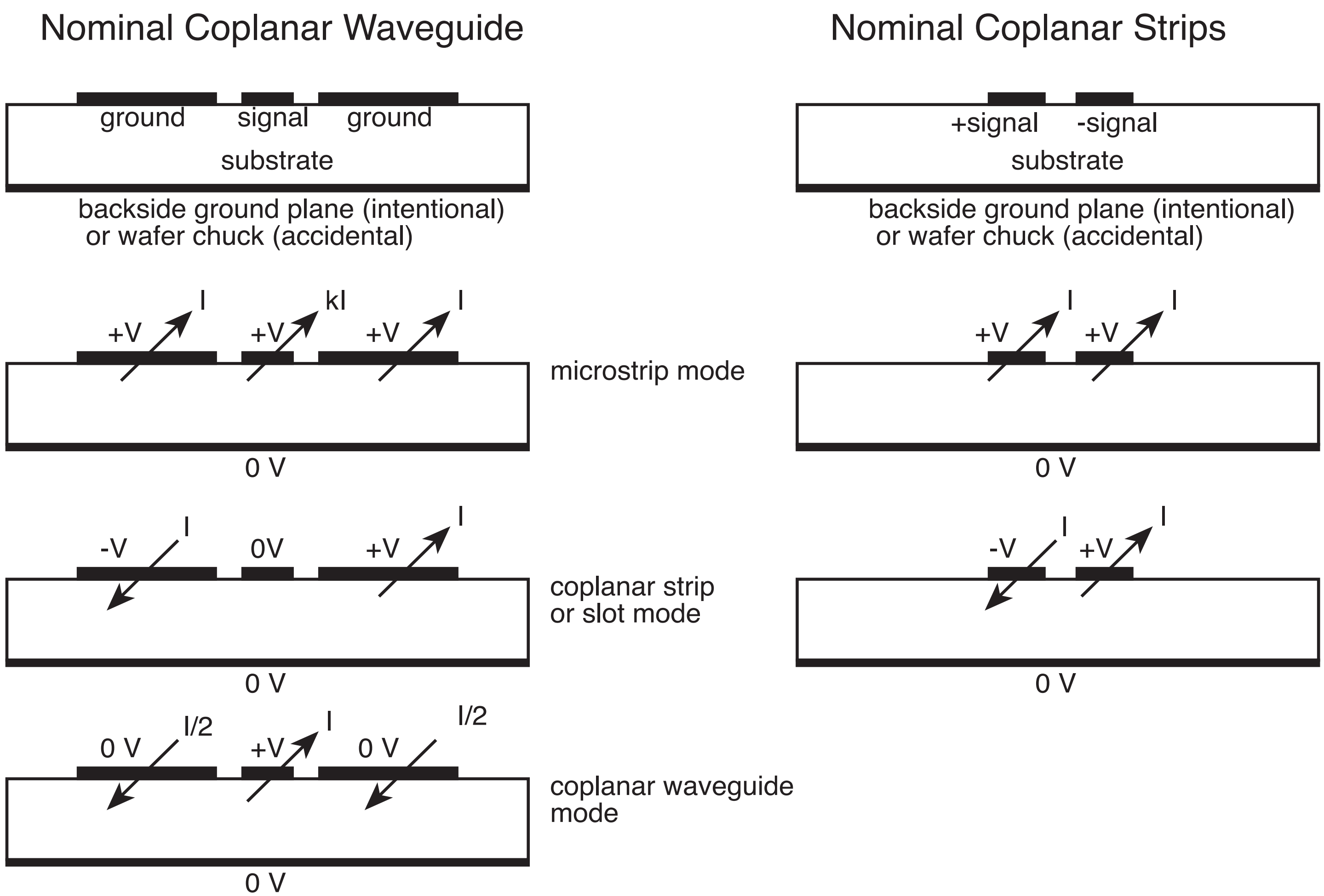


- Total number of quasi-TEM modes is one less than # of conductors
- Care must be taken to avoid excitation of parasitic modes
- unexpected results will otherwise arise...

## General Rules for Avoiding Parasitic Modes

1) Where do the currents flow?

2) Which conductors have what voltages for which modes?

Be aware that:

• currents must flow in the ground planes of unbalanced transmission lines. The currents flow close to the edge of the ground plane nearest the signal conductor.

• there are equal and opposite voltages on the 2 conductors of balanced transmission lines. This seriously restricts the types of junctions allowable.

# Example of parasitic mode excitation

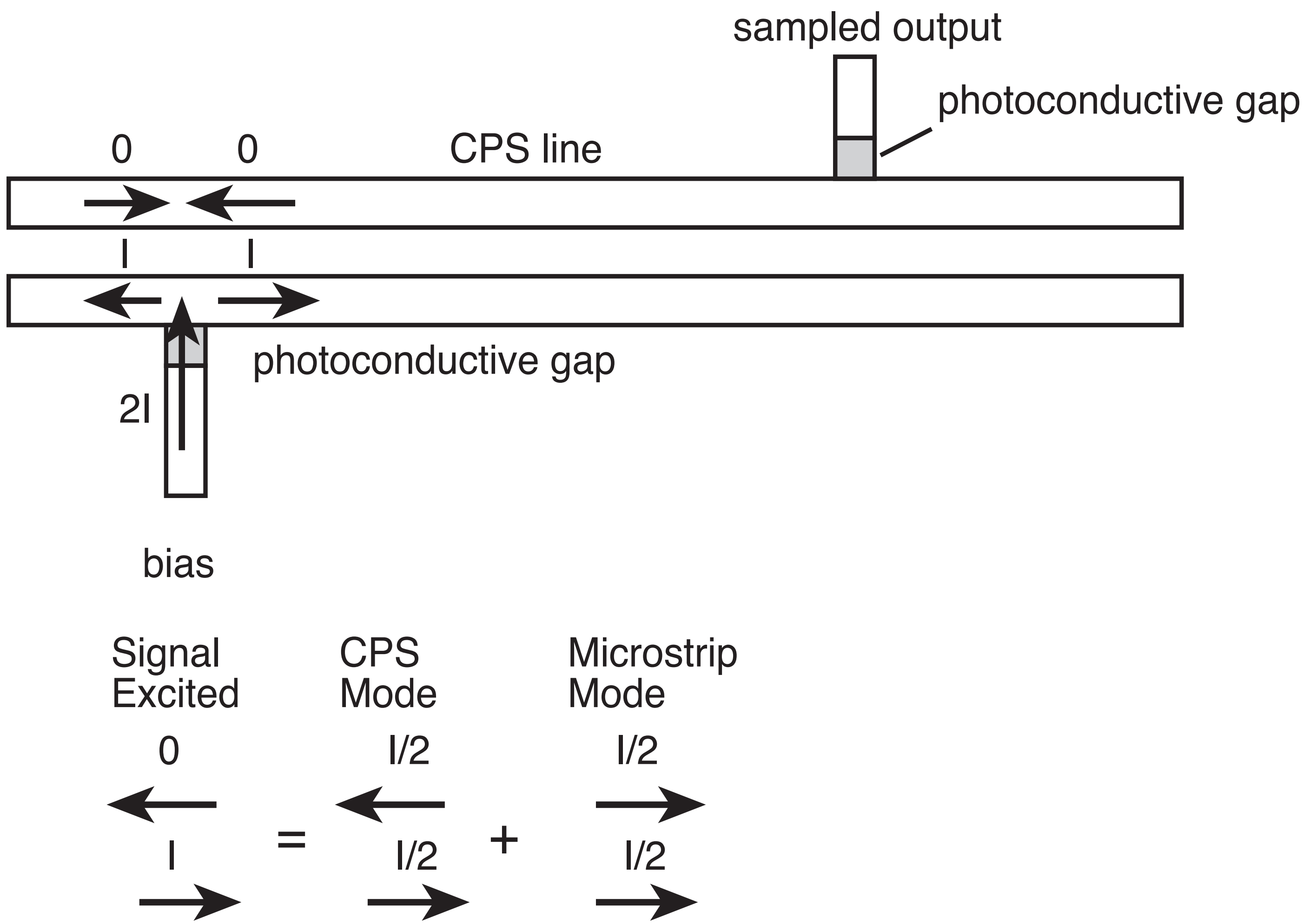


•Both pulse generator and sampling gap excite (sample) mixed microstrip and CPS mode. These propagate at different velocities and will separate in time as they propagate..

# Example of parasitic mode excitation

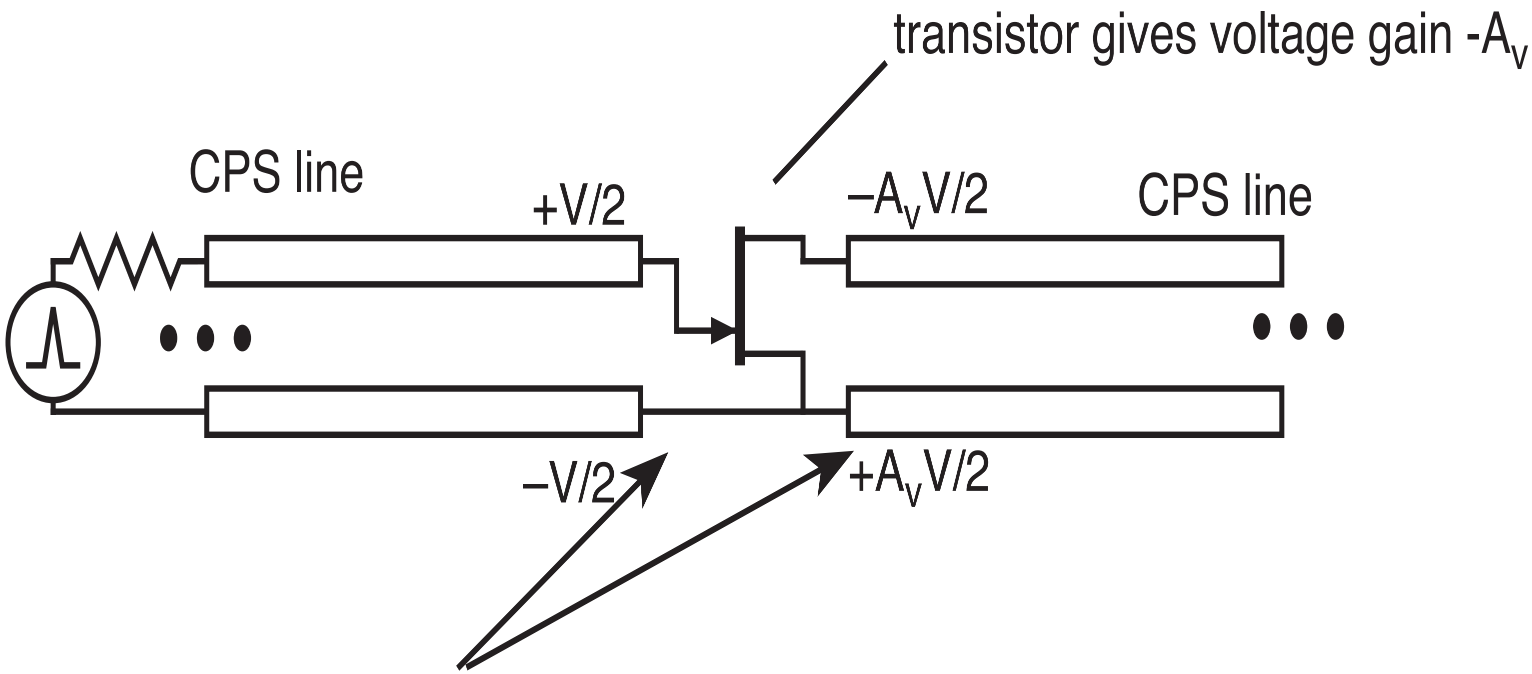


- potentials don't match!
- microstrip modes must be excited to equalize potentials.
- circuit load impedances include contributions from microstrip modes
- resonances will result from boundary conditions on microstrip modes

- CPS line is a balanced line with no ground connection. It cannot be used when a common-lead connection (ground) is needed, e.g. in testing a 2-port device.
- microstrip or CPW should be used in this application

## Example of parasitic mode excitation

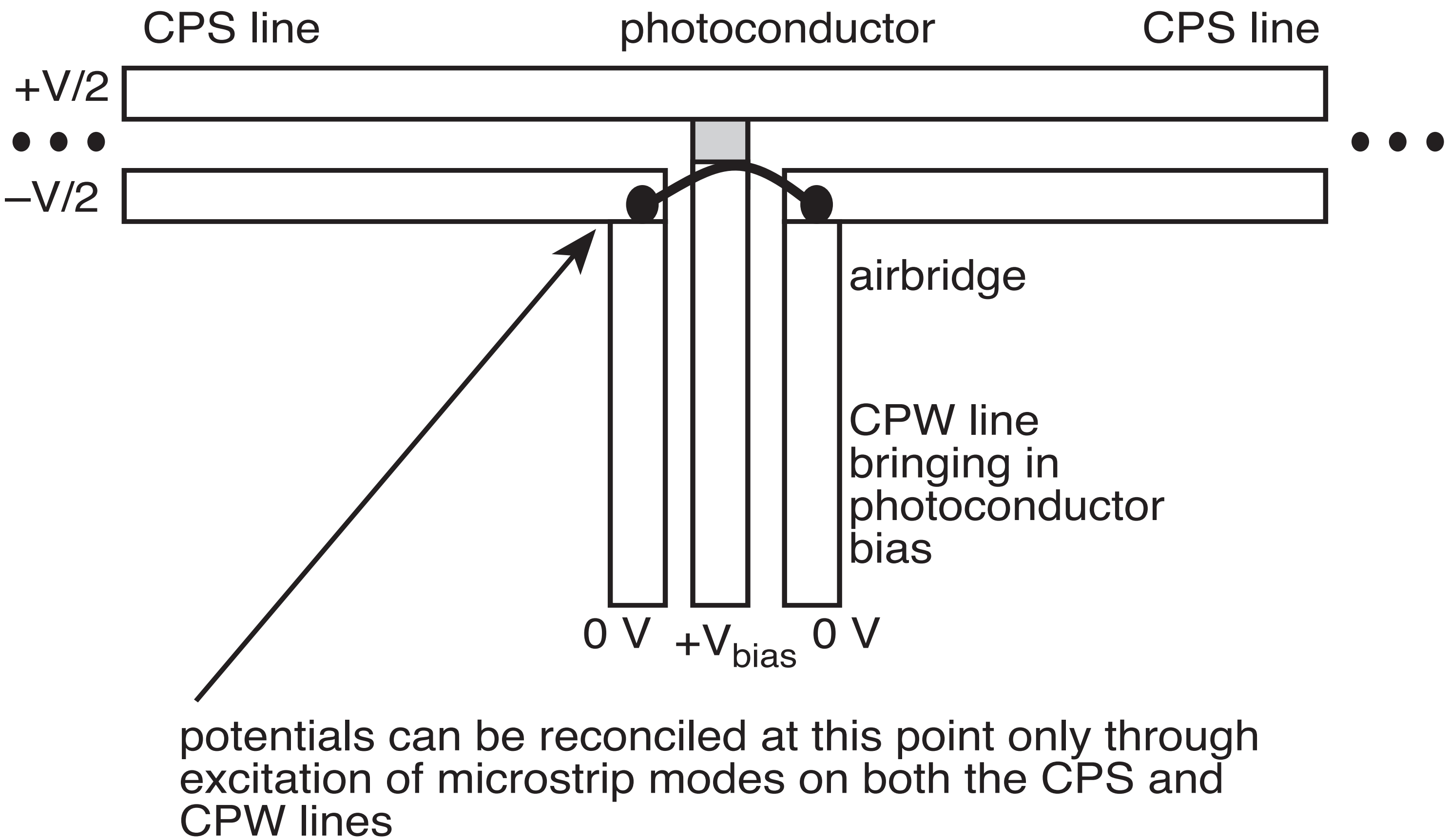


• CPS is usually a bad idea...

# Example of parasitic mode excitation

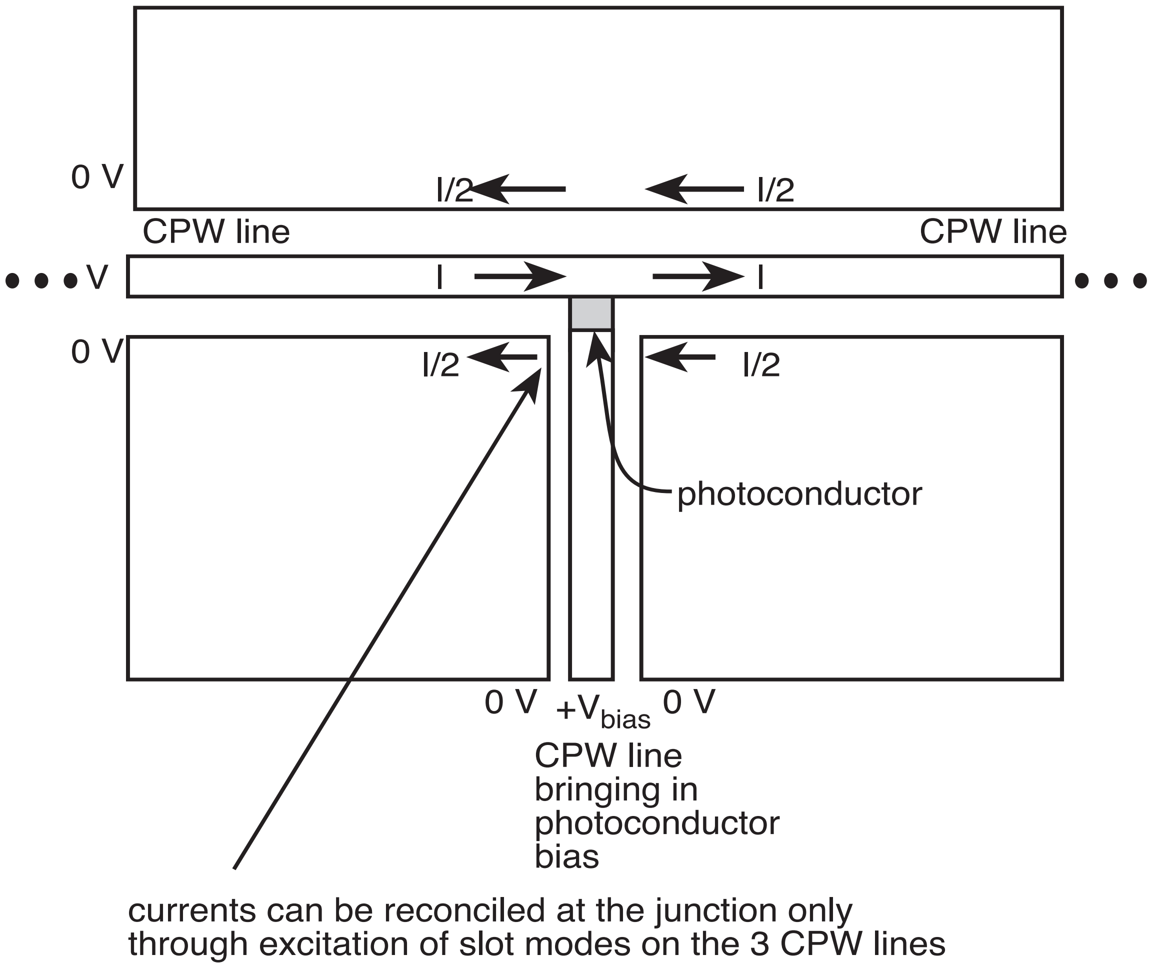


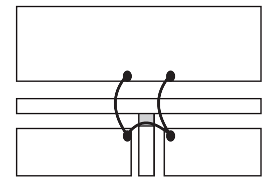

The problem can be fixed by strapping the junction with air-bridges

# Transmission Lines: In summary

## •Radiation Losses

(Coplanar waveguide as example)

$$\alpha_{radiation}(dB/mm) \propto (S+2W)^2 f^3$$

Line impedance constrains S/W
Narrower lines are better

## •Skin Losses:

$$\alpha_{skin}(dB/mm) \propto (W)^{-1} f^{1/2}$$

Wider lines are better

For any frequency, there is an optimum W for lowest loss. Lower $\varepsilon_r$ substrates have lower radiation losses..Alternatives are air-bridge CPW, etched-substrate CPW

Semi-rigid coaxial cable: lower loss than on-wafer lines
connector bandwidths to 65 GHz. 130 GHz connectors are in development.

## Antennas

# Picosecond On-Wafer Antennas

## Frequency-independent antennas

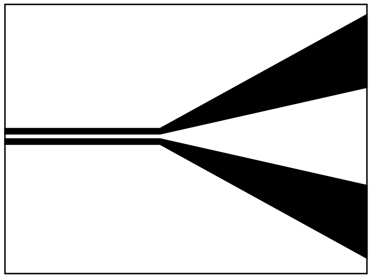

tapered CPS ("V" antenna)

CPS feed

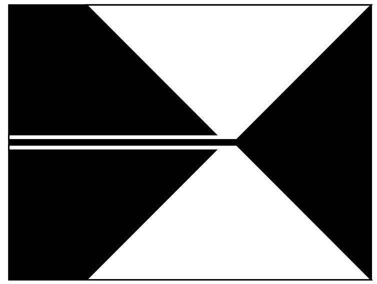

bowtie antenna (CPW feed)

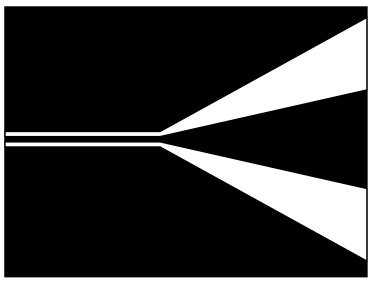

tapered CPW (Slot"V" antenna)

CPW feed

These are all travelling-wave antennas. Radiation impedance, group delay, and far-field patterns are all frequency-independent above the antenna cutoff

## Resonant antennas

metal

substrate

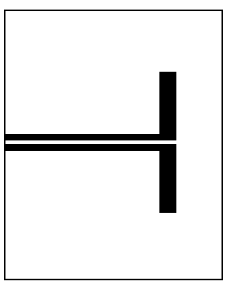

dipole antenna CPS feed

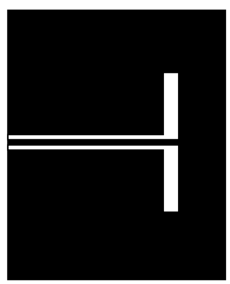

slot antenna (magnetic dipole)

CPW feed

all these require substrate lenses

Other monolithic antennas:

log periodic (not truly frequency independent)

exponential spiral (frequency-dependent polarization)

See Rutledge reference

# Substrate Lenses

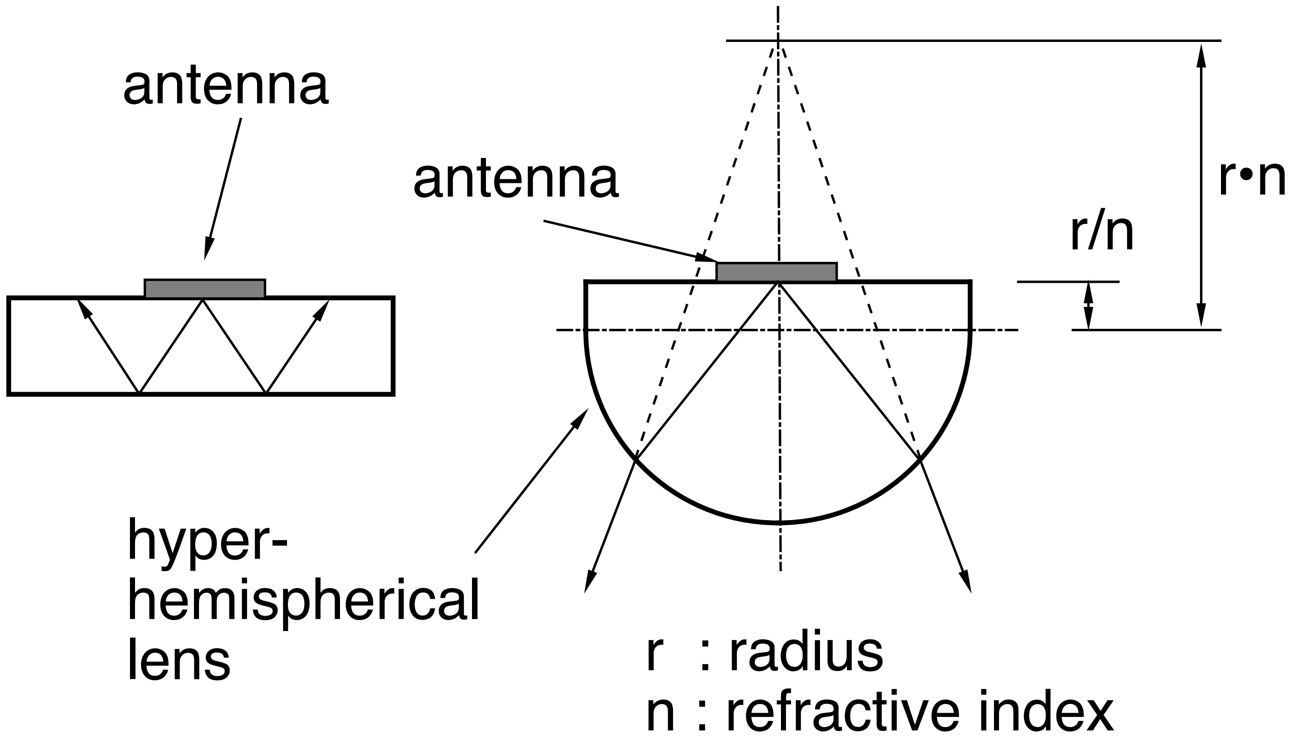


•Energy primarily radiated into substrate
•Trapped (Snell's law) into substrate slab modes
•Substrate lens allows radiation to escape, but efficiency still relatively poor for high-ε substrates. Hyperhemisphere gives some collimation
• Lens must be several wavelengths diameter at longest wavelength of interest.

# Radiation Distribution on tapered CPS antenna

$z_{peak}$=168 mm-GHz ($\theta_1$=5°)

$z_{peak}$=106 mm-GHz ($\theta_1$=10°)

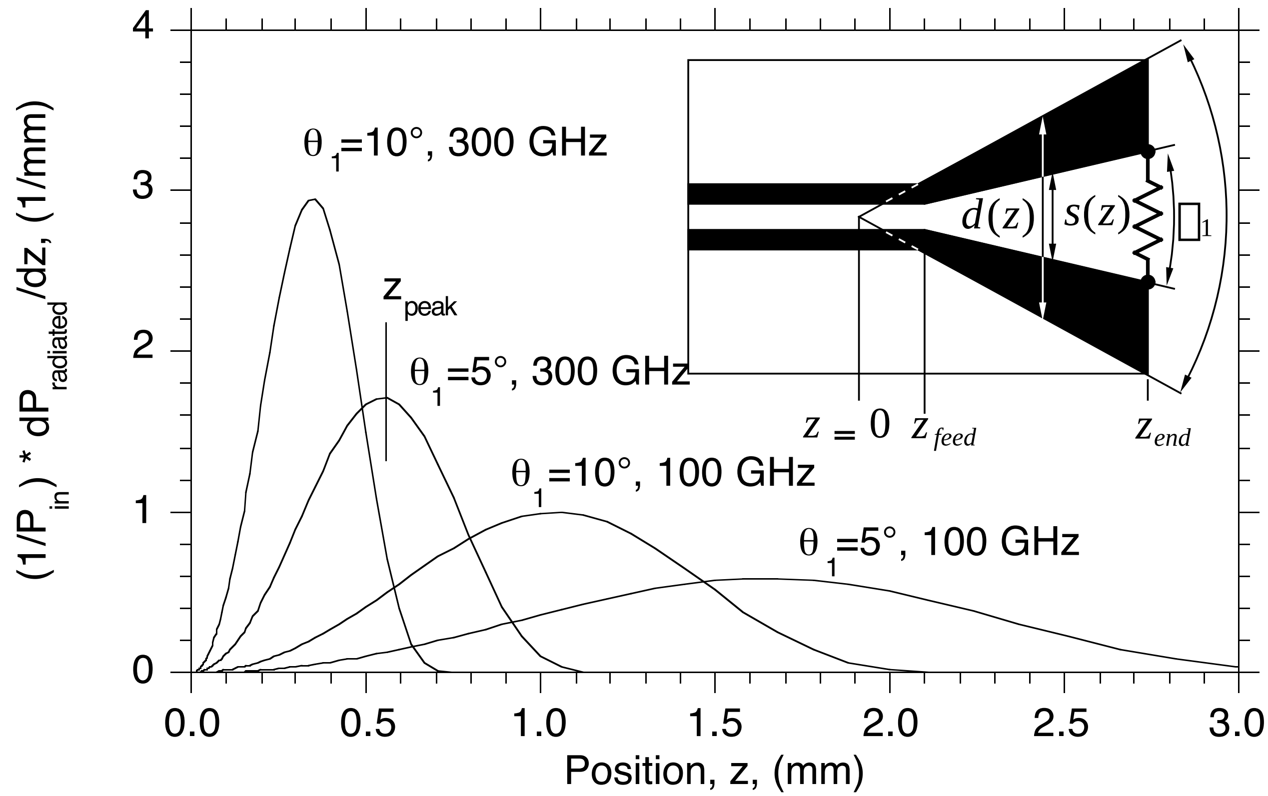


- Length ($\Delta z$) of radiation distribution proportional to wavelength.
- Width W proportional to length $\Delta z$, radiating area proportional to $\lambda^2$.
- Far-field radiation pattern independent of wavelength.

# Circuit Design

- Summary of fundamental gain-frequency limits.
- A few examples of high-speed circuits

The intention here is to give an overview of

...how active devices are modeled

...relevant device figures of merit & their influence on circuit performance

...this is of importance to researchers involved in optical probing of electronic devices: what measurements provide useful descriptive information to the device physicist and circuit designer?

# Device Figures-of-Merit

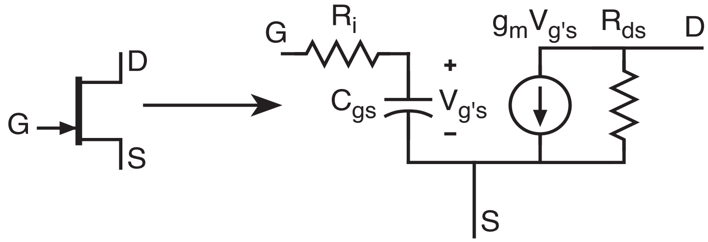


Top: simplified FET equivalent-circuit model

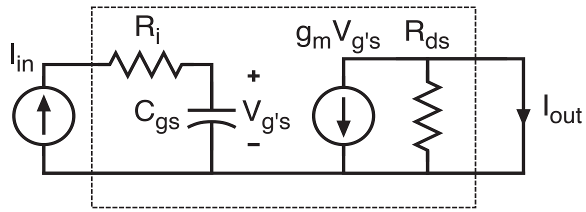


Center: definition of short-circuit current gain (Iout/In)

Current-gain cutoff frequency:

$$\left\| I_{out} / I_{in} \right\| = 1 \ \text{ at } f = f_{\tau}$$

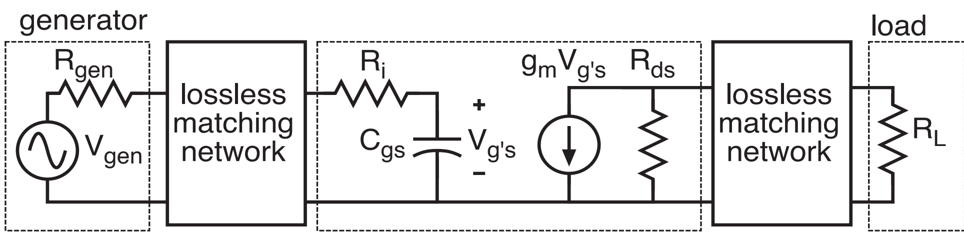


obaining the maximum power gain requires impedance-matching on input & output. Power gain cutoff frequency

$$\left\| P_{out} / P_{in} \right\| = 1 \ \text{ at } f = f_{\max}$$

Expressions for ft and fmax are given elsewhere in these notes...

# Device Figures of Merit

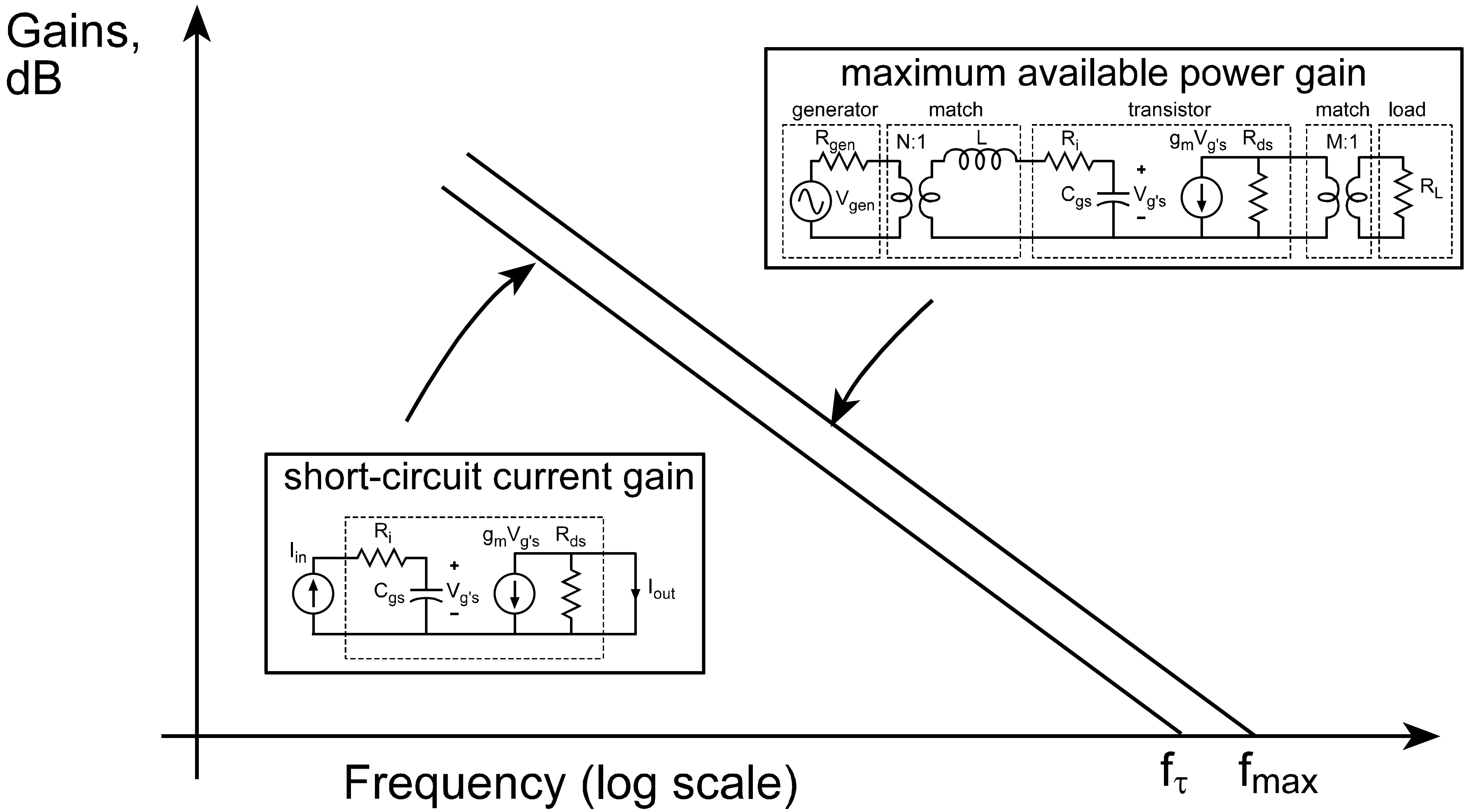


$$2\pi f_t = g_m / C_{gs} = 1/\tau_{gate} \rightarrow \text{depends on carrier transit times}$$

$$2\pi f_{\max} = \frac{f_\tau}{2}\sqrt{\frac{R_{ds}}{R_i}} \quad \rightarrow \text{also depends on parasitics}$$

# Resistively-Loaded Transistor Circuits

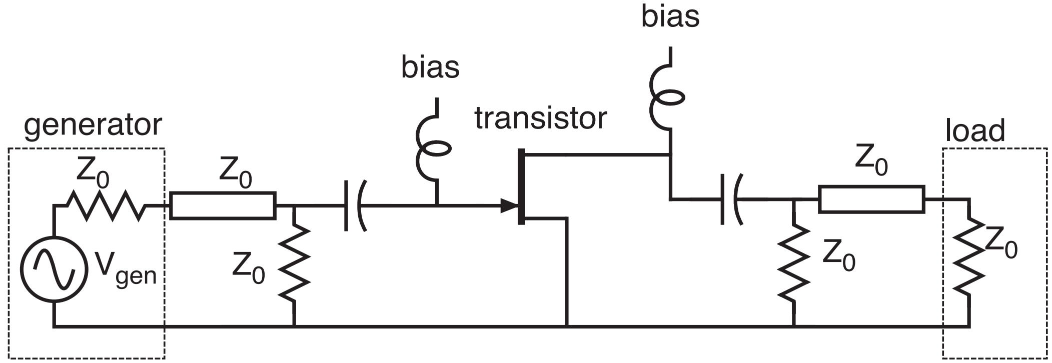


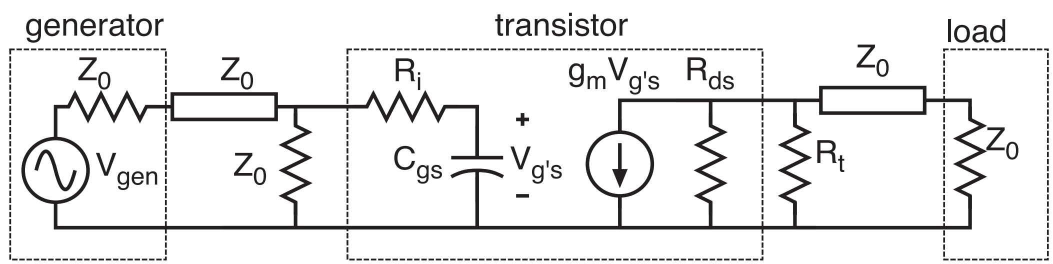


- Broadly representative of most analog high-frequency amplifiers.
- Bandwidth limited by capacitance-charging time of Cgs.
- Big transistor gives big gm, big Cgs, hence big gain, small bandwidth.
- Small transistor gives small gm, small Cgs, hence small gain, small bandwidth.

- Assuming that: (1) Generator and load impedances are equal and (2) fmax >>ft (Ri and Rds have small effect)...

Gain -bandwidth product given by ratio of gm to Cgs, eg. by ft !

# Resistively-Loaded Transistor Circuits 2

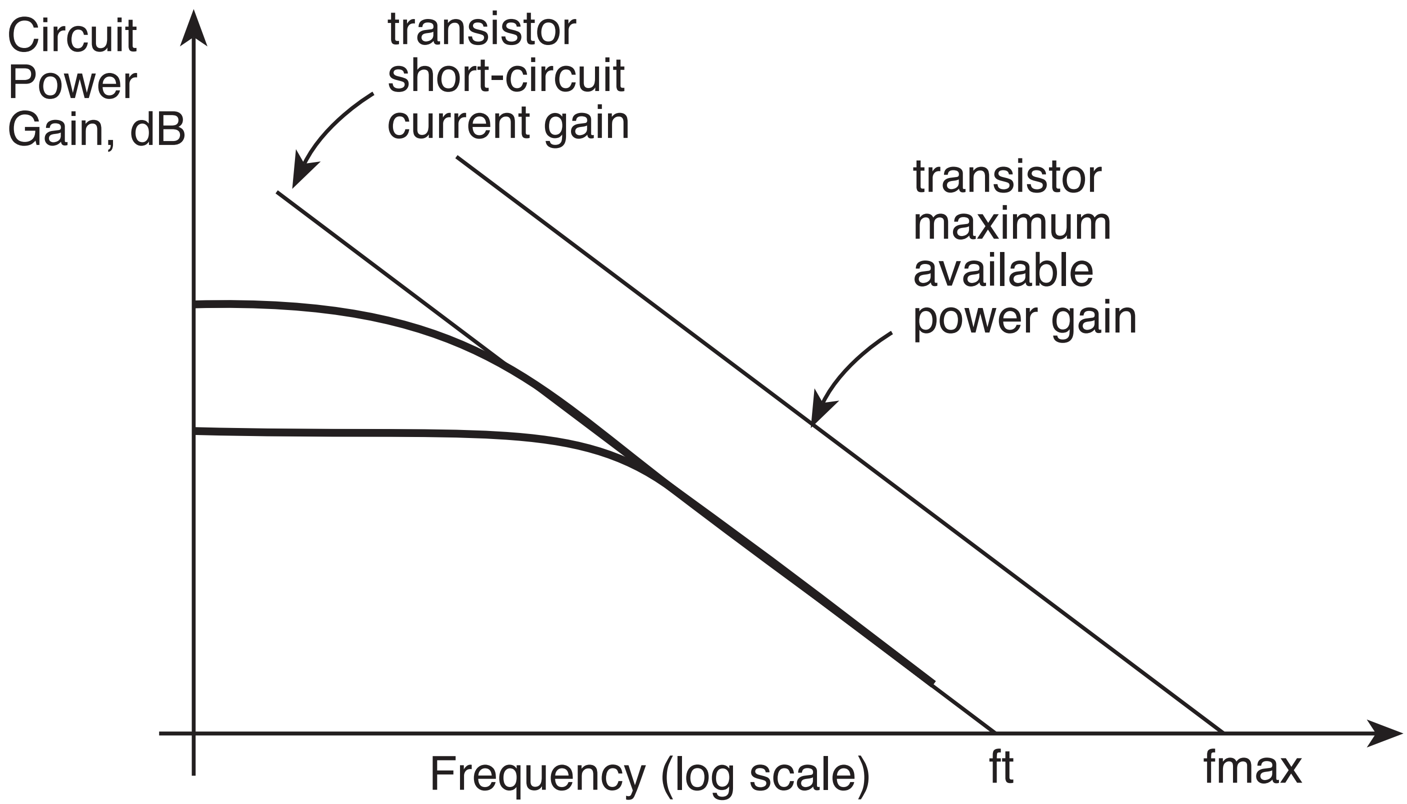


- Big transistors give large gain, low bandwidth
- Small transistor give small gain, high bandwidth
- Gain-bandwidth product limited to transistor short-circuit current-gain cutoff frequency if
  (1) Equal generator and load resistances
  (2) fmax much bigger than ft

# Classes of Circuits: Resistively Loaded

general

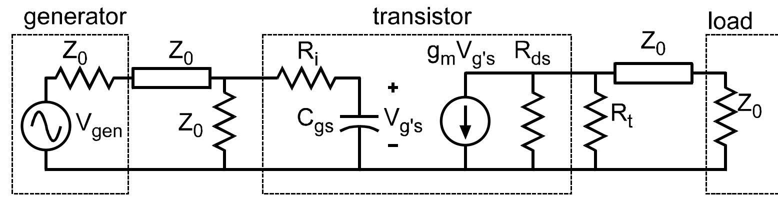


example

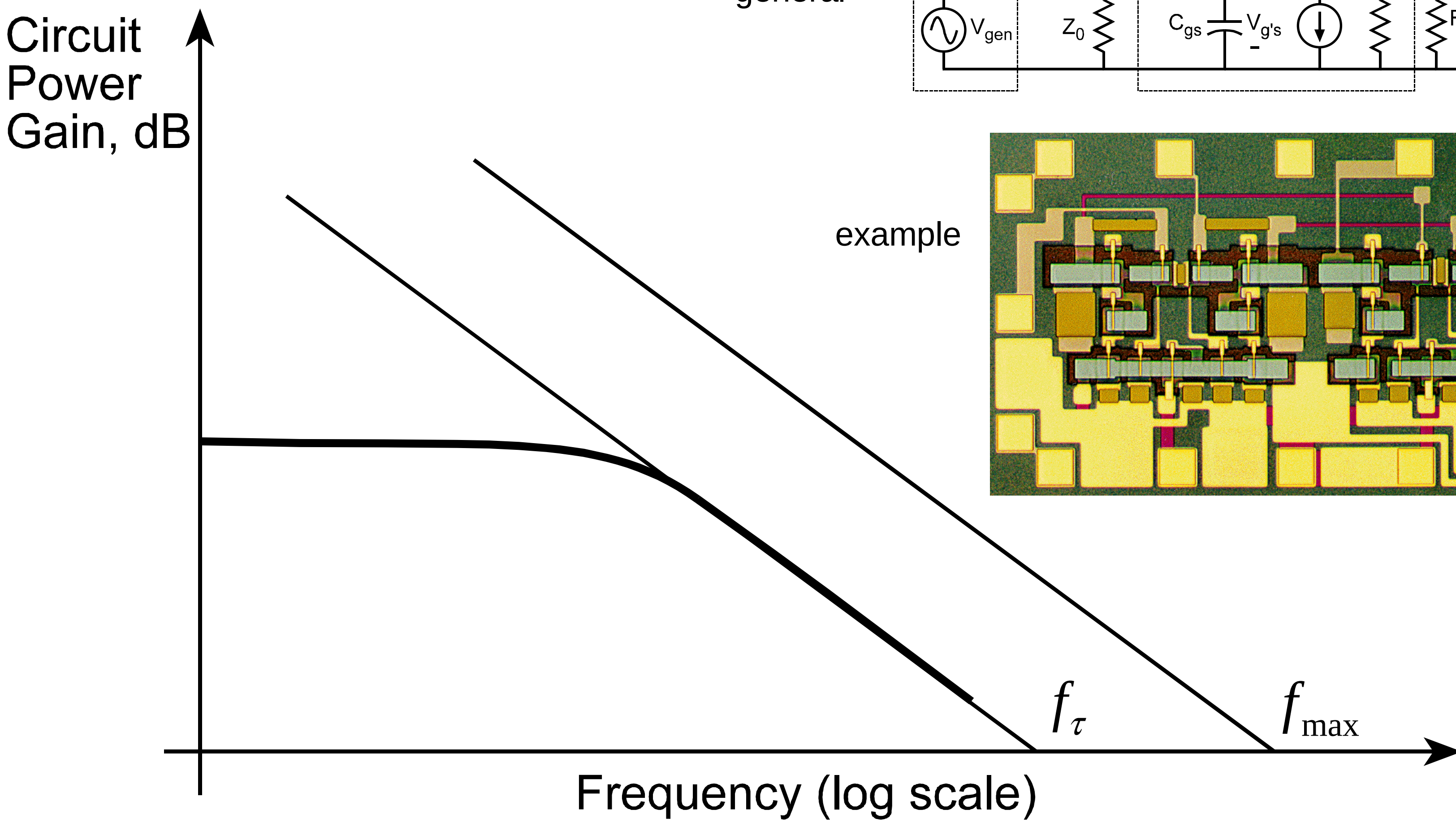


Advantage: simple elemenatry circuit --> suitable for building complex ICs

Limitation: gain-bandwidth products << transistor power-gain cutoff frequency

# Representative Resistive-Loaded Circuits

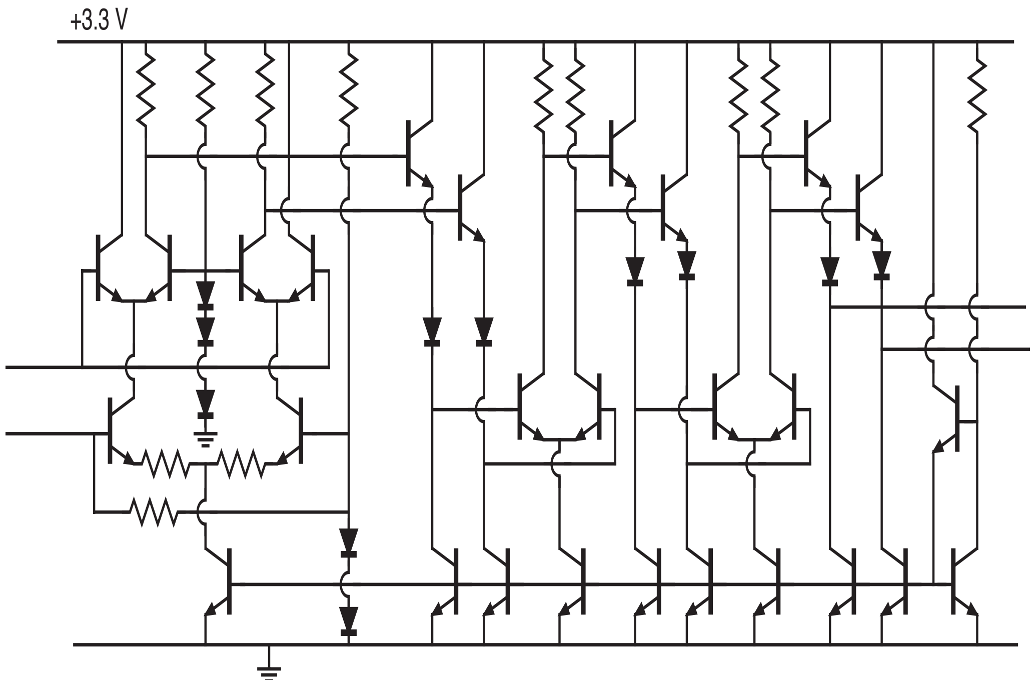


Broadband AGC amplifier for fiber-optic receiver

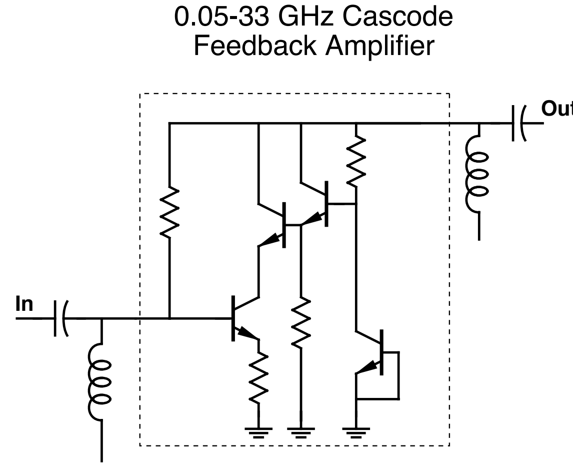


Broadband single-stage resistive feedback amplifier

Stage gain-bandwidth products at or below ft.

# Reactively-Matched Transistor Circuits 1

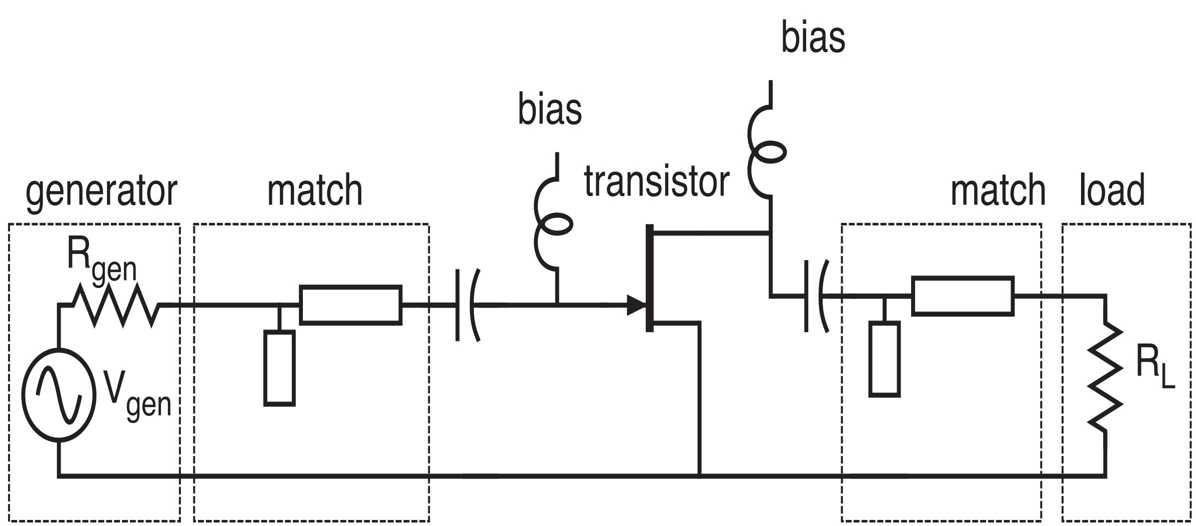


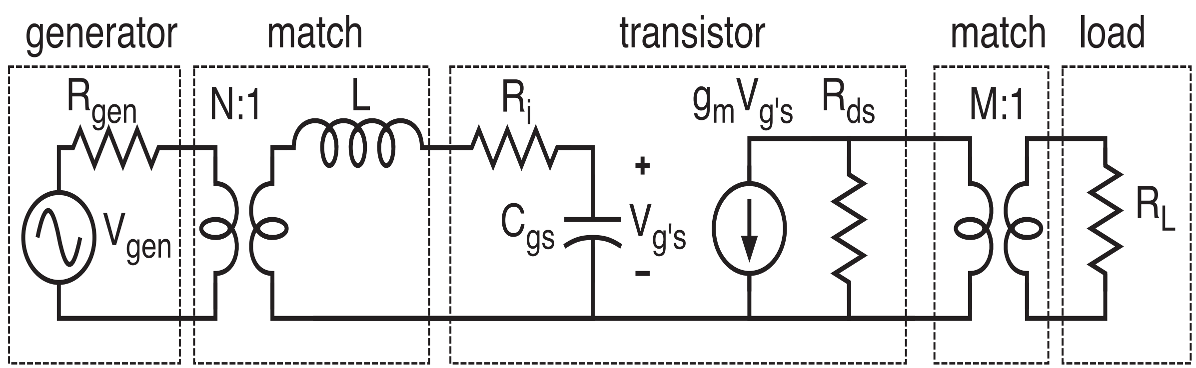


•Tuning networks on transistor input and output provide maximum power transfer, power gain obtained is maximum available from device.

*Tuning (impedance-matching) network are fundamentally narrowband (Fano's inequality)

Maximum available gain is obtained from the transistor, but only over a small frequency range.

# Reactively-Matched Transistor Circuits 2

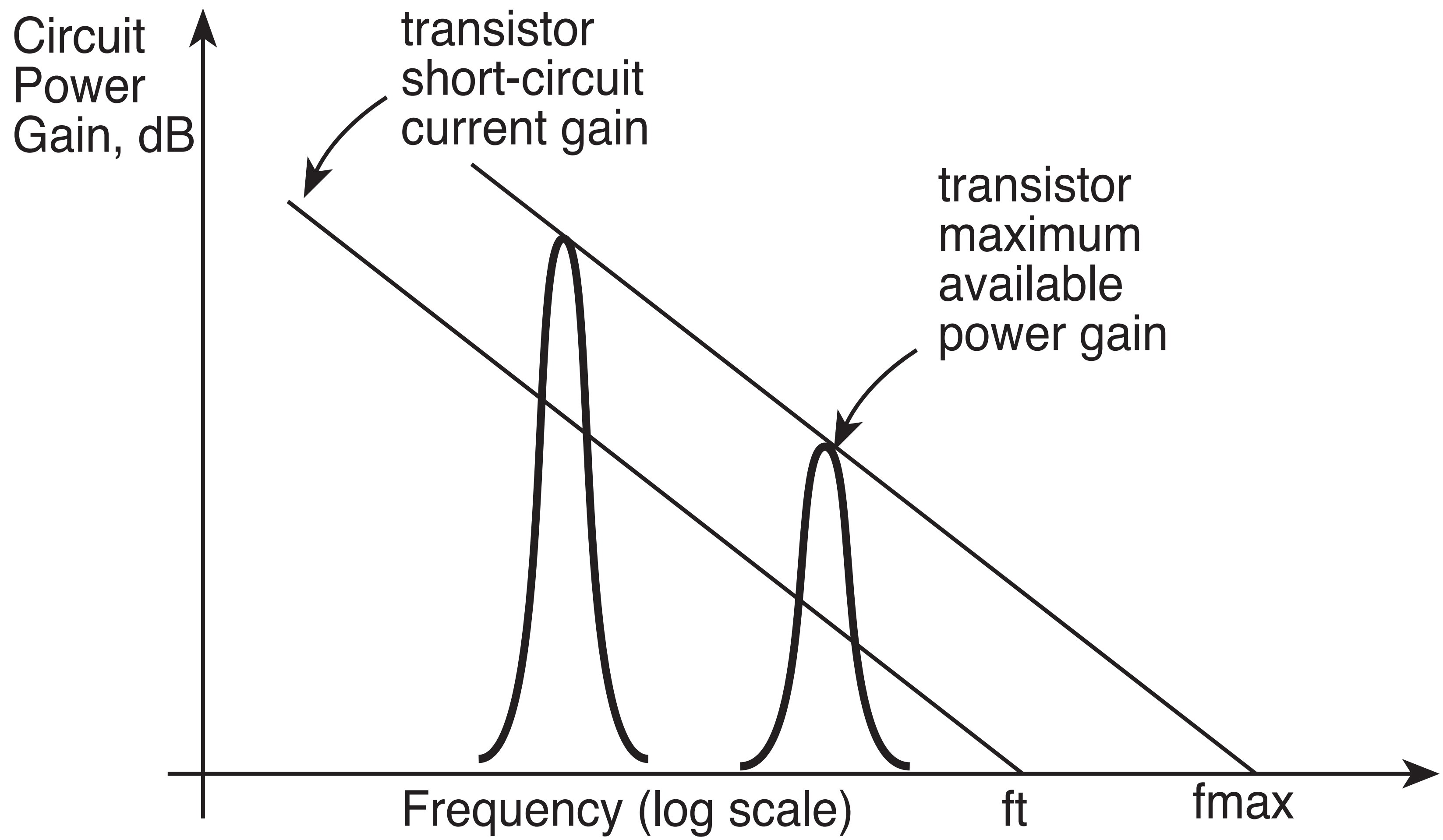


- Transistor maximum available power gain obtained over narrow bandwidth
- Accptable for narrow-band applications, not for broaband or digital

# Classes of Circuits: Reactively Tuned

general

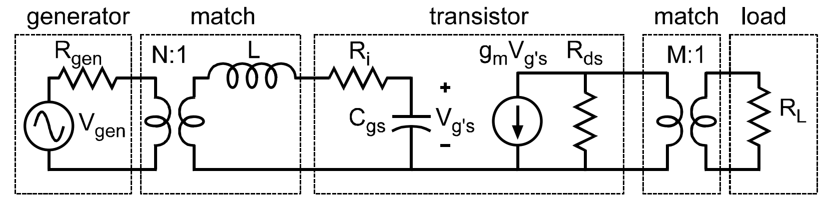


example

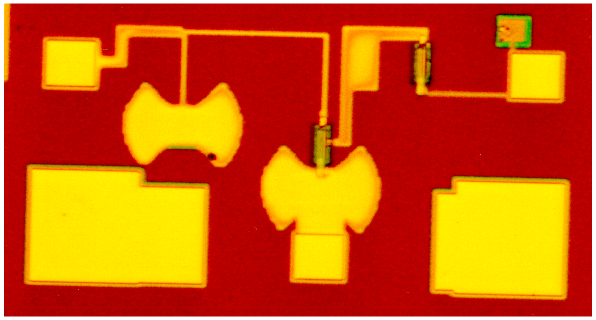

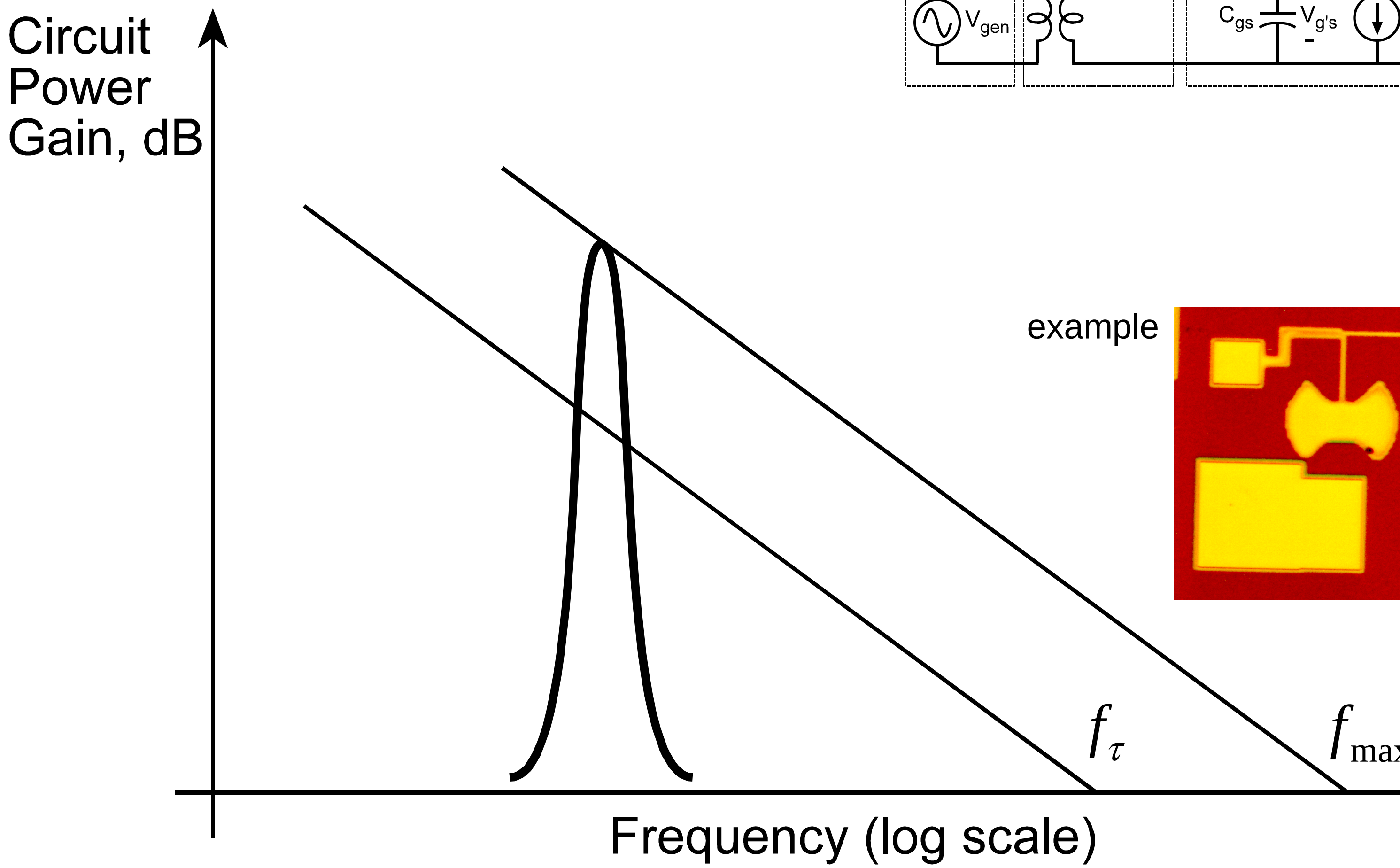


Advantage: gain equal to maximum available….over maximum bandwidth of ~ ft

Limitations: bandpass characteristics, large dimensions of tuning networks

# Distributed Circuits 1

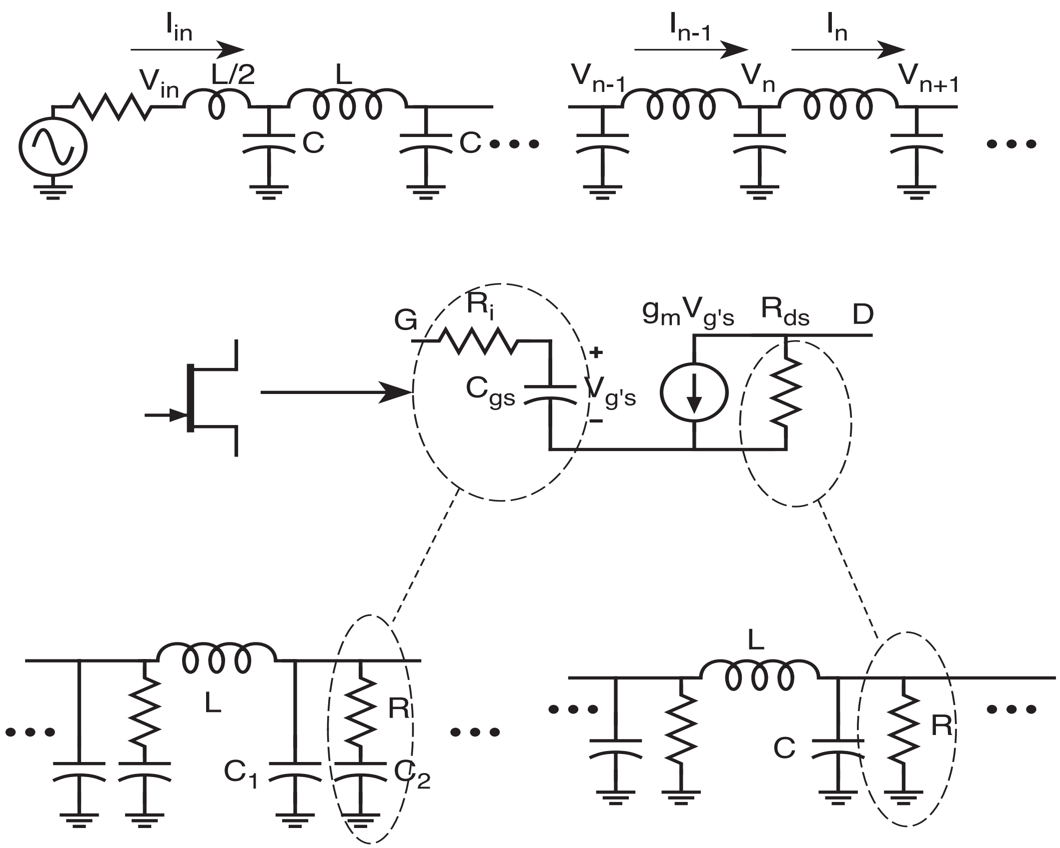


- A ladder network of Ls and Cs acts as a transmission line of impedance

$$Z_o = \sqrt{L / C}$$

...for frequencies below its Bragg frequency

$$f_{Bragg} = 1 / \pi\sqrt{LC}$$

- Transistor capacitances absorbed into synthetic transmission lines.
- Transistor resistance introduce transmission-line losses

- Distributed networks eliminate capacitance charging time as performance limit
- Line losses (caused by transistor fundamental, power-dissipating parasitics)- limits performance by introducing line losses.

# Distributed Circuits 2

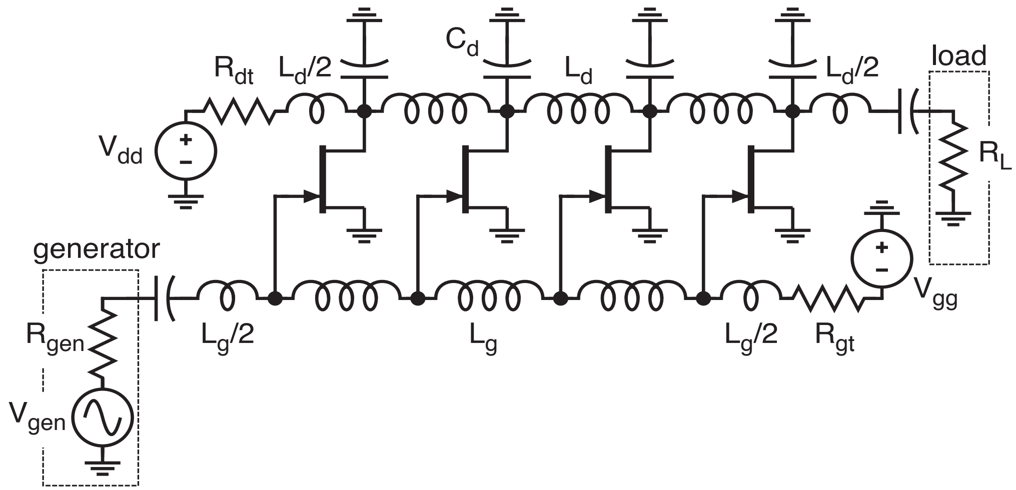


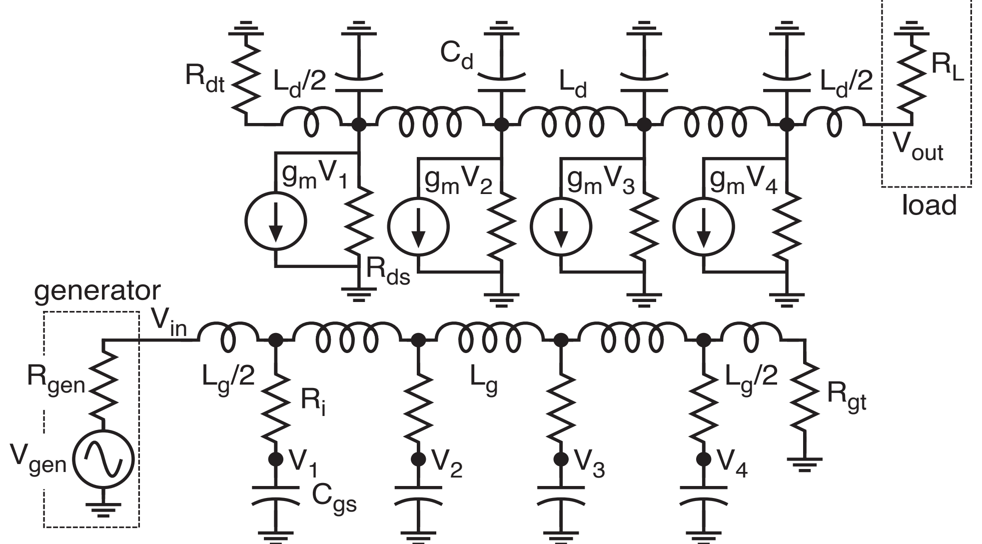


FET traveling-wave amplifier

- FET capacitances absorbed into synthetic lines.
- Capacitance charging times eliminated
- Feasible gain-bandwidth determined by gate, drain line losses
- Losses result from FET resistive parasitics.
- These resistive parasitics also determine FET fmax.

- Under idealized conditions, circuit gain-bandwidth product approaches transistor fmax.

# Distributed Circuits 3

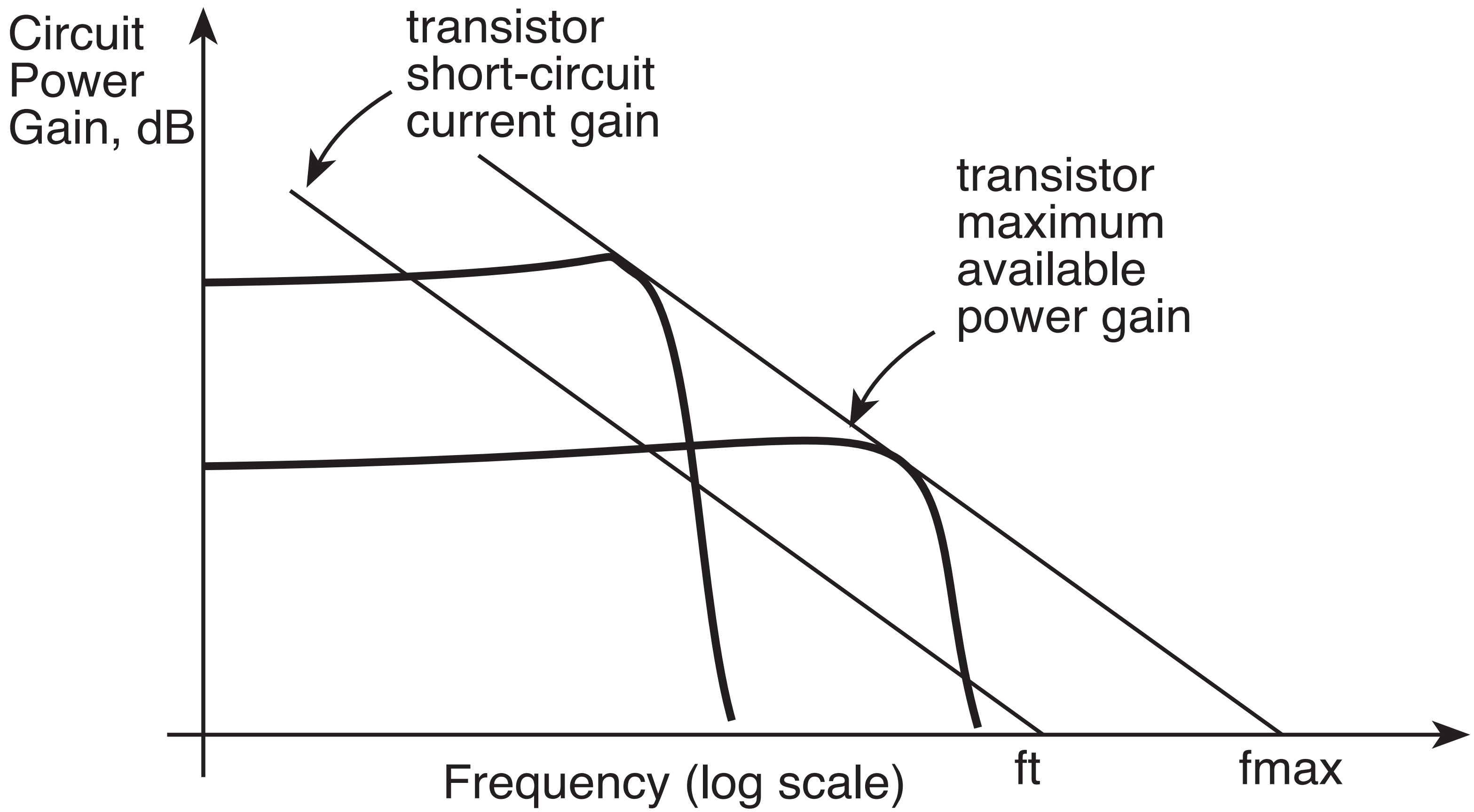


- Gain-bandwidth product can approach transistor power-gain cutoff frequency
- Somewhat idealized discussion: Real TWAs often limited somewhat below fmax if one is not free to choose generator & load impedance independently
- Gain-bandwidth very close to fmax always obtainable by capacitive division.

# Classes of Circuits: Distributed

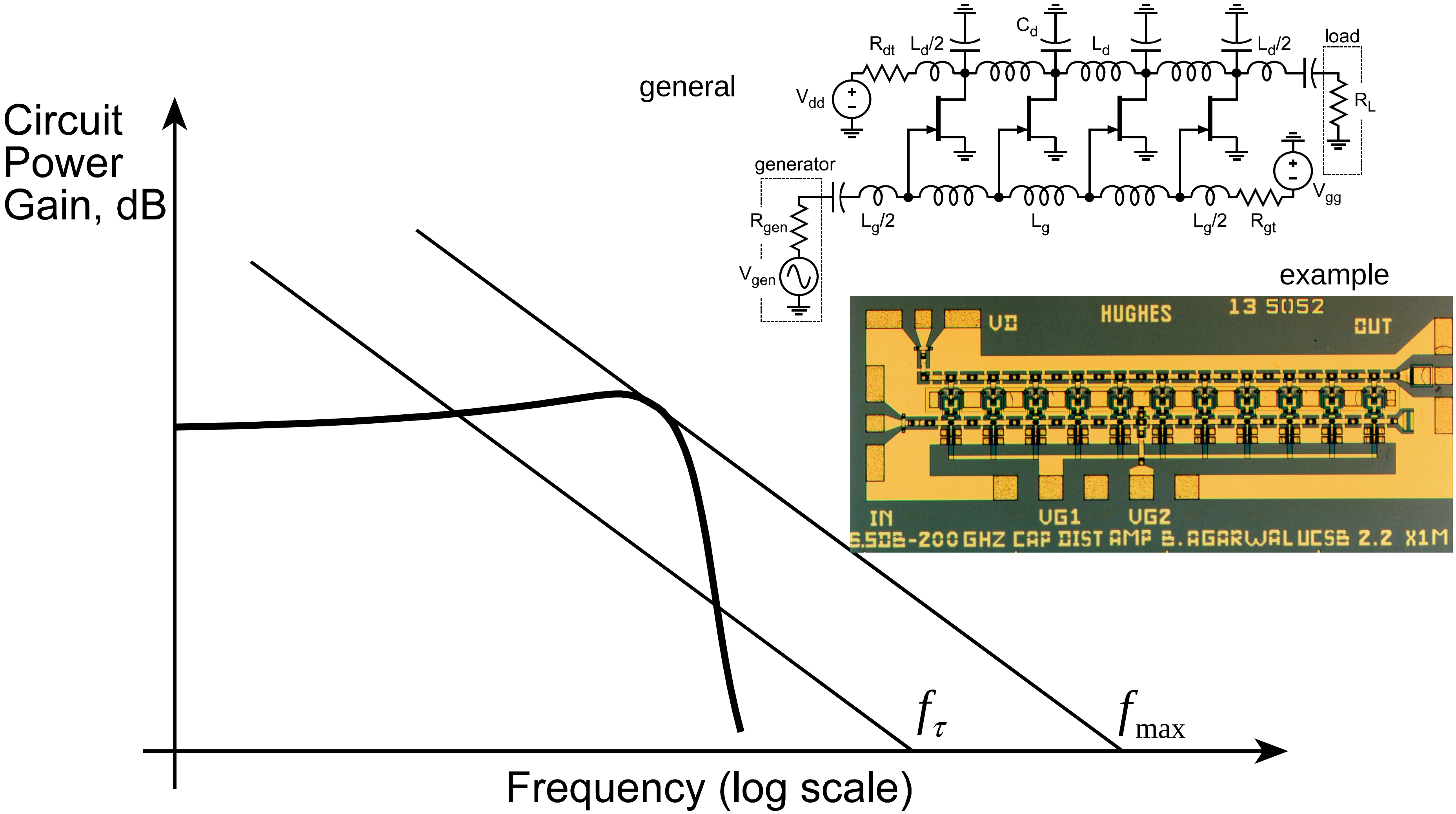


Advantage: gain-bandwidth products equal to transistor fmax

Limitation: size and complexity, signal delay renders unusable for logic, feedback

# Capacitive-Division Traveling-Wave Amplifiers

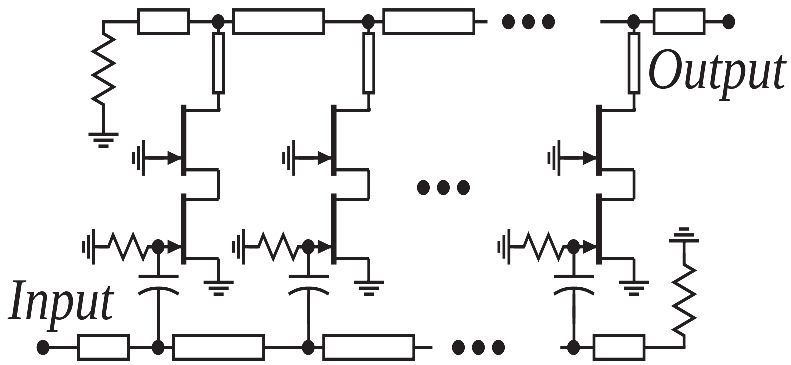


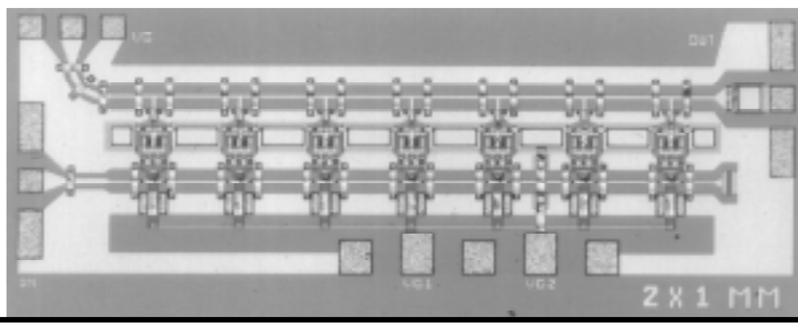


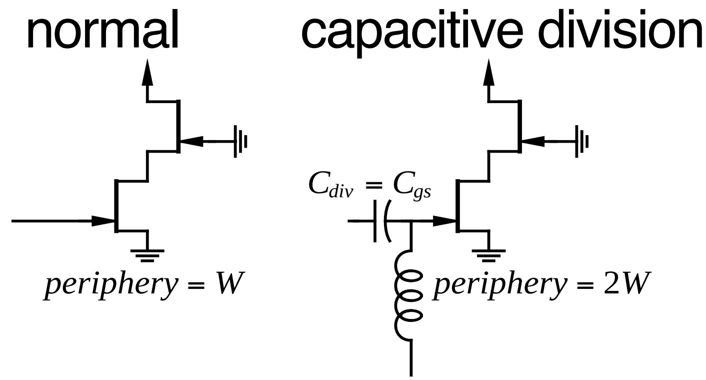


same transconductance,
same input capacitance,
but 2:1 improved series input resistance: increases bandwidth

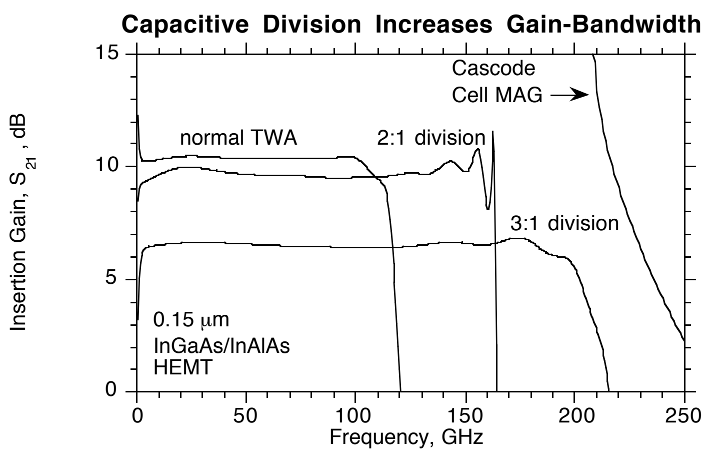


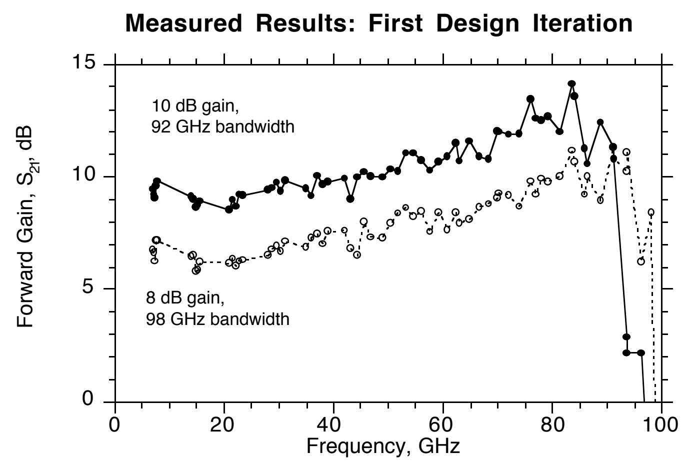

# 155 GHz HEMT Distributed Amplifier

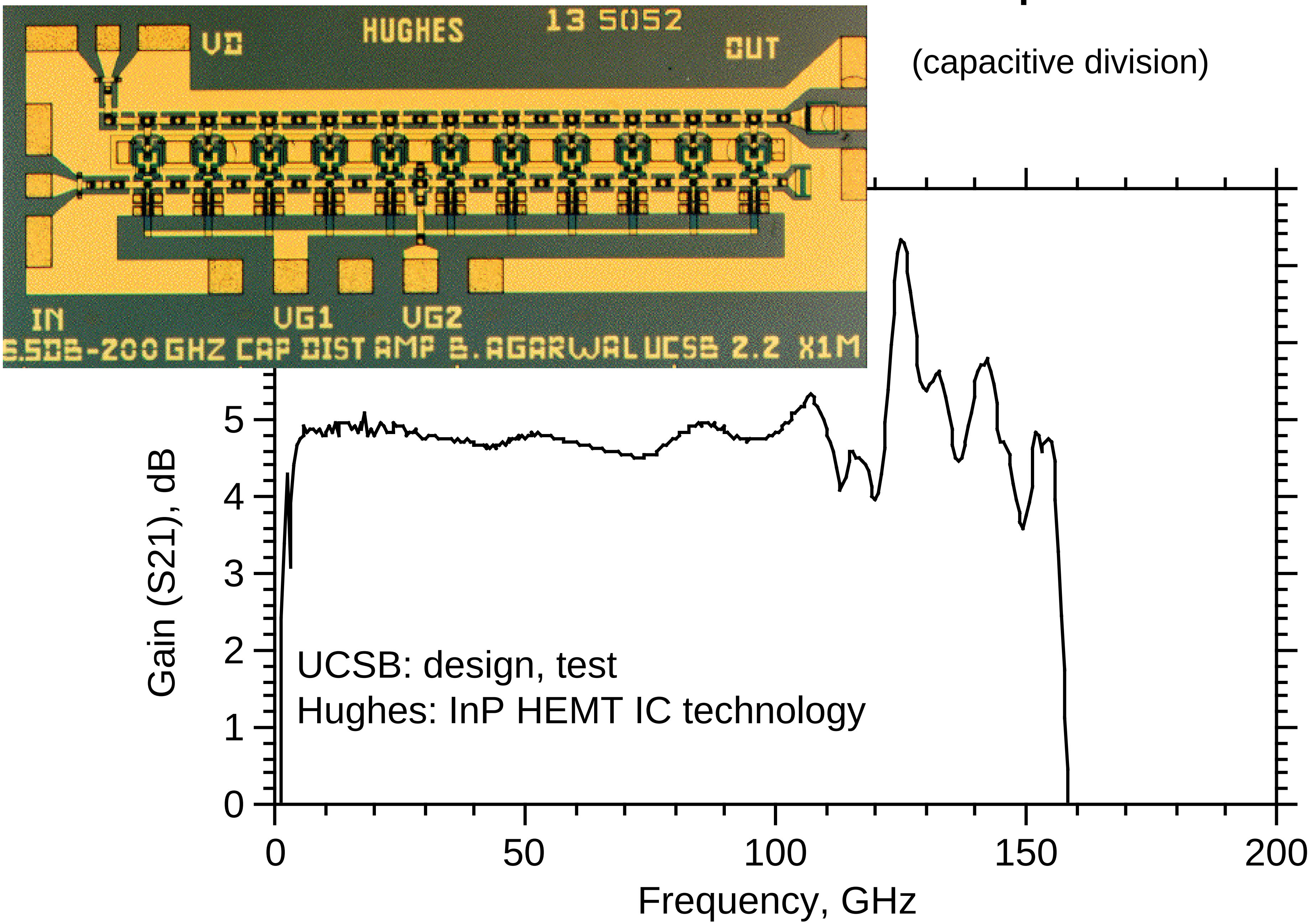

# $F_t$ multiplier: Principle of Operation

## Simple Stage

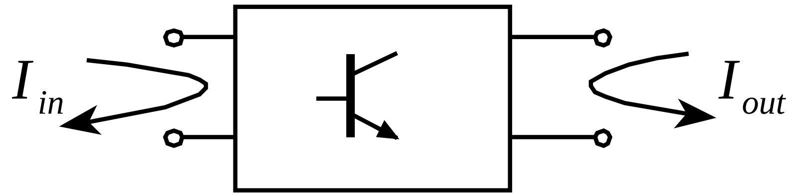


$$\frac{I_{out}}{I_{in}} = \frac{1}{j}\left(\frac{f_\tau}{f}\right)$$

## $f_t$ Doubler

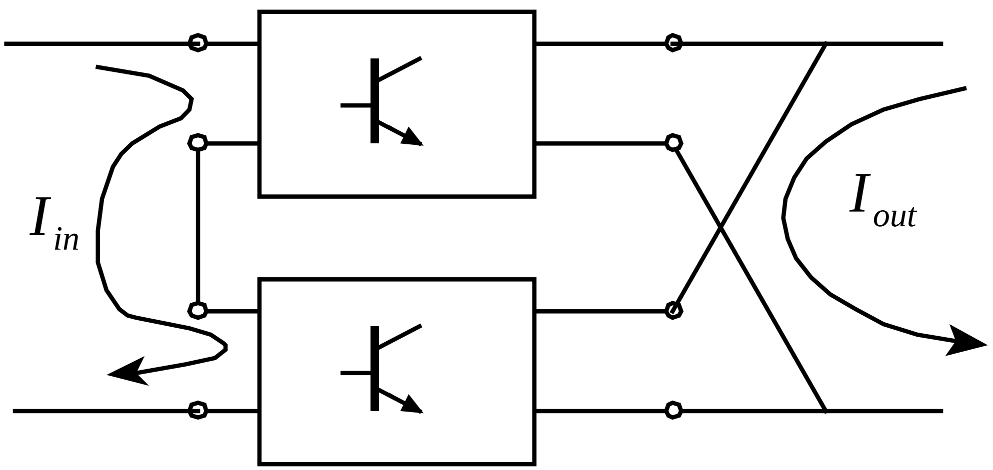


$$\frac{I_{out}}{I_{in}} = \frac{1}{j}\left(2 \cdot \frac{f_\tau}{f}\right)$$

*Inputs connected in series, outputs connected in parallel*
*output currents add*
*current gain is twice that of single stage, $f_t$ is doubled*

# $f_t$ Doublers: Implementation

Differential Pair

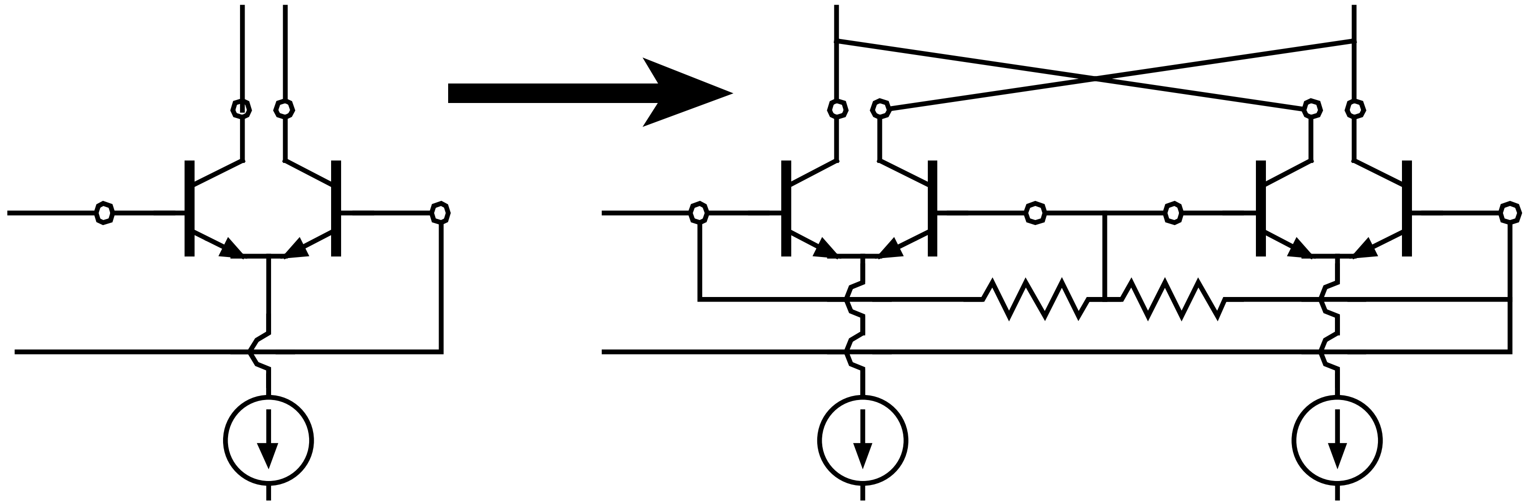

Single-ended (and emitter-follower)

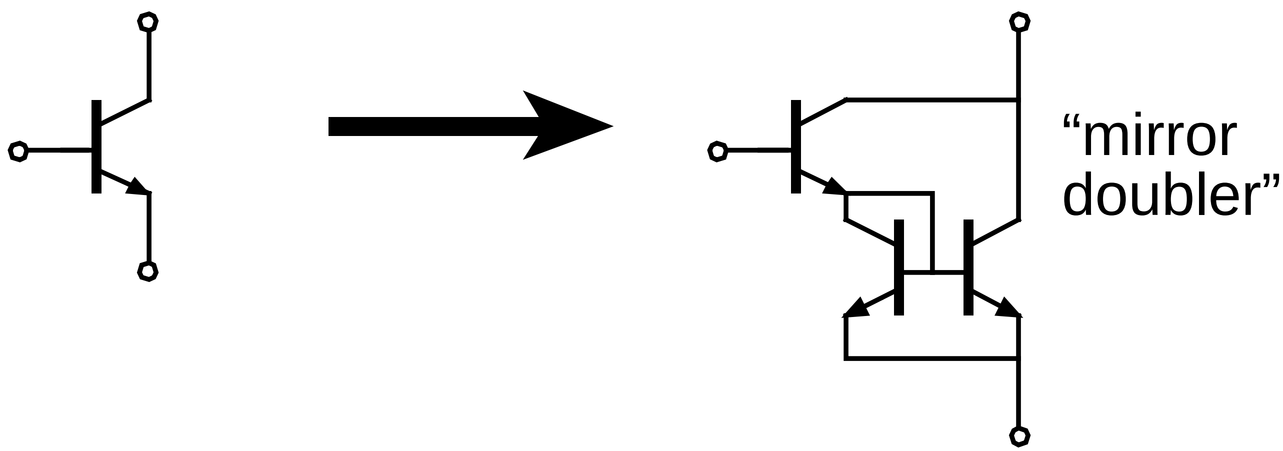

# Circuit Gain-bandwidth Limits: $F_t$ and $F_{max}$

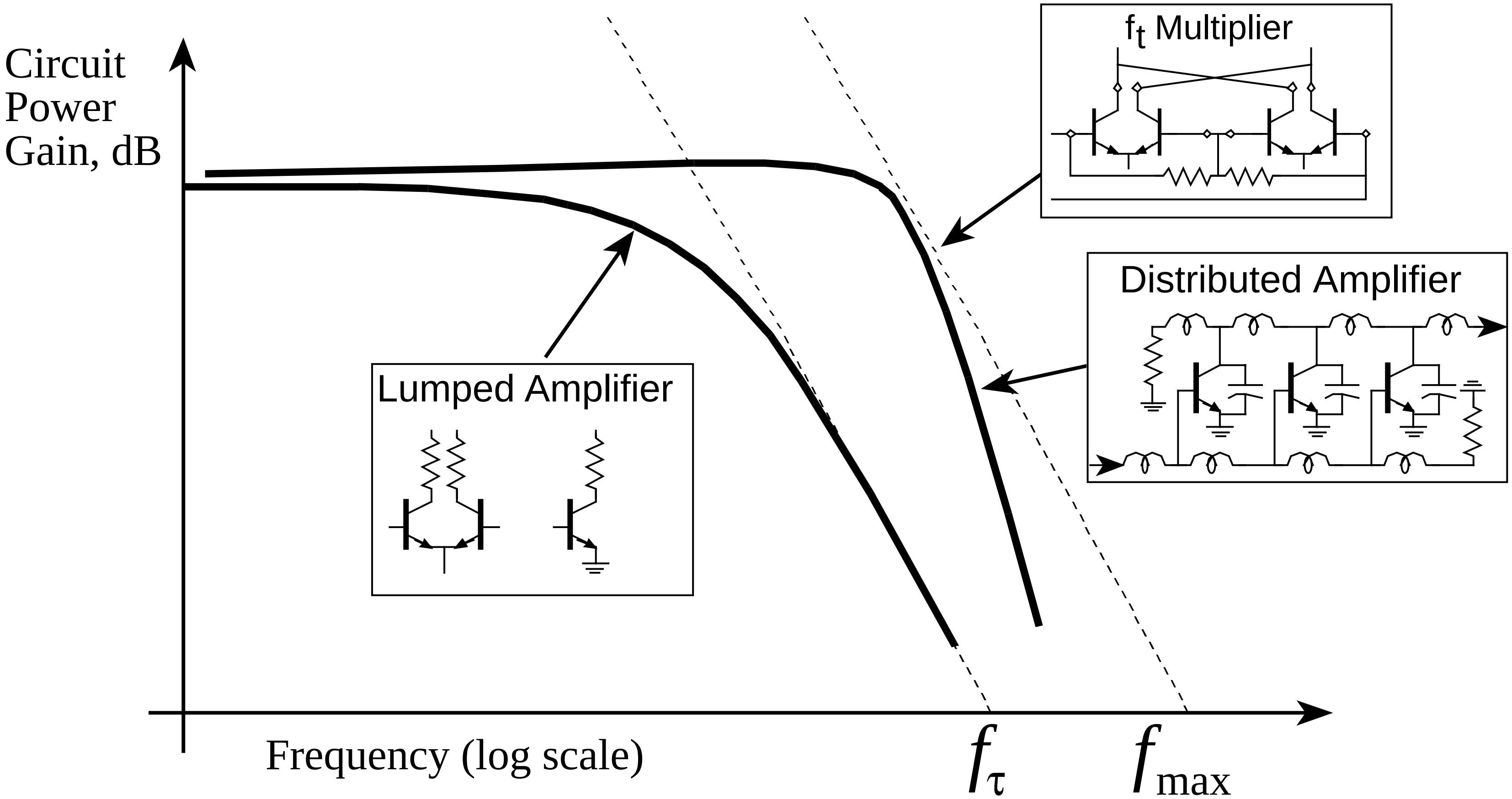


Lumped circuits: limited by $f_{max}$ and $f_t$

Distributed circuits: limited only by $f_{max}$

*$f_t$ multipliers: also limited only by $f_{max}$*

# Observations: High Frequency Circuit Design

Current-gain cutoff frequency
determined by carrier transit times

Power gain cutoff frequency
*also* determined by RC charging parasitics

Reactively tuned circuits: classical microwave design
narrow bandwidths, big circuits

Distributed circuits:
“optimal” , but complexity & delay serious limits

Resistively loaded circuits: classical analog design
circuit bandwidths below transistor limits
*ft-muliplier brings bandwidths close to fmax-limit*

# Nonlinear Wave Propagation Devices

Shock-wave nonlinear transmission lines
NLTL-gated diode sampling circuits
Soliton NLTL impulse compressors & frequency multipliers
Traveling-Wave RTD pulse generators

These devices exploit distibuted circuit priciples presented above
General principle: use of distributed circuit yeilds performance determined by fundamental limits of the semiconductor device, rather than capacitance charging times.

# NLTL Techology

Subpicosecond electronic pulse generation & detection

Principles of operation: nonlinear wave propagation

Basis of performance: THz bandwidth of Schottky diodes

- Shock-wave NLTLs
- Soliton NLTLs
- Diode sampling circuits

Bandwidths now ≈700-1000 GHz, ≈0.3–0.5 ps pulses
Technological limit is at ≈2-3 times greater bandwidth.

# Electrical Sampling Circuits

Used in Sampling Oscilloscopes, TDRs, and network analyzers

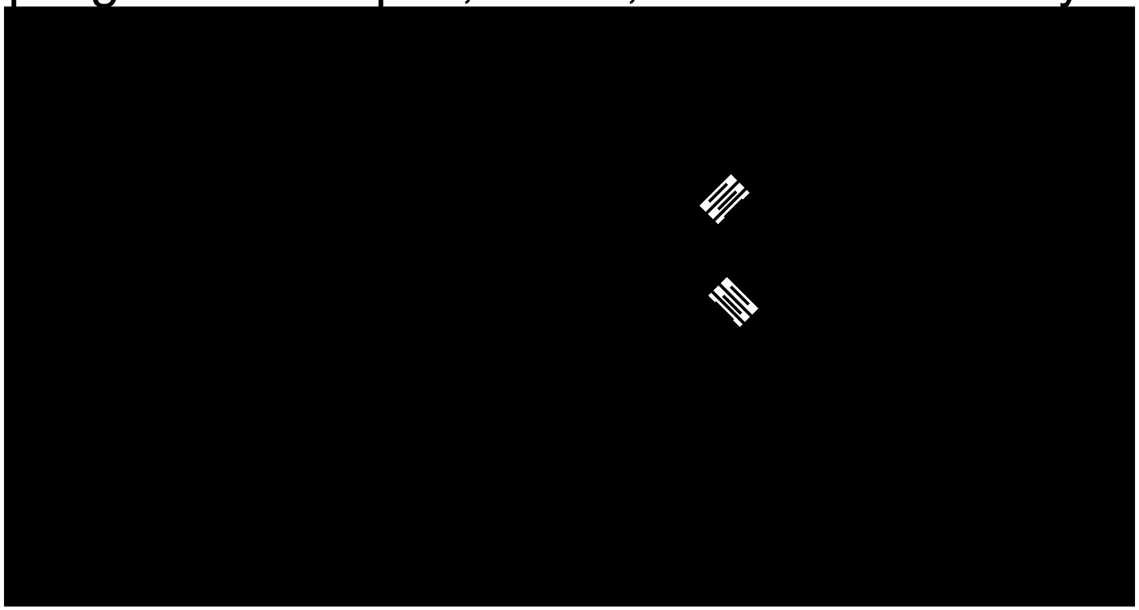

**R·C Risetime at Input**

$$T_{RC} = 2.2\left(\frac{Z_0}{2}\right)\left(2C_{Diode}\right)$$

**Aperture Risetime**

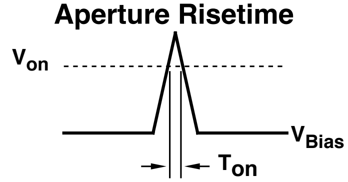


**Total Effective Risetime**

$$T_{EFF} = \sqrt{T_{ON}^2 + T_{RC}^2}$$

Schottky diodes are readily made with ≈5 fF junction capacitance and ≈2 THz R-C cutoff frequencies. The primary bandwidth limitation of sampling circuits is thus the duration of the strobe pulse used to gate the diodes. Previously, silicon step-recovery diodes (≈25 ps $T_f$) had been used.

# Stucture and Equivalent Circuit of NLTL

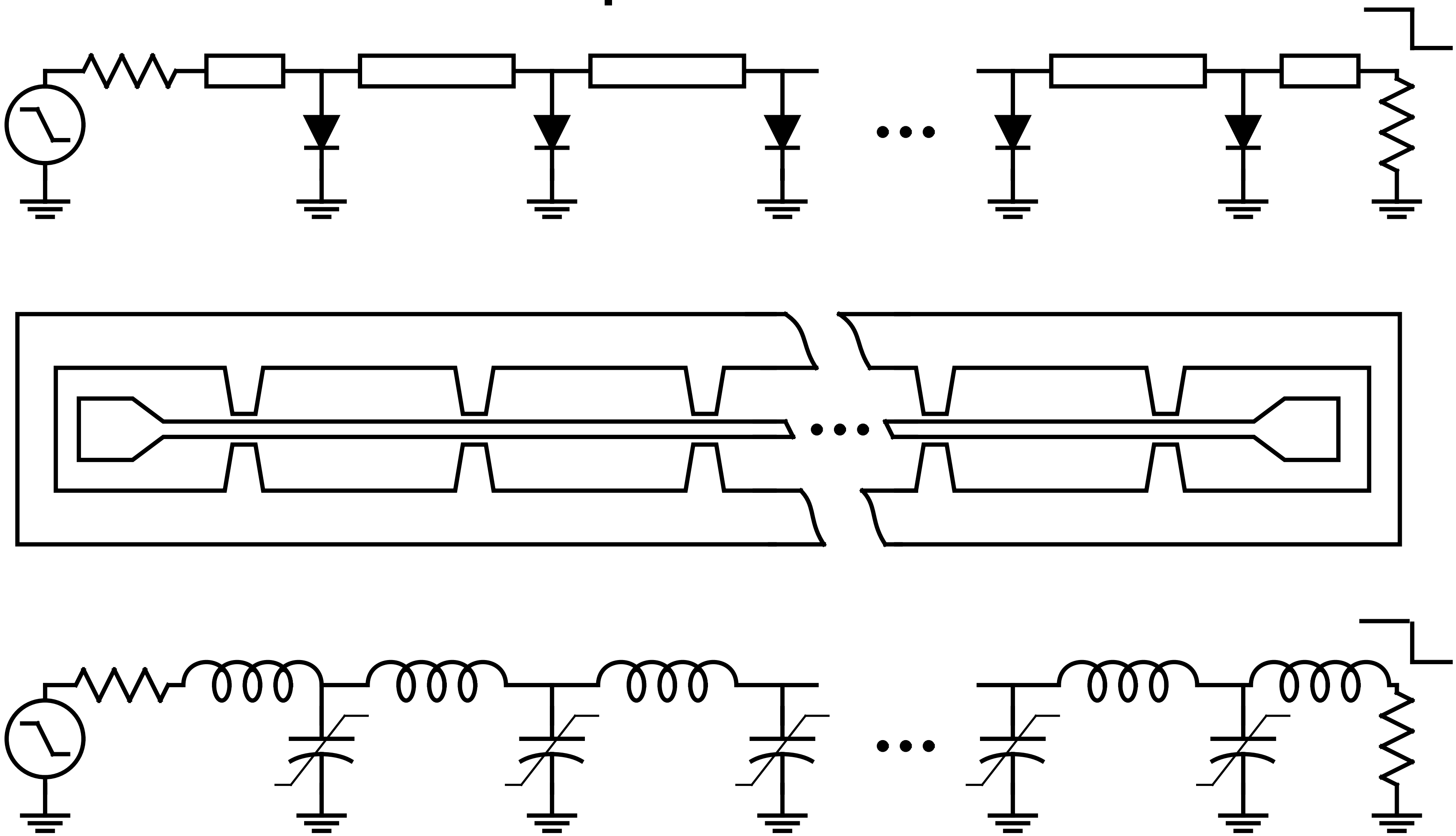

# Wavefront Compression by NLTL

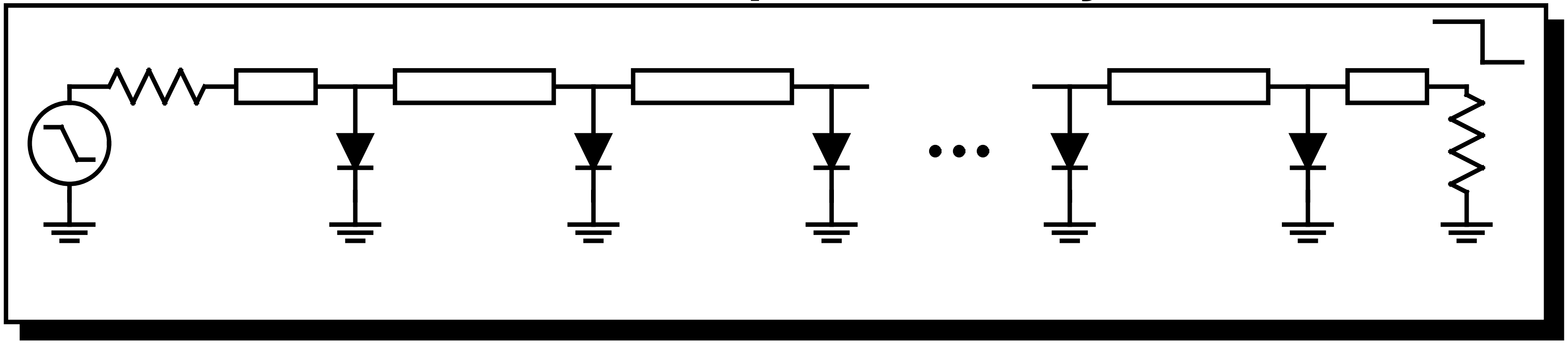

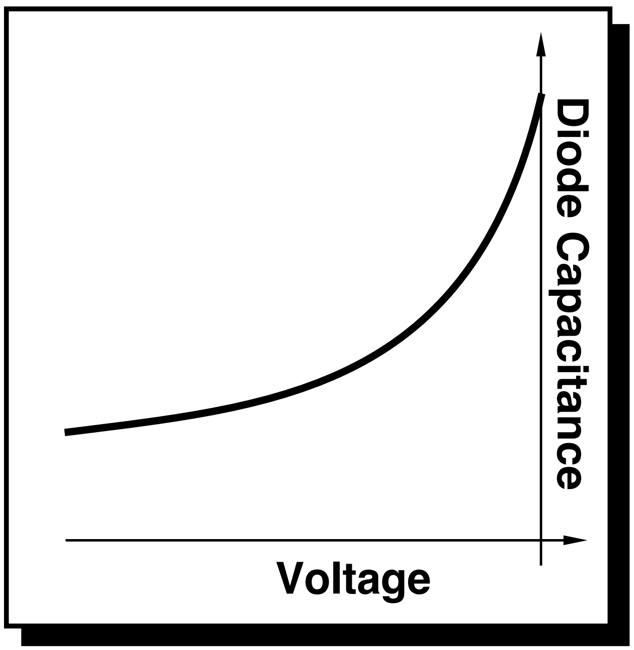


$$T_{delay} = \sqrt{L(C_{diode} + C_{line})}$$

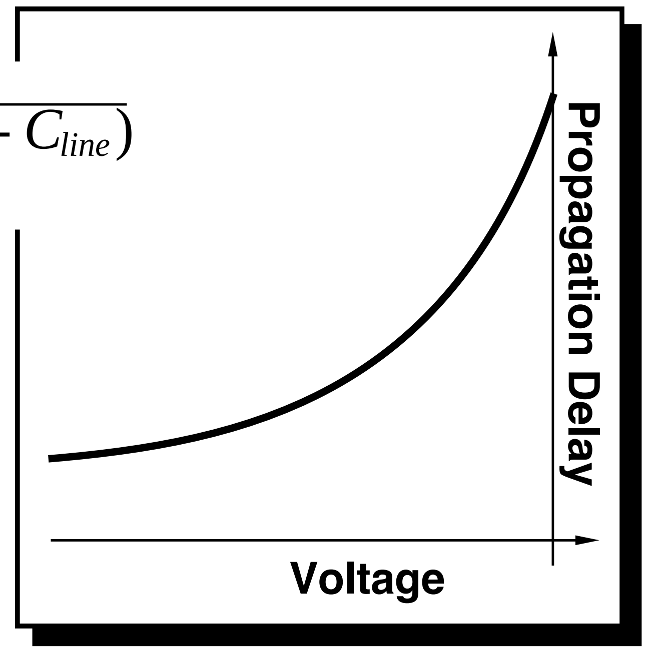

# SPICE Simulation of Shock formation

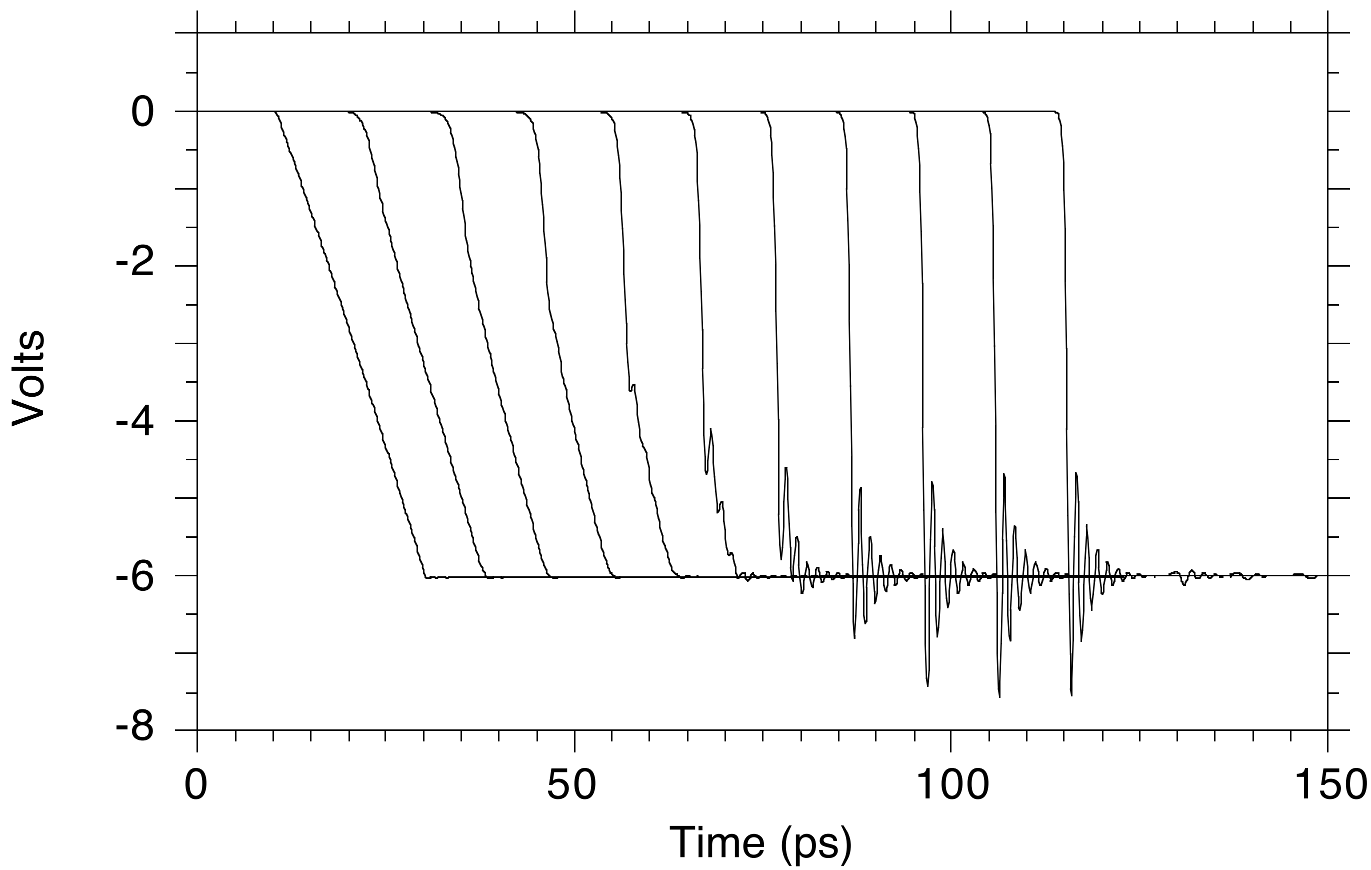

## Limits to NLTL Shock-Wave Transition Time

• Periodic-Network (Bragg) Frequency

The periodic structure results in a sharp filter cutoff inversely proportional to the diode spacing. WIthin lithographic limits, this can easily be 1-2 THz.

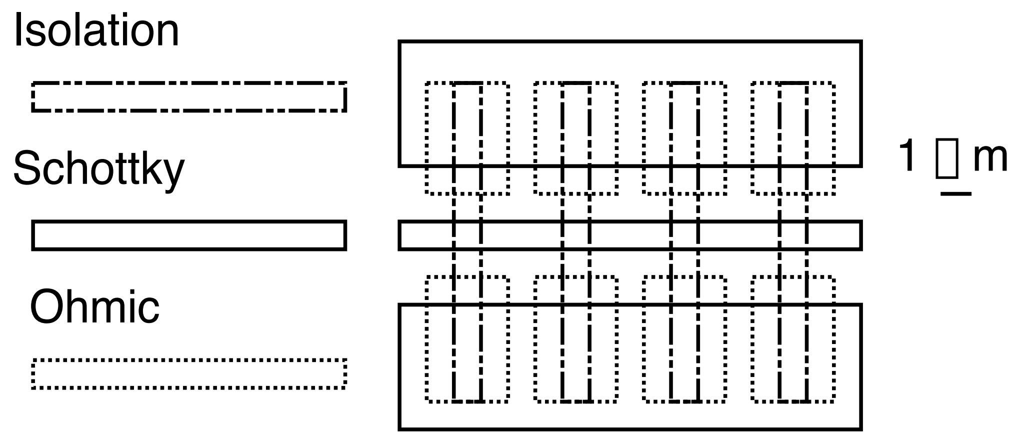


•Diode Cutoff Frequency

The fundamental limit of the technology.

Falltime limited to $T_f f_{diode} = 1.4\,ps \cdot THz$

10 THz diodes: 0.14 ps predicted shock-waves

# Shorted-Line Differentiator for Impulse Generation

## Symmetric Impulse Generation with CPW/CPS Balun/Differentiator

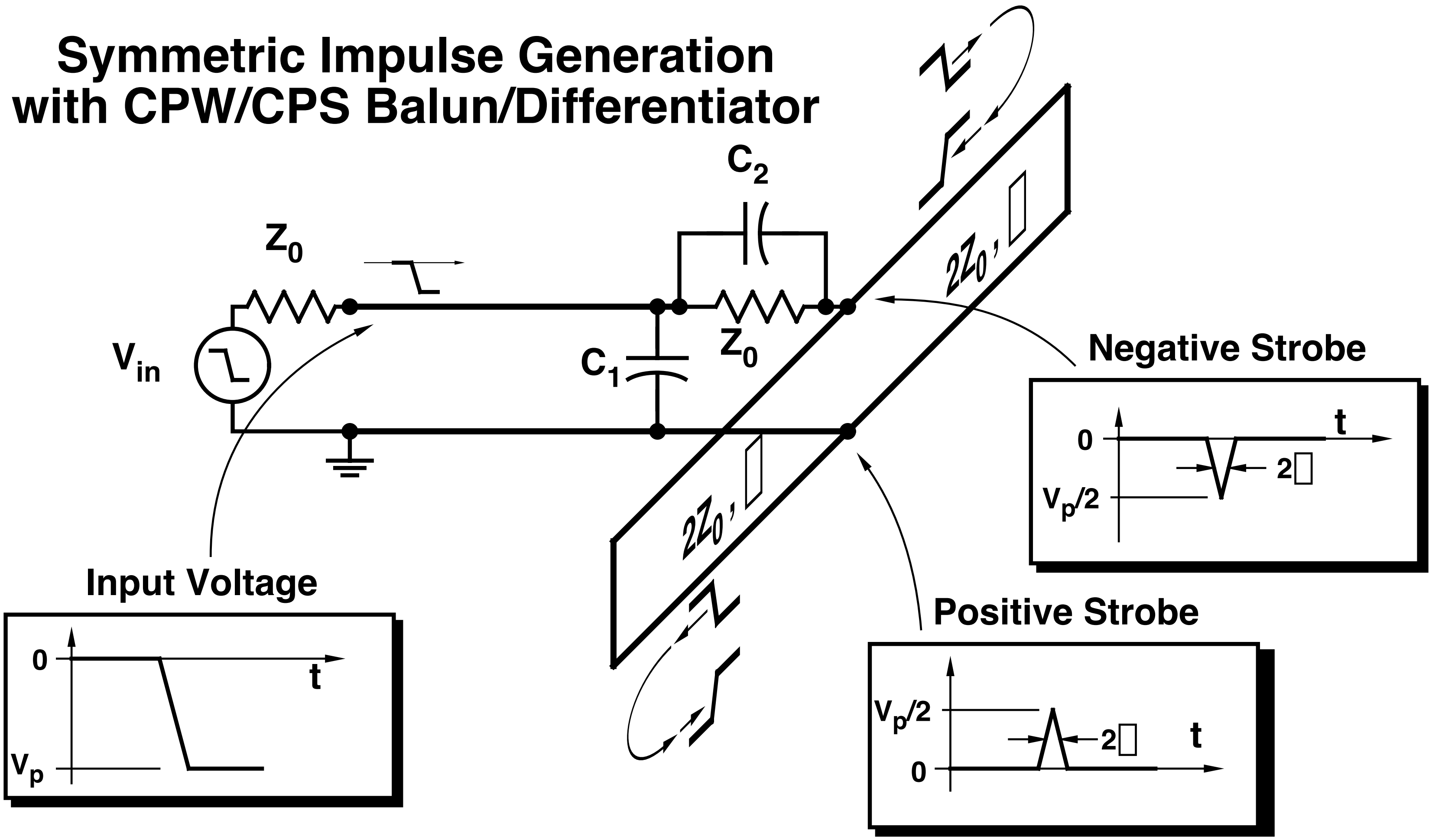

# NLTL-Strobed Sampling Circuit Layout

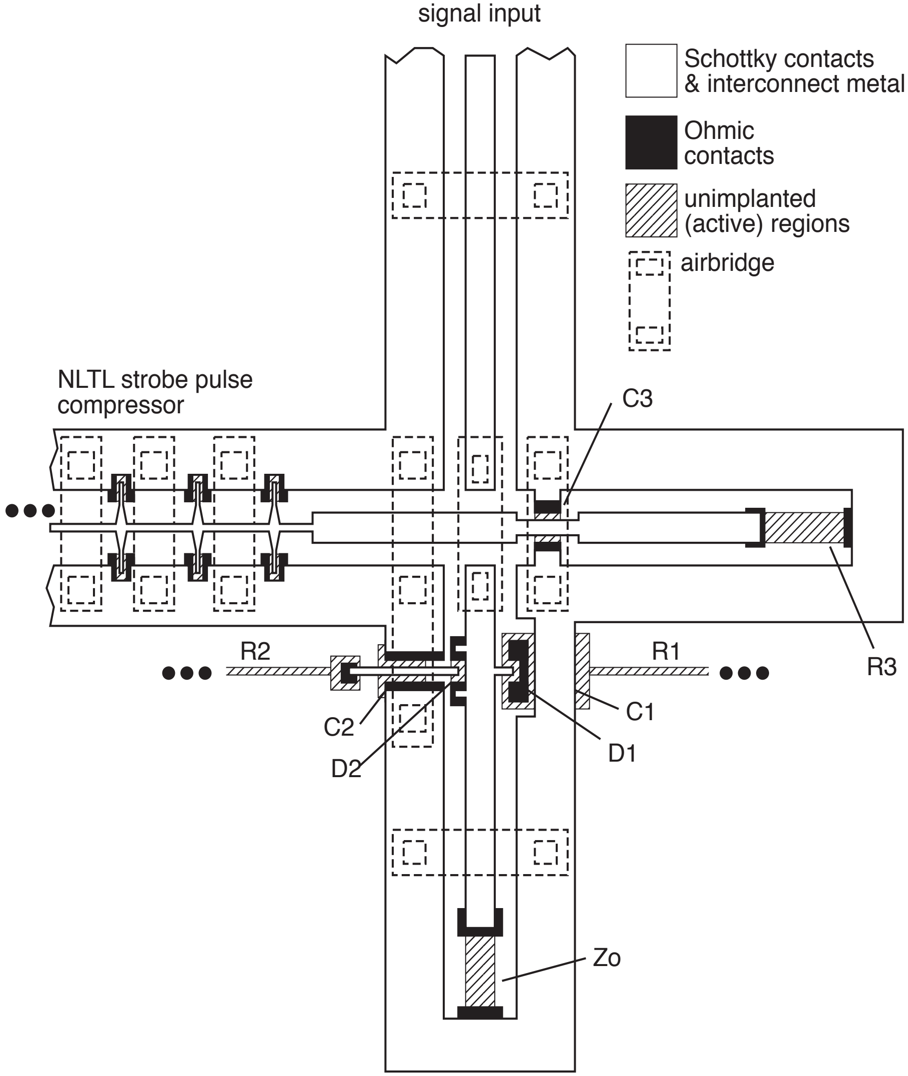


Implementation of the shorted line balun-differentiator exploits the deliberate excitation of CPS modes at the junction between two CPWs.

## NLTL-Strobed Sampling Circuit

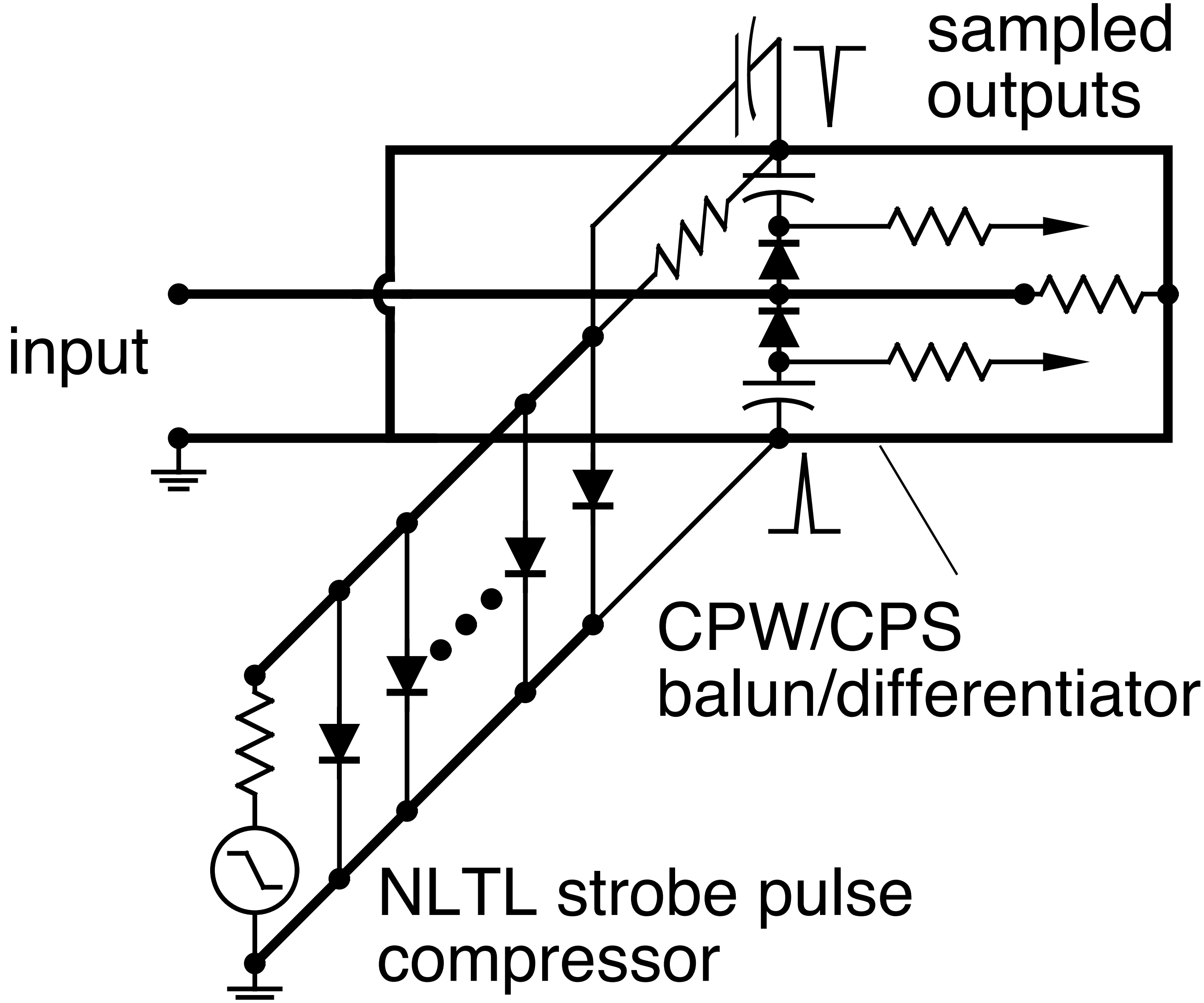

# NLTL output measured by sampling circuit

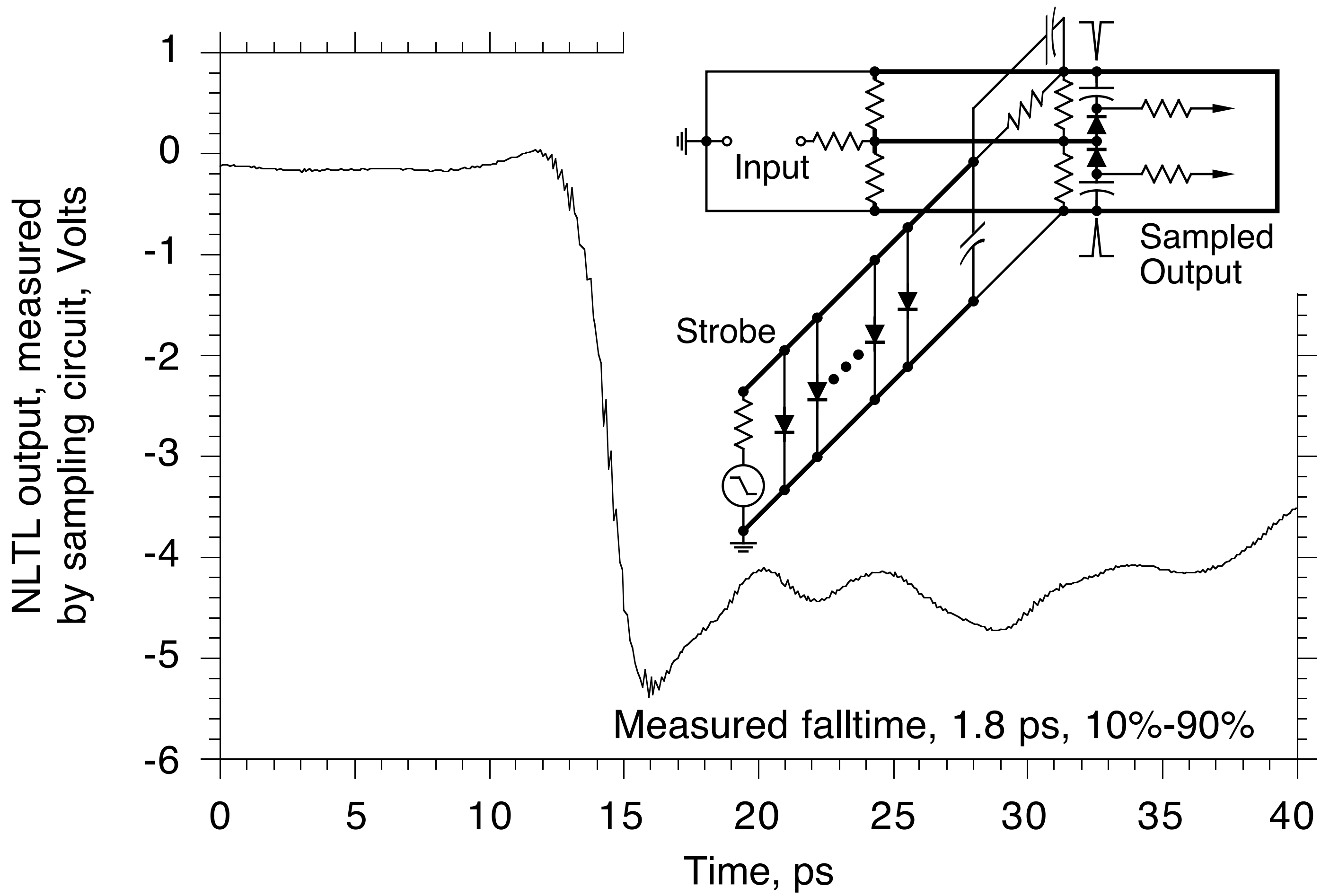

# Increasing NLTL bandwidth

- need increased diode cutoff frequency
- need increased Bragg Frequency.
  - small diodes at small spacings then causes problems:
  - narrow transmission lines with very high skin effect losses
  - diode spacing comparable to diode's physical size
  - diode-to- transmission line junction comparable to diode spacing
    - hence large junction (pad) parasitics
- difficulties mitigated using elevated coplanar waveguide with top-contacted diodes
  - high transmission line velocity increases diode spacings
  - low CPW dielectric constant: wide conductor, lower skin losses
  - diode contacted from TOP, junction (pad) parasistics eliminated

# Elevated CPW

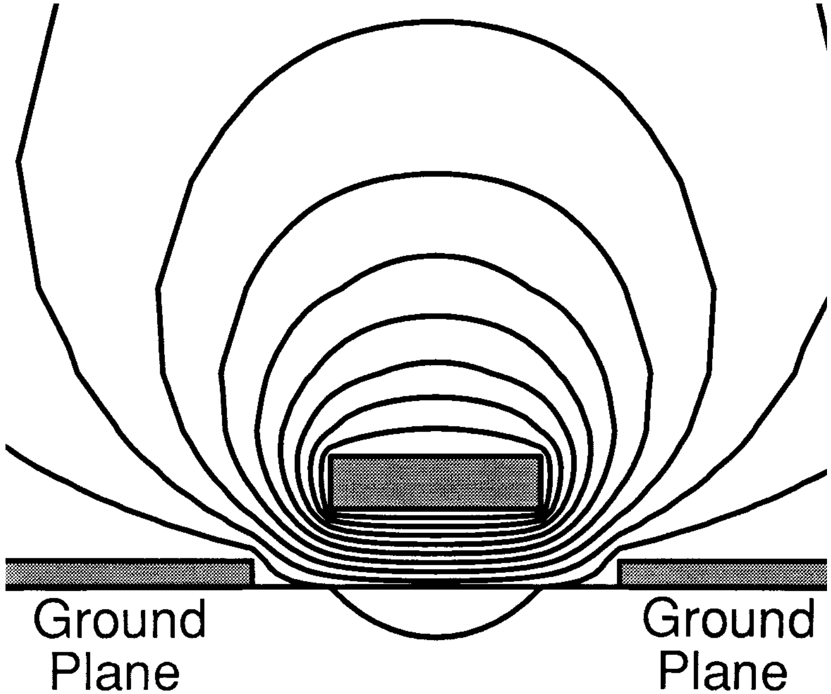


Transmission-line fields primarily in air.

Higher velocity.

Wider conductor needed for given Zo, hence lower skin-effect losses

Radiation losses lower (??) because of reduced field in substrate.

Less useful at lower frequencies: to be effective, conductor elevation must be comparable to conductor width. Lower-frequency (non-elevated) CPW can be made WIDER to reduce skin loss.

## Elevated CPW II

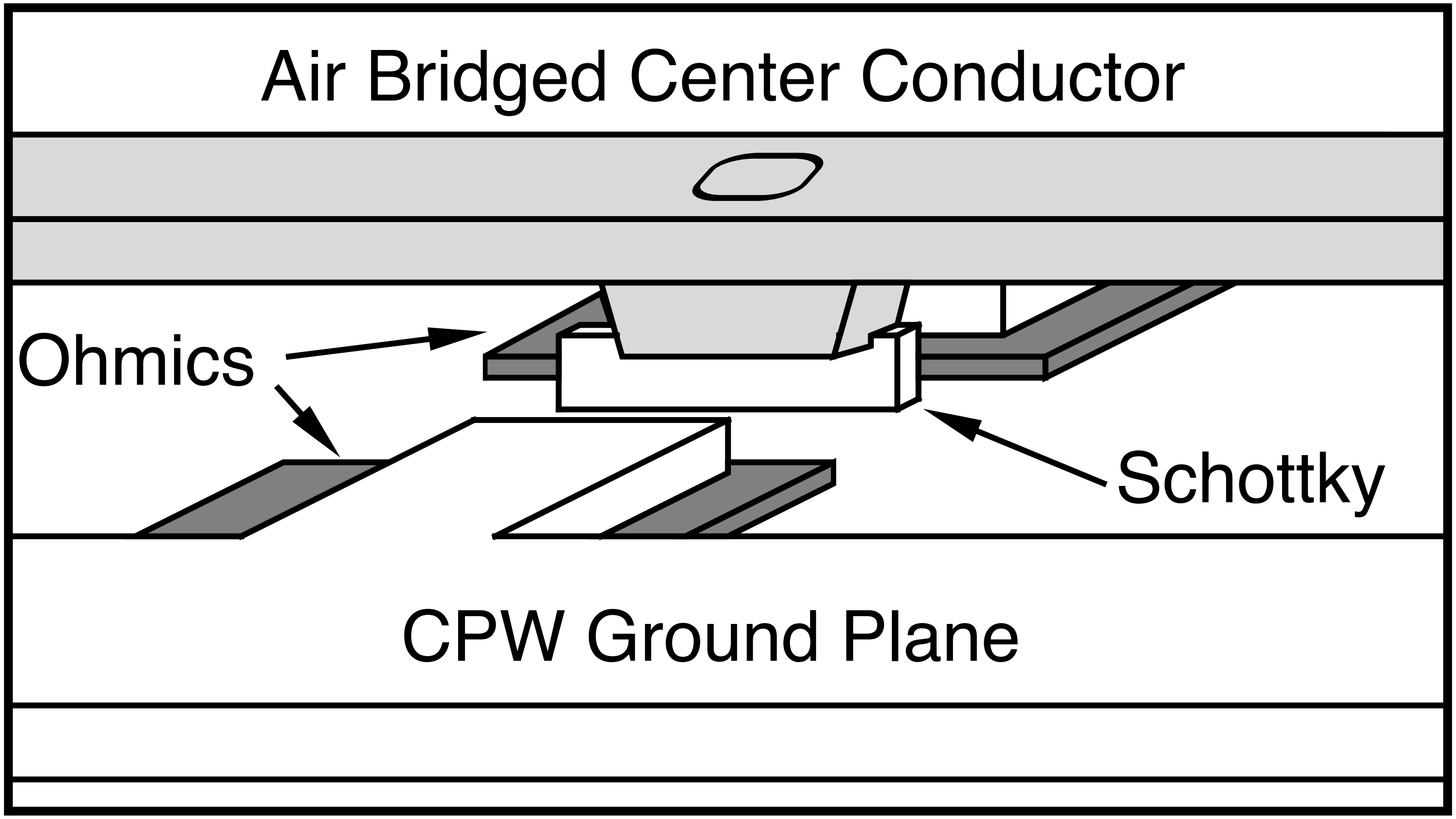


Perspective drawing showing the air bridged center conductor contacting the top of a diode. The Schottky contact is kept well away from the edge of the $H^+$ implanted region, which ends outside the ohmics.

## Elevated CPW III

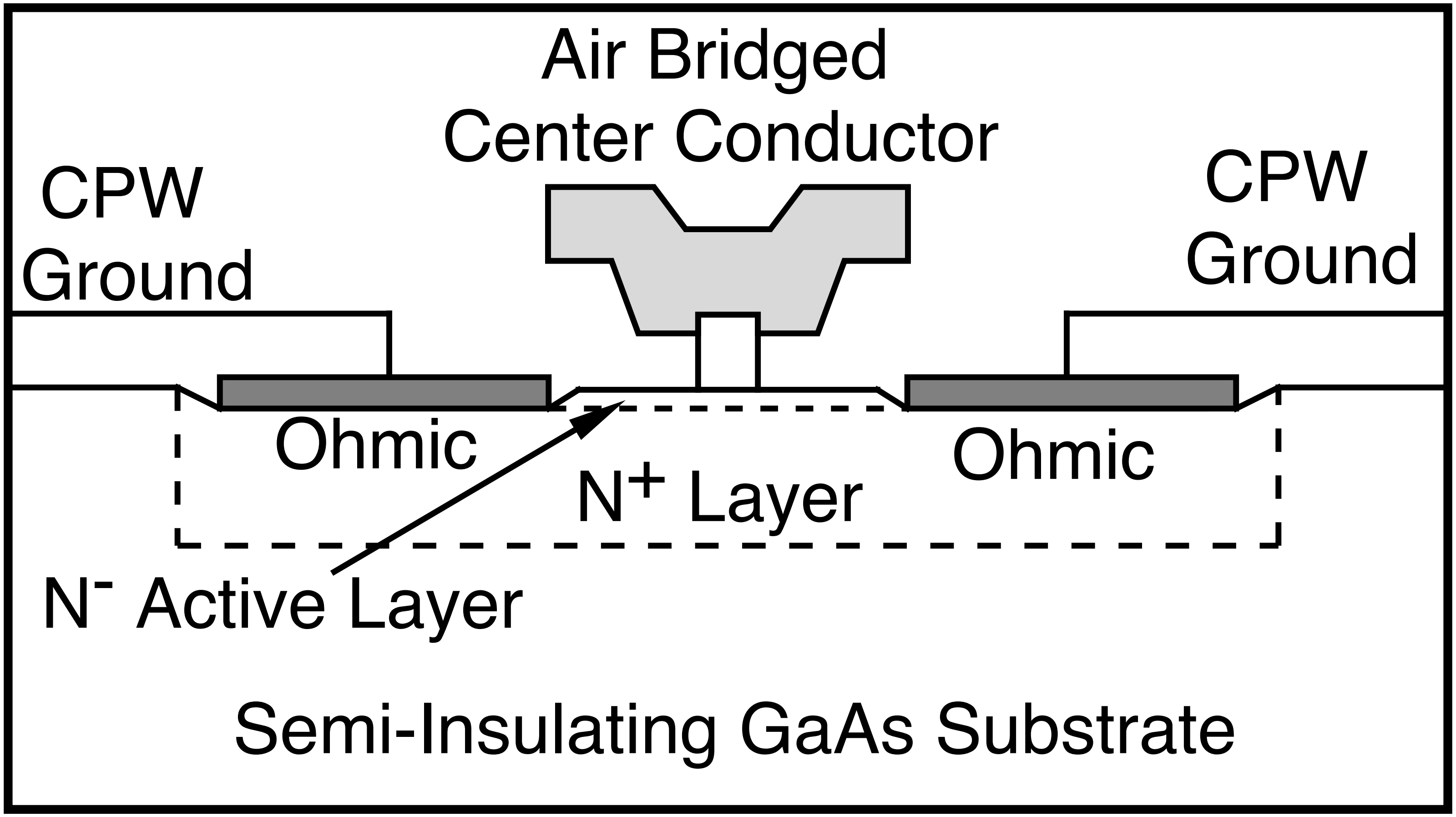


Cross section of the air bridge contacted diode. A layer of polyimide is used to keep the post off the substrate during electroplating. The ohmic contacts are recessed through the $N^-$ active layer to a heavily doped $N^+$ buried layer.

# Elevated CPW IV


S.E.M. image showing the air bridged center conductor of the coplanar waveguide contacting the tops of the diodes on the NLTL without touching the substrate.

# Elevated CPW V

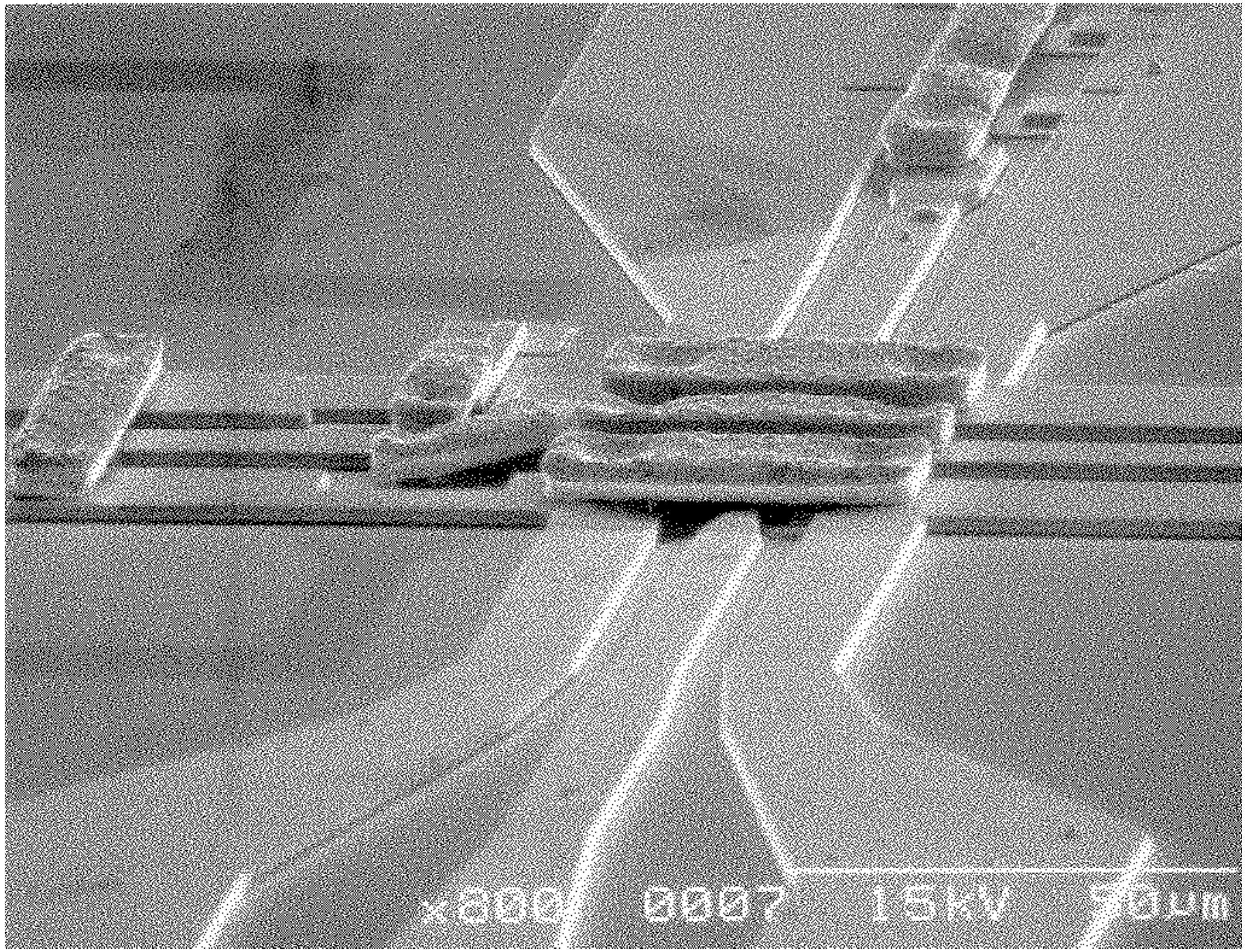


S.E.M. image of the sampling circuit and the output end of the NLTL that provides the strobe pulse to the two $1\,\mu m \times 1\,\mu m$ sampling diodes.

# NLTL output measured by sampling circuit

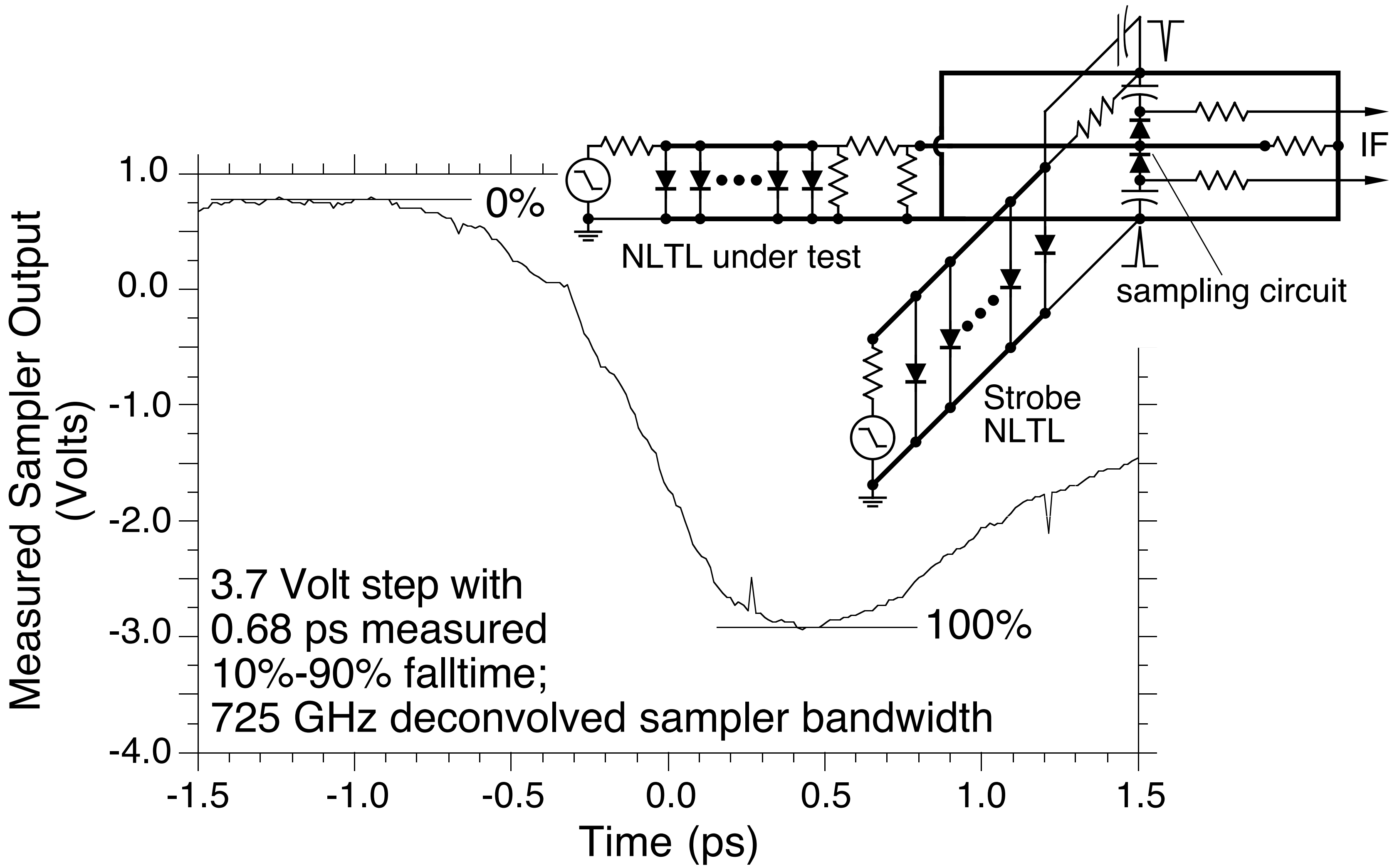

# GaAs Picosecond Optical Waveform Analyzer

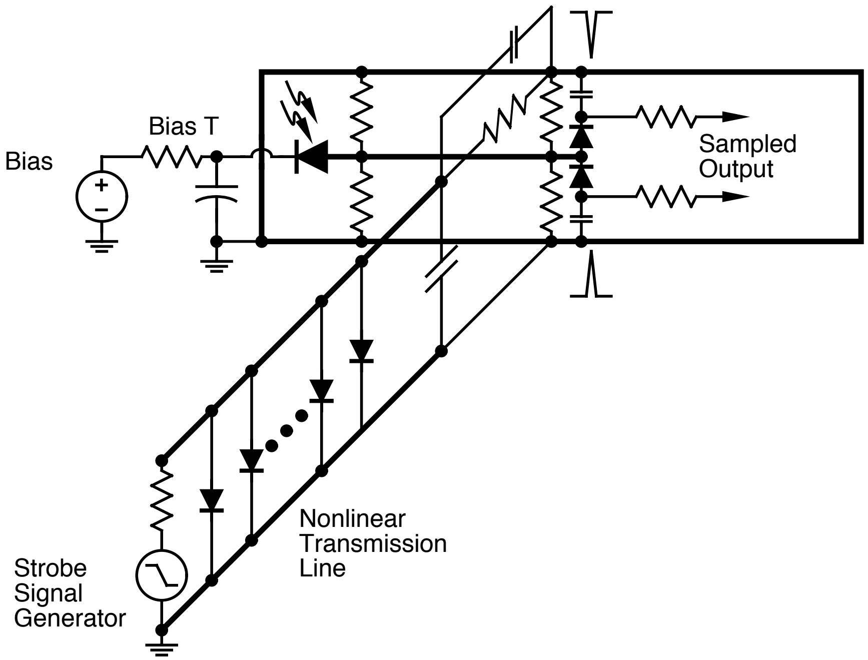


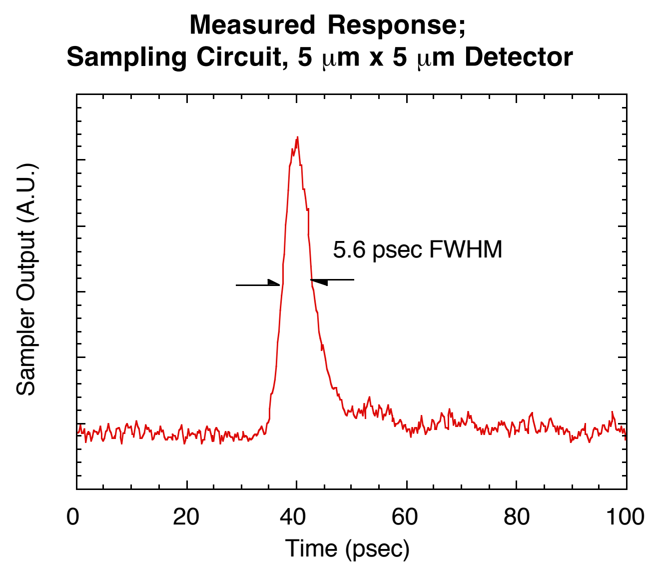

# Instruments and Measurements

# Instrumentation:  Motivation

## The Problem: Device vs Instrument Bandwidth

**Microwave transistor measurements: almost 10:1 frequency extrapolation**

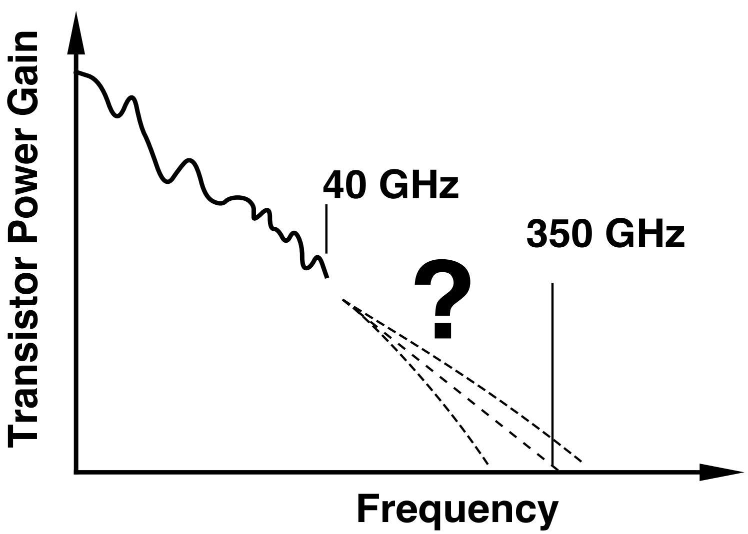


**Modern device bandwidth exceeds instrument bandwidth.**

**High-frequency device models must be**

**Poor understanding of devices.**

**Circuits above 60 GHz hard to measure.**

## Types of Instruments/ Measurements

### Conventional Electronic Measurements

- Network Analyzer
- Time Domain Reflectometer
- Sampling Oscilloscope
- Spectrum Analyzer

### Optoelectronic Techniques

- Photoconductive probing
- Electrooptic Sampling:Substrate Probing and Needle Probe

### On-wafer network analysis

- GaAs NLTL-based active probes
- Photoconductor-based probes

## Network Analysis

•Measures linear 2-port stimulus-response characteristics of a device

•Data usually presented as admittance or wave scattering parameters as a function of frequency.

•2 Purposes:

Functional measurements of a component (gain-frequency curve, etc.)

Device characterization and modelling

# Small-Signal Network Measurements

Restrict to linear devices (or nonlinear device in small-signal regime)

General device model:

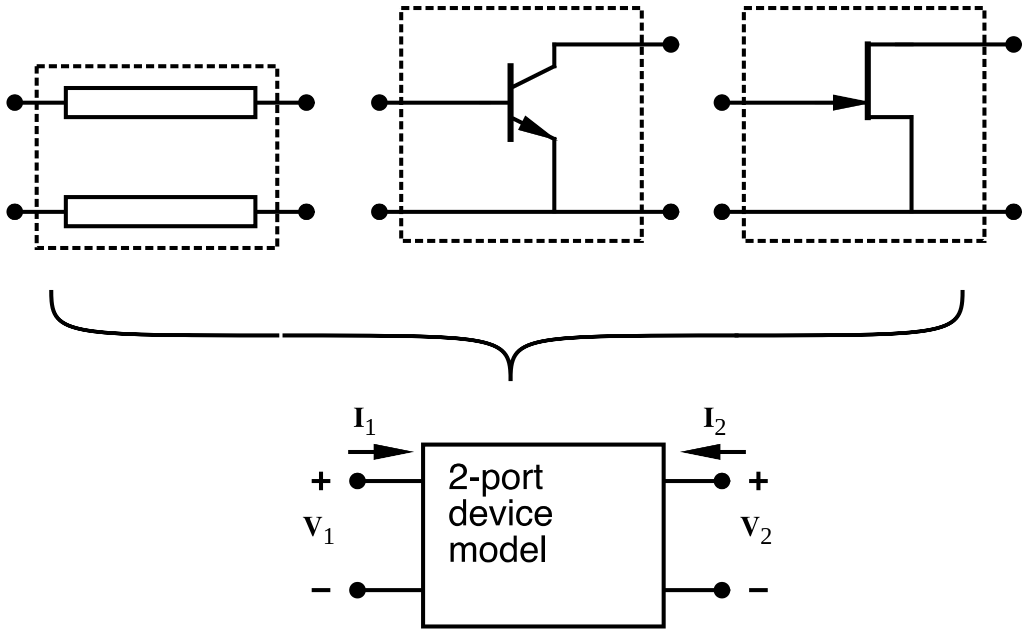


Frequency-domain description:

$$v_1(t) = V_1(\omega)e^{j\omega t},$$
$$i_1(t) = I_1(\omega)e^{j\omega t}, \text{ etc.}$$

$$\begin{bmatrix} I_1(\omega) \\ I_2(\omega) \end{bmatrix} = \begin{bmatrix} Y_{11}(\omega) & Y_{12}(\omega) \\ Y_{21}(\omega) & Y_{22}(\omega) \end{bmatrix} \begin{bmatrix} V_1(\omega) \\ V_2(\omega) \end{bmatrix}$$

Two-port Admittance parameters

# Microwave Scattering Parameters I.

## Waves on transmission lines:

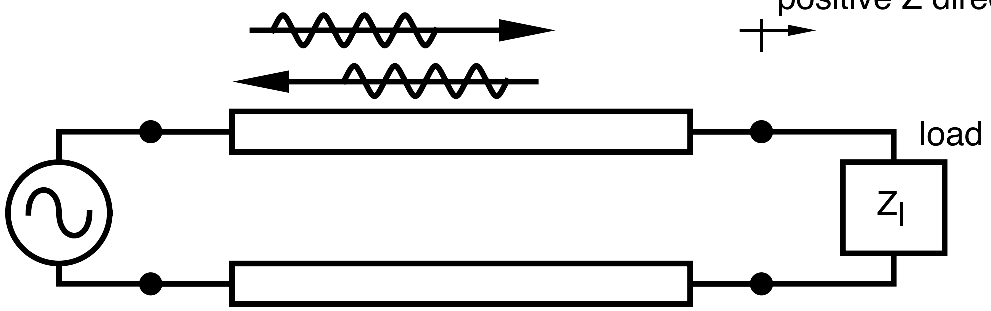


a,b: forward and reverse waves

Forward, reverse power: $|a|^2$, $|b|^2$

forward wave reverse wave

$$v(z,t) = a(t - z / velocity)\sqrt{Z_0} + b(t + z / velocity)\sqrt{Z_0}$$ Voltage

$$i(z,t) = \frac{a(t - z / velocity)}{\sqrt{Z_0}} - \frac{b(t + z / velocity)}{\sqrt{Z_0}}$$ Current

Voltage at any point: $v(z,t) = a(z,t)\sqrt{Z_0} + b(z,t)\sqrt{Z_0}$

Current at any point: $i(z,t) = a(z,t)/\sqrt{Z_0} - b(z,t)/\sqrt{Z_0}$

# Microwave Scattering Parameters II

Two-port parameters described in terms of incident and emanating waves from the device (when connected to transmission lines)

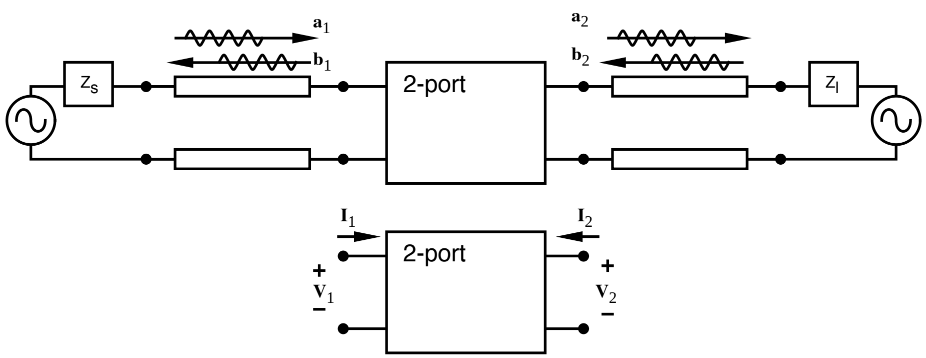


Equivalent S-parameter and Y-parameter models of a 2-port.

Scattering parameter model

$$\begin{bmatrix} b_1(\omega) \\ b_2(\omega) \end{bmatrix} = \begin{bmatrix} S_{11}(\omega) & S_{12}(\omega) \\ S_{21}(\omega) & S_{22}(\omega) \end{bmatrix} \begin{bmatrix} a_1(\omega) \\ a_2(\omega) \end{bmatrix}$$

Admittance parameter model

$$\begin{bmatrix} I_1(\omega) \\ I_2(\omega) \end{bmatrix} = \begin{bmatrix} Y_{11}(\omega) & Y_{12}(\omega) \\ Y_{21}(\omega) & Y_{22}(\omega) \end{bmatrix} \begin{bmatrix} V_1(\omega) \\ V_2(\omega) \end{bmatrix}$$

SInce $v = a\sqrt{Z_0} + b\sqrt{Z_0}$ and $i = a/\sqrt{Z_0} - b/\sqrt{Z_0}$, the scattering (S) parameters can be directly computed from the admittance (Y) parameters.

# Comments Regarding Transistor Testing

Subsequent notes will discuss laser-based testing of electronics. Key points in transistor measurements:

Are we measuring device or circuit performance? Device measurements are parametric (what ft, what fmax, what Cgs...?), while circuit measurements are functional (gain-bandwidth obtained, logic gain progation delay, pulse amplifier risetime, ...)

Device measurments should allow the device engineer to extract the linear model, from which figures-of-merit (ft, fmax) and device physical parameters (capacitances, resistances, transit times) are determined. The circuit engineer will want a circuit model of the device, described either as above (capacitances, resistances, transit times) or by a black-box linear 2-port description.

Pulse "response time" measurements with unspecified bias conditions, signal levels, and generator and load impedances are of little significant value. Linear or large-signal nonlinear operation will give quite different behavior. Bandwidth (risetime) is a function of gain becuase of gain-bandwidth limits. Very short RC charging times may be obtained by driving the transistor through very low impedances, but the circuit may be providing no power gain under such conditions...

# The Microwave Network Analyzer

Measurement of (linear / small signal) 2-port network parameters in the frequency domain.

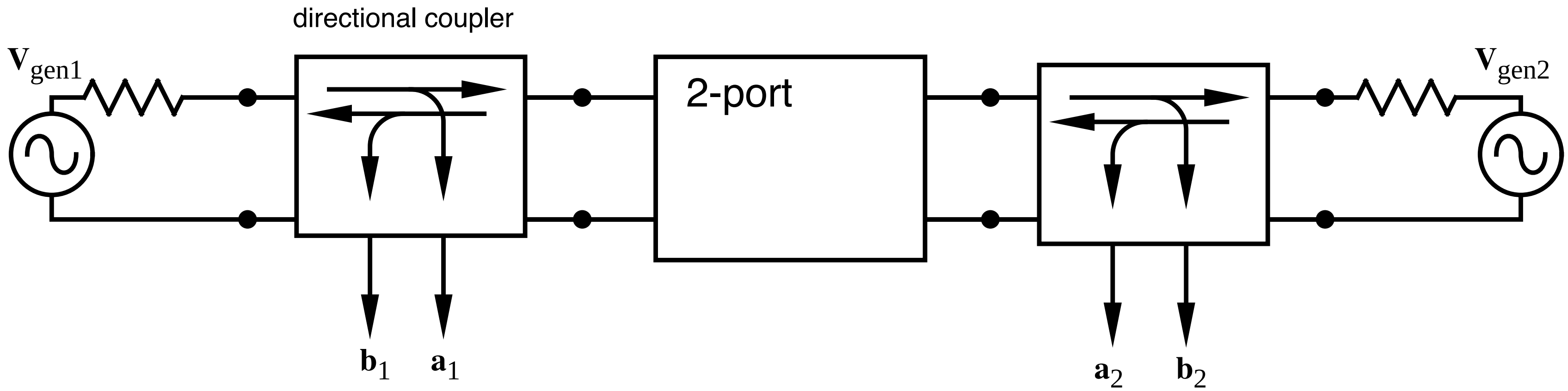


Swept-frequency sources ($V_{gen1}$ and $V_{gen2}$ ) are alternately applied to the 2-port input and output, and the incident and emanating waves measured with directional couplers.

Calibration: amplitude/phase contributions of cabling (etc.) between the instrument and the d.u.t. are corrected for by first measuring a series of devices of known characteristics in place of the d.u.t. , either 50Ω load, open, short, and through line, or a series of through lines of differing lengths ("LRL")

# Block Diagram: Microwave Network Analyzer

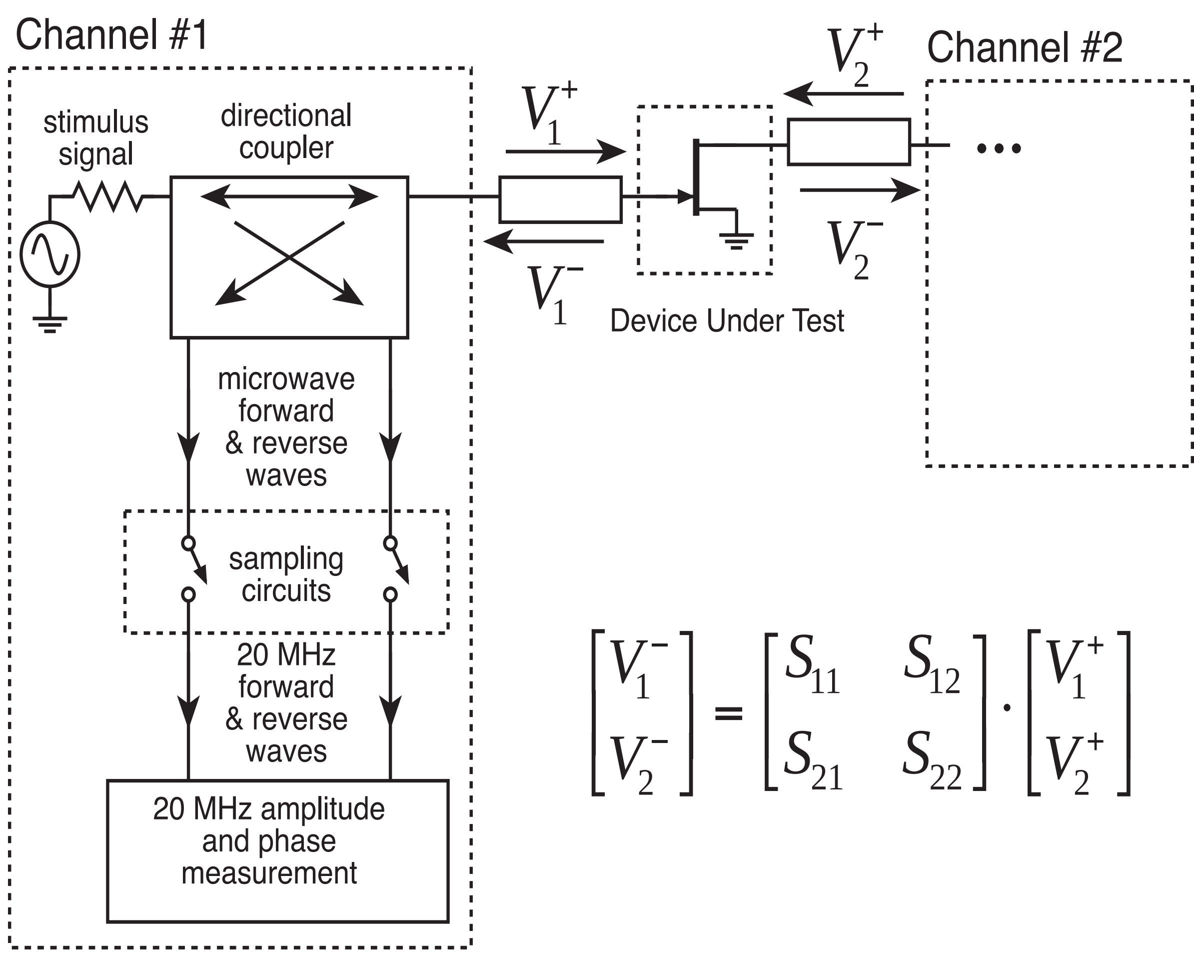


$$\begin{bmatrix} V_1^- \\ V_2^- \end{bmatrix} = \begin{bmatrix} S_{11} & S_{12} \\ S_{21} & S_{22} \end{bmatrix} \cdot \begin{bmatrix} V_1^+ \\ V_2^+ \end{bmatrix}$$

Bandwidth limits include

available connectors and cables,

sampling circuits,

signal source frequency range

## Performance of modern network analyzers:

After Calibration: DC-110 GHz instrument
(Coaxial-based system, using coplanar microwave wafer probes)

Amplitude accuracy, 0 dB signal: $\approx \pm 0.05$ dB

Phase accuracy, 0 dB signal: $\approx \pm 3°$

Directivity*: $\approx$ -40 dB
*Measured reflection magnitude for a zero-reflection device

Given accurate calibration standards, network analyzers can provide very precise device models. Competing optical techniques offering wider bandwidth must attain competitive accuracy. This places stringent demands on laser intensity stability (and often laser pulse timing stability).

# Example Measurement with DC-40 GHz NWA

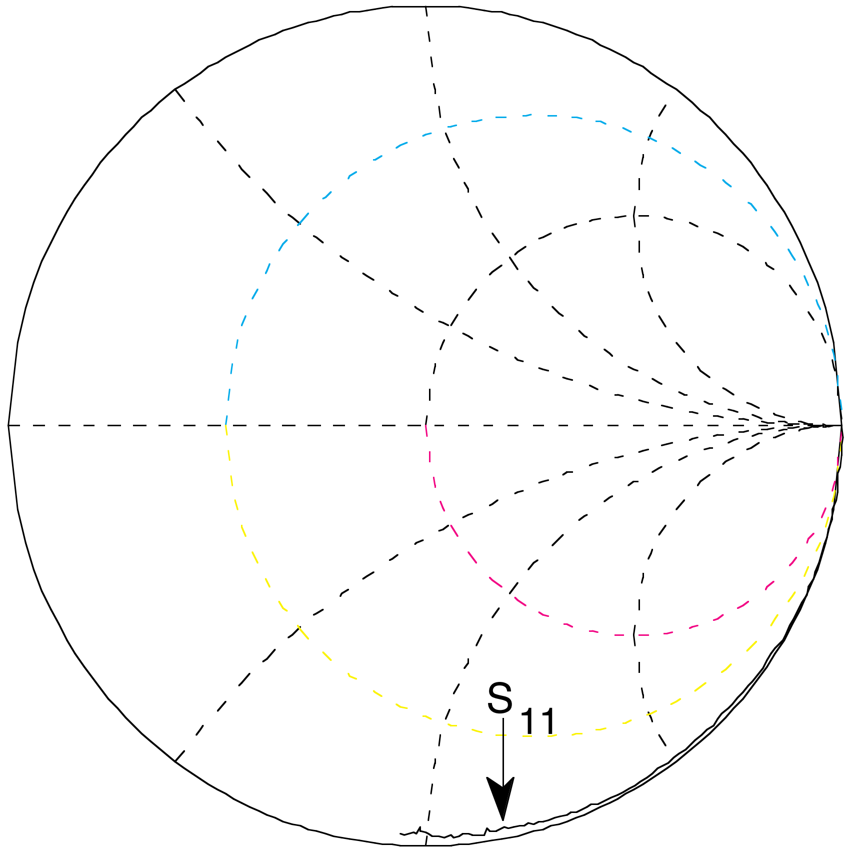


Impedance measurement of a 4 THz Schottky diode. Device Q is 100 at 40 GHz, hence S11 differs from 0 dB by ≈0.05 dB. Instrument accuracy is sufficient to observe the diode resistance!

# Time-domain reflectometry:

Measurement of the 2-port network small-signal parameters in the time domain: Yields same information as the swept-frequency analyzer (?).

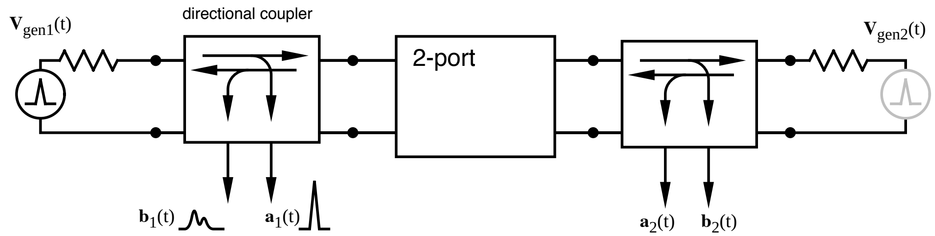


First method uses directional couplers to separate incident & reflected waves

$s_{ij}(t)$ is simply the inverse Fourier transform of $S_{ij}(\omega)$:

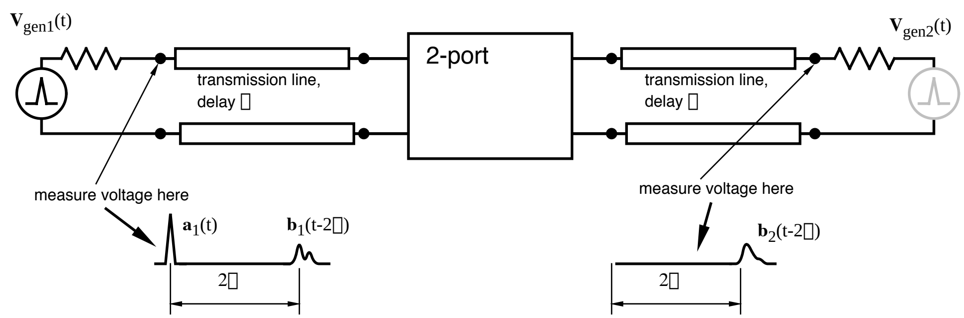


Using a delay line with delay longer than the duration of the stimulus signal, the incident & emanating waves are separated in time, eliminating (?) the need for directional couplers.

## Problems with Time-Domain NWA Measurements, I

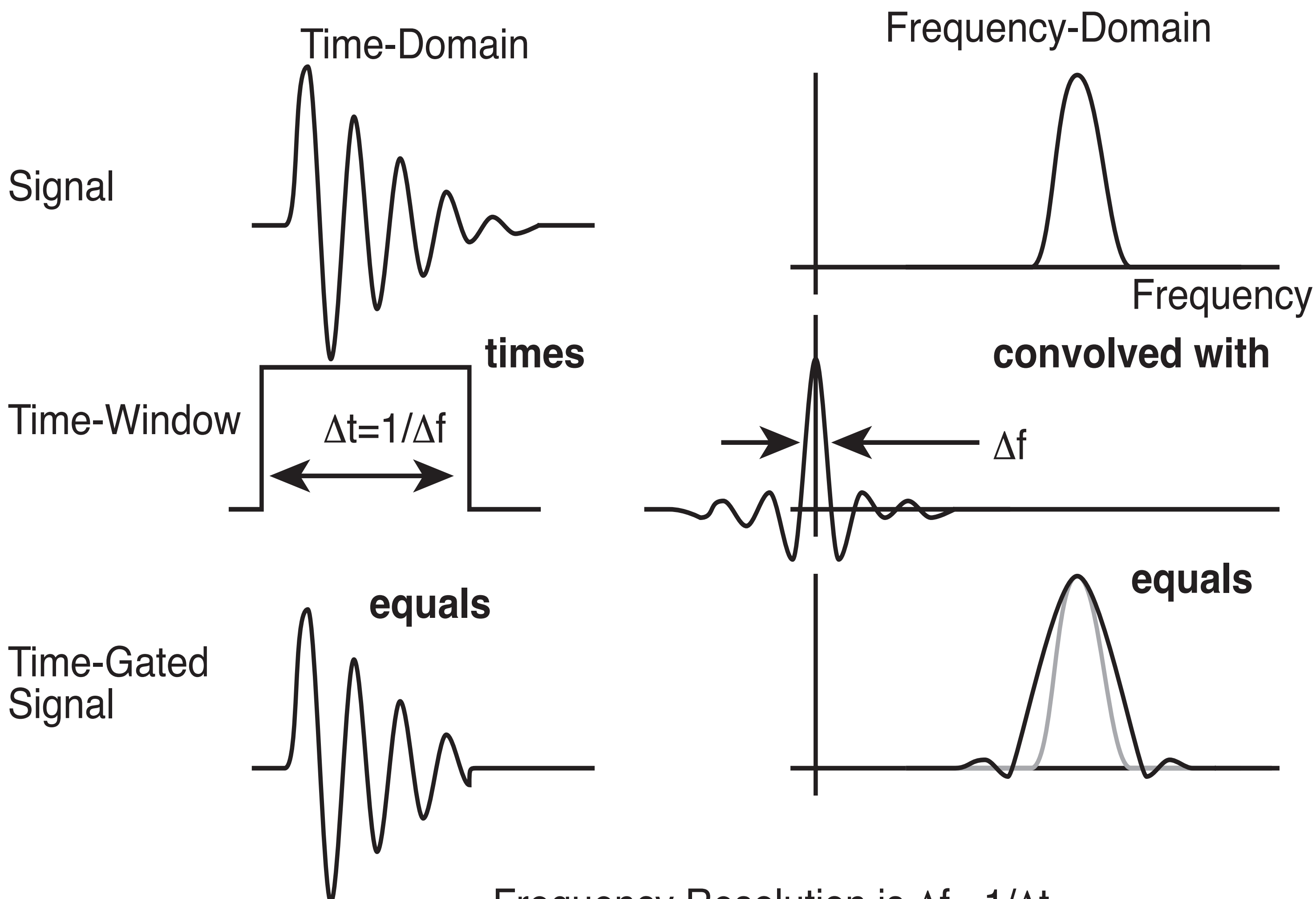


Frequency Resolution is $\Delta f = 1/\Delta t$

- While time-gating eliminates spurious responses, frequency resolution is lost.

# Problems with Time-Domain NWA, II

## Spectrum Downconversion by Sampling

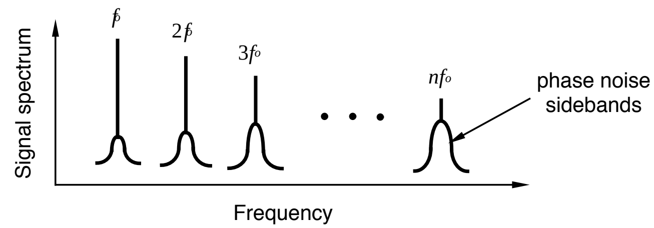


Sampling Circuit Input

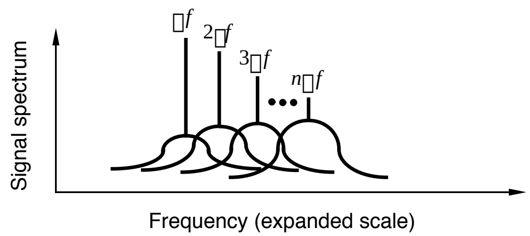


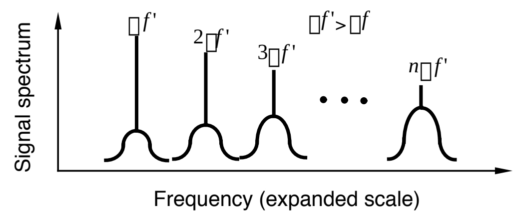


Sampling Circuit Output

- **Aliasing of phase-noise sidebands degrades noise performance if scan rate is below phase-noise bandwidth**

•System imperfections (phase, amplitude noise) and DUT nonlinearity cause mutual interference between spectral lines under measurment

- Other problems: sharing bits of resolution in A-D converter between harmonics
- Conclusion: Commercial NWAs use swept-frequency stimulus for good reason

.

## Signal Measurements

Samping oscilloscope

Time waveform of signal. Commercial instruments to 50 GHz (NLTL based...).

Spectrum Analyzer

Measures power spectrum of signal. Commercial instruments: 40 GHz with coaxial inputs, to 325 GHz in waveguide.

## Optoelectronic Measurement Techniques

Sampling Devices and Systems

Electrooptic Sampling

Photoconductive Sampling

# Sampling Devices, Optoelectronic and Electronic

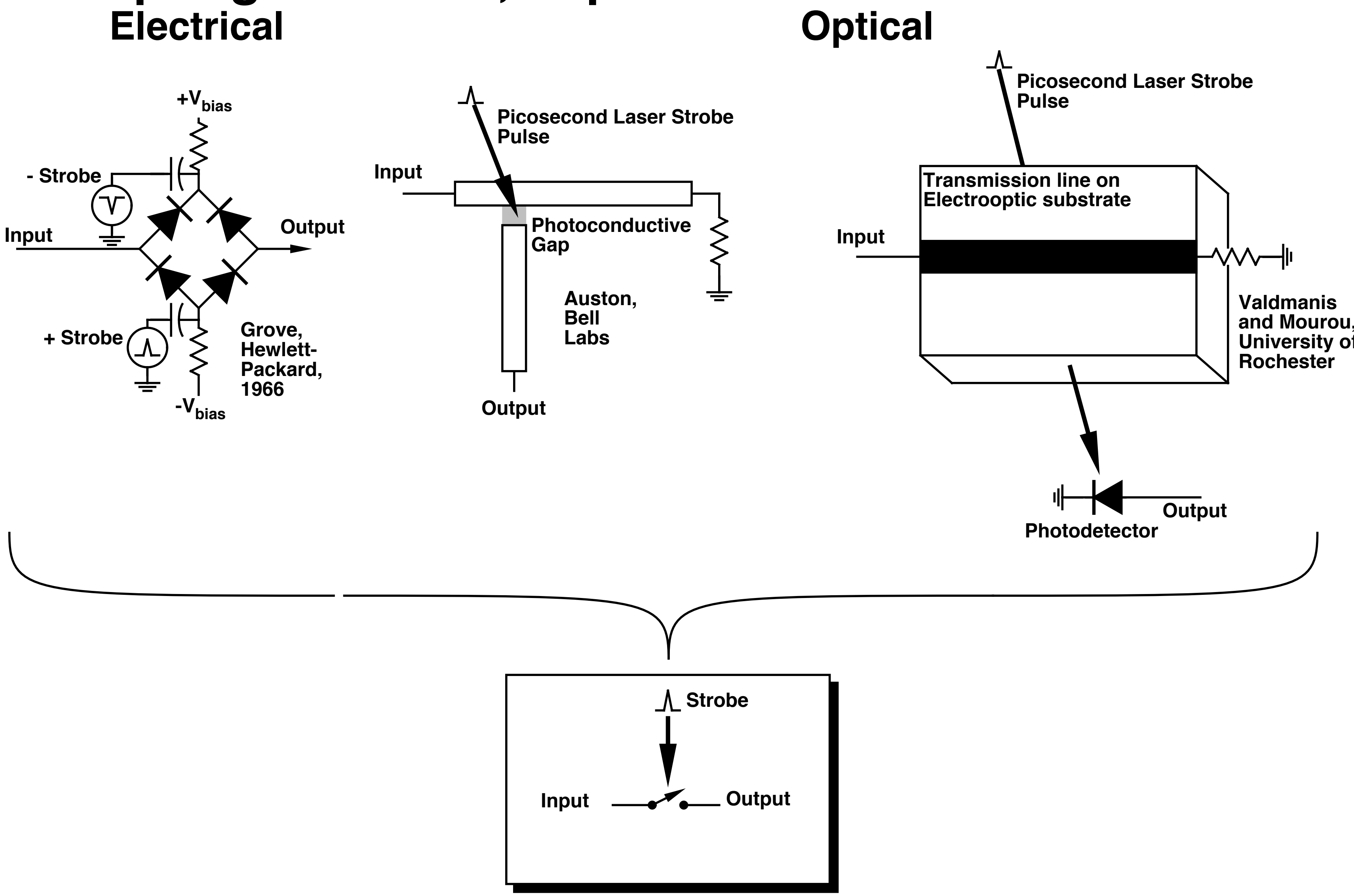

# Sampling

Reducing the repetition frequency (bandwidth) of a signal so that it can be measured with low-frequency instruments

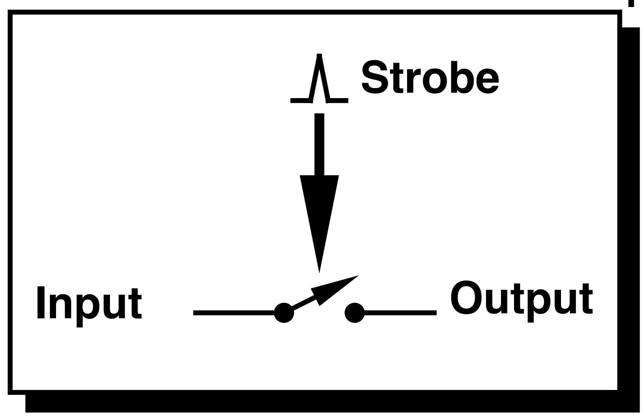


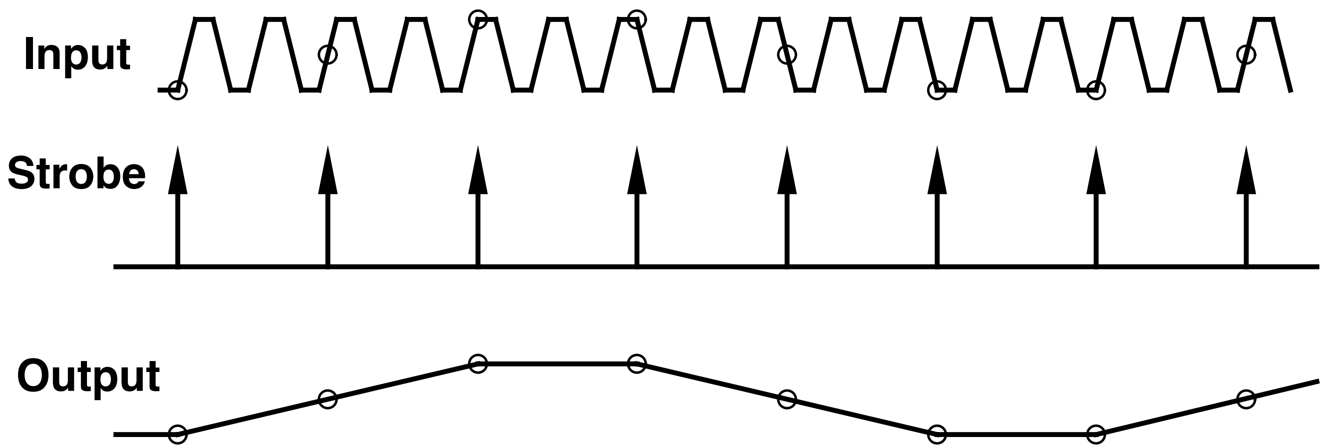


If the strobe signal has repetition frequency $f_0$ and the input signal has repetition frequency $nf_0+\Delta f$, the sampled output will be at frequency $\Delta f$.

# Laser Sampling and Timing Jitter

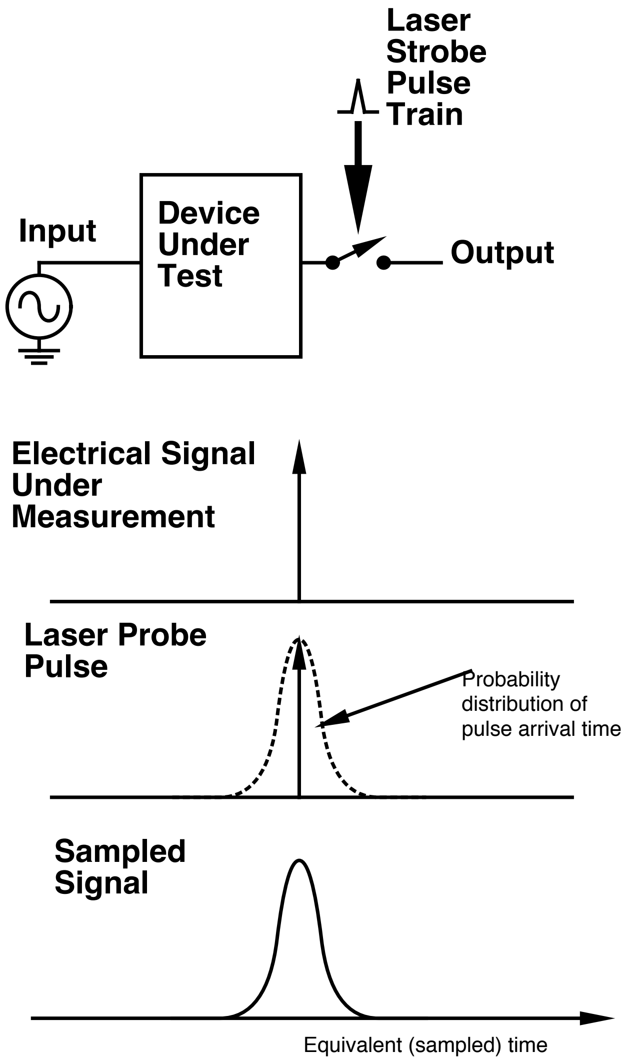


Mode-locked lasers derive their pulse repetition rate from the cavity round-trip time. This resonator, in terms of the laser intensity modulation intensity envelope, has relatively poor Q (poor finesse) and pulsed lasers have substantial pulse timing fluctuations.

Relative timing fluctuations of the laser and electrical signal source degrade the system time resolution.

Good microwave synthesizer: ≈0.2 ps rms jitter

Mode-locked YAG laser: ≈3-10 ps rms
(0.3 ps if phase-locked)
CPM laser: ≈5 ps rms jitter

# The pump-probe technique

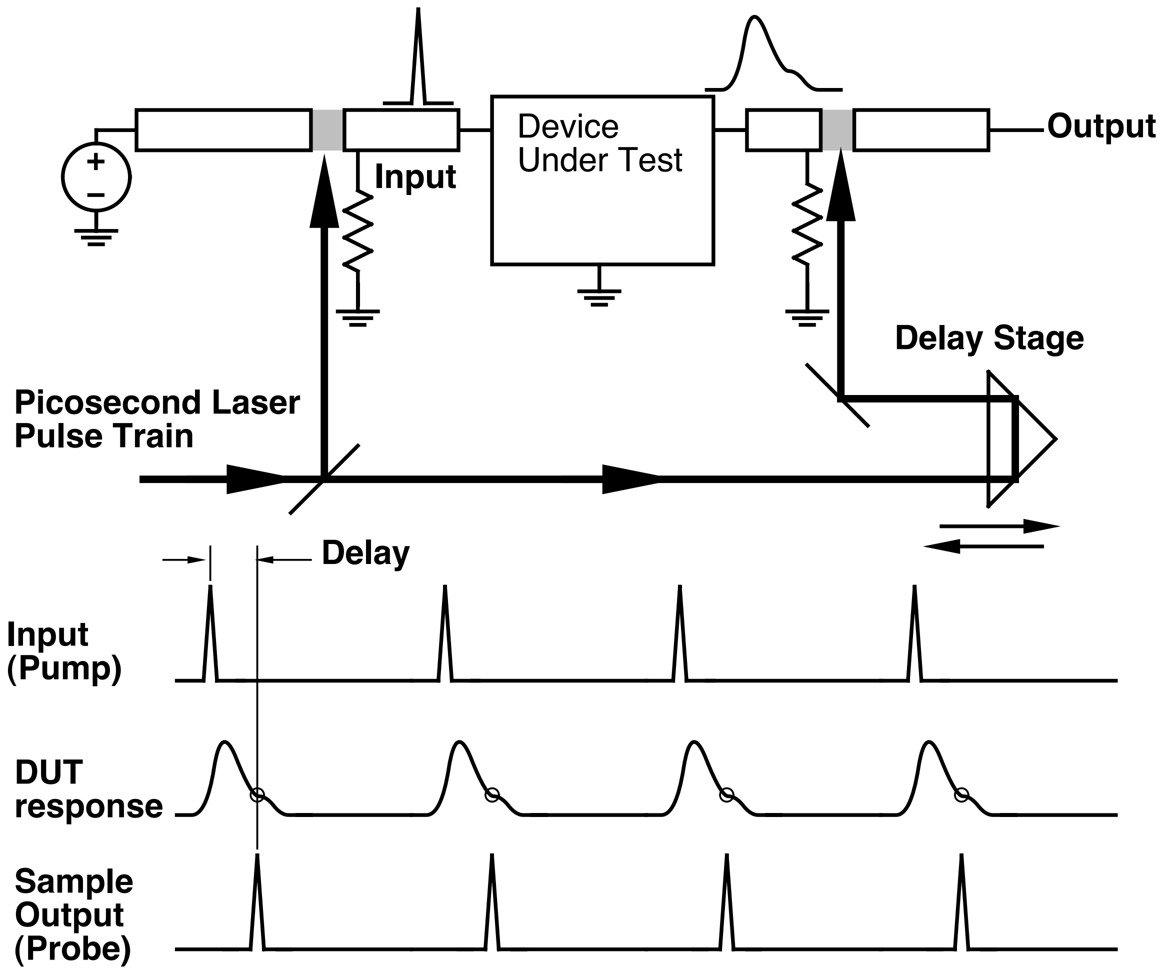


Because the stimulus and probing signals are derived from the same laser pulse, laser pulse timing fluctuations have no effect on the measurement.

technique limited to stimulus-response measurements

# Photoconductive Characterization of Devices

<u>Purpose</u>: 2-port small-signal network measurements. <u>Method</u>: time-domain reflectometry/ transmission using photoconductive pulse generators and sampling gaps: Matloubian et. al., IEEE MGWL Vol. 1. No. 2, Feb. 1991

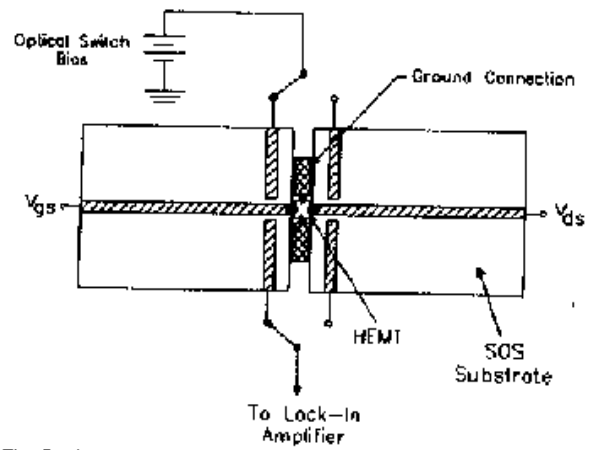


Fig. 2. Picosecond optoelectronic test fixture with HEMT wire-bonded to center microstrip lines.

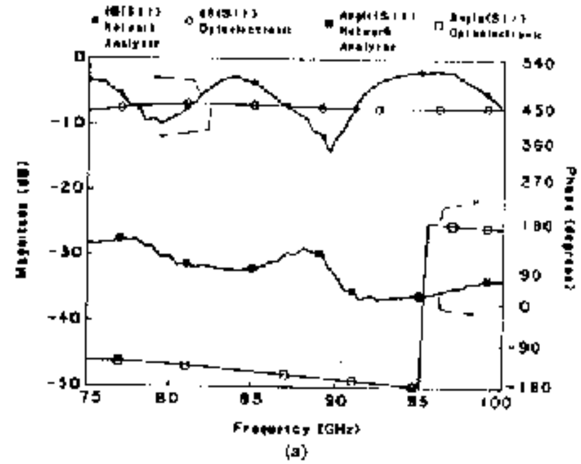


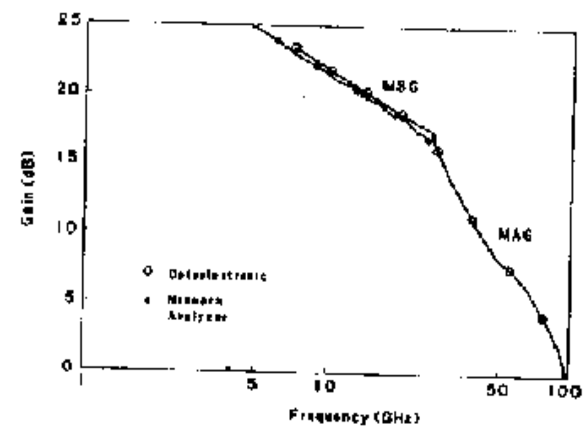


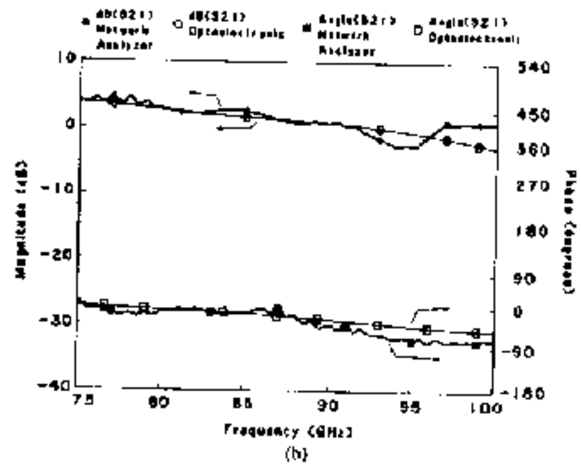

# Electrooptic Probing

Field-Induced birefringence in [100]-cut GaAs:

$$N_{[01\bar{1}]} - N_{[011]} = N_0^3 r_{41} E_{[110]}$$

A sub-bandgap probe beam is passed in the [100] direction through the substrate, and the birefringence measured with a polarization interferomenter. The interferometer output is proportional to the potential difference across the wafer.

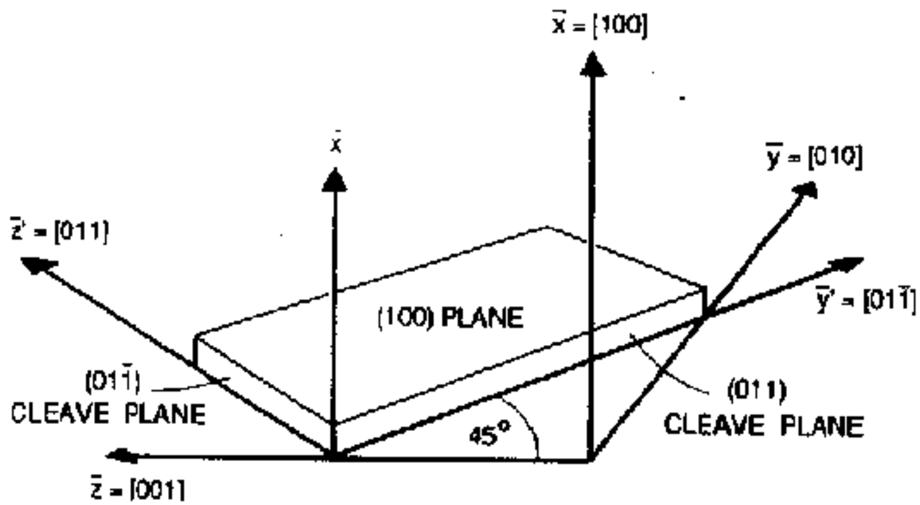


Principal axes and cleave planes in (100)-cut Gallium Arsenide.

# Gallium Arsenide electrooptic intensity modulator

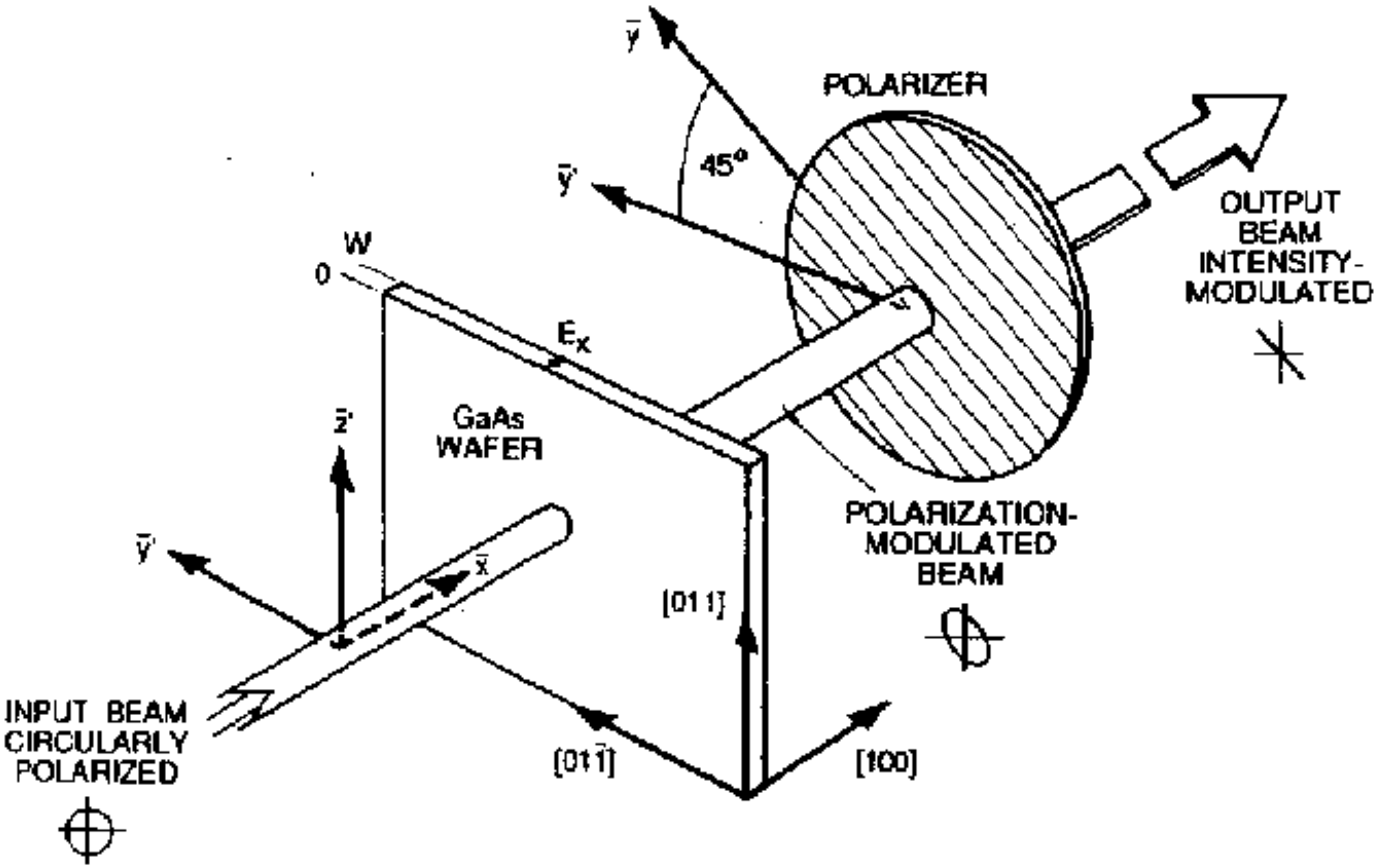

# Electrooptic: Frontside/backside probing

Frontside probing

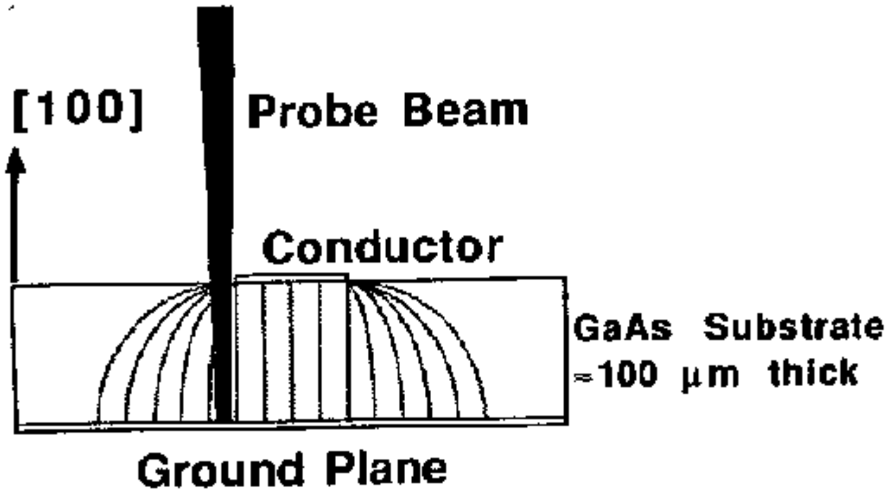


Backside probing

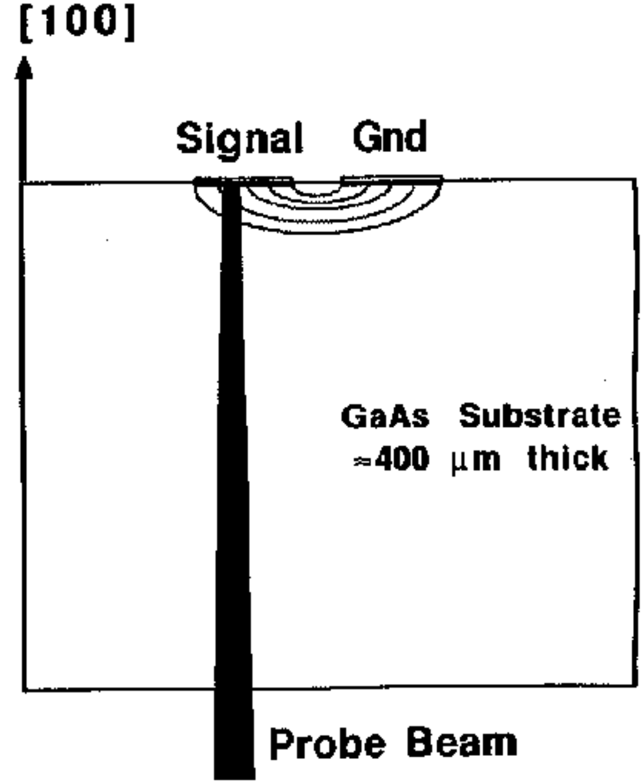

# Electrooptic Sampling System

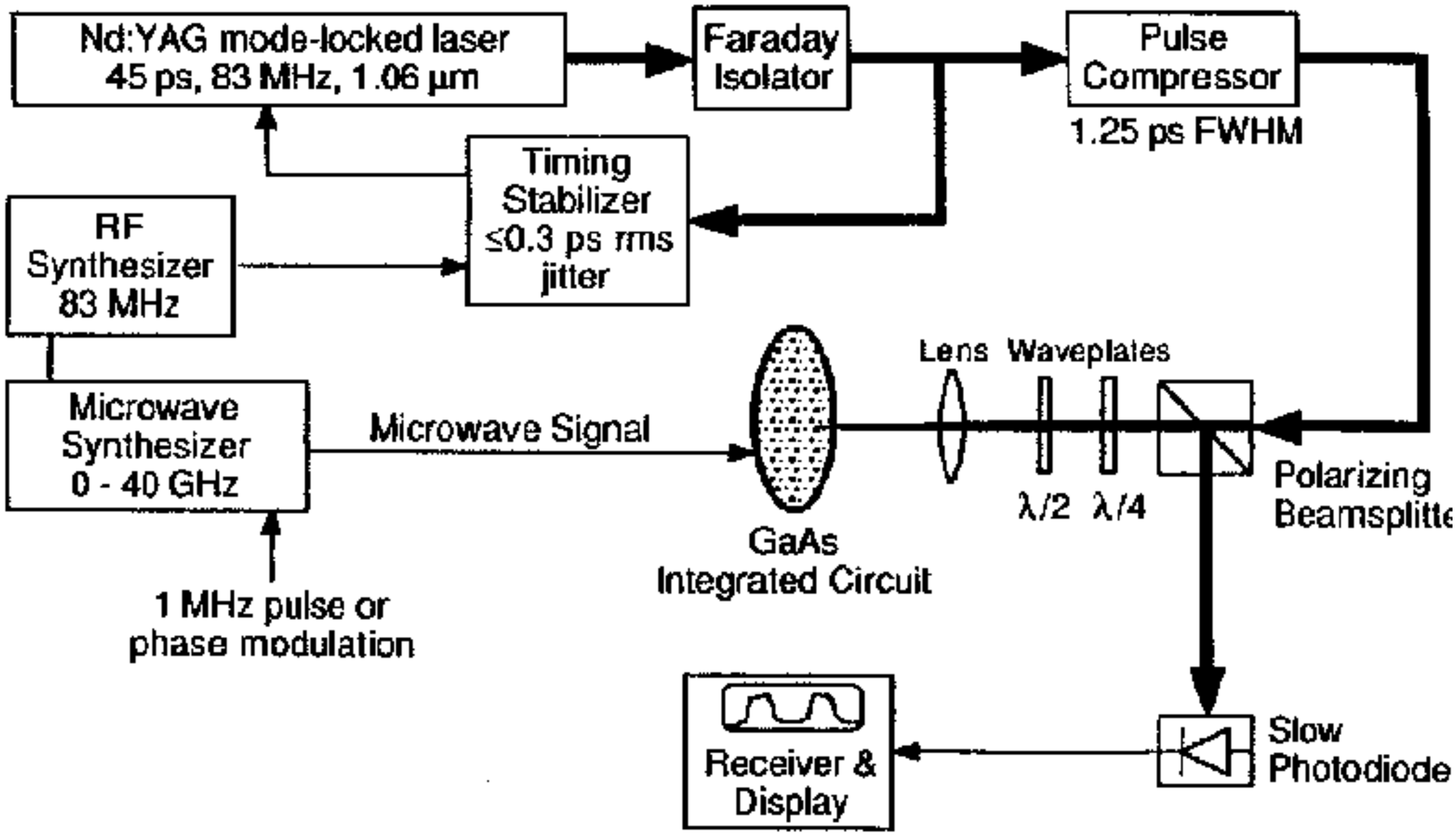

# Example Measurement: eo sampling

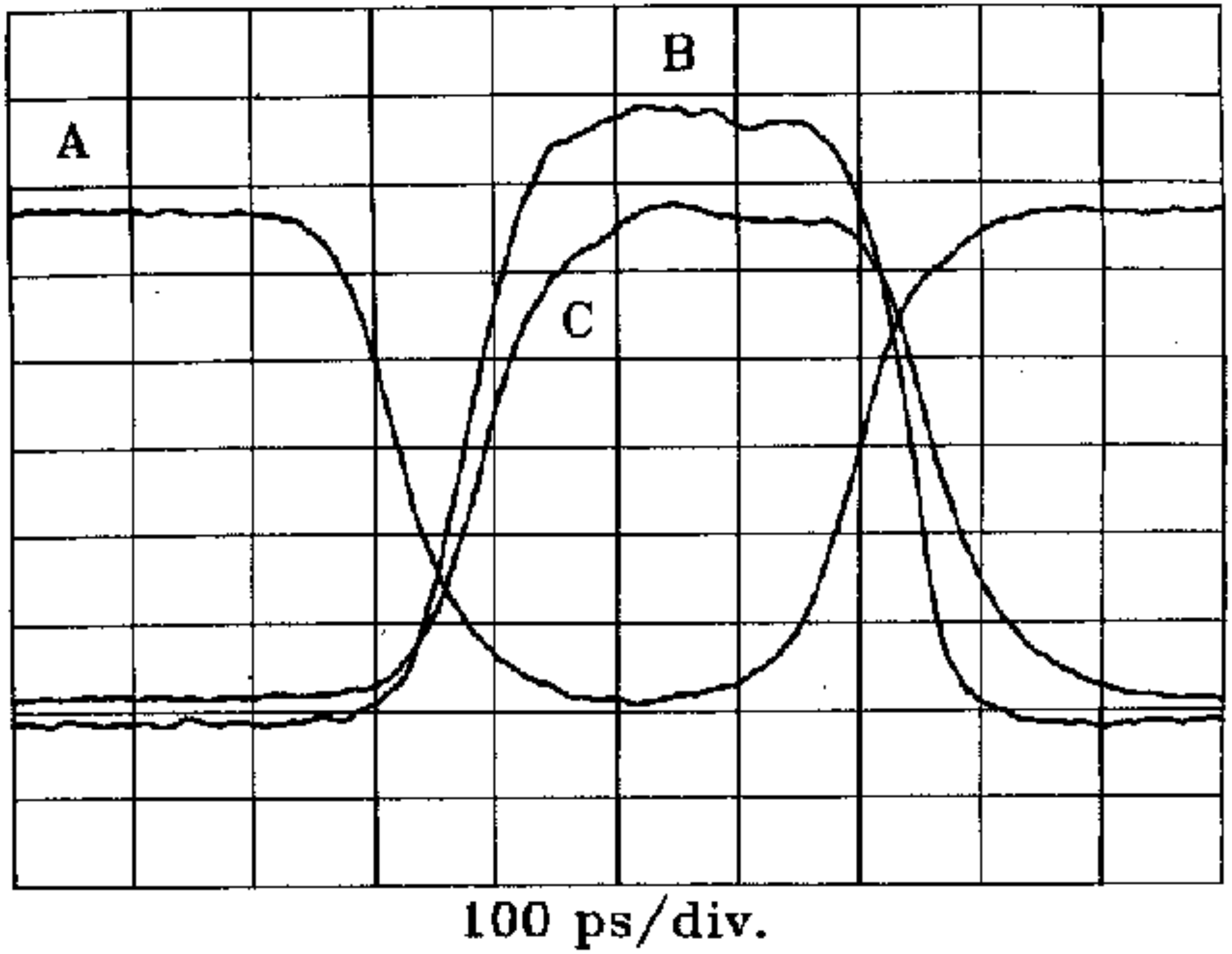


Voltage waveforms at the input (a), source-follower gate (b), and output (c) of a GaAs buffered-FET-logic inverter gate

# Electrooptic Sampling of Photodetectors

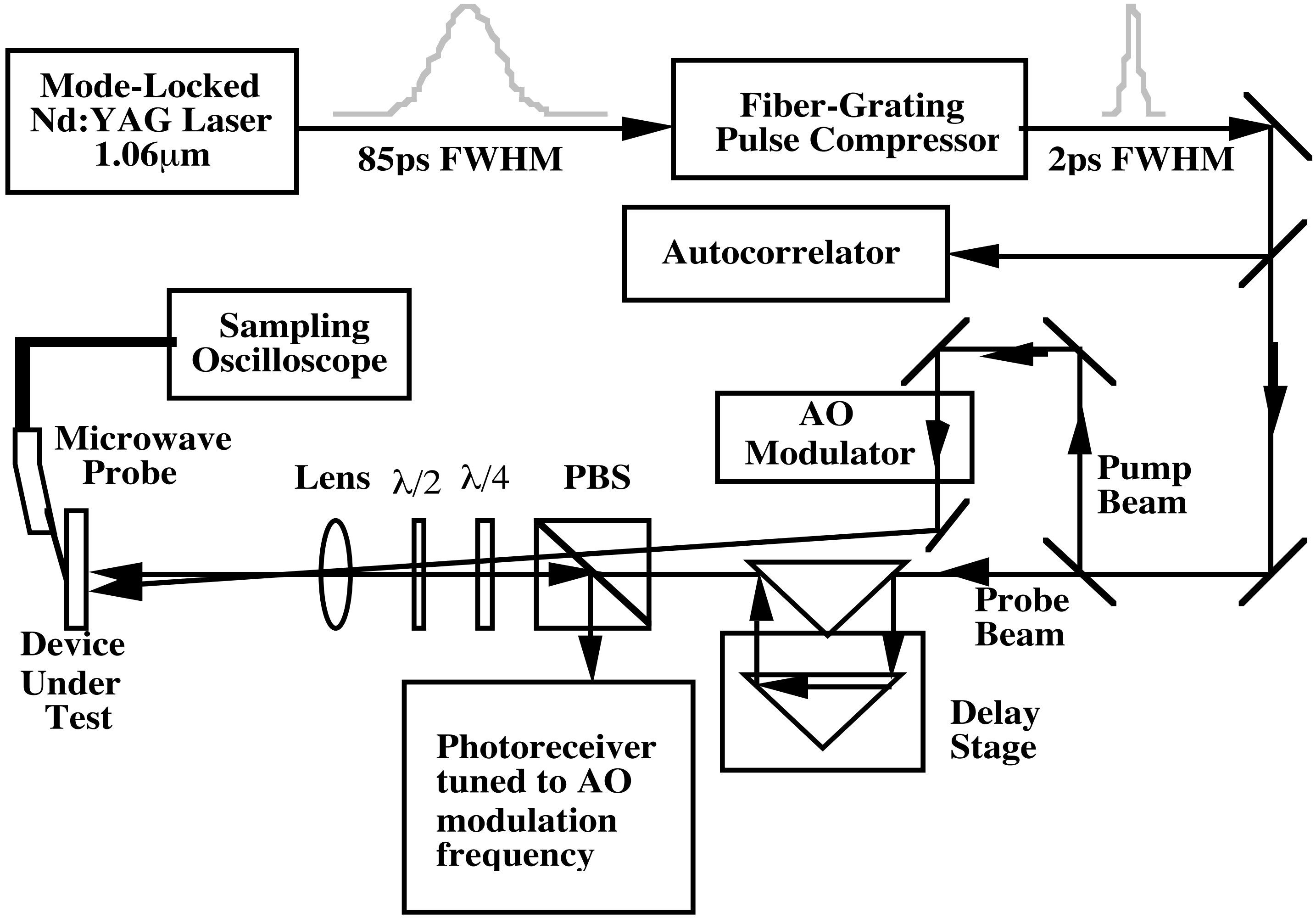

# Electrooptic Sampling of Photodetectors: Result

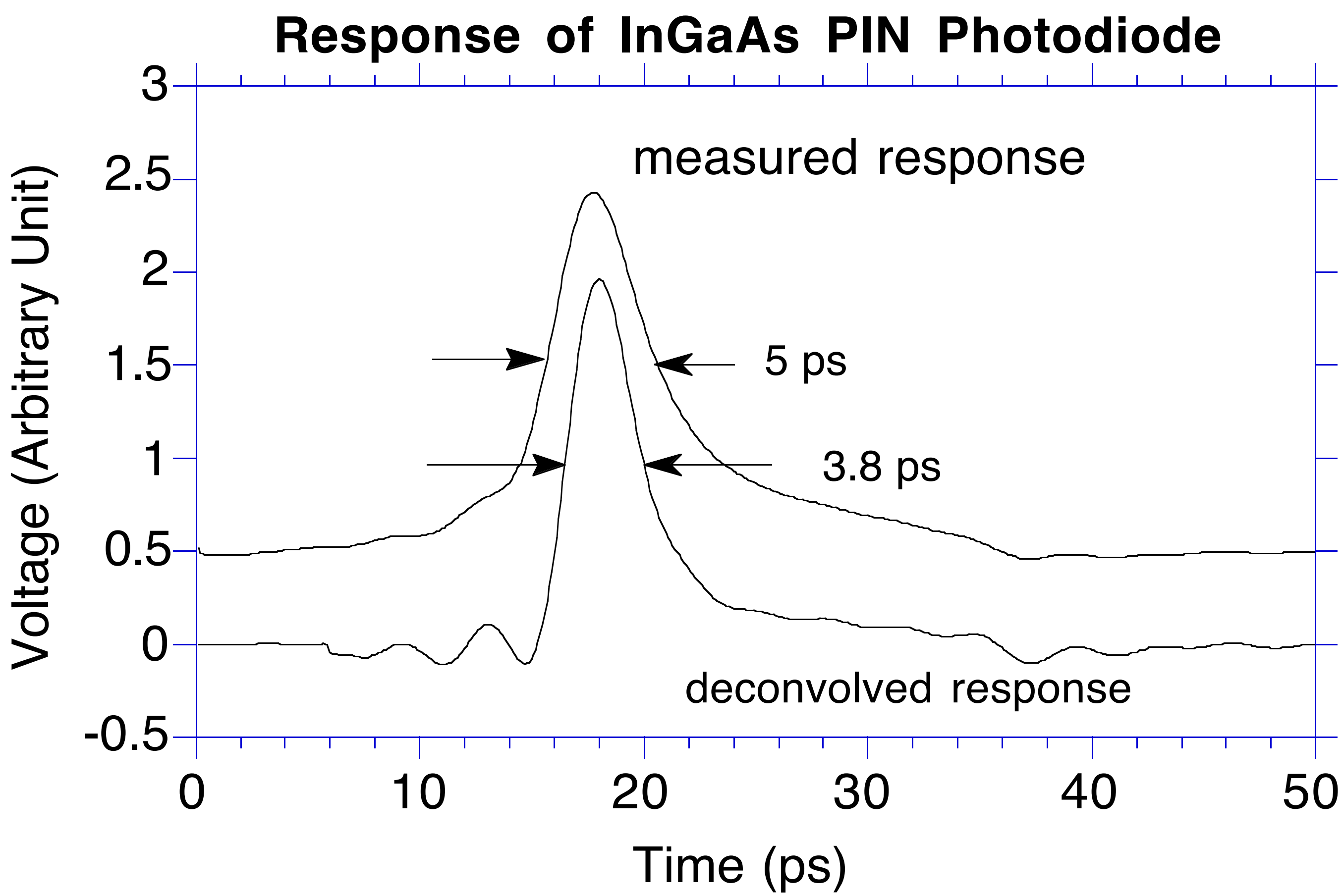

# Electrooptic Needle Probe

J.A. VALDMANIS

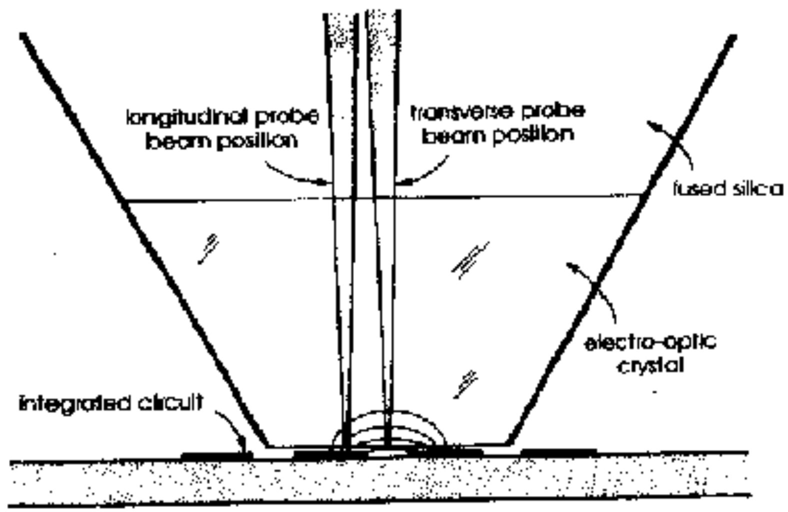


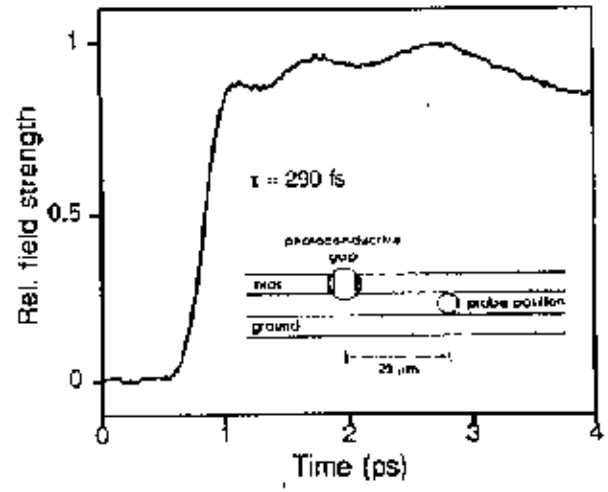


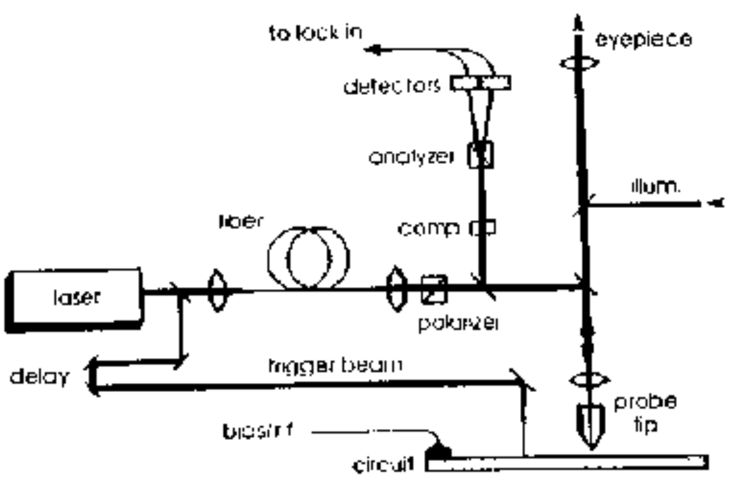

## Laser sources for optoelectronic measurements

### Colliding-pulse mode-locked dye laser:

Pulse durations <<100 fs.
Free-running laser (passively mode-locked): 5-10 ps rms timing jitter wavelengths above-bandgap in GaAs: not for electrooptic substrate probing. Relatively stable amplitude. Primary laser for femtosecond optoelectronic experiments.

### Synchronously-Pumped dye lasers

0.1-5 ps pulse durations. Primarily for wavelengths less than 900 nm (no substrate probing in GaAs).
Significant (1-3 ps rms) timing jitter. Stable amplitude

### Ti-Sapphire Laser

≈200 fs pulse widths, negligible wings, tunable wavelengths
Sibbet et. al. have timing-stabilized such lasers. Good choice.

## Laser sources for optoelectronic measurements II

### Nd:YAG laser & fiber-grating pulse compressor

Wavelength (1.06 μm) below-GaAs-bandgap; suitable for substrate probing.
Subpicosecond timing jitter attainable with feedback stabilization.
Poor spectral flatness (measurement error) due to wings on pulse.
Considerable low-frequency amplitude fluctuations, drift.
Power-dependent Raman scattering adds excess noise above shot noise, limiting input power to fiber, and thereby limiting usable pulse compression to ≈1 ps outputs with single-stage compression.

### Mode-locked & gain-switched semiconductor diode lasers

Area of intense research. Low phase noise for actively mode-locked devices, particularly those with external optical cavities. Pulse widths ranging from ≈0.1 ps to 2-5 ps, dependent on pulse repetition frequency. Adiabatic soliton compression looks like a breakthrough

# Compressed YAG Autocorrellation: "wings"

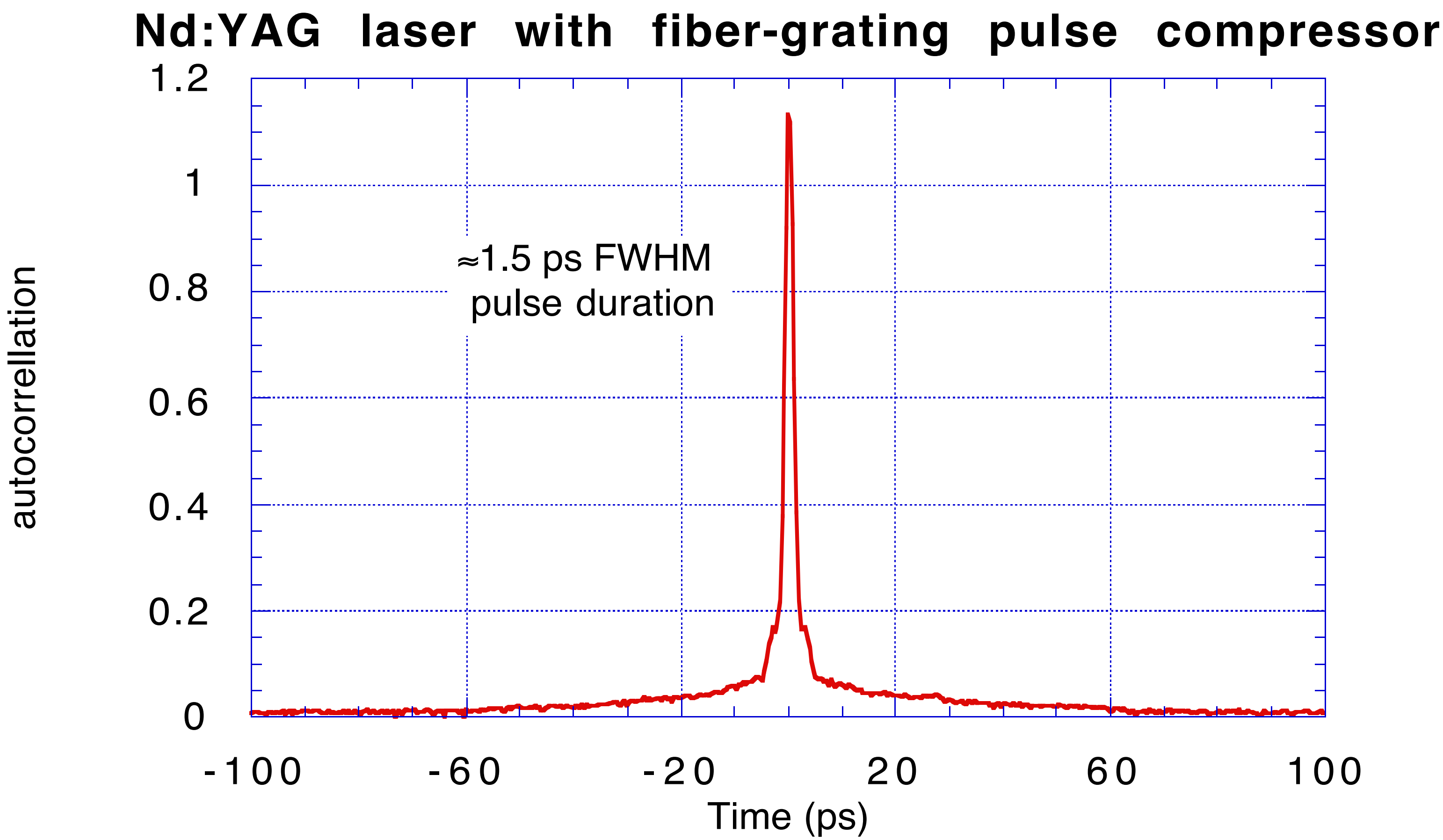

# Compressed YAG Power Spectrum

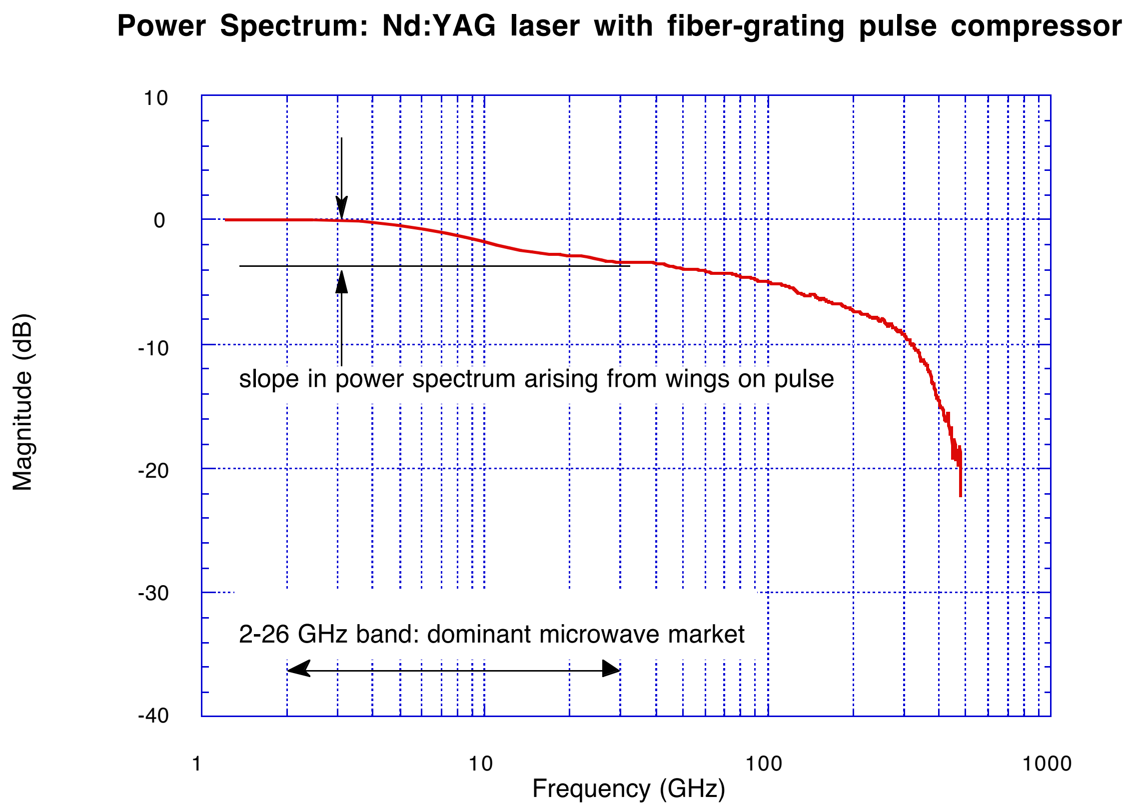


"Wings" cause errors in low-frequency measurement response .
Intensity fluctuations from compressor degrade repeatability
Raman scattering adds (≈10-50 dB) to shot noise, limiting compression ratios attainable with low noise

# phase noise theory and measurement

Laser timing and amplitude fluctuations:

$$I(t) \cong \overline{P}T\big(1 + N(t)\big)\sum_{-\infty}^{+\infty} \frac{1}{\sigma_t\sqrt{2\pi}} \exp\Big[-\big(t - nT - J(t)\big)^2 \;\; 2\sigma_t^2\Big]$$

Laser Spectrum

$$S_I(\omega) \approx \overline{P}^2 \exp\big(-\omega^2\sigma_t^2\big)\sum_{-\infty}^{+\infty}\begin{bmatrix} 2\pi\delta(\omega - \omega_0) \quad \ldots\text{laser harmonics} \\ +S_N(\omega - \omega_0) \quad \ldots\text{AM sidebands} \\ +n^2\omega_l^2 S_J(\omega - \omega_0) \quad \ldots\text{FM sidebands} \end{bmatrix}$$

# phase noise theory and measurement

I(t) laser intensity

P=average intensity

T=pulse repetition period

$\sigma_t$ =RMS pulse width

N(t)=intensity fluctuations

J(t) timing fluctuations

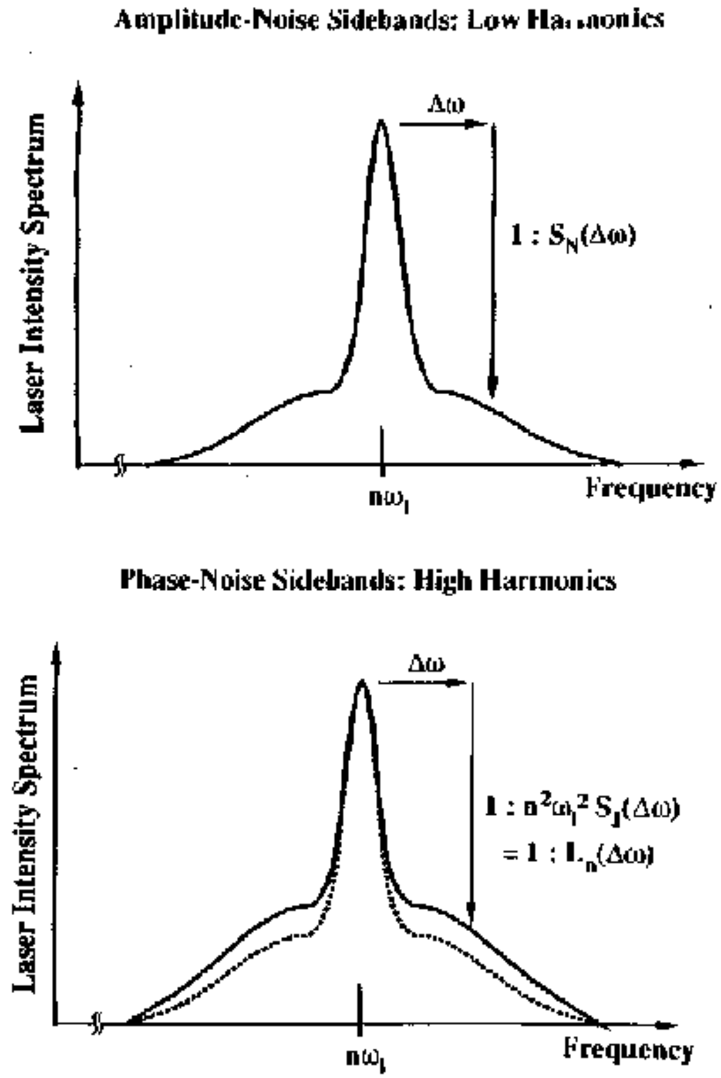

# phase noise integration

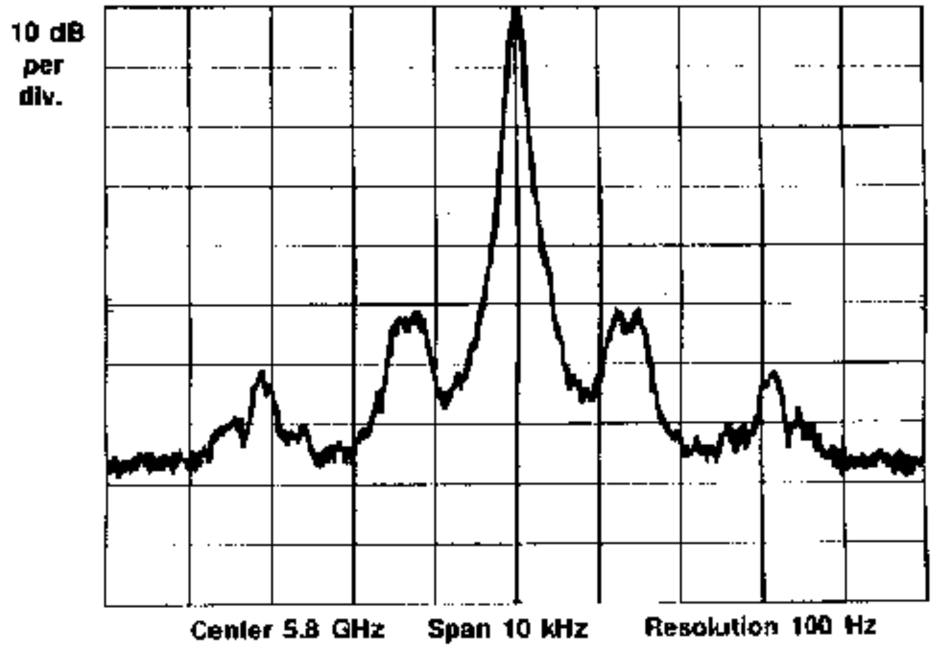


$$\left\| J^2(t) \right\| = \sigma_J^2 = \frac{1}{\pi} \int_{\omega_{low}}^{+\omega_l/2} S_J(\omega)\, d\omega$$

$\omega_{low}$ is the low - frequency limit of integration

$\approx \pi / T,$ where $T$ is the period of observation

In words: Power in sidebands divided by power in carrier is mean-squared phase deviation in radians. Divide by the radian frequency to obtain the timing deviation

# Laser Timing Stabilization

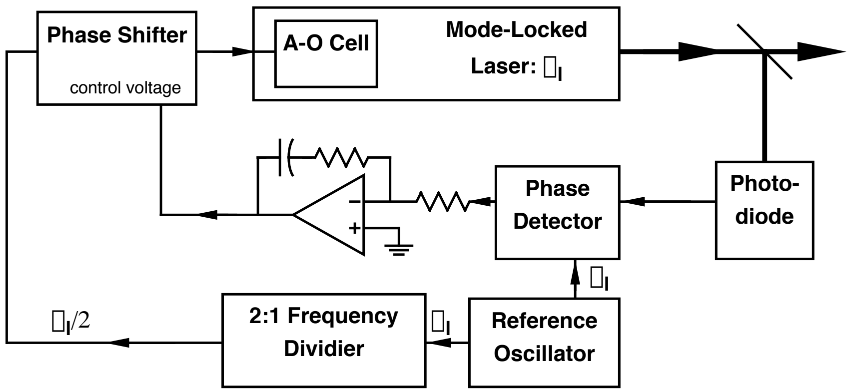


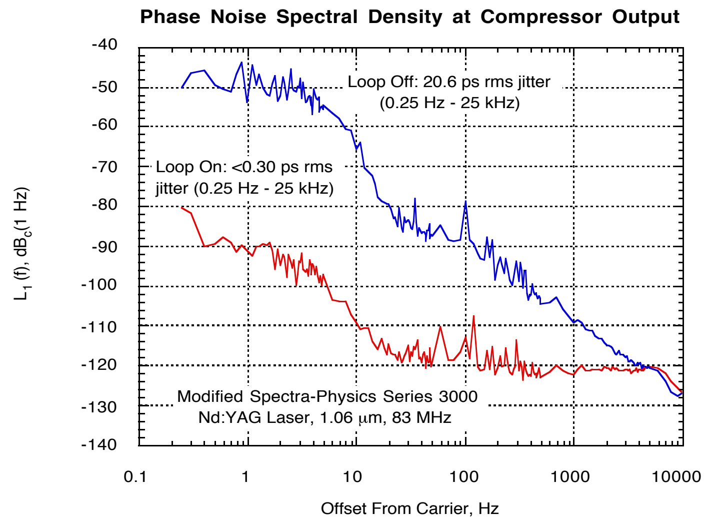


This method is applicable to any actively mode-locked laser.
Passively mode-locked lasers can be phase-locked by introducing an electrically-controlled cavity tuning element

# On-Wafer Network Analysis

- photoconductive sampling probes
  - external probes for S-parameter measurements
  - internal-node probes
- NLTL/diode sampling IC probes for waveform & network measurements
- STM/AFM probes

# Active Probes

## Highly Reproducible Optoelectronic Wafer Probes with Fiber Input

M. D. Feuer, S. C. Shunk, P. R. Smith[1], H. H. Law[1], C. A. Burrus[2] and M. C. Nuss

AT&T Bell Labs, 101 Crawfords Corner Rd., Holmdel, NJ 07733-3030
[1] AT&T Bell Labs, 600 Mountain Ave., Murray Hill, NJ 07974-0636
[2] AT&T Bell Labs, 791 Holmdel-Keyport Rd., Holmdel, NJ 07733-0400

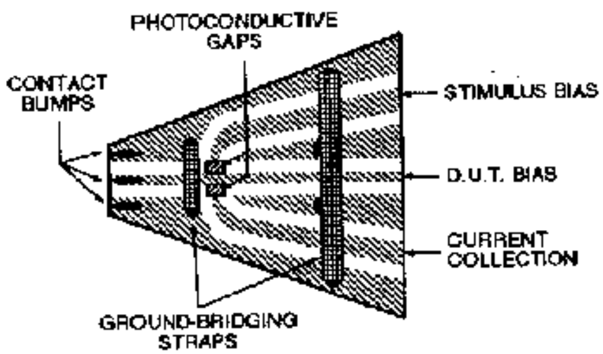


Figure 1. Schematic layout of optoelectronic wafer probe with ground-bridging straps. Optical pulses are introduced through the back of the probe substrate. The system provides high bandwidth, throughput and accuracy.

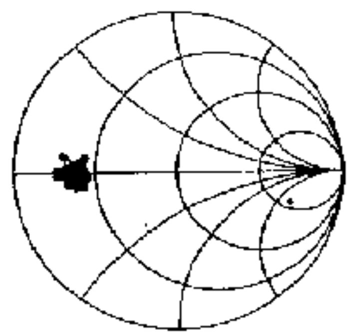

Figure 2. S11 of a thin-film resistor with a dc resistance of 12.5 ohm, from dc to 125 GHz at 2.5 GHz intervals, after full correction with vector accuracy enhancement.

## Subpicosecond GaAs Wafer Probe System

M. S. Shakouri, A. Black †, D. M. Bloom

*Edward L. Ginzton Laboratory, Stanford UniversityStanford, CA 94305*
*† Now at Gadzoox Microsystem, Los Gatos, CA.*

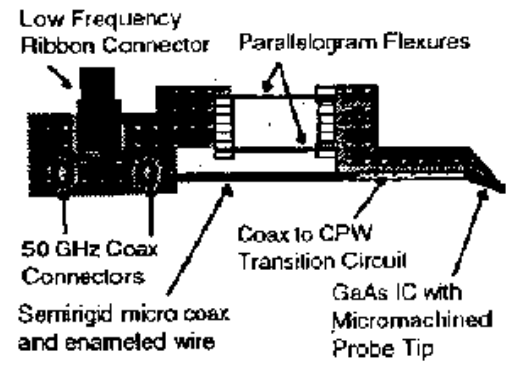


FIG. 1. GaAs Wafer Probe Assembly

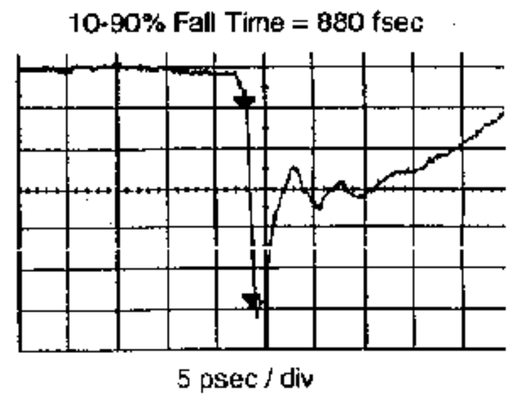

# On-Wafer Signal Measurements

## Novel High-Impedance Photoconductive Sampling Probe for Ultra-High Speed Circuit Characterization

Joungho Kim, Yi-Jen Chan*, Steven Williamson, John Nees, Shin-ichi Wakana, John Whitaker, Dimitris Pavlidis*

Center for Ultrafast Optical Science, *Center for High Frequency Microelectronics
The University of Michigan, EECS
2200 Bonisteel, 1006 IST
Ann Arbor, MI48109-2099

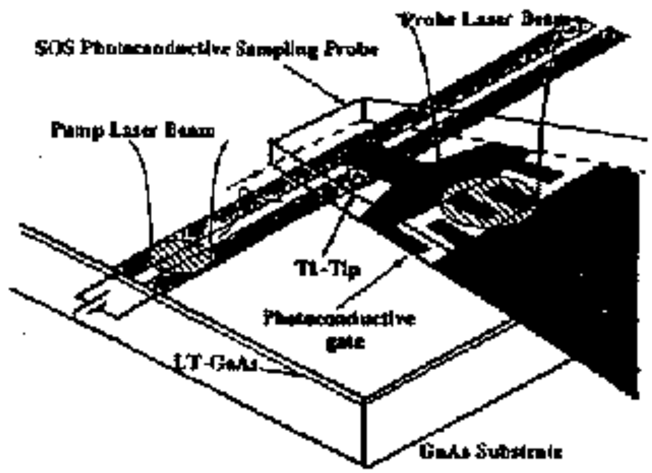


Fig.1 Experimental set-up to measure short electrical pulses propagating along a coplanar strip. We used 120-fs Ti-Sapphire laser for pump and probe beam.

# NLTL-based Probe for On-Wafer Network Analysis

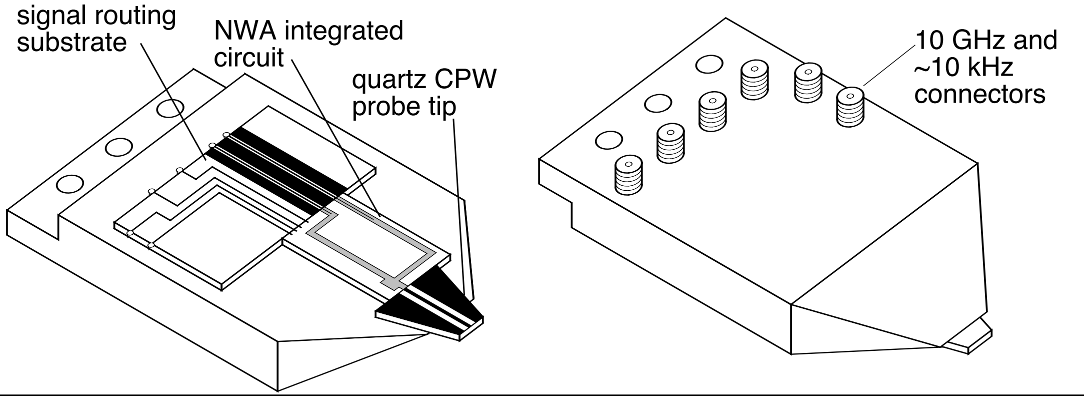


NLTL-based IC coupled to DUT through wideband CPW-on-quartz probe tip

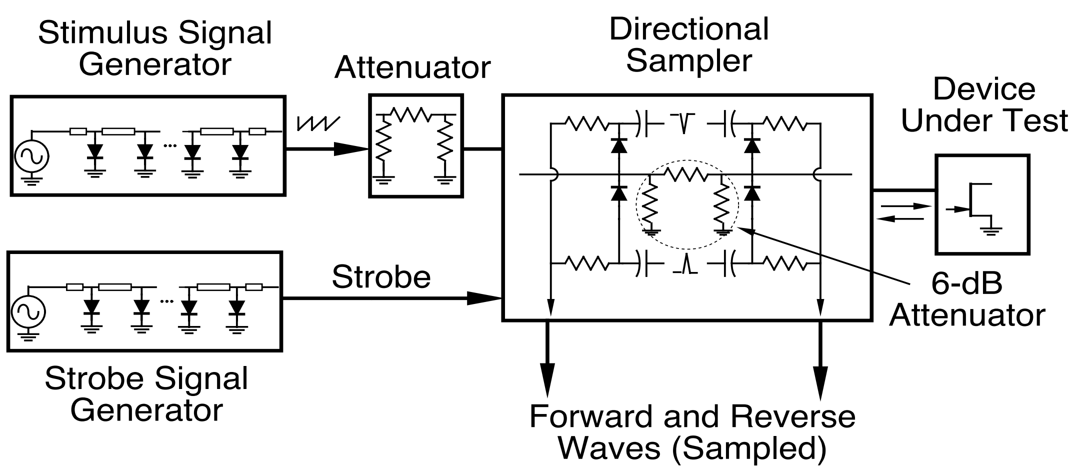


measurements made in frequency domain with pulsed stimulus signal. Forward & reverse waves separated by directional sampler, not by time-gating.

# System Block Diagram

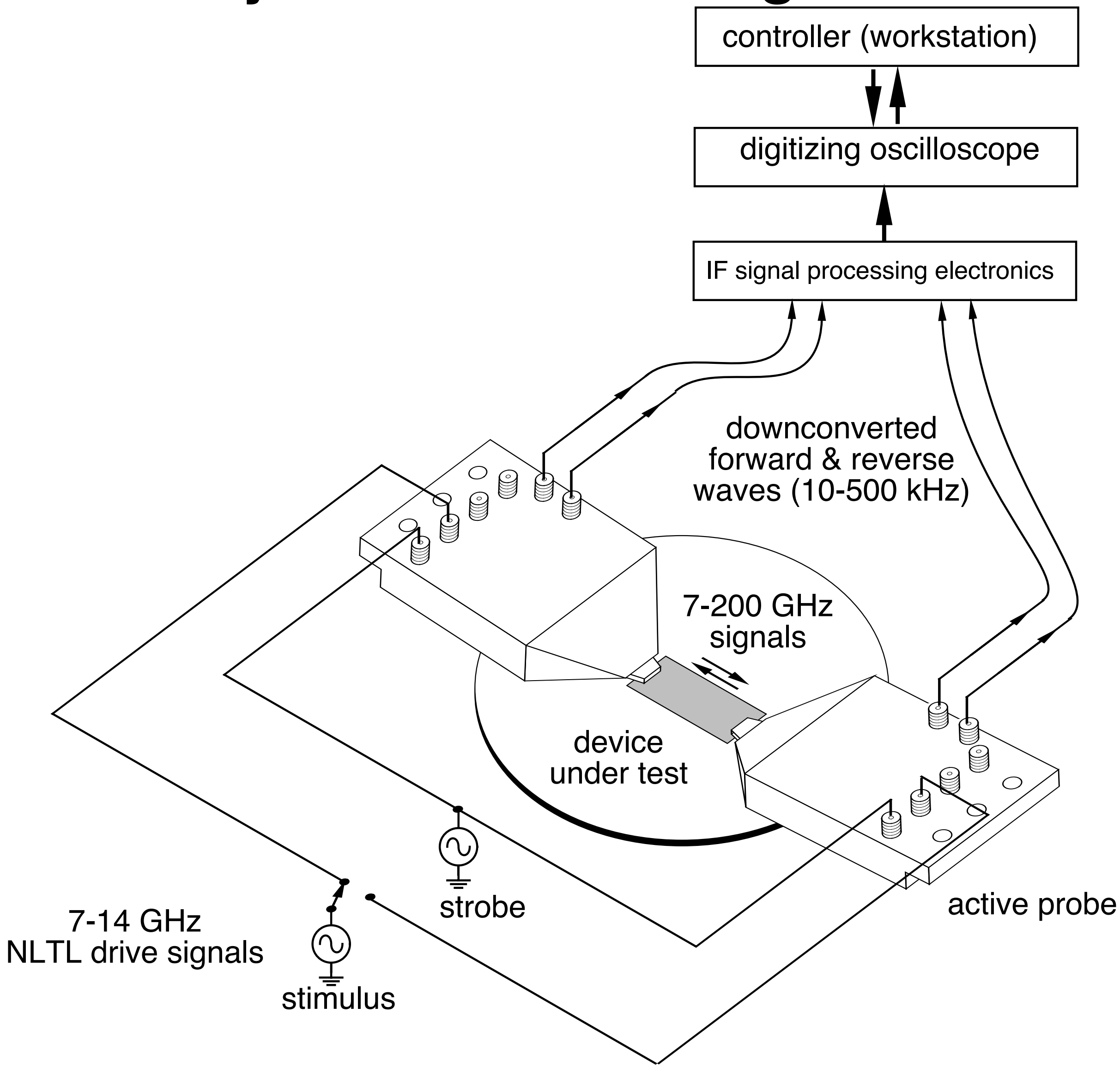

# NLTL-based active probe pulse response

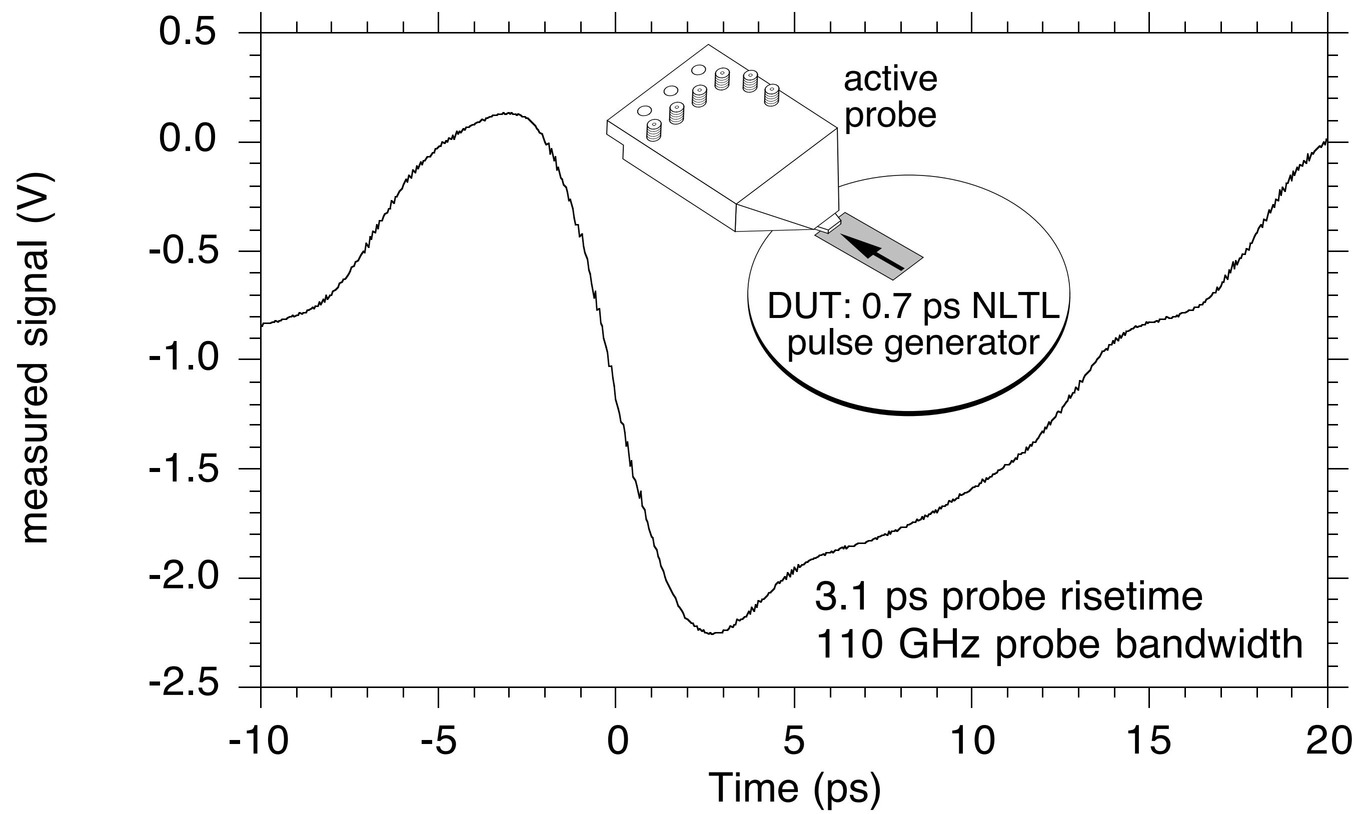

# Measurements with active probe

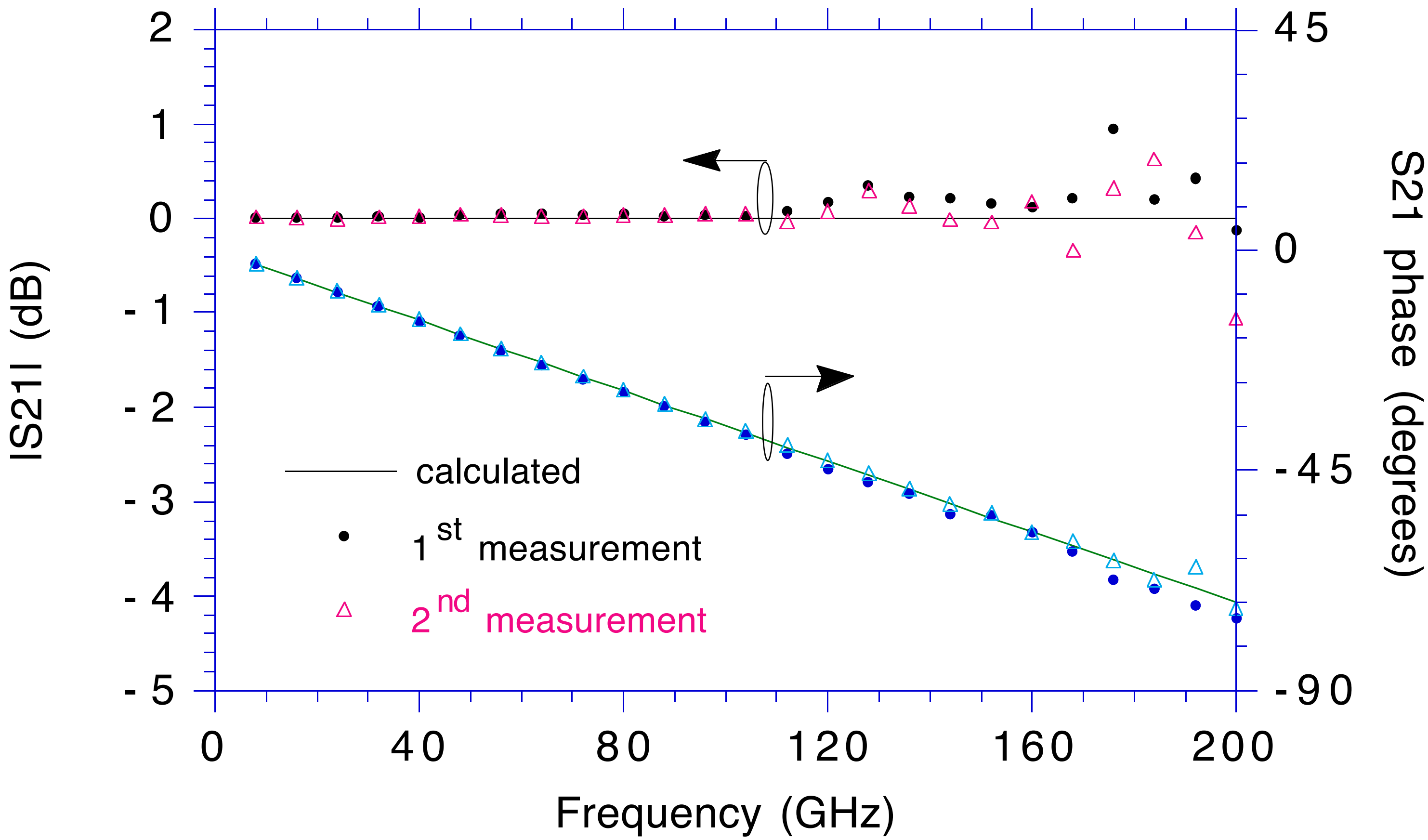

# Measurements with active probe

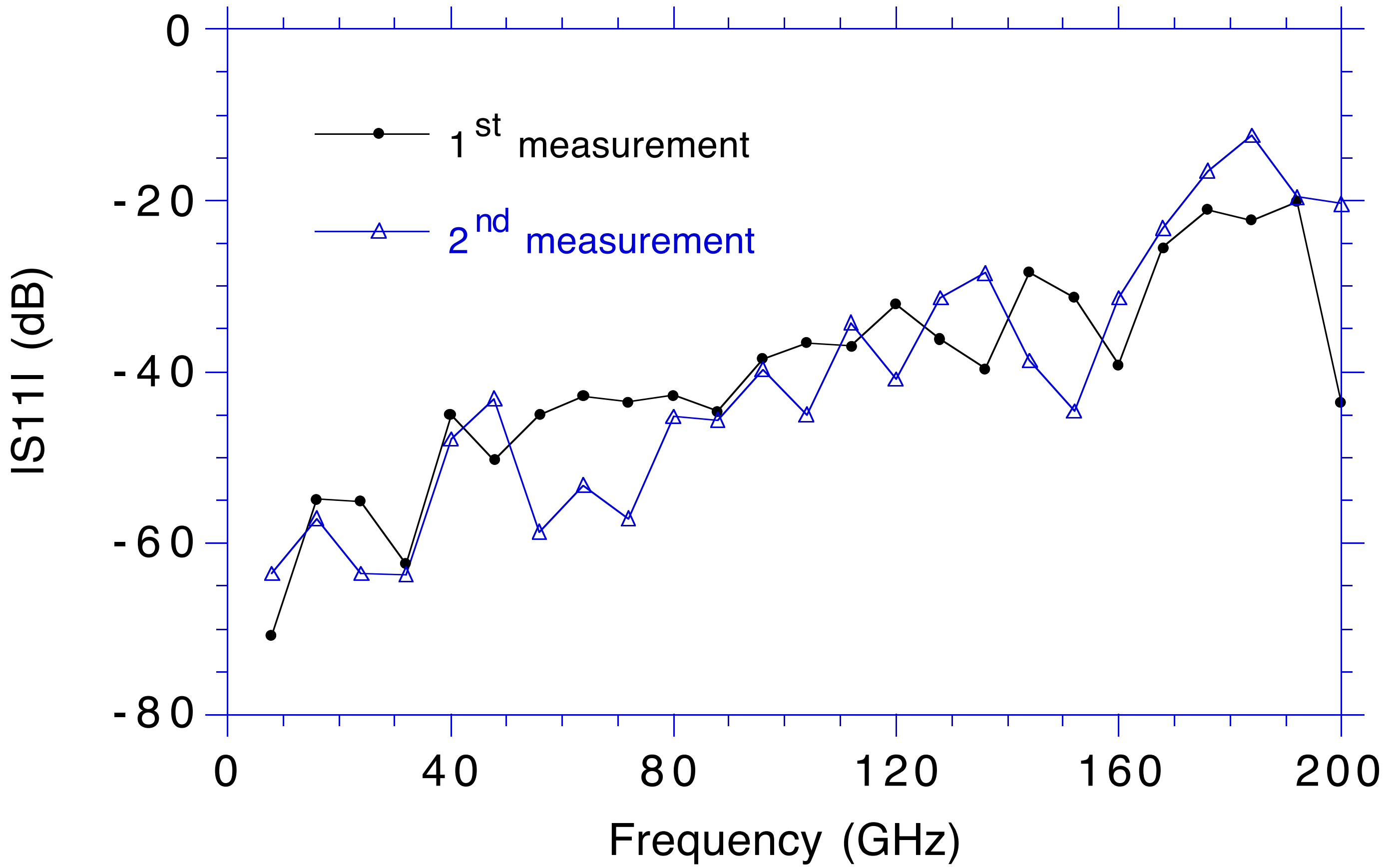

# Measurements with active probe

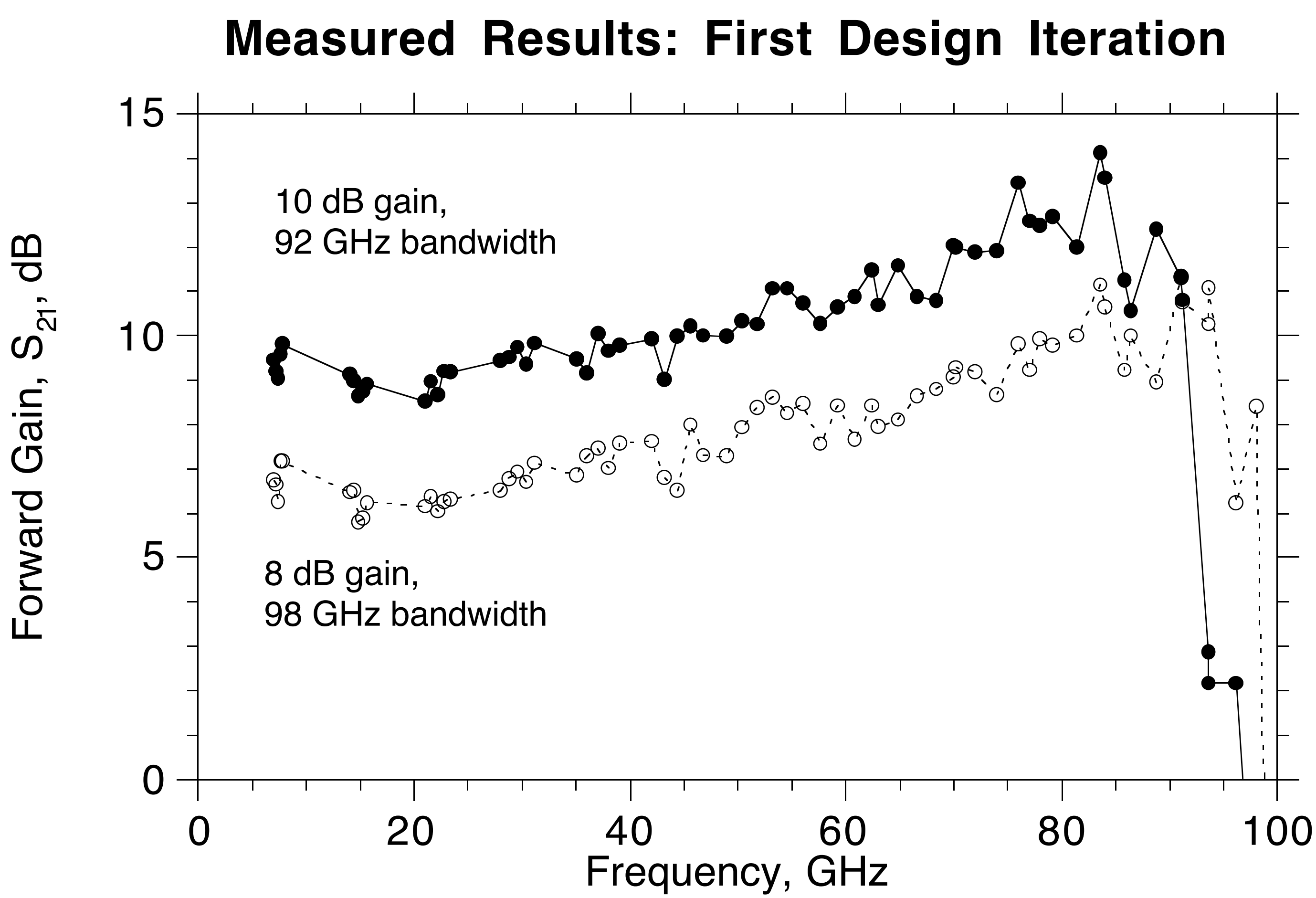


(capactiive-division TWA shown earlier.

# AFM active probe

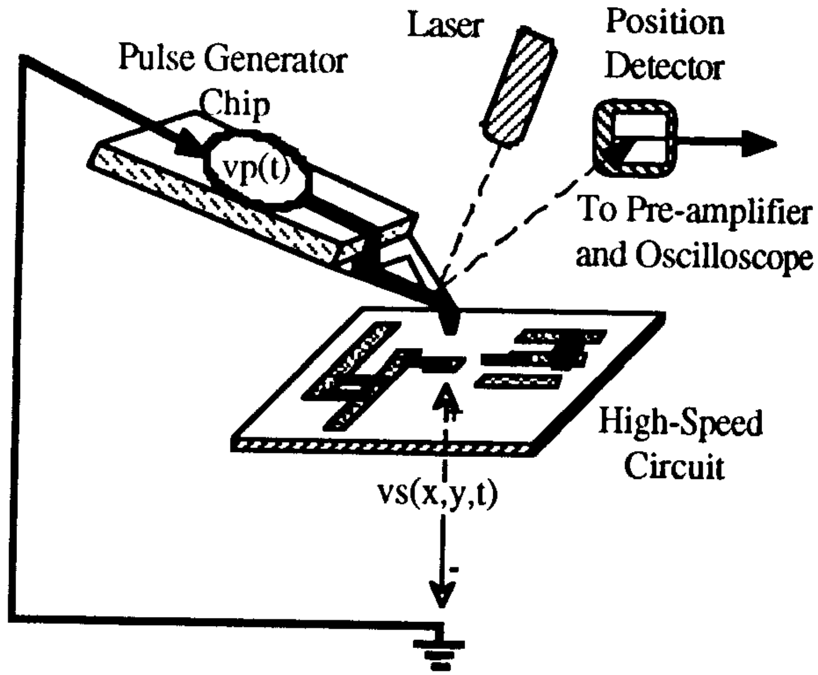


**Figure 1.** High-speed SFM probe system.

- Ho et al , 1995 Ultrafast Electronics & Optoelectroncis conference
- Force on AFM tip proportional to voltage squared--provides nonlinearity to sample DUT signal with pulse train applied through AFM tip.
- Bettina et al, 1997 UFEO conference: NLTL pulse generator, ~ 1 ps resolution

# pico-/femto- second laser spectroscopy

(mm-Wave and sub-mm-wave Gain-Frequency Measurement System)

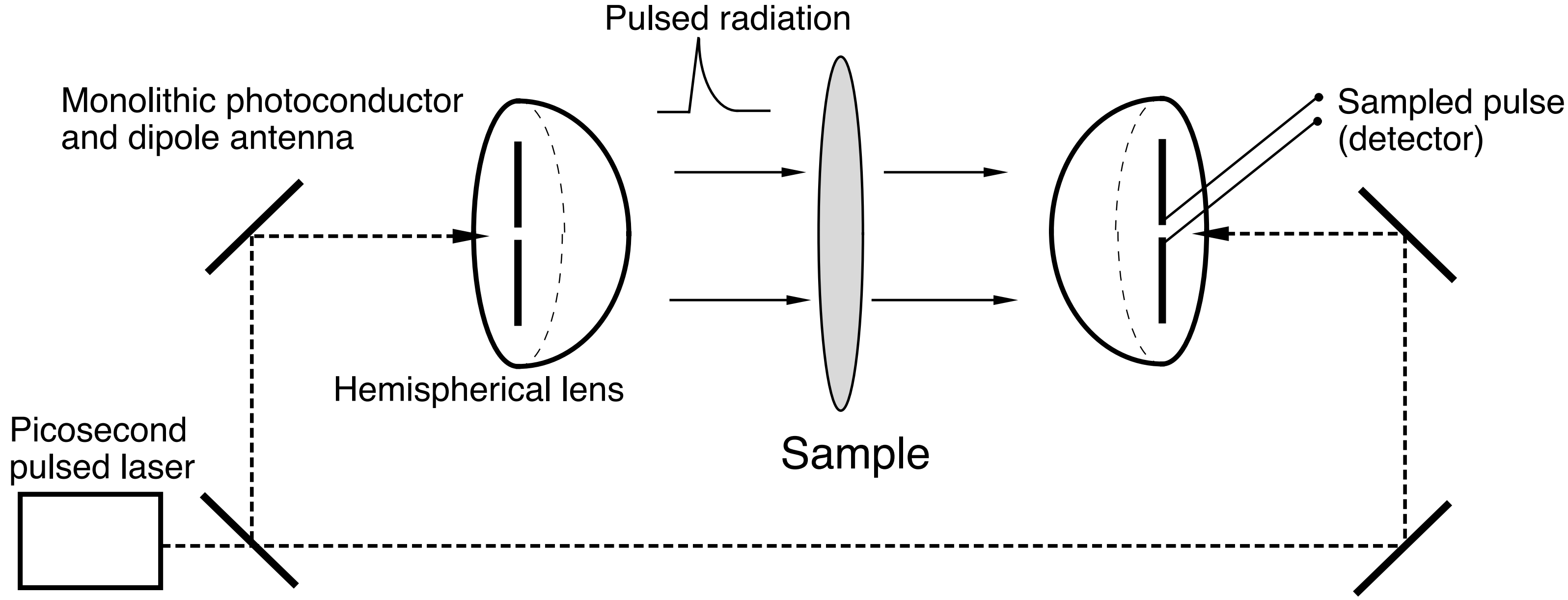


- Broadband: ≈1.5 THz demonstrated
- need picosecond laser (big, $$)

Purpose: measurements of materials and sub-mm-wave components

# (sub)picosecond Laser Spectroscopy: Exter et al.

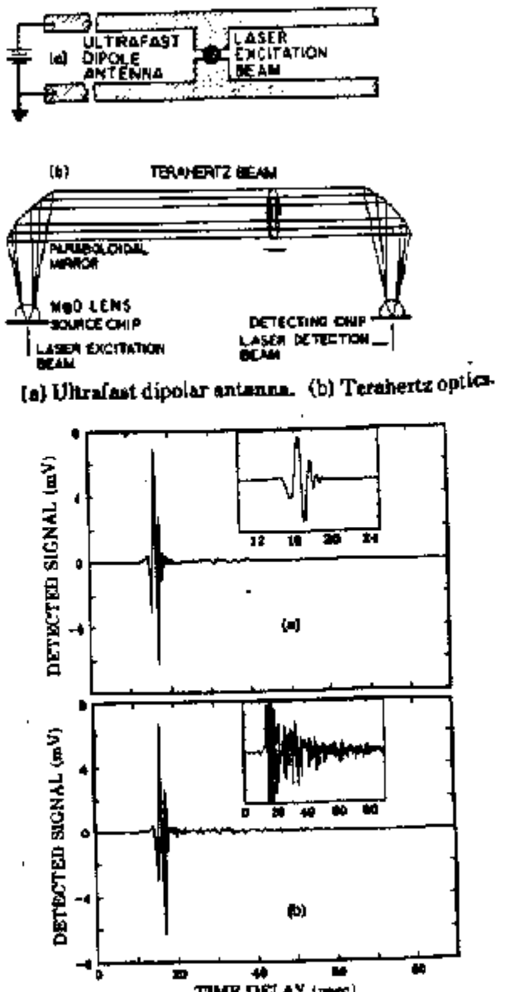


Fig 3-2 (a) Measured electrical pulse of the freely propagating terahertz beam in pure nitrogen. The inset shows pulse on an expanded time scale. (b) Measured electrical pulse with 1.5 Torr of water vapor in the enclosure. The inset shows pulse on a 20× expanded vertical scale.

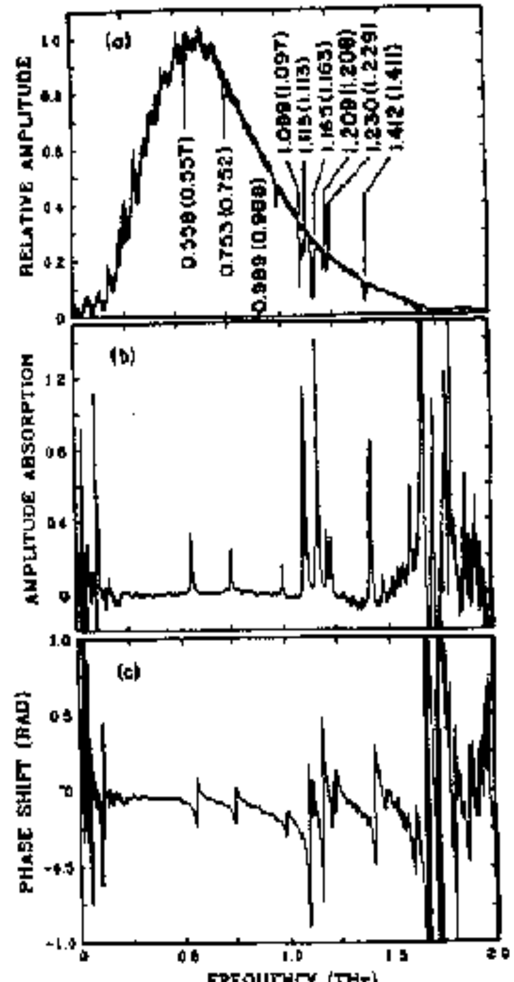


Fig 3-3 (a) Amplitude spectra of Figs. 2(b) and 2(c). (b) Amplitude absorption coefficient obtained from Fig. 3(a). (c) Relative phase of the spectral components of Fig. 3(a).

# NLTL-based Transmitter and Receiver

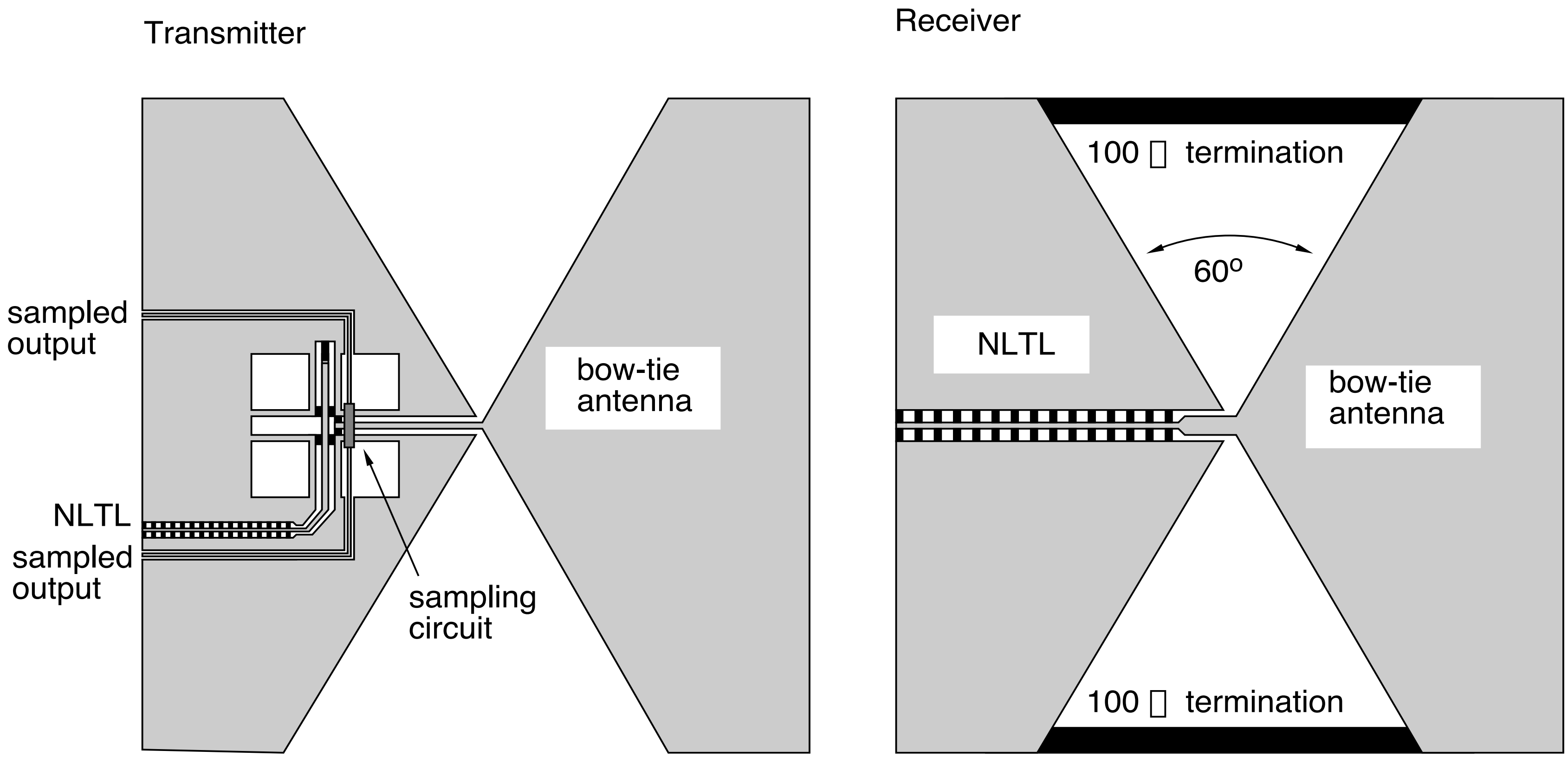

# Free-Space mm-Wave Measurement System

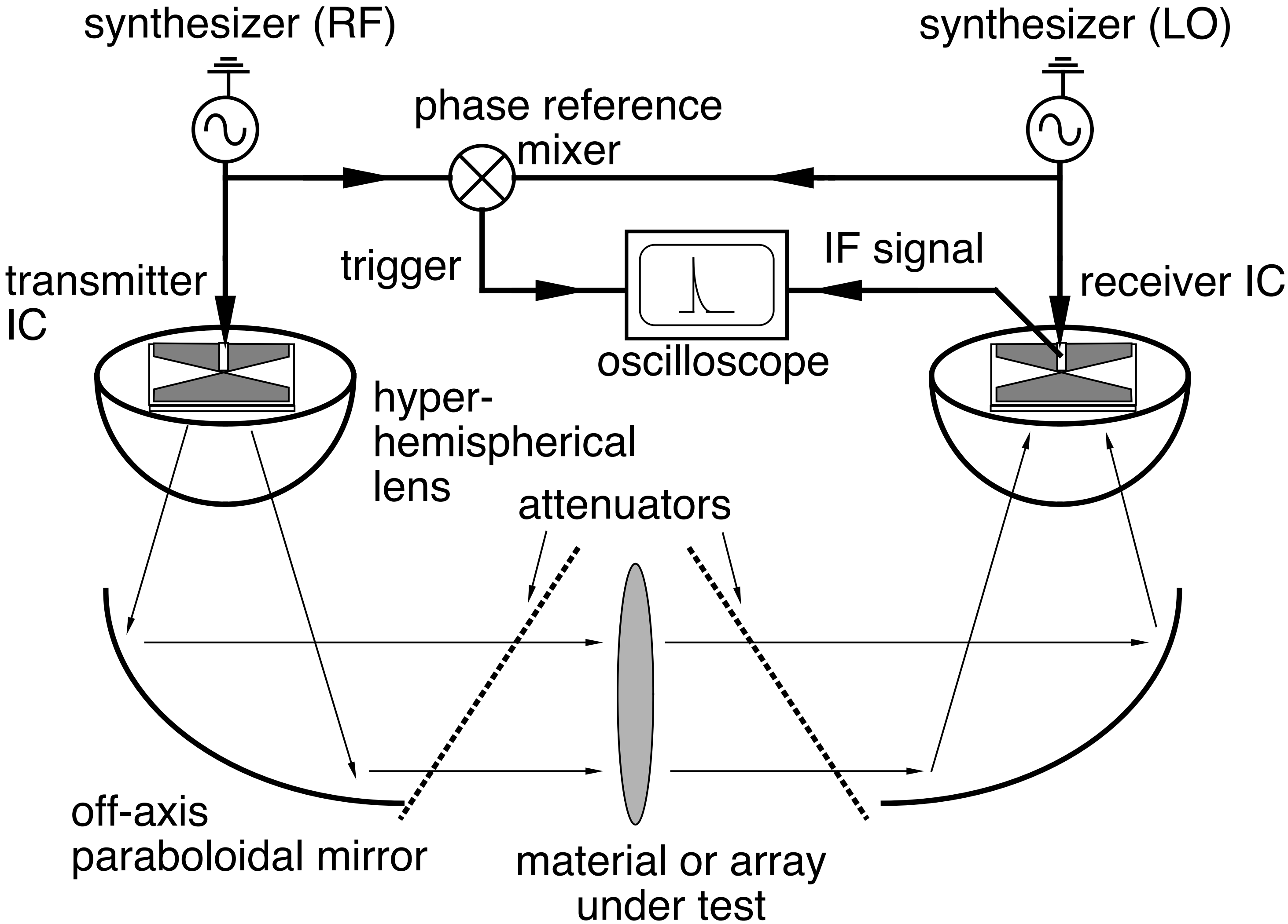

# Measured Signal with NLTL-based system

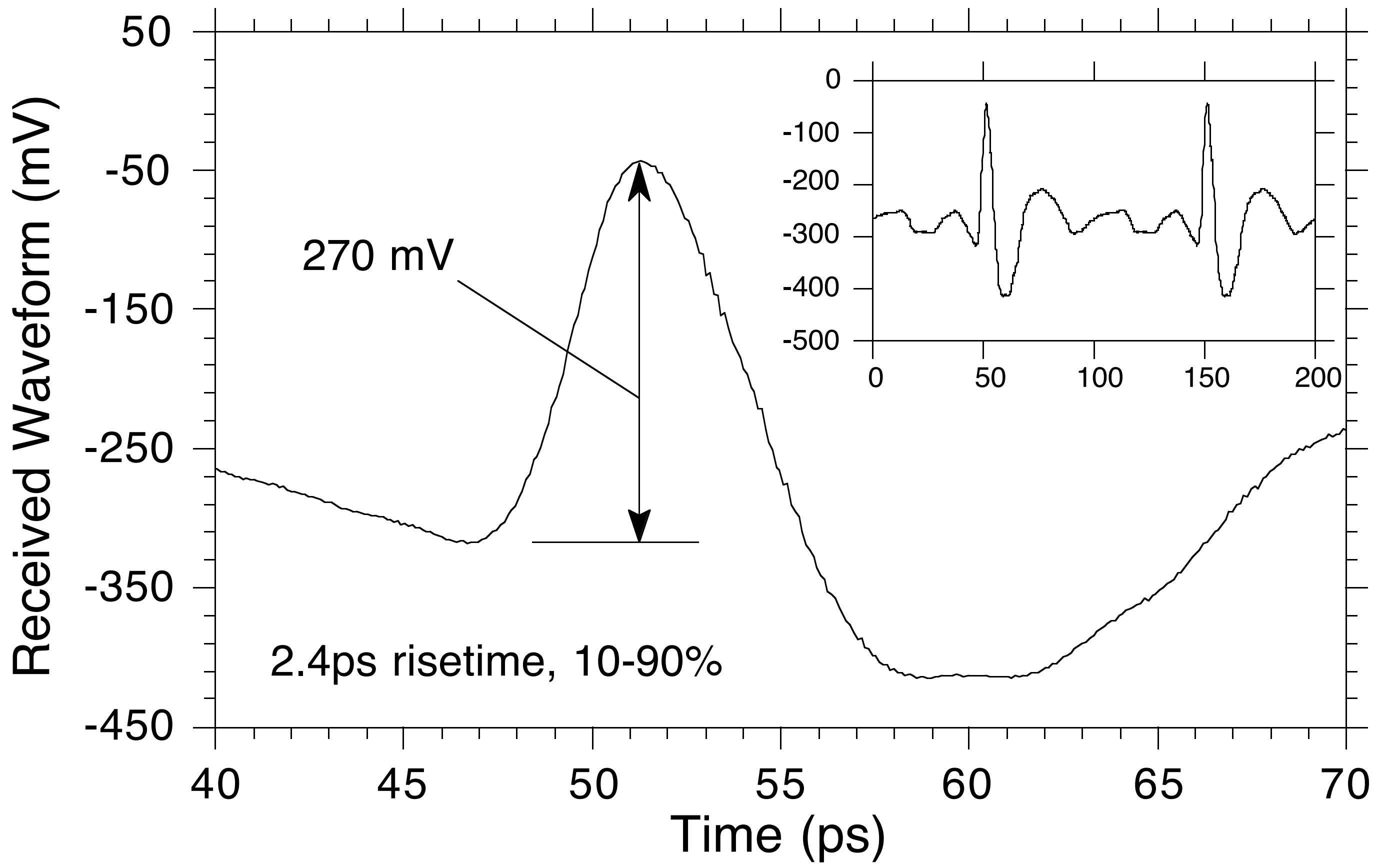

# measurement with NLTL-based system

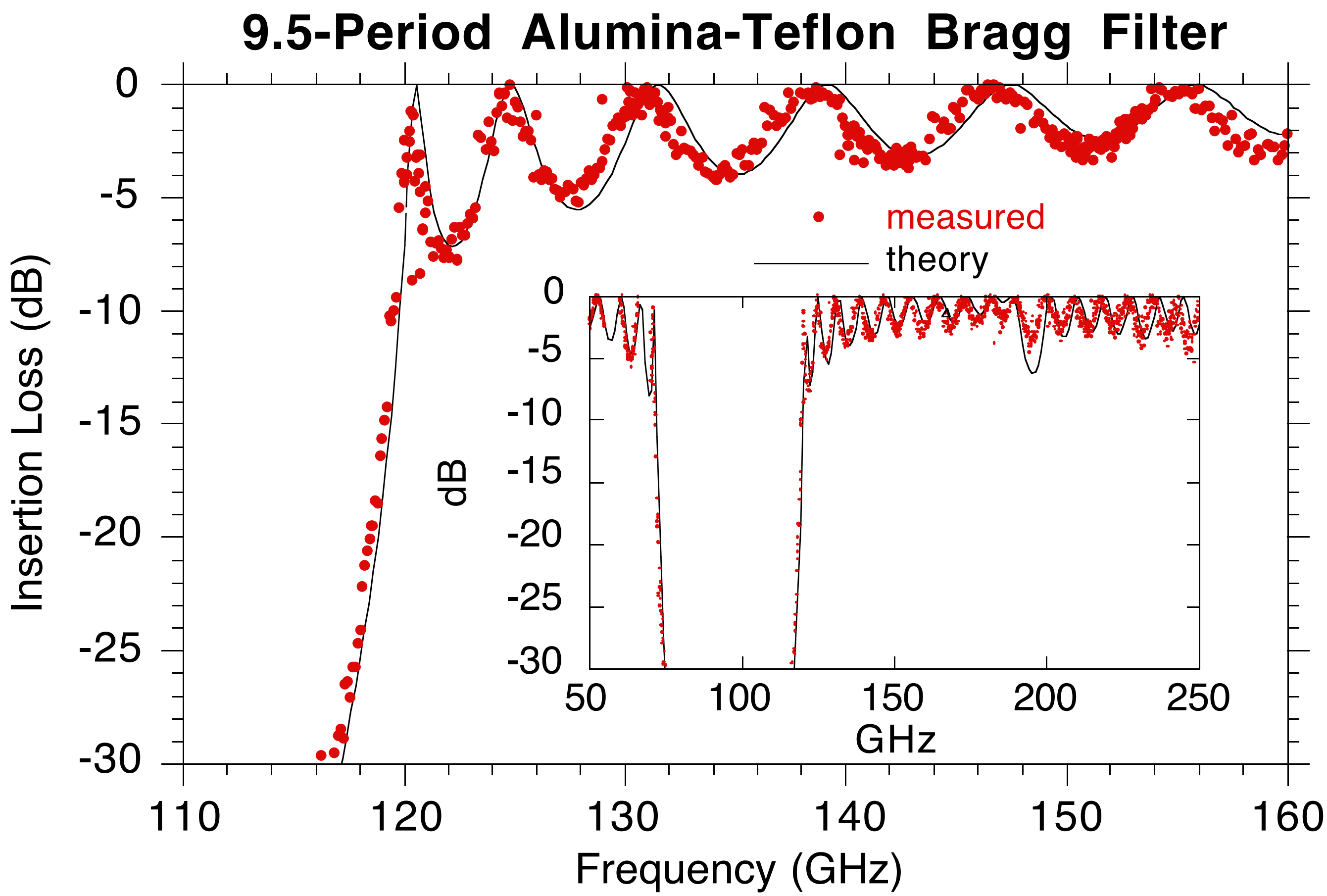

# measurement with NLTL-based system

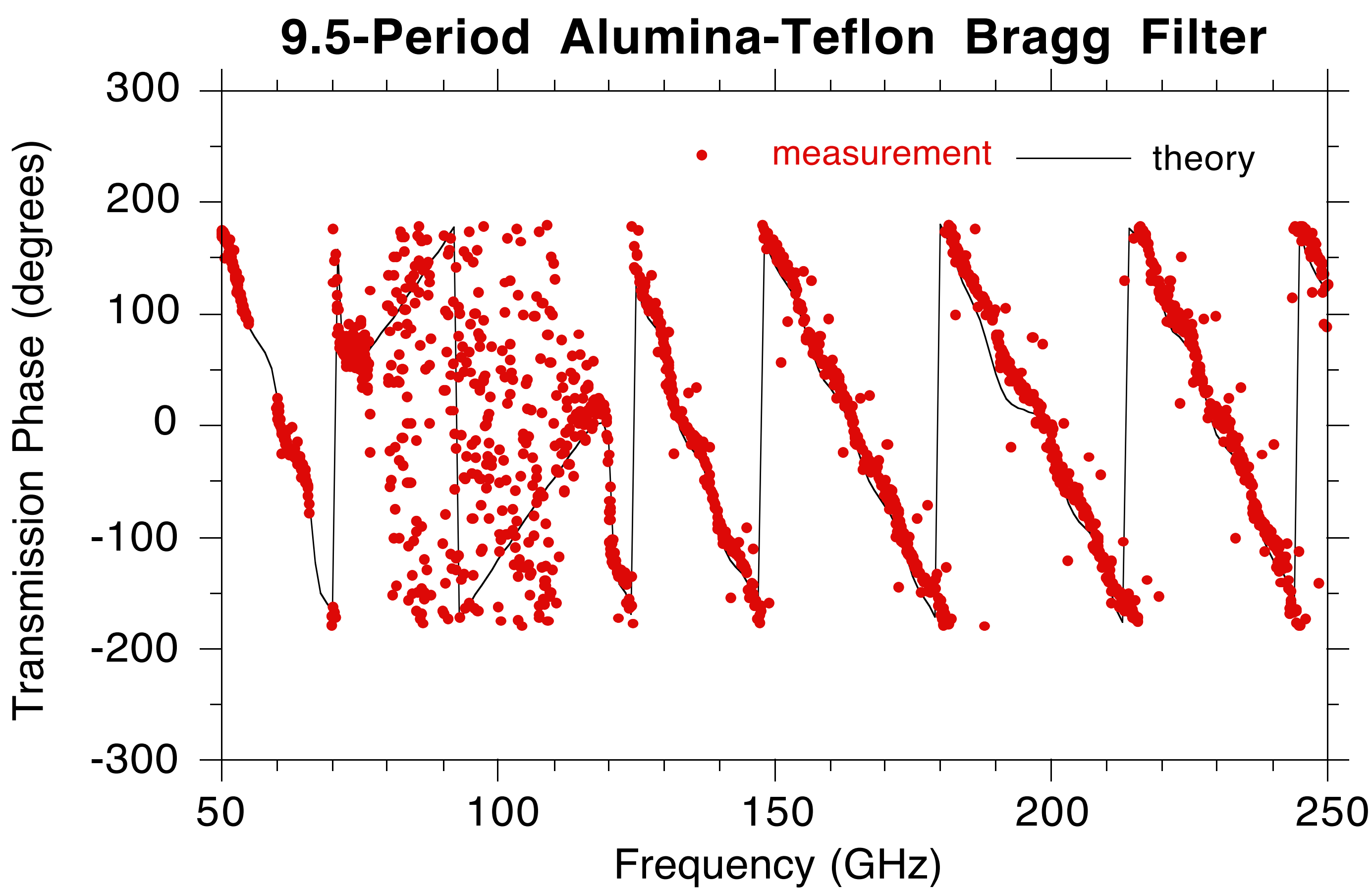

Appendix sections:

Soliton NLTL impulse compressors
Traveling-wave RTD pulse generators

# RTD Array Oscillators for THz signal generation

- Power per device is small.
- Combine outputs from array of ≈1000-10,000 SRTD oscillators.
- Cavity resonator defines oscillation frequency, provides strong coupling between array elements

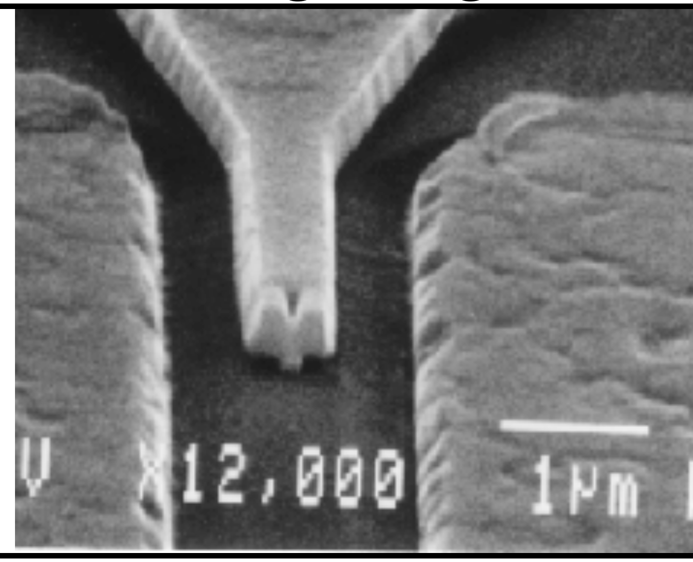


Array oscillator layout

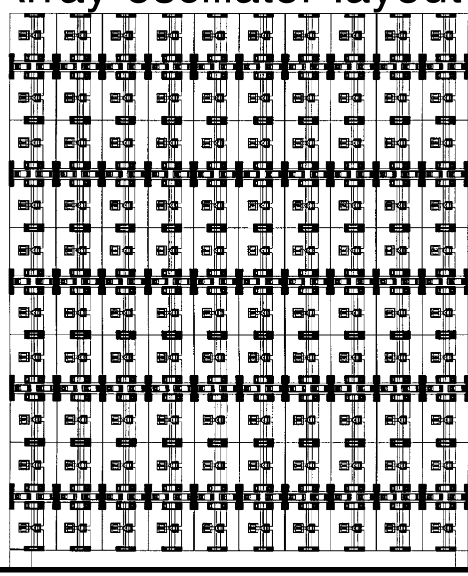

Quasi-optical Array Oscillator:

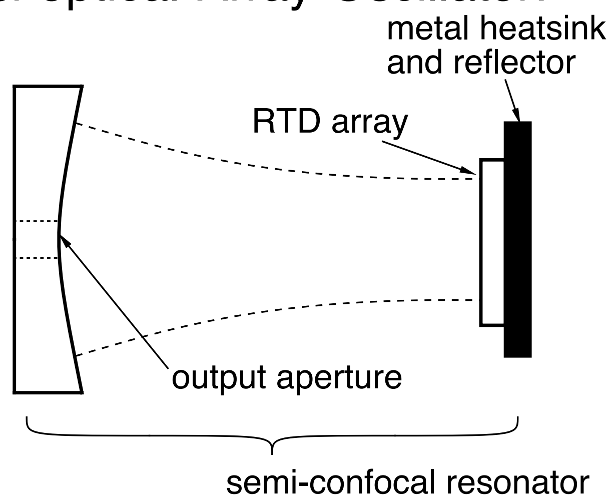

# A Critical Issue: Suppression of Bias Circuit Oscillations

## Oscillator: array in resonator

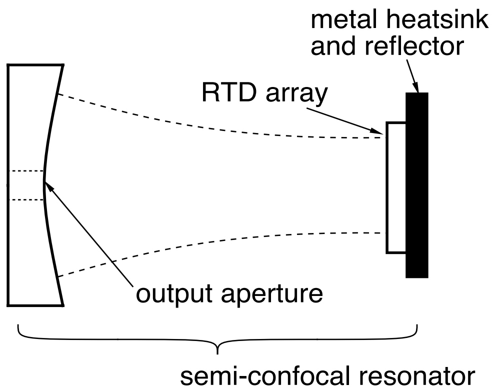


--------------------------------------------

## Array: negative-resistance plane

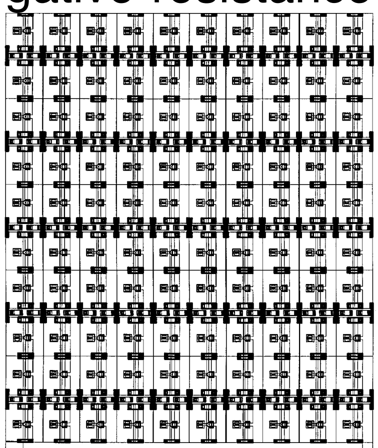

## Array unit cell: RTD with bias stabilization

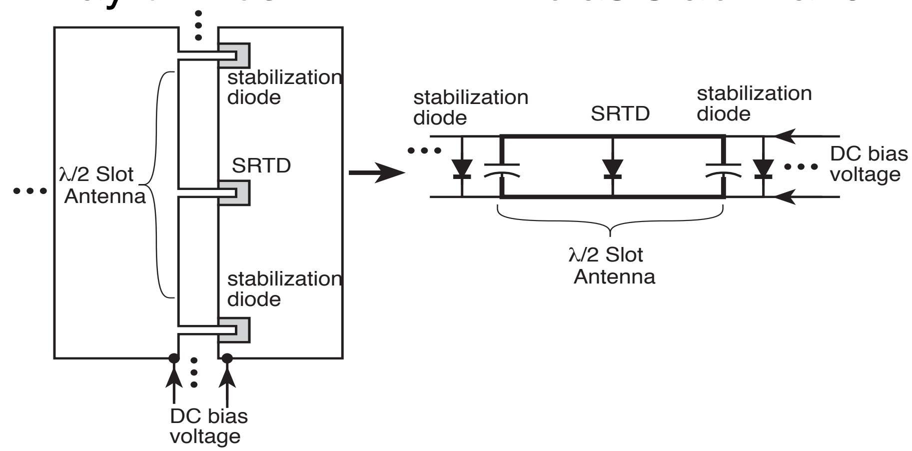


- Without stabilization, bias circuit stability issues limit power to $\approx$ 0.5 mW.

- integrated Schottky stabilizer diodes

# Maximum RTD Output Power

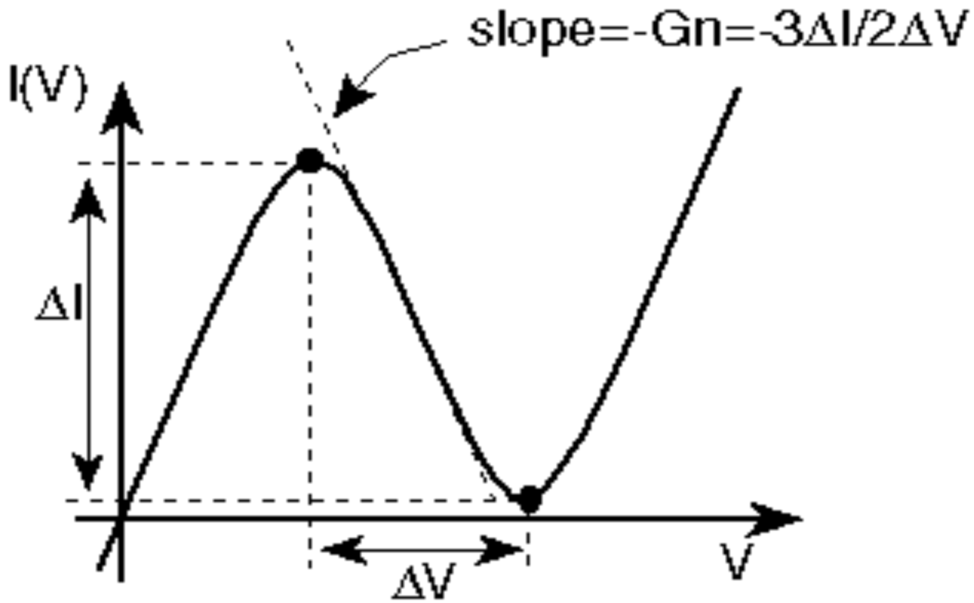


- Cubic Polynomial fit to RTD I-V charactersitics
- Peak negative conductance: $G_n = 3\Delta I / 2\Delta V$
- Maximum RTD output power:

$$P_{\max} = (3/16)\Delta I \Delta V (1 - f^2 / f_{\max}{}^2)$$

- In terms of $G_n$: $P_{\max} = (\Delta V^2 G_n / 8)(1 - f^2 / f_{\max}{}^2)$

## Conditions for Stability

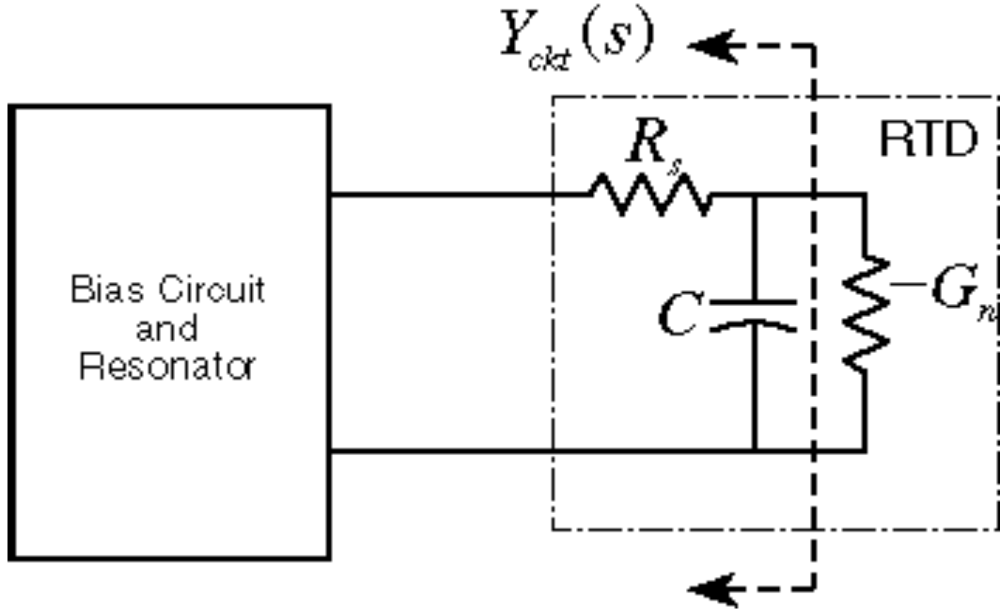


- Find complex frequencies $s_i = \sigma_i + j\omega_i$ at which $Y_{ckt}(s) = G_n$
- Necessary and sufficient condition for stability is $\sigma_i < 0$
- A sufficient condition for stability is

$$\mathrm{Re}[Y_{ckt}(j\omega)] = G_{ckt}(j\omega) > G_n$$

- At all frequencies where stability is demanded the external circuit should present a low impedance

## Power Limitations Imposed by Stability Requirements

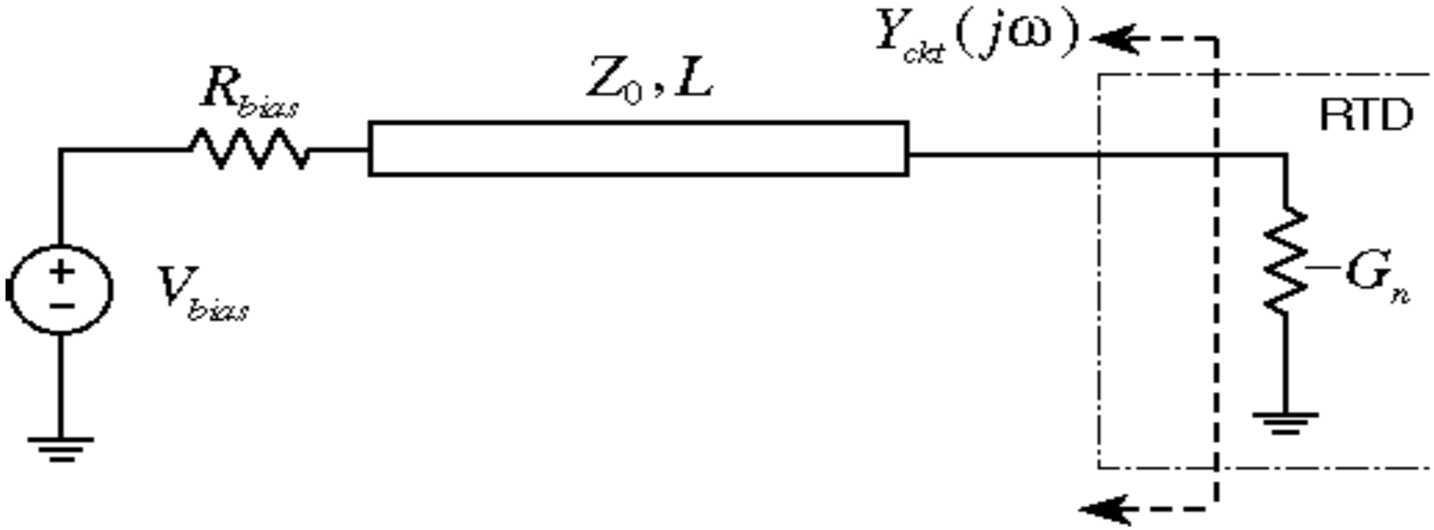


- A sufficient condition for stability is $\mathrm{Re}[Y_{ckt}(j\omega)] = G_{ckt}(j\omega) > G_n$
- DC stability demands that $1/R_{bias} > G_n$: $P_{\max} = \Delta V^2 / 8R_{bias}$
- Stability at other frequencies constraints $R_{bias} = Z_0$:

$$P_{\max} = \Delta V^2 / 8Z_0$$

- Power limitation eliminated if $L < \lambda / 4$: On wafer bias stabilizer at submm-wave frequencies

# RTD Bias Stabilization using shunt Schottky diodes

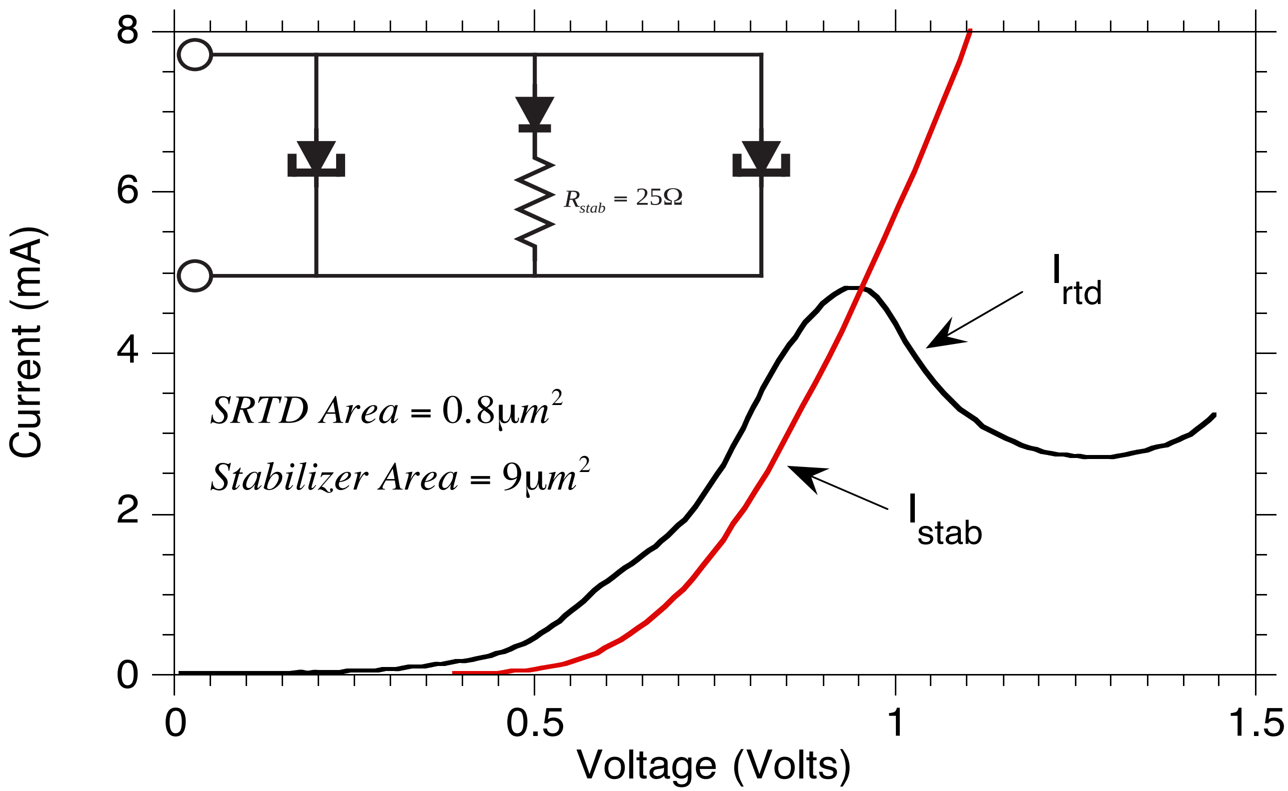


- 2 SRTDs share a stabilizer with $R_{stab} = 25\Omega$
- Easily extended to larger SRTDs by area scaling

# Slot Antenna Coupled RTD Oscillator

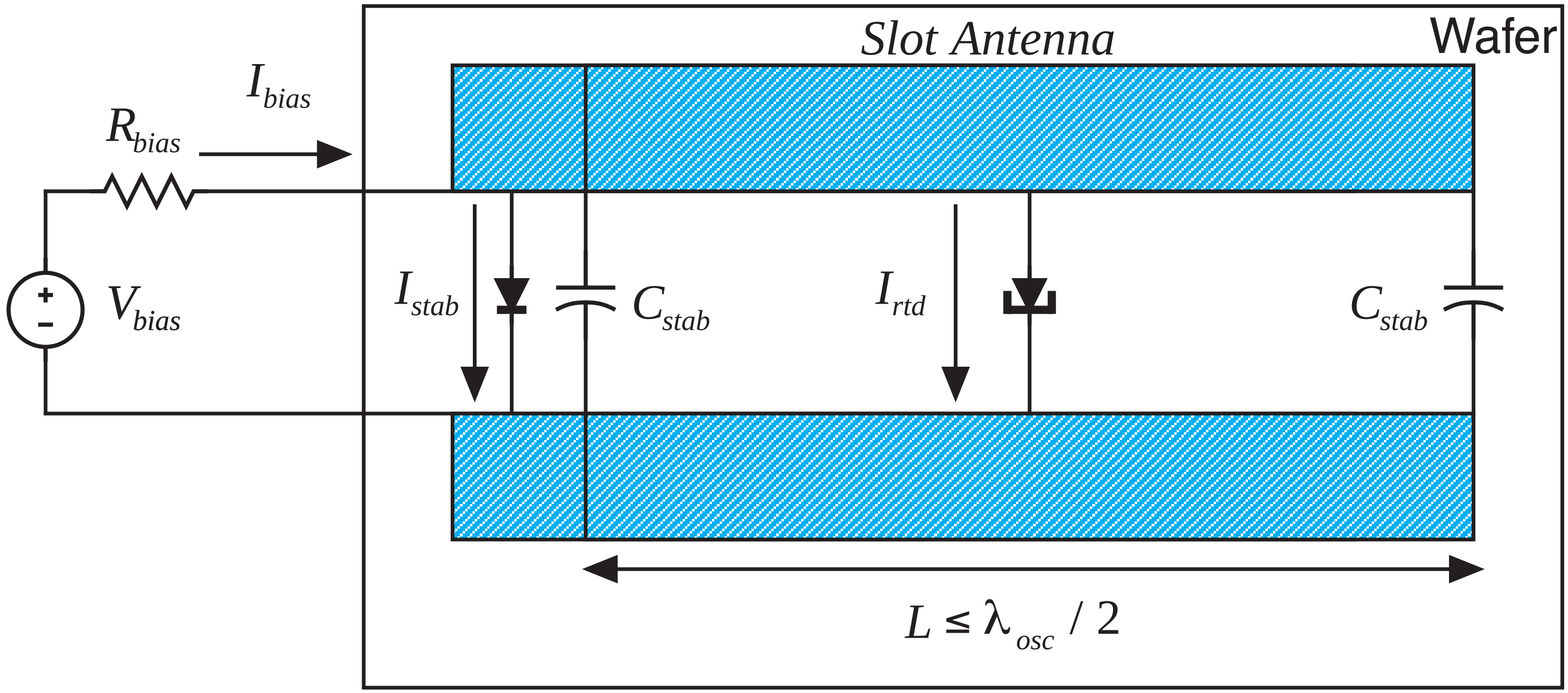


- Slot Antenna: Resonating and Radiating element
- SRTD capacitance detunes the slot length
- Easily extended to arrays

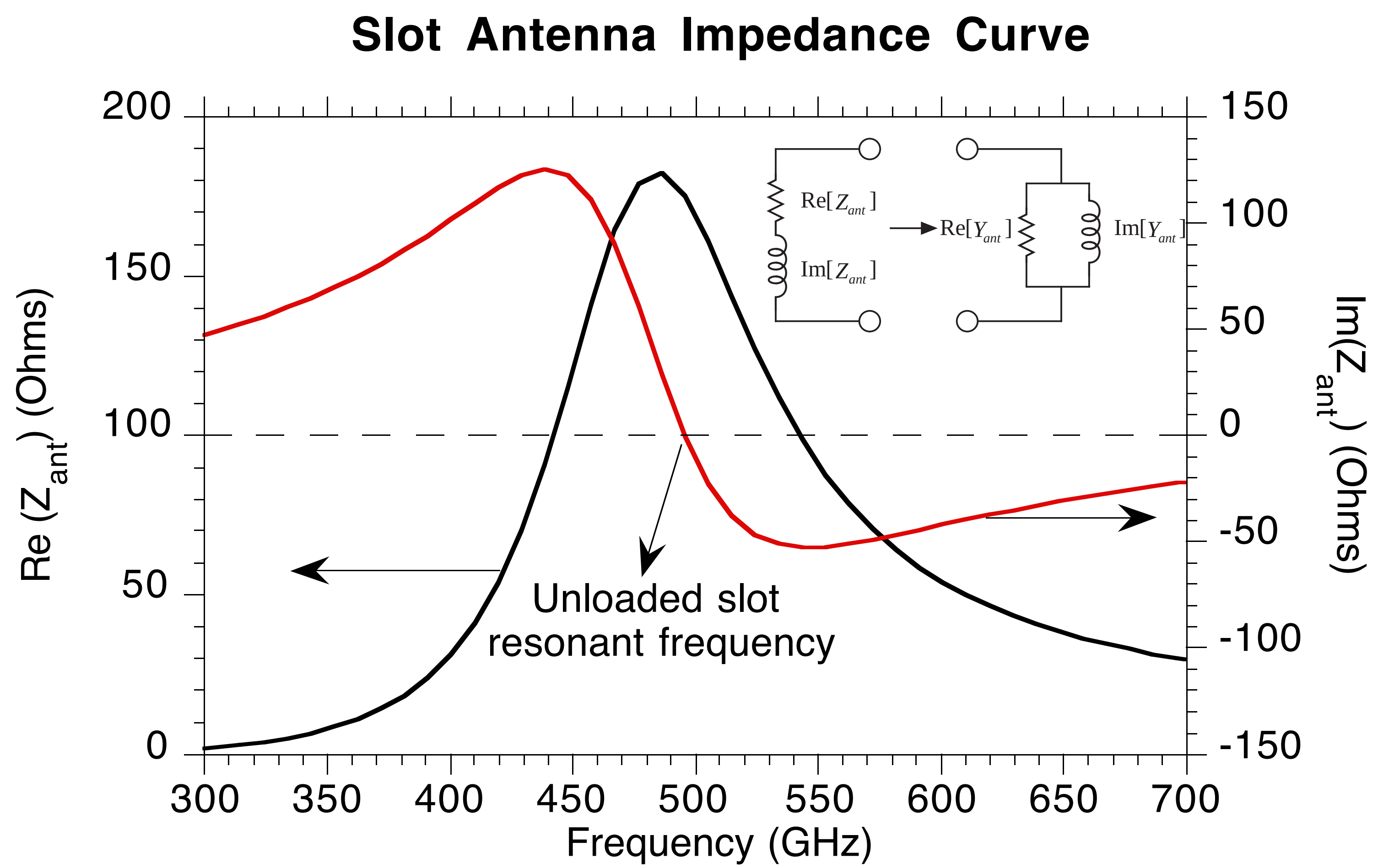

Slot Antenna Impedance Curve
Re (Z_ant) (Ohms)
Im(Z_ant) (Ohms)
Frequency (GHz)
Unloaded slot
resonant frequency
Re[Z_ant]
Im[Z_ant]
Re[Y_ant]
Im[Y_ant]

# InGaAs/AlAs SRTDs with InGaAs/InAlAs Schottky stabilizer diodes

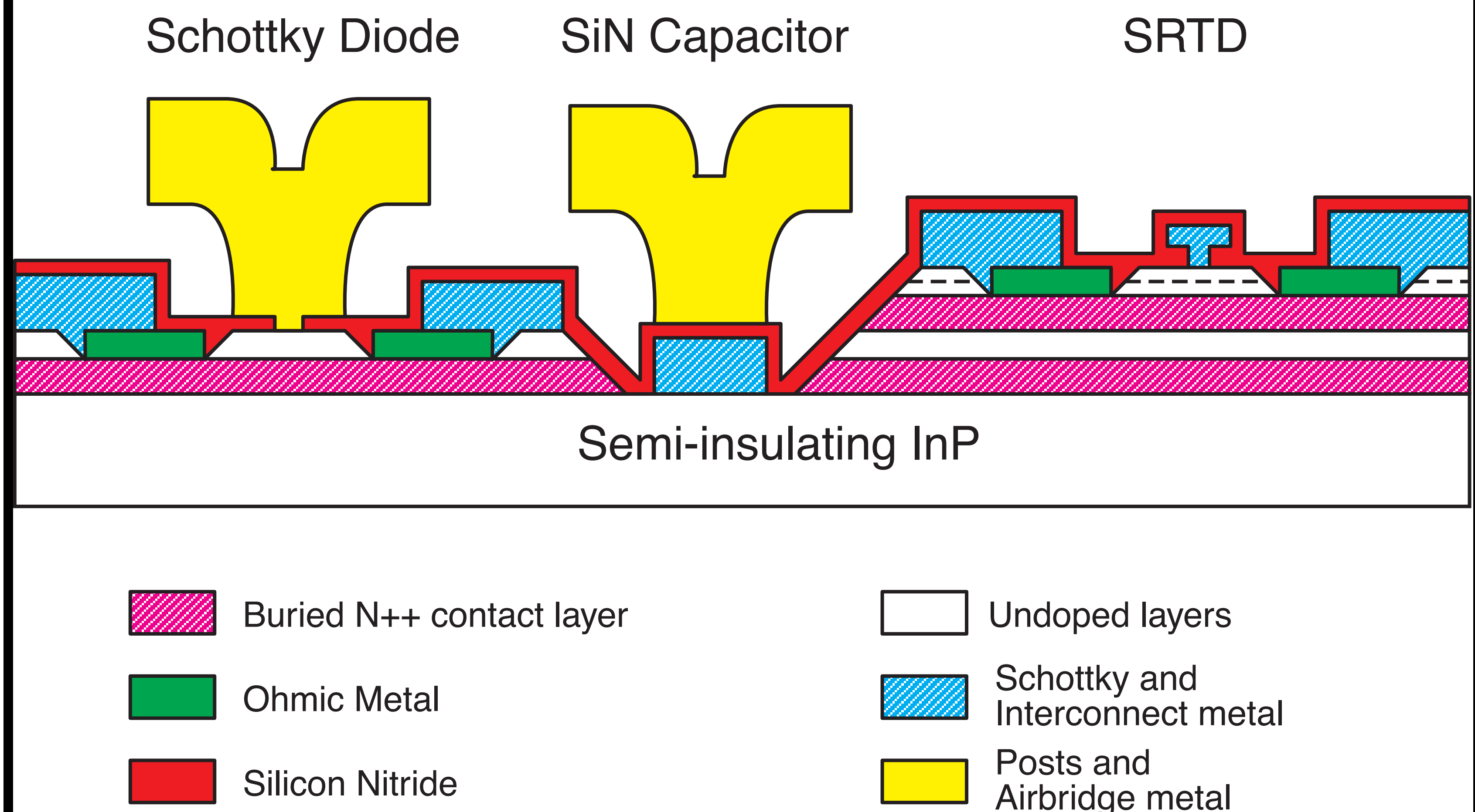

# Oscillator Array

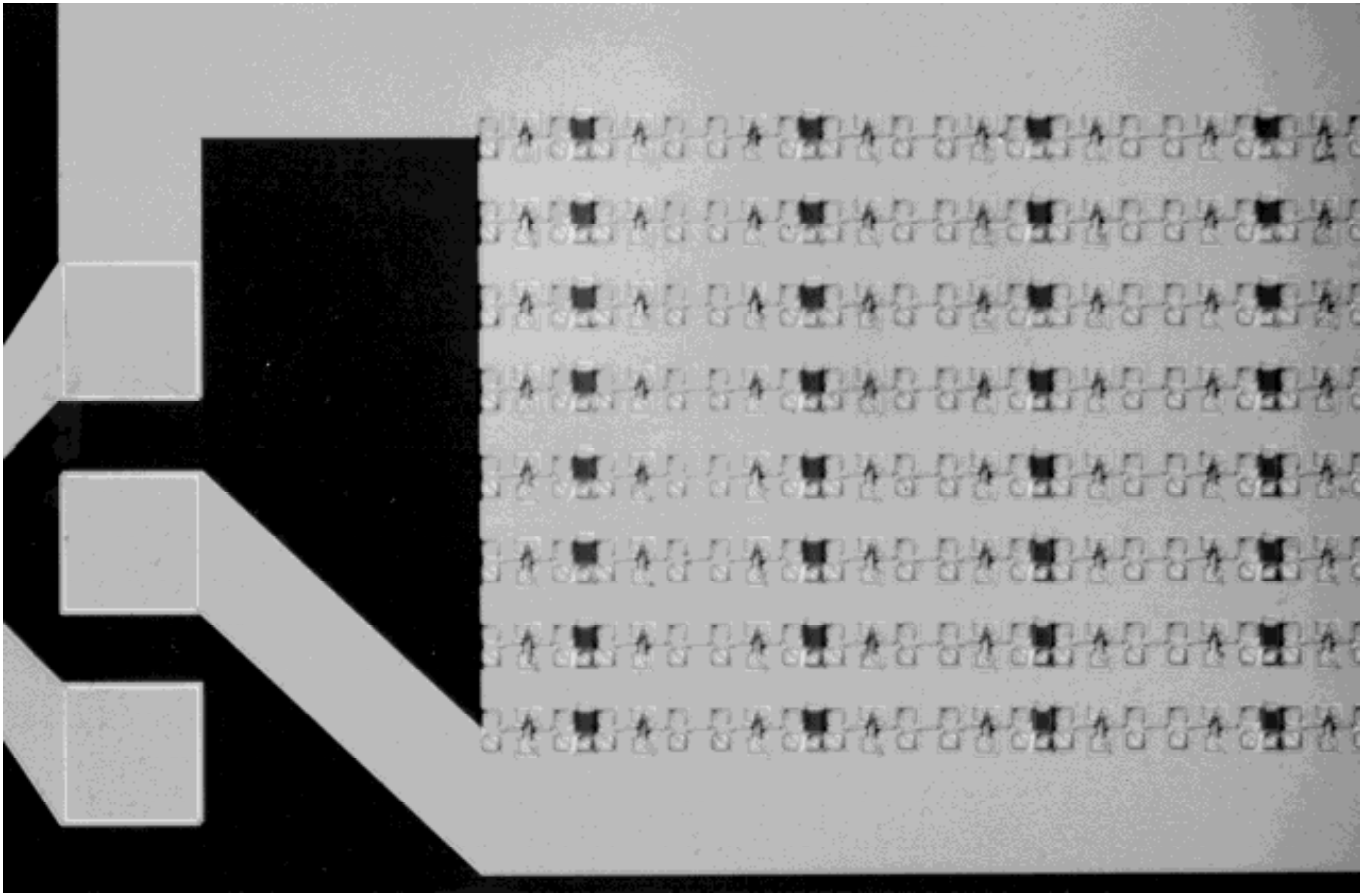

## Quasi-optical Setup for Testing Submm-wave Oscillators

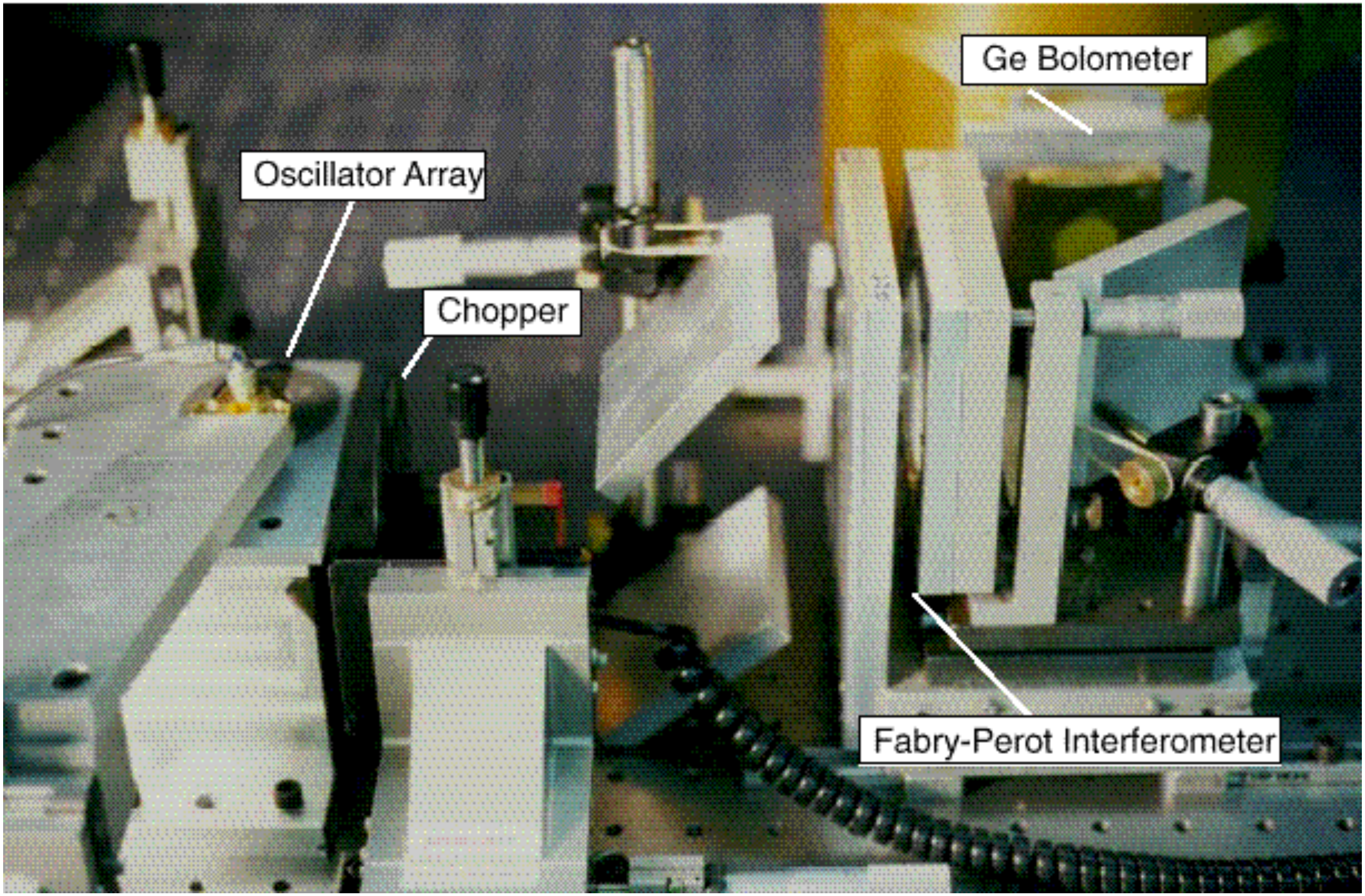

**Bolometer output Vs Mirror displacement for a 64-element array at 800 GHz**

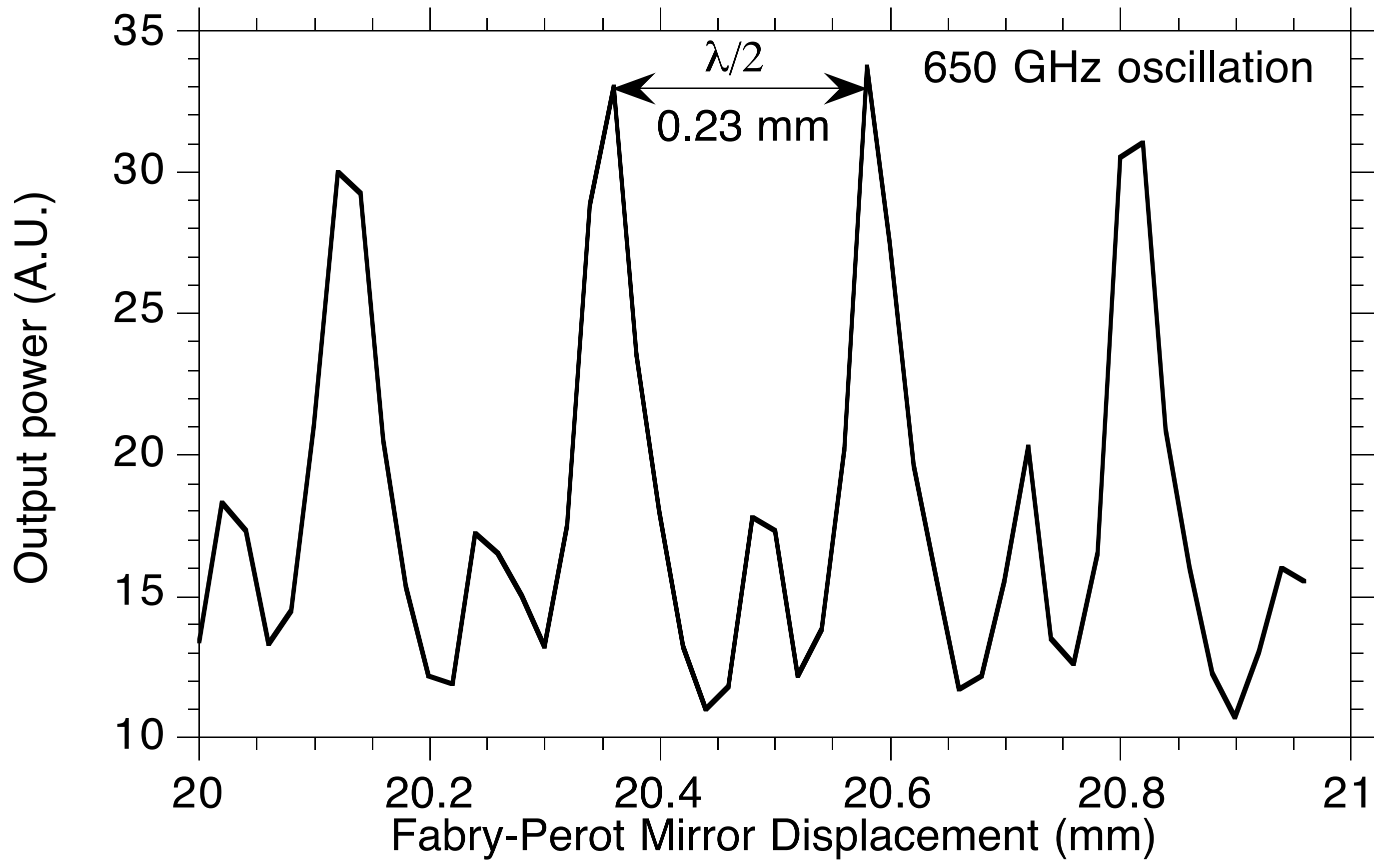

## Soliton NLTLs: Impulse Compression

Shock-wave devices:
competition of nonlinearity against dissipation
wavefronts compressed into shock-waves
picosecond step-functions are formed

Soliton-propagation devices:
competition of nonlinearity against dispersion
input waveforms decompose into sets of solitons
appropriate scaling: compression of impulses
picosecond large-amplitude impulses are formed.

# Signal Distortion on NLTLs

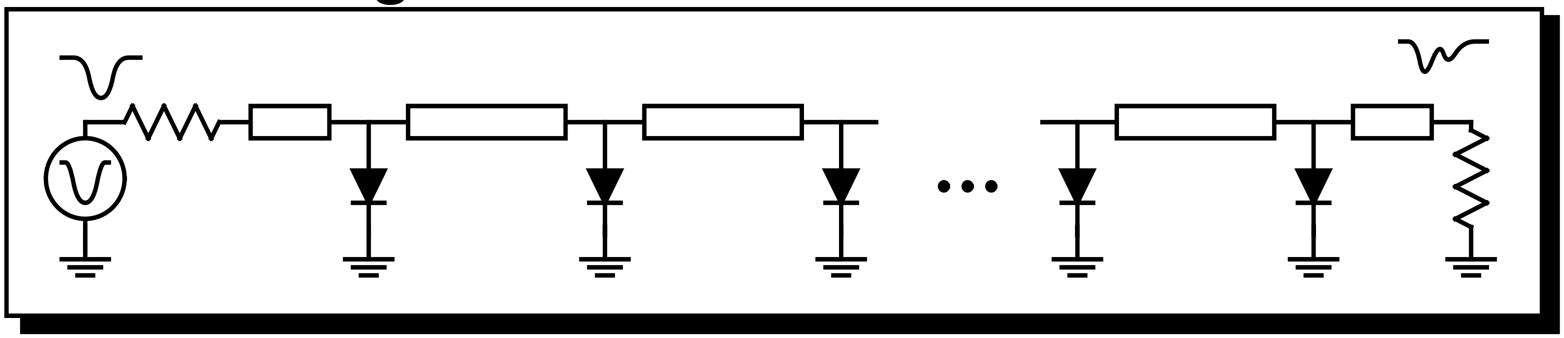

**Diode Nonlinear Reactance**

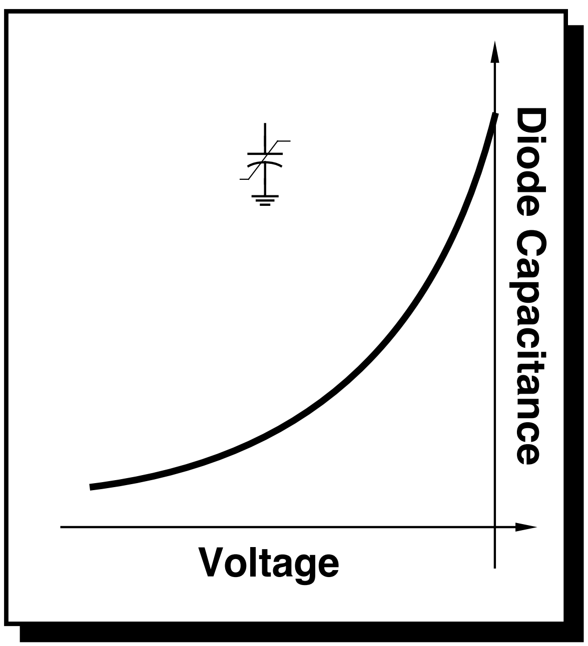


**Periodic-Network (Bragg) Dispersion**

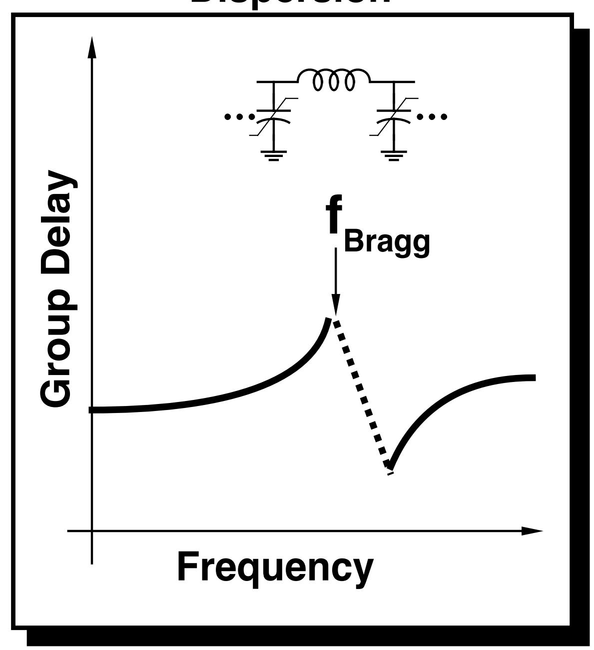

## Solitary Waves on NLTLs

•Pulse waveforms for which nonlinearity and dispersion are in opposition

•Propagate without dispersion

•Larger amplitude solitary waves propagate faster

•Larger amplitude solitary waves have shorter duration

•Solitary wave duration inversely proportional to Bragg frequency.

# Soliton Collision

**Solitons: solitary waves which are undistorted after collisions.**

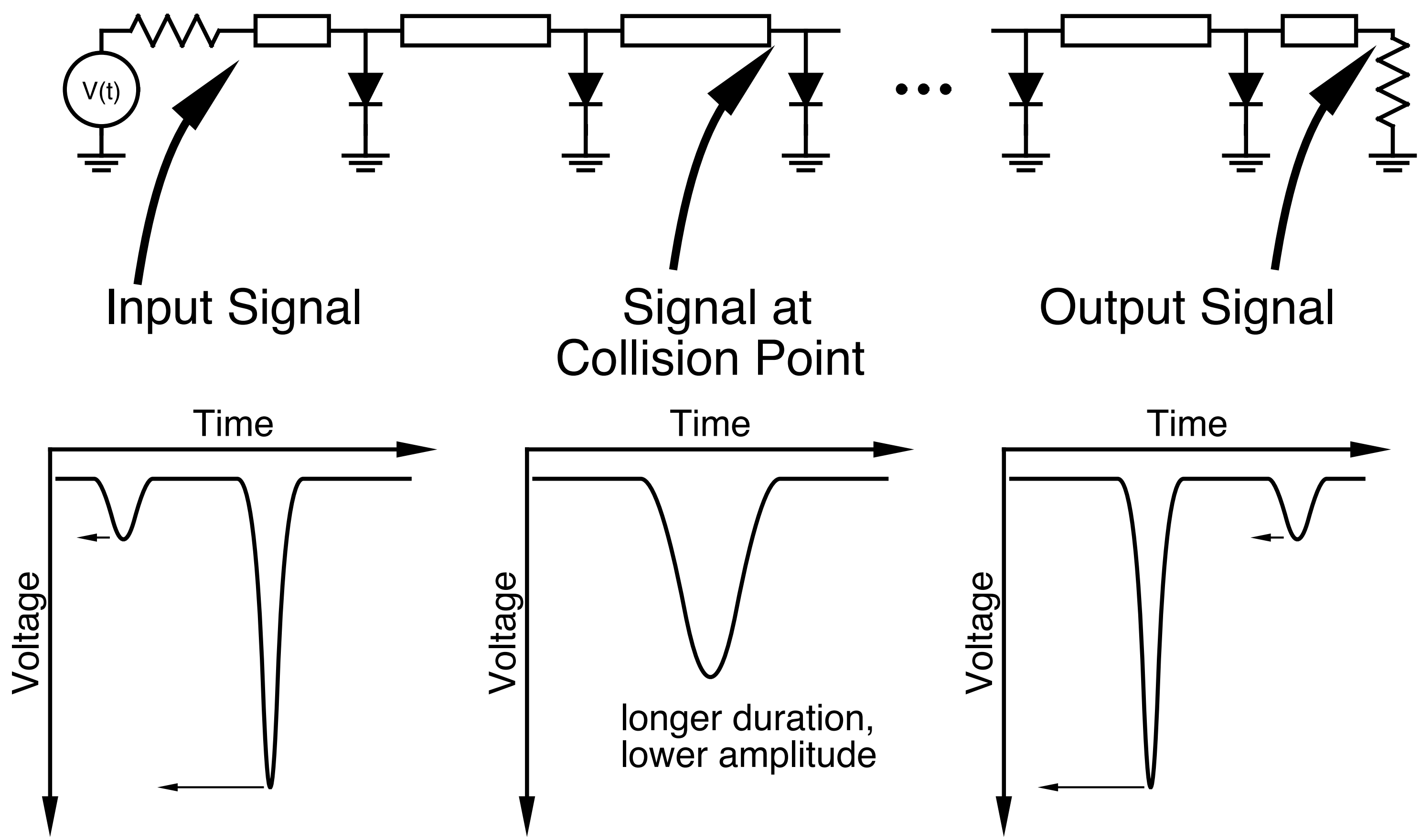

# Compression through Soliton Decomposition

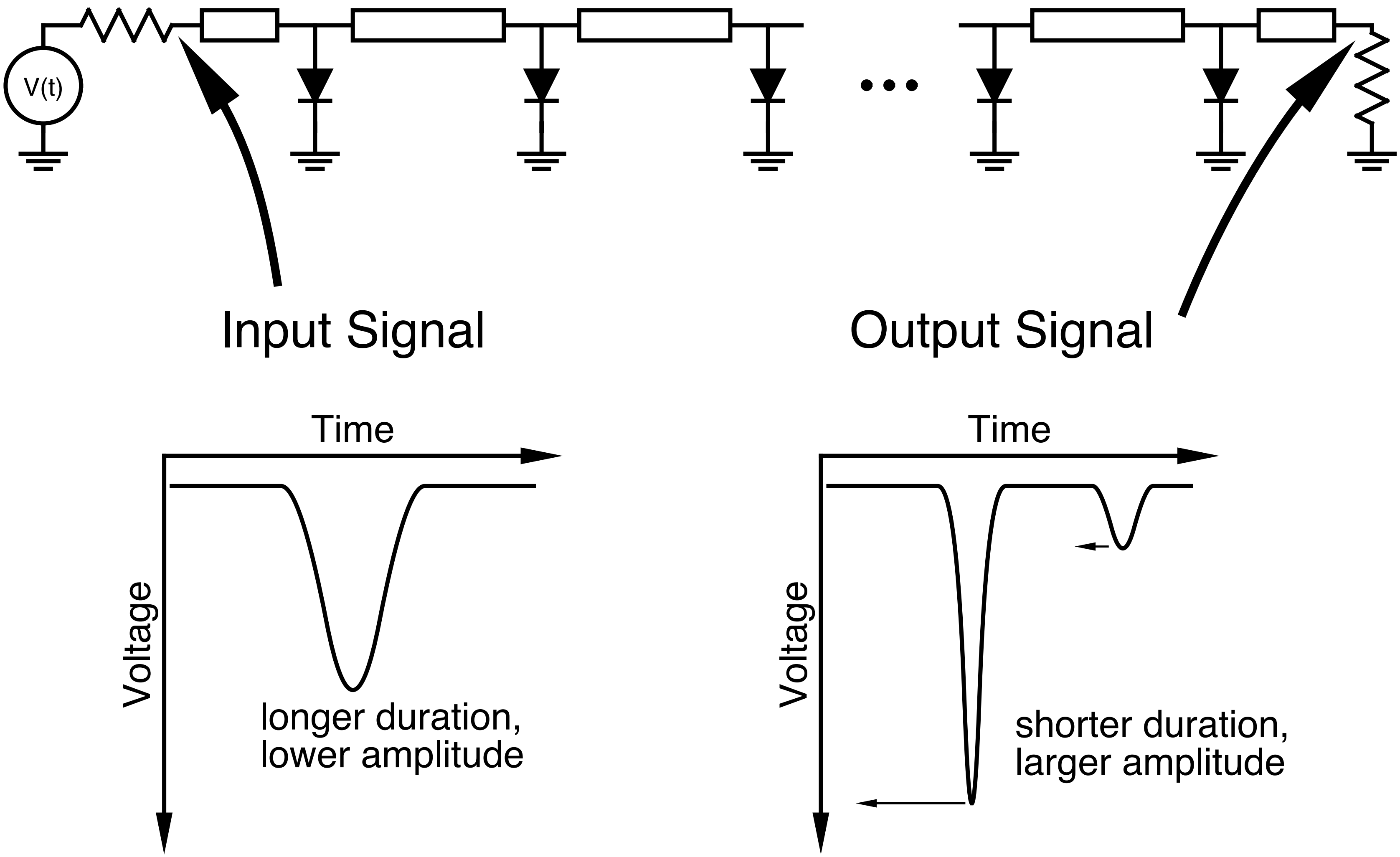

# Uniform Line: Limited Compression Ratio

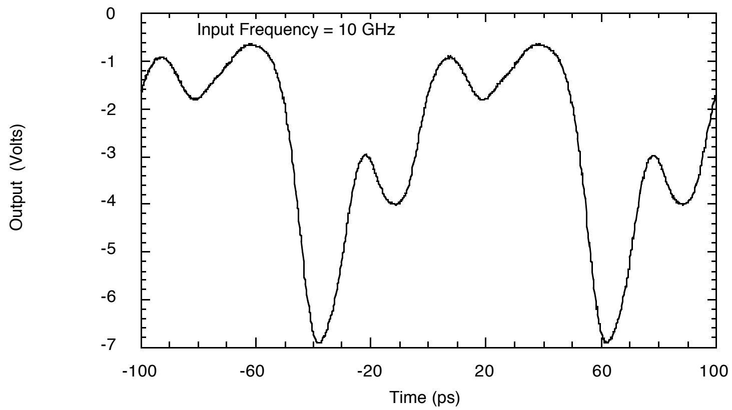


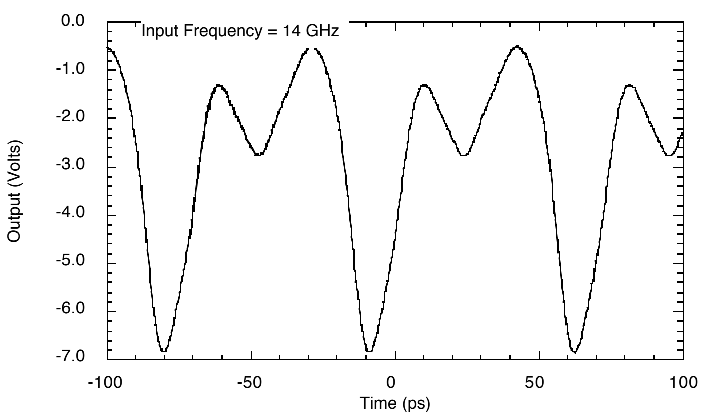


Line has ≈35 GHz Bragg frequency.

Pulse widths ≈$1/4f_{Bragg}$ will split into 2 solitons.

Longer pulses will split into 3 or more solitons per cycle.

Compression ratio limited to approximately 2.5:1

# Compression by Repeated Soliton Splitting

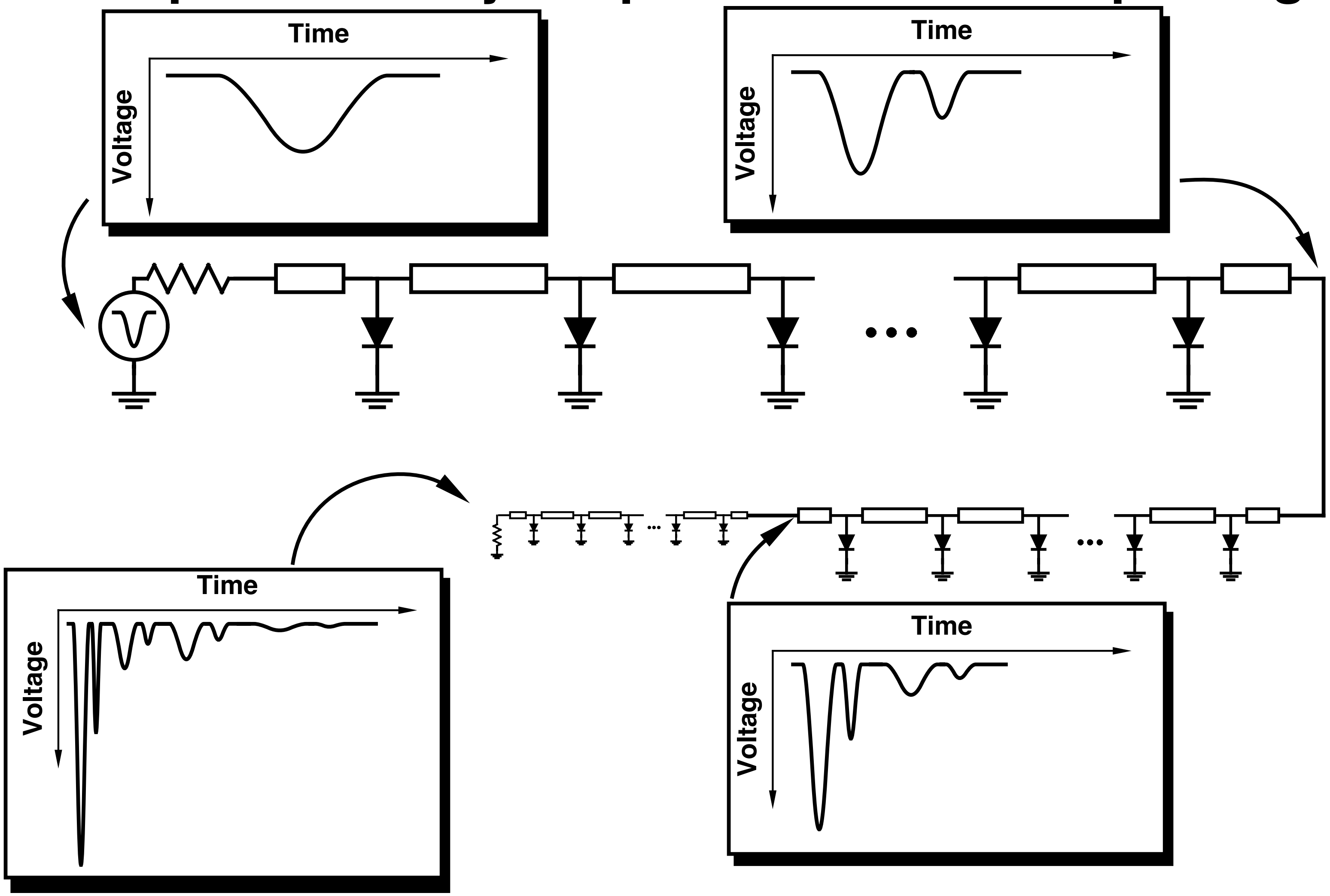

# Compression on a 2-Step Line

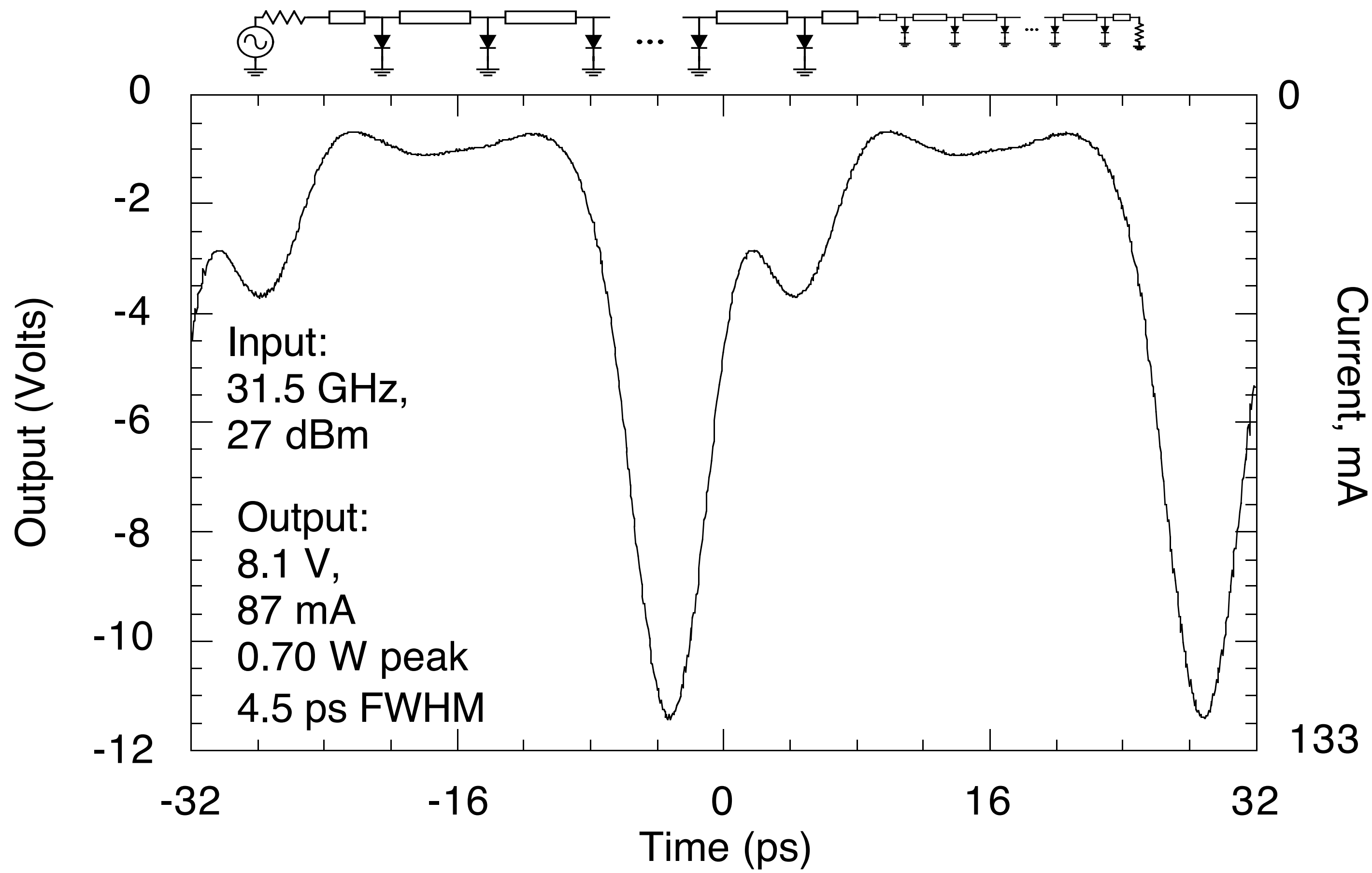

# Continuous Compression on a Tapered Line

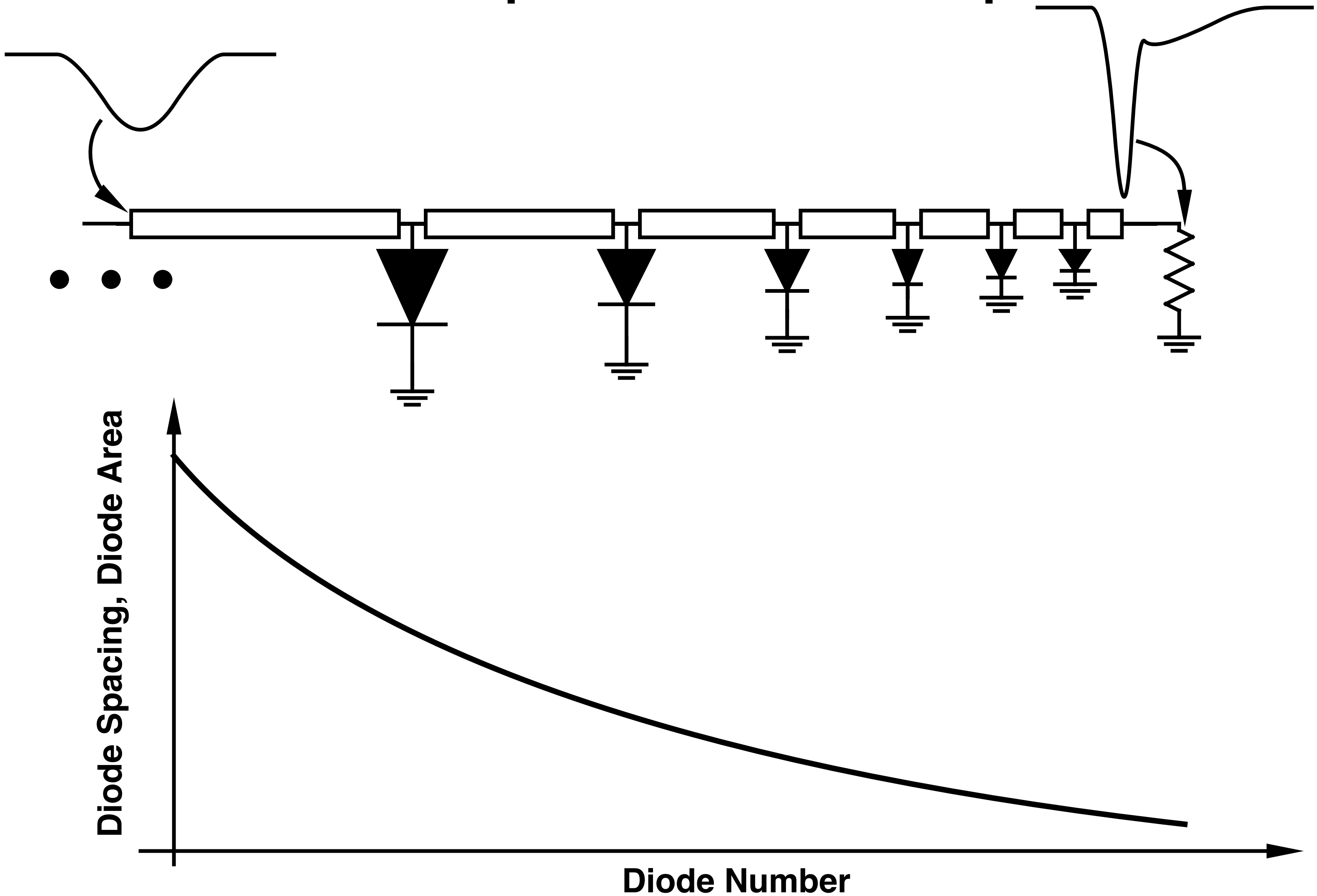

# Result: Tapered Impulse Compressor

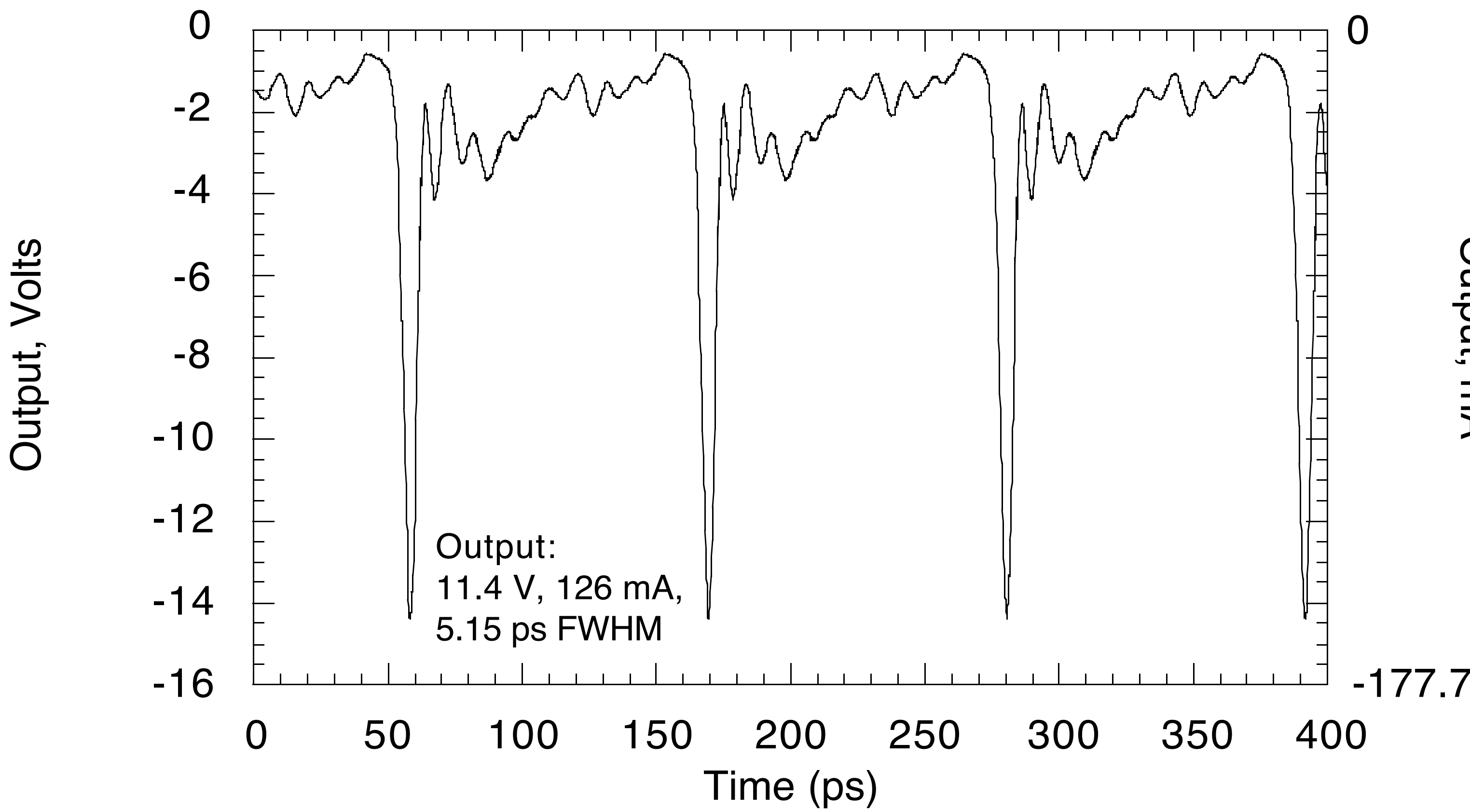

## Soliton Impulse Compressors: Summary

•Current performance
≈2:1 amplitude gain but limited bandwidth (5 ps measured, 2 ps theoretical).

• Fundamental limits:
Soliton (as opposed to shock) formation requires $f_{Bragg} << f_{diode}$.
2 THz (14 V Breakdown) diodes then should permit 2 ps FWHM pulses.
Faster diodes have lower breakdown voltages.
(Epitaxial or wired) series diodes may permit high $f_{diode}$ and high $V_{BR}$.

Compared to Shock-Wave NLTLs:
Poorer compression/length (bigger die, expensive)
≈2:1 poorer (theoretical) pulse performance (above)
much poorer experimental pulse performance
≈3 times larger output voltage (9 times in power)

# Traveling-Wave RTD Pulse Generator

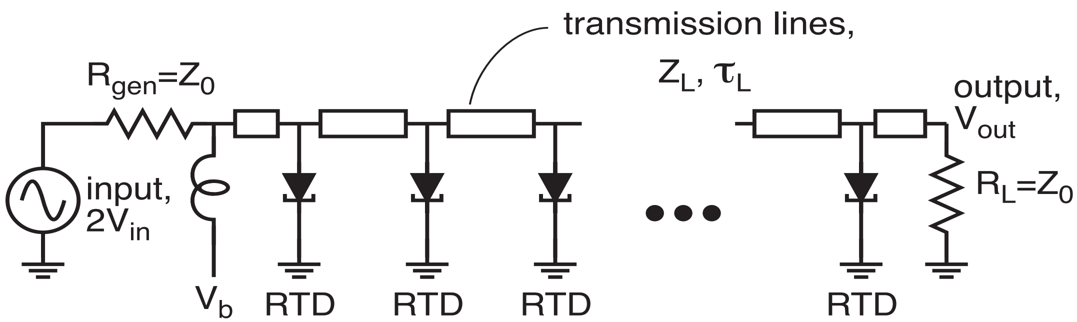


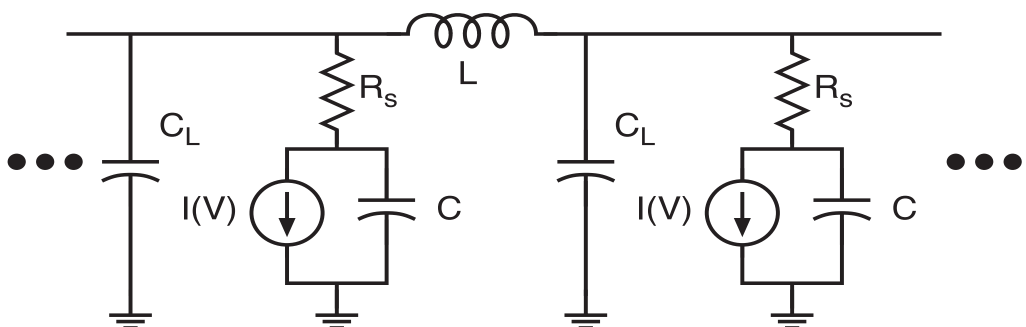


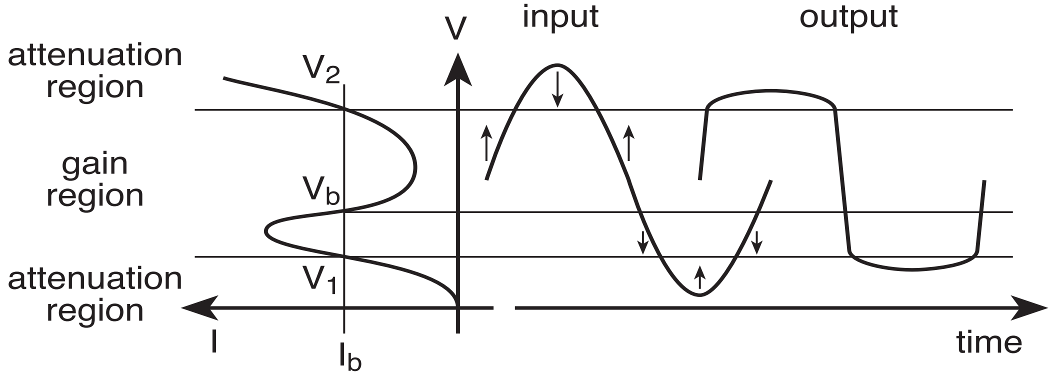


$$T_{10\%-90\%} \cong (\ln 0.9 - \ln 0.1) 2C\sqrt{R_n R_s} = 0.70 / f_{max}$$

TWRTD is a distributed structure

Capacitance charging times are eliminated

risetimes limited by $f_{max}$

if Rs<<Rn, TWRTD is several times faster than lumped RTD

NOT useful for logic : fast risetime, long delay.

# Lumped- vs Traveling-Wave RTD Risetimes

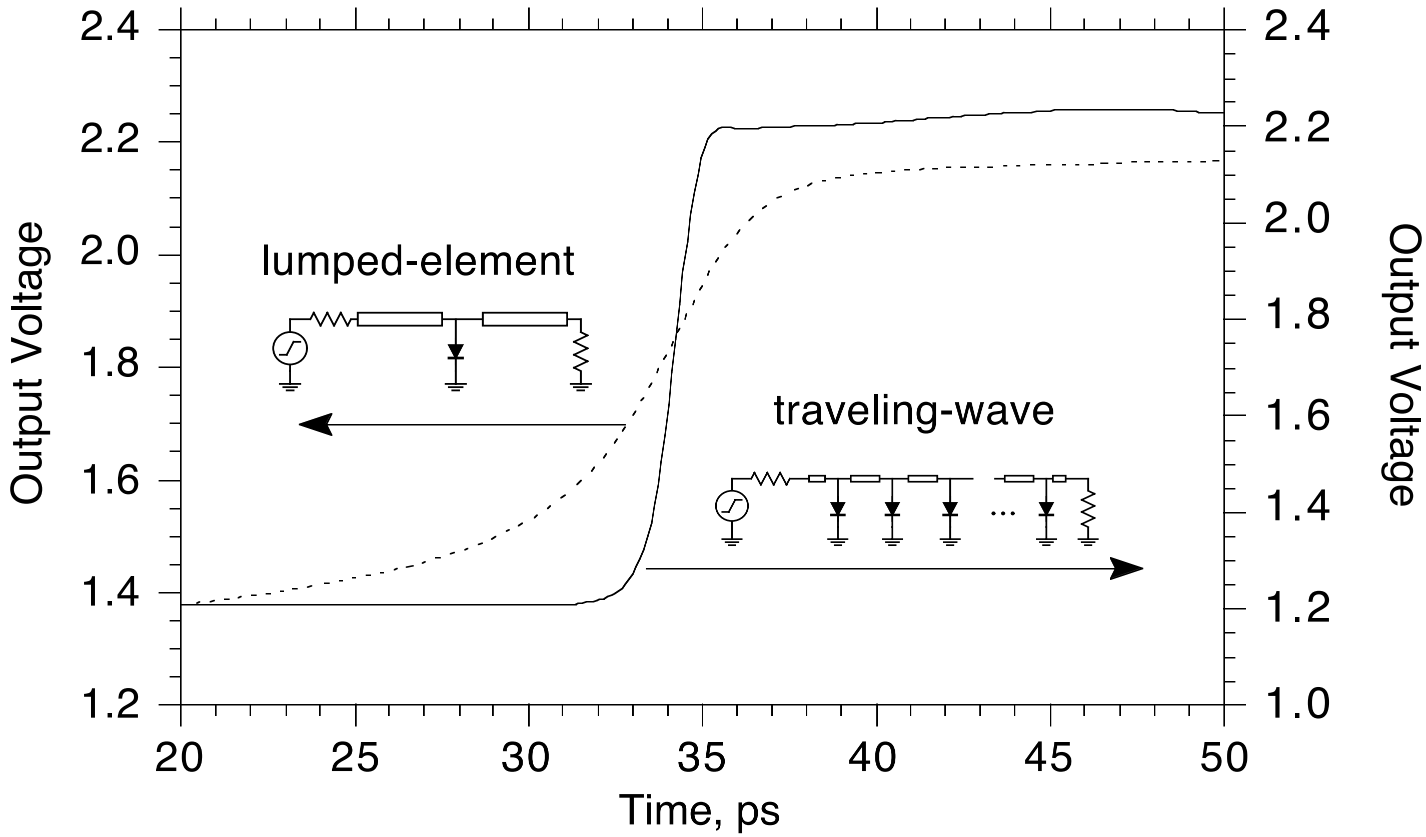


For RTD with low $R_S$, TWRTD is several times faster.

# TWRTD Measured Output Waveform

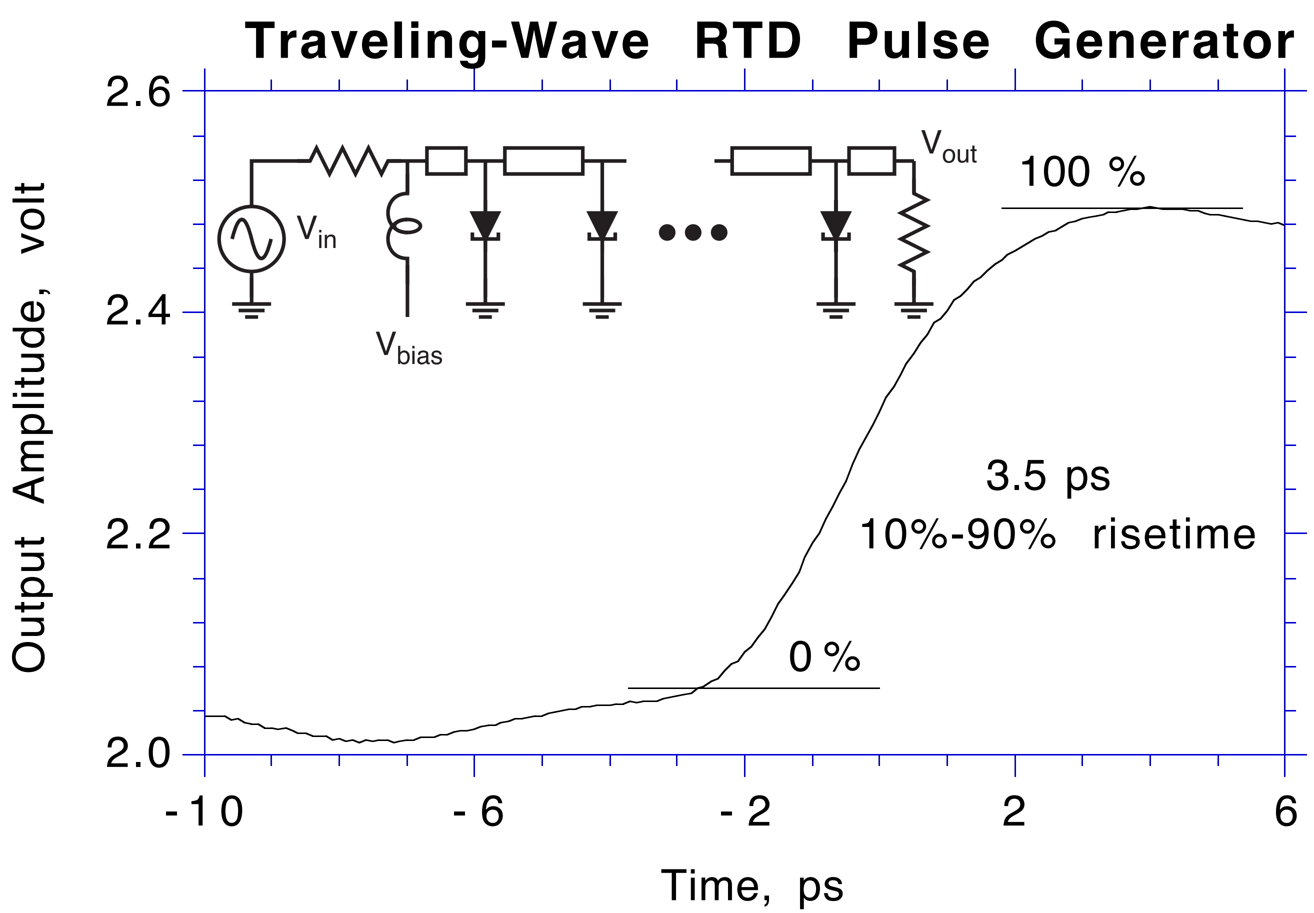


(measured with an .NLTL-based active probe )

# References

CLEO Short Course, Ultrafast Electronics and Optoelectronics, 1998


## Photodetectors

G. Lucovsky, R.F.Schwarz, and R.B. Emmons, "Transit-Time Considerations in p-i-n Diodes", Journal of Applied Physics, Vol. 35, No. 3, March 1964, pp. 622-628.

V. L. Dalal, "Hole Velocity in p-GaAs", Applied Physics Letters, Vol. 16, No. 12, 15 June 1970, pp. 489-491.

Y.-G. Wey, Kirk S. Giboney, J.E. Bowers, and M.J.W. Rodwell, "110 GHz Double Heterostructure GaInAs/InP p-i-n Photodiode", *Postdeadline paper presented at* the 1993 IEEE/OSA conference on Ultrafast Electronics and Optoelectronics, January 25-27, San Francisco. Proceedings to be published by the OSA.

S.Y. Wang, D.M. Bloom, "100 GHz Bandwidth Planar GaAs Schottky Photodiode", Electronics Letters, Vol. 19, No. 14, 7 July 1983, pp. 554-555

D.G. Parker, P.G. Say, A,M, Hanson and W. Sibbett, "110 GHz High-Efficiency Photodiodes Fabricated from Indium Tin Oxide/GaAs", Electronics Letters, 22 November 1989, pp s66-s67

B.J. VanZeghbroeck, W. Patrick, J.-M. Halbout, and P. Vettinger, "105-GHz bandwidth metal-semiconductor-metal photodiode", IEEE Electron Device Letters, Vol. 9, No. 10, Oct. 1988, pp. 527-529.

## Photoconductors

*Photoconductive Devices*

D. H. Auston, "Impulse Response of Photoconductors in Transmission Lines", IEEE J Quant Elect., Vol. QE-19, No. 4, April 1983

J.T. Darrow, S-C Zhang, D.H. Auston, and J.D. Morse, "Saturation Properties of Large-Aperture Photoconducting Antennas", IEEE J Quant Elect, Vol 28, No. 6, June 1992

S. Gupta, S.L. Williamson, Y. Chen, J.F. Whitaker, and F.W. Smith, "Ultrafast Dectors using III-V Epilayers Grown by Molecular-Beam-Epitaxy at Low Temperatures", Laser Focus World, July 1992

*TeraHertz Spectroscopy using photoconductors*

D. H. Auston and M. C. Nuss, " Electro-optic generation and detection of femtosecond electrical transients", IEEE, Quantum Electron., Vol. 24, pp. 184-197, 1988.

G. Arjavalingam, Y. Pastrol, J. M. Halbout and G. V. Kopcsay, "Broad-band microwave measurements with transient radiation from optelectronically pulsed antenna", IEEE, Trans. MTT., Vol. 38, No.5, pp. 615-621, May, 1990.

N. Katzenellenbogen and D. R. Grischkowsky, "Efficient generation of 380 fs pulses of THz radiation by ultrafast laser pulse excitation of a biased metal-semiconductor interface", Appl. Phys. Lett., Vol.58, No.3, pp. 222-224, January, 1991.

*On-Wafer Network Analysis Using Photoconductors*

M.D. Feuer, S.C. Shunk, P.R. Smith, H.H. Law, C.A. Burrus, and M.C. Nuss, "Highly reproducible optoelectronic wafer probes with fiber input", 1993 IEEE/OSA conference on Ultrafast Electronics and Optoelectronics, January 25-27, San Francisco. Proceedings to be published by the OSA.

**Step-Recovery Diodes:**

J. L. Moll and S.A. Hamilton, "Physical Modeling of the Step Recovery Diode for Pulse and Harmonic Generation Circuits", IEEE Proc., Vol. 57, No. 7, July 1969, pp. 1250-1259.

M. Tan, S. Wang, and D. Mars, "GaAs double heterostructure step recovery diodes," 1990 IEEE Device Research Conference, Santa Barbara, CA.

Mamoru Kurata, "Design Considerations of Step Recovery Diodes with the Aid of Numerical Large-Signal Analysis", IEEE Trans. Electr. Dev., Vol, ED-19, No. 11, Nov. 1972.

K. Schünemann and Jörg Muller, "A charge-control model of the PIN Diode", IEEE Trans Electr. Dev., Vol. ED-23, No. 10, Oct. 1976.

**Resonant Tunnel Diodes**

E.R. Brown, C.D. Parker, A.R. Calawa, M.J. Manfra, C.L. Chen, L. J. Mahoney, W.D. Goodhue, J. D.Söderström, and T. C. McGill, "High Frequency resonant-tunneling oscillators", Microwave Optical Technology Letters, vol. 4, pp. 19-23, 1991.

D.H. Chow, J. N. Schulman, E. Özbay, and D. M. Bloom, "Investigation of $In_{0.53}Ga_{0.47}As/AlAs$ resonant tunneling diodes for high-speed switching", Appl. Phys. Lett., Vol. 61, No. 14, 5 October 1992, pp. 1685-1687.

E. R. Brown, J. R. Söderström, C. D. Parker, L. J. Mahoney, K. M. Molvar, and T. C. McGill, "Oscillations up to 712 GHz in InAs/AlSb resonant-tunneling diodes", Appl. Phys. Lett. 58, 2291-2293 (1991).

E.R. Brown, T.C.L.G. Sollner, C.D. Parker, W.D. Goodhue, and C.L. Chen, "Oscillations up to 420 GHz in GaAs/AlAs resonant tunneling diodes", Appl. Phys. Lett., Vol. 55, No. 17, 23 October 1989, pp. 1777-1779

E.R. Brown, W.D. Goodhue, and T.C.L.G. Sollner, "Fundamental Oscillations up to 200 GHz in resonant tunneling diodes and new estimates of their maximum frequency of oscillation from stationary-state tunneling theory" , J. Appl. Phys., Vol. 64, No. 3, 1 Aug. 1988, pp. 1519-1529.

S.K. Diamond, E. Özbay, M.J.W. Rodwell, D.M. Bloom, Y.C. Pao, and J.S. Harris, "Resonant Tunneling Diodes for Switching Applications," Applied Physics Letters, 54 (2),
pp. 153-155, January 9, 1989.

M. Reddy, M.J. Mondry, M.J.W. Rodwell, S.C. Martin, R.E. Muller, R.P. Smith, D.H. Chow, and J.N. Schulman, "Fabrication, DC, and Microwave Characteristics of Submicron Schottky-Collector AlAs/$In_{0.53}Ga_{0.47}As$/InP Resonant Tunneling Diodes", Journal of Applied Physics, Vol 77, No. 9, 1 May 1995, pp. 4819–4821.

M. Reddy, S.C. Martin, A.C. Molnar, R.E. Muller, R.P. Smith, P.H. Siegel, M.J. Mondry, M.J.W. Rodwell, and S.J. Allen, Jr., "Monolithic Schottky-Collector Resonant Tunnel Diode Oscillator Arrays to 650 GHz " *IEEE Electron Device Letters*, Volume 18, No. 5, May 1997, pp. 218-221.

**Terahertz Technology (Radio Astronomy and Imaging)**

See the IEEE Proceedings, special issue on Terahertz technology, November 1992. Review Papers on Schottky diodes, Transmission lines, antennas, multipliers, quasi-optical arrays, and Terahertz spectroscopy

**100 GHz-5 THz Schottky Diodes**

K. Lundien, R.J. Mattauch, J. Archer, and R. Malik, "Hyperabrupt Junction Varactor Diodes for Millimeter-Wavelength Harmonic Generators", IEEE Trans. on MTT, vol. MTT-31, 1983, pp. 393-397

K.S. Champlin and G. Eisenstein, "Cutoff frequency of submillimeter Schottky-barrier diodes", IEEE Trans MTT, Vol MTT-26, No. 1, Jan. 1978.

C.O. Weiss and A. Godone, "Harmonic Mixing and Detection with Schottky Diodes up to the 5 THz Range", IEEE J. Quantum Electr., Vol QE-20, No. 2, February 1984.

## Transmission Lines and Antennas

D. B. Rutledge, D. P. Neikirk, and D. P. Kasilingam. "Integrated-Circuit Antennas" in Infrared and Millimeter Waves, K. J. Button, Ed., Vol. 10, pp. 1-90, New York: Academic Press, 1984. Also covers transmission line radiation losses

R. C. Compton, R. C. McPhedran, Z. P. Popovic, G. M. Rebeiz, P. P. Tong and D. B. Rutledge, "Bow-Tie Antennas on a Dielectric Half-Space: Theory and Experiment", IEEE, Trans. Antenna Propag., AP-35, pp. 622-631, June, 1987.

A. Moussessian and D. B. Rutledge, "A Millimeter-Wave Slot-V Antenna", IEEE AP-S (antennas and propagation) International Symposium, July 1992, Chicago, IL

R.L. Wigington and N.S. Nahman, "Transient Analysis of Coaxial Cables Considering Skin Effect", Proc. IRE, February 1957.

Reinmut Hoffmann, Handbook of Microwave Integrated Circuits, Artech House, Norwood, MASS, 1987. This is a good general reference for transmission line design formulas.

## Transistors

U. K. Mishra, A.S. Brown, and S.E. Rosenbaum: "DC and RF performance of 0.1 µm Gate Length AlInAs-GaInAs Pseudomorphic HEMTs" In Technical Digest, 1988 International Electron Device Meeting, Dec. 11-14, San Francisco.

Shoji Yamahata, Kenji Kurishima, Hiroshi Ito, Yutaka Matsuoka, "Over-220-GHz ft-and-fmax InP/InGaAs Double-Heterojunction Bipolar Transistors with a New Hexagonal-Shaped Emitter", Proceedings, 1995 IEEE GaAs IC Symposium.

W. E. Stanchina, J. F. Jensen, R. H. Walden, M. Hafizi, H. -C. Sun, T. Liu, G. Raghavan, K. E. Elliott, M. Kardos, A. E. Schmitz, Y. K. Brown, M. E. Montes and M.Young, ‘‘An InP-Based HBT Fab for High-Speed Digital, Analog, Mixed-Signal and Optoelectronic ICs”, GaAs IC Symp. Tech. Dig, 1995, pp. 31-34.

Y. Matsuoka, S. Yamahata, S. Yamaguchi, K. Murata, E. Sano, and T. Ishibashi ‘‘IC- oriented self-aligned high-performance AlGaAs/GaAs ballistic collection transistors and their applications to high-speed ICs”, IEICE Trans. on Electron., vol. E76-C, pp. 1392-1401, 1993.

S. Yamahata, K. Kurishima, H. Ito and Y. Matsuoka, ‘‘Over-220-GHz- $f_\tau$ -and- $f_{\max}$ InP/InGaAs Double-Heterojunction Bipolar Transistors with a New Hexagonal-Shaped Emitter”, GaAs IC Symp. Tech. Dig., 1995, pp. 163-166.

S. Yamahata, K. Kurishima, H, Nakajima, T. Kobayashi and Y. Matsuoka, ‘‘Ultra-High $f_{\max}$ and $f_\tau$ InP/InGaAs Double-Heterojunction Bipolar Transistors with Step-Graded InGaAsP Collector”, GaAs IC Symp. Tech. Dig. , 1994, pp. 345-348.

T. Ishibashi, H. Nakajima, H. Ito, S. Yamahata and Y. Matsuoka, ‘‘Supressed Base-Widening in AlGaAs/GaAs Ballistic Collection Transistors”, Device Research Conf. Tech. Dig. , 1990, pp. VIIB-3.

Q. Lee, B. Agarwal, R. Pullela, D. Mensa, J. Guthrie, L. Samoska, M. Rodwell, " A > 400 GHz $f_{\max}$ Transferred Substrate Heterojunction Bipolar Transistor IC Technology”, IEEE Electron Device Letters, March 1998

## Electrooptic Sampling

J. A. Valmanis, G. A. Mourou, and C.W. Gabel, "Subpicosecond electrical sampling", IEEE J Quant Elect, QE-19, (1983)

J. A. Valdmanis and S.S. Pei, "A non-contact picosecond prober for integrated circuit testing", in *Picosecond Electronics and Optoelectronics*, Springer-Verlag, New York, 1987

B. H. Kolner and D. M. Bloom, "Direct Electrooptic Sampling of Transmission-Line Signals Propagating on a GaAs substrate", Electronics Letters, Vol. 20, pp. 818-819, 1984.

K.J. Weingarten, M.J.W. Rodwell, and D.M. Bloom, "Picosecond Sampling of GaAs Integrated Circuits," IEEE Journal of Quantum Electronics, Vol. 24, No. 2, pp. 198-220 February, 1988.

## Diode Sampling Circuits (non-NLTL-based)

W. M. Grove, "Sampling for oscilloscopes and Other RF systems, DC Through X-band", IEEE Trans on MTT, Vol. MTT-14, No. 12, Dec. 1966, pp. 629-635.

J. Merkelo and R.D. Hall, "Broad-Band Thin-Film Signal Sampler", IEEE J. of Solid-State Circuits, Vol. SC-7, No. 1, February 1972, pp. 50-54.

## Nonlinear Transmission Lines

*Basic Principles: Electrical Shock-Waves and Solitons*

Fermi, Pasta, and Ulam, "Studies of Non Linear Problems" in: Enrico Fermi, Collected Papers, Volume II, (page 266),University of Chicago Press.

Landauer, R. :"Parametric Amplification along Nonlinear Transmission Lines", J. Appl. Phys., 1960, Vol. 31, No. 3, pp. 479-484.

Khokhlov, R.V. "On the Theory of Shock Radio Waves in Non-Linear Lines", Radiotekhnika i elektronica, 1961, 6, No.6, pp. 917-925.

A. Scott, Active and Nonlinear Wave Propagation in Electronics, Wiley-Interscience, New York, 1970. This provides a wide overview of the literature with many references.

R. Hirota and K. Suzuki, "Theoretical and Experimental Studies of Lattice Solitons in Nonlinear Lumped Networks", IEEE Proc., Vol. 61, No. 10, Oct. 1973, pp. 1483-1491.

A.C.Scott, F.Y.F. Chu, and D.W.McLaughlin, "The Soliton: A New Concept in Applied Science" IEEE Proc, Vol. 61, No. 10, Oct. 1973, pp. 1443-1482.

C.R. Wilson, M.M. Turner, and P. W. Smith, "Electromagnetic Shock Wave generation in a lumped element delay line using nonlinear ferroelectric capacitors", Appl Phys Lett, Vol 56, No 24, 11 June 1990.

*Shock-Wave NLTLs and Sampling Circuits*

M.J.W. Rodwell, S. T. Allen, R. Y. Yu, M. G. Case, M. Reddy, E. Carman , J. Pusl, M. Kamegawa, Y. Konishi, and R. Pullela, "Active and Nonlinear Wave Propagation Devices in Ultrafast Electronics and Optoelectronics", Invited Paper, IEEE Proceedings, Vol. 82, No. 7, July 1994, pp. 1037-1058.

M. J. W. Rodwell, M. Kamegawa, R. Yu, M. Case, E. Carmen, K. S. Giboney, "GaAs Nonlinear Transmission Lines for Picosecond Pulse Generation and Millimeter-Wave Sampling", IEEE, Trans. MTT., Vol. 39, No.7, July, 1991.

R. A. Marsland, C. J. Maden, D. W. Van Der Weide, M. S. Shakouri, and D. M. Bloom, "Monolithic Integrated Circuits for MM-Wave Instrumentation", in Technical Digest, GaAs IC Symposium, New Orlens, La. October, 7-10, 1990.

S.T. Allen, U. Bhattacharya, M.J.W. Rodwell: "4 THz Sidewall-Etched Varactors and their application in Sub-mm-Wave Sampling Circuits", Electronics Letters, Vol. 29, No. 25, 9 December 1993, pp. 2227-2228

*Soliton Devices*

Michael Case, Eric Carman, Ruai Yu, and M.J.W. Rodwell, "Picosecond Duration, Large-Amplitude Impulse Generation Using Electrical Soliton Effects" Applied Physics Letters, Vol. 60, no. 24, 15 June 1992, pp. 3019-3021.

*Applications: Network Analysis, Spectroscopy, Photodetector Integration*

Ruai Yu, Madhukar Reddy, Joe Pusl, Scott Allen, Michael Case, and Mark Rodwell, "Full Two-Port On-Wafer Vector Network Analysis to 120 GHz Using Active Probes", .1993 IEEE Conference on Microwave Theory and Techniques, June, Atlanta, Ga

M.S. Shakouri, A. Black, D.M. Bloom, "Subpicosecond GaAs Wafer Probe System" in proceedings, OSA meeting on Ultrafast Electronics and Optoelectronics, January 1993, San Francisco.

Y. Konishi, M. Kamegawa, M. Case, R. Yu, M.J.W. Rodwell, and D.B. Rutledge, "Picosecond Spectroscopy Using Monolithic GaAs Circuits", Applied Physics Letters, Vol. 61, No 23, 7 Dec. 1992.

E. Özbay, K. D. Li, and D.M. Bloom, "2.0 ps, 150 GHz GaAs Monolithic Photodiode and All-Electronic Sampler", IEEE Phot. Tech. Lett., Vol. 3, No. 6, June 1991, pp. 570-572.

M. Kamegawa, K. Giboney, J. Karin, M.Case, R. Yu, M.J.W. Rodwell, and J.E. Bowers, "Picosecond GaAs Monolithic Optoelectronic Sampling Circuit", IEEE Photonic Technology Letters, Vol. 3, No. 6, June 1991, pp. 567-569.

**Laser Timing Stabilization:**

M.J.W. Rodwell, D.M. Bloom and K.J. Weingarten, "Subpicosecond Laser Timing Stabilization," IEEE Journal of Quantum Electronics, Vol. 25, No. 4, pp. 817-827, April, 1989.